UNIVERSITÀ DEGLI STUDI DI NAPOLI "FEDERICO II"

DOTTORATO IN SCIENZE VETERINARIE XXIX CICLO

TESI

"Marine Biotechnology: a sea of new resources and solutions for ocean and human health"

Candidato	**Tutor**	**Co-Tutor**
Dott. Christian Galasso	Dott.ssa Giovanna Romano	Dott.ssa Clementina Sansone

DOTTORATO IN SCIENZE VETERINARIE - Segreteria *Dott.ssa Maria Teresa Cagiano*
Coordinamento - *Prof. Giuseppe Cringoli*

A Carolina, forza, sostegno e futuro della mia vita personale e professionale.

A papà e mamma, ai nonni e alla mia famiglia tutta, parte integrante di questo traguardo.

INDEX

LIST OF ABBREVIATION

°C	degree Celsius
15-HEPE	(±)-15-hydroxy-5Z,8Z,11Z,13E,17Z-eicosapentaenoic acid
5-HEPE	(±)-5-hydroxy-6E,8Z,11Z,14Z,17Z-eicosapentaenoic acid
A. andersoni	*Alexandrium andersoni*
A549	lung adenocarcinoma cell line
ACTB	actin-beta
AFC	7-amino-4- trifluoromethyl-coumarin
AIFM1	Apoptosis Inducing Factor, Mitochondria Associated 1
AKR1C2	Aldo-keto reductase family 1, member C2
ANOVA	Analysis of variance
ATCC	American Type Culture Collection
ATOX1	ATX1 antioxidant protein 1 homolog
ATP6V1G2	V-type proton ATPase subunit G 2
B2M	beta-2-microglobulin
BAX	BCL2 Associated X Protein
BCL2	B-Cell CLL/Lymphoma 2
BCL2L11	Bcl-2-like protein 11
BEAS-2B	normal lung/brunch epithelial cell line
BECN1	Beclin 1
BIRC3	baculoviral IAP repeat containing 3
BLAST	Basic Local Alignment Search Tool
Blastn	Nucleotide-nucleotide BLAST
Blastp	Protein-protein BLAST
Bp	base pair
BP10	Blastula protease 10
CCL5	Chemokine (C-C motif) ligand 5
CCMP	Culture Collection of Marine Phytoplankton
cDNA	complementary Deoxyribonucleic Acid
CDSs	coding DNA sequences
CH_2Cl_2	Dichloromethane
$CHCl_3$	chloroform
Chl *a*	Chlorophyll a
Chl *b*	Chlorophyll b
COHH	Centers for Oceans and Human Health;
COLO 205	colorectal adenocarcinoma cell line
CRADD	CASP2 and RIPK1 domain containing adaptor with death domain
Ct	cycle threshold
CYCS	cytochrome c somatic
DECADIENAL	2-*trans*,4-*trans*-decadienal
DECATRIENAL	2-trans-4-trans-7-cis-decatrienal
DEPC	Diethylpyrocarbonate
DEVD	Aspartic acid-Glutamic acid-Valine- Aspartic acid
DHCR24	24-dehydrocholesterol reductase
DHCR24	24-dehydrocholesterol reductase
DMEM	Dulbecco's modified Eagle's medium
DNA	DeoxyriboNucleic Acid
dNTP	deoxynucleotide triphosphate

DPPH	2,2-Di(4-tert-octylphenyl)-1-picrylhydrazyl
DPR	Decreto del Presidente della Repubblica
DPYSL4	dihydropyrimidinase-related protein 4
E	efficiency
ECVAM	European Centre for the Validation of Alternative Models
EDTA	Ethylenediaminetetraacetic acid
EIF5B	eukaryotic translation initiation factor 5B
ELISA	enzyme-linked immunosorbent assay
EMBOSS	European Molecular Biology Open Software Suite
EPI-200	human epidermal tissue model
ERA-NET- MBT	European Research Area - Network - Marine Biotech;
FADD	Fas Associated Death Domain
FAHs	fatty acid hydroperoxides
FASLG	Fas ligand
FBS	Fetal Bovine Serum
FOXM1	Forkhead box M1
FSW	Filtered Sea Water
g	Relative Centrifugal Force (RCF) or G-Force
GADD45	growth arrest and DNA-damage-inducible protein
GPX1	Glutathione peroxidase 1
GPX4	Glutathione peroxidase 4
GSTP1	Glutathione S-transferase pi 1
H. sapiens or HS	*Homo sapiens*
H_2O_2	dihydrogen peroxide
HAT	Human Airway Trypsin-like protease
HEPEs	Hydroxy-EicosaPentaEnoic acids
HepETEs	Epoxyalcohols
HEPTADIENAL	2-*trans*,4-*trans*-heptadienal
HIF1A	Hypoxia-inducible factor 1-alpha
hpf	hours post fertilization
HPLC	High Performance Liquid Chromatography
HPRT	1hypoxanthine phosphoribosyltransferase
HSP90AA1	Heat shock protein 90kDa alpha A
HUBs	highly connected nodes
IC50	half maximal inhibitory concentration
IGF1R	insulin-like growth factor 1 receptor
KCl	Postassium chloride
KCNIP1	Kv channel-interacting protein 1
LC-MS/MS	liquid chromatography-mass spectrometry
LOXs	Lipoxygenases
MCL1	induced myeloid leukemia cell differentiation protein-Mcl-1
MeOH	methanol
ml	millilitres
MTase	MethylTransferase enzyme
n-BuOH	*n*-butanol
NCBI	National Center for Biotechnology Information
NEAA	non-essential amino acids
NF-kB	Nuclear Factor Kappa B
ng	nanogram
nm	nanometres
NOAA	National Oceanic and Atmospheric Administration

OCTADIENAL	2-*trans*,4-*trans*-octadienal
OCTATRIENAL	2-*trans,*4-*trans*,7-octatrienal
OHHI	Oceans and Human Health Initiative
P. lividus or Pl	*Paracentrotus lividus*
p38 MAPK	p38 mitogen-activated protein kinase
p53	Tumor Protein P53
PARP1	Poly ADP-Ribose Polymerase 1
PBS	Phosphate-Buffered Saline
PCR	Polymerase Chain Reaction
PDLIM1	PDZ and LIM domain 1
PGE_2	prostaglandin E_2
PINK1	PTEN Induced Putative Kinase
Pl-Z12–1	zinc-finger transcription factor
PMSF	phenylmethylsulfonyl fluoride
PRDX5	Peroxiredoxin 5
PTGR1	Prostaglandin reductase 1
PUAs	Polyunsaturated Aldehydes
PUFAs	Polyunsaturated Fatty Acids
qPCR	quantitative Polymerase Chain Reaction
R	expression ratio
R^2	regression coefficient
REST	Relative Expression Software Tool
RIMAR	Research Infrastructures for MArine biological Resources
RIP	Receptor-Interacting Protein
RIPA	radioimmunoprecipitation assay
RIPK_2	Homeodomain Interacting Protein Kinase 2
RIPK4	Receptor Interacting Serine/Threonine Kinase 4
RNA	RiboNucleic Acid
RNase	Ribonuclease
ROS	Reactive Oxigen Species
RPLP0	large ribosomal protein P0
RSC	Radical scavenging capacity
S. purpuratus or Sp	*Strongylocentrotus purpuratus*
SD	Standard Deviation
SIRT2	Sirtuin 2
SIVA	CD27 - binding pro-apoptotic protein
SLC7A11	Solute carrier family 7 member 11
SOD2	Superoxide dismutase 2, mitochondrial
SPE	Solid Phase Extraction
SYBR Green	N', N'-dimethyl-N-[4-[(E)-(3-methyl-1,3-benzothiazol-2-ylidene) methyl]-1-Phenylquinolin-1-ium-2-yl]-N-propylpropane-1,3-diamine
T. suecica	*Tetraselmis suecica*
TAE	Tris-Acetate-EDTA buffer
Taq	*Thermus aquaticus* DNA polymerase
tBlastn	Protein-nucleotide BLAST
Tm	temperature melting
TNF_R1	TNF Receptor Superfamily Member 1A
TNF_R2	TNF Receptor Superfamily Member 1B
TNFR1	Tumor Necrosis Factor Receptor 1
TNFR16	Tumor Necrosis Factor Receptor 16
TNFR27	Tumor Necrosis Factor Receptor 27

TNFRSF25	Tumor Necrosis Factor ligand superfamily member 25
TNFSF8	Tumor Necrosis Factor ligand superfamily member 8
TNF-α	Tumor Necrosis Factor-alpha
TRAF2	TNF receptor-associated factor 2
TRAIL_R1	TNF Receptor Superfamily Member 10a
TRIDECANAL	*trans*-2-tridecanal
UKL1	Unc-51 Like Autophagy Activating Kinase
UKL3	Unc-51 Like Autophagy Activating Kinase 3
WI38	normal diploid human lung fibroblasts
XIAP	X-linked inhibitor of apoptosis
Z-VAD-FMK	N-Benzyloxycarbonyl-Val-Ala-Asp(O-Me) fluoromethyl ketone
µm	micrometer
µM	microMolar
µmol	micromol

LIST OF FIGURES

FIGURE 1.11: (**A**) *Paracentrotus lividus* 48 hours plutei after incubation in decadienal at 1.32 μM (b), 2.63 μM (c), 3.95 μM (d) and 5.26 μM (e) compared to control embryo (a). (**B**) Percentage of abnormal sea urchin larvae after 48 hours of treatment with several decadienal concentration ranging from 1.32 μM to 6.58 μM. Control is reported as 0 μM decadienal concentration. Yellow bars = retarded larvae; blue bars = abnormal pluteus larvae; red bar = abnormal gastrulae and blastulae; green = dead pre-hatched embryos. Values (means ± S.D.; N = 600) are the results of three different experiments (modified from Romano et al., 2010).

FIGURE 1.12: Active mitochondria visualised by the mitochondrial-specific fluorescent dye Mito tracker within *Paracentrotus lividus* egg before the fertilization (**A** and **B**); egg 10 minutes after the elevation of the fertilization envelope (**C** and **D**); embryos at 50 min post fertilization (**E** and **F**); embryos at 50 min post fertilization incubated with 5 μg ml^{-1} decadienal (**G** and **H**). Upper panels are images in transmitted light; lower panels are the same images in fluorescent light. (Modified from Romano et al., 2011).

FIGURE 1.13: Schematic representation of molecular cell death pathways activated by the three different PUAs in lung adenocarcinoma cell lines A549. Red arrows indicate signal transduction via activated by decadienal; blue arrows indicate signal transduction via activated by octadienal; green arrows indicate signal transduction via activated by heptadienal (from Sansone et al., 2014)

FIGURE 2.1: Schematic representation of *in vitro* experiment for the treatment of sea urchin *Paracentrotus lividus* embryos with different concentrations of heptadienal (2 μM, 2,5 μM, 3 μM, 5,5 μM and 6 μM) for 5 hours, 21 hours and 48 hours.

FIGURE 2.2: the flowchart show the several steps needed for the bioinformatic study of *Paracentrotus lividus* database. This analysis started from aminoacid sequences from *Homo sapiens*, and, passing though *Strongylocentrotus purpuratus*, identified and annotated ortholog protein and nucleotide sequences from our model organism.

FIGURE 3.1: Morphological effects of five different heptadienal concentrations (2.0 μM, 2.5 μM, 3.0 μM, 5.5 μM and 6.0 μM) on sea urchin *Paracentrotus lividus* embryo development. For each concentration of pure compound, embryos at the pluteus stage were analysed under the microscope and divided in 'Normal plutei' and 'Abnormal plutei'. The ratio between the two different morphological groups is expressed as percentage respect to the entire number of embryos examined.

FIGURE 3.2: Pictures obtained by inverted microscope showing some examples of different types of malformations induced in Paracentrotus lividus plutei at 48 hours post fertilization (hpf) after incubation with the three polyunsaturated aldehydes (**B**, **C**, **D**, **E**, **F**, **G** and **H**) in comparison with the normal conformation (**A**) of the control. Embryos were fixed with 4% of paraformaldehyde (modified from Varrella et al.,2014).

FIGURE 3.3: Extrinsic apoptotic pathway: (**A**, **C**, **E** and **G**) Multialignment of aminoacid sequences AIFM1, RIPK4, TNFR16 and TNFR27 from *Homo sapiens*, *Strongylocentrotus purpuratus* and *Paracentrotus lividus*. (**B**, **D**, **F** and **H**) Complex intron-exon structure of the *P. lividus* genes involved in extrinsic apoptosis.

FIGURE 3.4: Phylogenetic tree showing the inferred evolutionary relationship among various members of the Receptor Interacting Serine/Threonine Kinase (RIPK) superfamily from *Homo sapiens*, *Strongylocentrotus purpuratus* and *Paracentrotus lividus*.

FIGURE 3.5: Phylogenetic analysis showing the inferred evolutionary relationship among various members of the Tumor Necrosis Factor Receptor (TNFR) superfamily from *Homo sapiens*, *Strongylocentrotus purpuratus* and *Paracentrotus lividus*.

FIGURE 3.6: Intrinsic apoptoc pathway: (**A**, **C** and **E**) Multialignment of aminoacid sequences of BAX, BCL2 and PARP from *Homo sapiens*, *Strongylocentrotus purpuratus* and *Paracentrotus lividus*. (**B**, **D** and **F**) Complex intron-exon structure of the *P. lividus* genes involved in intrinsic apoptosis.

FIGURE 3.7: Autophagy: (**A**, **C**, **E** and **G**) Multialignment of aminoacid sequences of BECN, PINK, ULK1 and ULK3 from *Homo sapiens*, *Strongylocentrotus purpuratus* and *Paracentrotus lividus*. (**B**, **D**, **F** and **H**) Complex intron-exon structure of the *P. lividus* genes involved in intrinsic apoptosis.

FIGURE 3.8: Phylogenetic tree that represents the evolutionary relationship among various members of the Unc-51 Like Autophagy Activating Kinase (ULK) superfamily from *Homo sapiens*, *Strongylocentrotus purpuratus* and *Paracentrotus lividus*.

FIGURE 3.9: Efficiency amplification was calculated for each primer pair, generating a standard curves with serial 10-fold dilutions of the calibrator's cDNA sample by using the cycle threshold (Ct) value versus the logarithm of each dilution factor and using the equation $E=10^{-1}/\text{slope}$.

FIGURE 3.10: Gene expression study by Real Time q-PCR of twelve genes involved in three different death cell signaling pathway in embryos incubated with increasing heptadienal concentrations (2 µM, 2.5 µM, 3 µM, 5.5 µM and 6 µM) and collected at a specific developmental stage of *P. lividus*: early blastula (5 hpf). (**A**) Gene expression levels of Aifm1, Ripk, Tnfr16, Tnfr27 and Nf*k*B (involved in extrinsic apoptosis). (**B)** Gene expression levels of Bax, Bcl2 and Parp (involved in intrinsic apoptosis). (**C**) Gene expression levels of Ulk1, Ulk3, Pink and Becn1 (involved in autophagy). Data are reported as a fold difference (mean ± SD), compared to control embryos in sea water without heptadienal. Fold differences greater than ±2 were considered to be significant.

FIGURE 3.11: Gene expression study by Real Time q-PCR of twelve genes involved in three different death cell signaling pathway in embryos incubated with increasing heptadienal concentrations (2 µM, 2.5 µM, 3 µM, 5.5 µM and 6 µM) and collected at a specific developmental stage of *P. lividus*: early prisma (21 hpf). (**A**) Gene expression levels of Aifm1, Ripk4, Tnfr16, Tnfr27 and Nf*k*B (involved in extrinsic apoptosis). (**B**) Gene expression levels of Bax, Bcl2 and Parp (involved in intrinsic apoptosis). (**C**) Gene expression levels of Ulk1, Ulk3, Pink and Becn1 (involved in autophagy). Data are reported as a fold difference (mean ± SD), compared to control embryos in sea water without heptadienal. Fold differences greater than ±2 were considered to be significant.

FIGURE 3.12: Gene expression study by Real Time q-PCR of twelve genes involved in three different death cell signaling pathway in embryos incubated with increasing heptadienal concentrations (2 µM, 2.5 µM, 3 µM, 5.5 µM and 6 µM) and collected at a specific developmental stage of *P. lividus*: pluteus stage (48 hpf). (**A**) Gene expression levels of Aifm1, Ripk, Tnfr16, Tnfr27 and Nf*k*B (involved in extrinsic apoptosis). (**B**) Gene expression levels of Bax, Bcl2 and Parp (involved in intrinsic apoptosis). (**C**) Gene expression levels of Ulk1, Ulk3, Pink and Becn1 (involved in autophagy). Data are reported as a fold difference (mean ± SD), compared to control embryos in sea water without heptadienal. Fold differences greater than ±2 were considered to be significant.

FIGURE 3.13: Gene expression study by Real-Time qPCR of thirteen genes involved in three different death cell signaling pathways in A549 cell line treated with 5 µM of heptadienal for 2 hours. (**A**) Gene expression levels of AIFM_1, RIPK_2, TRAIL_R1, TNF_R1, TNF_R2 and Nf*k*B (involved in extrinsic apoptosis). (**B**) Gene expression levels of BAX, BCL_2 and PARP (involved in intrinsic apoptosis). (**C**) Gene expression levels of ULK_1, ULK_3, PINK and BECN_1 (involved in autophagy). Data are reported as a fold difference (mean ± SD), compared to control A549 cells without heptadienal. Fold differences greater than ±2 were considered significant.

FIGURE 8.1: Chemical characterization of ethanol/water crude extract. (**A**) HPLC chromatogram of pigments from the ethanol/water extract of the green microalga *Tetraselmis suecica*. (**B**) Table describes peak identification, retention time, abbreviations and online spectral characteristics of the ethanol/water extract of the green microalga *Tetraselmis suecica*.

FIGURE 8.2: Chemical characterization of ethanol/water crude extract. (**A**) LC-PDA-ESI+MS/MS analysis of the carotenoid pool in the ethanol/water extract of *Tetraselmis suecica*. (**B**) Table describes for each peak retention time, maximum of absorbance (expressed in nm), ESI^+-MS (expressed in *m/z*), ESI^+-MS/MS (expressed in *m/z*) and relative names of the chemical components of the ethanol/water extract of the green microalga *Tetraselmis suecica*.

FIGURE 8.3: *In vitro* repairing activity of *Tetraselmis suecica* ethanol/water extract against H_2O_2 treatment. (**A**) Human lung adenocarcinoma cells (A549) treated with various concentrations of *T. suecica* extracts for 24 and 48 h. Cell viability was determined using the MTT assay and expressed as the percentage of control growing cells. (**B**) Cell viability of lung adenocarcinoma cells (A549) treated with various concentrations of H_2O_2 (0.3 mM, 3 mM, 30 mM and 300 mM) for 24 and 48 h . (**C**) Effect of extract on cell viability of A549 cells following exposure to H_2O_2 prior to extract treatment at 2 μg ml^{-1}, 5 μg ml^{-1}, 10 μg ml^{-1}, 25 μg ml^{-1}, 50 μg ml^{-1}, 100 μg ml^{-1}, 200 μg ml^{-1} and 400 μg ml^{-1}. Three independent assays were performed in triplicate; data are shown as mean ±S.D. Significant differences between treated groups were determined using Students-t test (*) and ANOVA followed by Dunnett's test (#). Crosshatched symbols denote significant differences between treatments and control (#$p<0.05$).

FIGURE 8.4: Histograms showing the results of gene expression analysis. **(A, B,** and **C)** Effect of *Tetraselmis suecica* ethanol/water extract at three different concentrations (100 μg ml^{-1}, 200 μg ml^{-1} and 400 μg ml^{-1}) on oxidative stress gene expression in H_2O_2-treated human lung adenocarcinoma cells (A549). A549 cells were pretreated with H_2O_2 (30 mM = 12 μg ml^{-1}) for 1 h prior to extract treatments (100, 200 and 400 μg ml^{-1}) and harvested 2 h later. **(D)** Negative control for the evaluation of the effect of *Tetraselmis suecica* ethanol/water extract (without any injury pre-treatment) at three different concentrations (100, 200 and 400 μg ml^{-1}) on oxidative stress gene expression in human lung adenocarcinoma cells (A549). Three independent assays were performed in triplicate and the data are expressed as mean ±S.D. Expression values greater or lower than a two-fold difference with respect to the controls were considered significant.

FIGURE 8.5: The effect of *Tetraselmis suecica* ethanol/water extract on oxidative stress protein expression in H_2O_2-treated human lung adenocarcinoma cells (A549). (**A**, **B** and **C**) Three independent assays were performed in triplicate and the data shown are mean ±S.D. The values above the blots represent the densitometric analysis of the photographic sheets measuring the variation in protein expression. The values of the bands are normalized versus actin and represented as ratio between the expression of single protein and actin. Asterisks denote significant differences compared to controls (*$p\leq0.05$ and **$p<0.005$).

FIGURE 8.6: The effect of ethanol/water extract from *Tetraselmis suecica* on prostaglandin PGE_2 serum-release induced by H_2O_2 -treatment in human lung adenocarcinoma cells (A549). (**A**) Average PGE_2 concentration (pg μl^{-1}) determined by ELISA in culture medium of cells treated with 100, 200 and 400 μg ml^{-1} of the extract for 24 h. (**B**) Average of the PGE_2 concentration (pg μl^{-1}) determined by ELISA in culture medium of cells treated with 100, 200 and 400 μg ml^{-1} of extract for 24 h after pretreatment with 30 mM (= 12 μg ml^{-1}) of H_2O_2 for 1 h. Asterisks denote significant differences compared to controls (*$p\leq0.05$ and **$p<0.005$) and determined using Students-t test.

FIGURE 8.7: Response of EpiDerm^{TM} tissue cultures after topical application of 30 mM (= 12 µg ml^{-1}) H_2O_2 for 1 h prior to *Tetraselmis suecica* ethanol/water extract treatment (200 µg ml^{-1}) showing the repairing effect of the extract after H_2O_2 treatment. Three independent assays were performed in triplicate; data are shown as mean ±S.D. Significant differences between treated groups were determined using Students-t test (*p≤0.05) and ANOVA. NC = not treated. Ts 200 µg = 200 µg *T. suecica* extract; H_2O_2 + Ts 200 µg = epidermal tissue pretreated with H_2O_2 for 1 h and recovered with extract.

FIGURE 8.8: Effect of an *n*-butanol extract of the dinoflagellate *Alexandrium andersoni* on lung adenocarcinoma (A549) and colorectal carcinoma (HT-29) cancer cell lines. Percentage of viable cells for A549 (**A**) and HT-29 (**B**) were calculated with the MTT viability assay. Values are reported as mean ± S.D. compared to controls (100% viability). Concentrations tested were 10, 50, 100, 200 and 400 µg ml^{-1} for 24 and 48 h. Asterisks denote statistically significant differences with a p value ≤0.0001.

FIGURE 8.9: Histograms showing the effects of *Alexandrium andersoni n*-butanol extract on the expression levels of target genes in lung adenocarcinoma A549 (**A)** and in colorectal adenocarcinoma HT-29 (**B**) cell lines. Gene expression analysis was conducted after 2 h of treatment with 400 µg ml^{-1} of extract; error bars represent ±S.D.

FIGURE 8.10: Histograms showing the effects of *Alexandrium andersoni n*-butanol extract on the expression levels of target proteins. (**A**) TNFR1, (**B**) RIP-k1, (**C**) DR3 and (**D**) control (actin) in lung adenocarcinoma A549 cells. Immunoblot analysis shows that the extract induced TNF signaling after 24 h. Asterisk denotes significant increase in protein levels. **p≤0.05 versus control; error bars represent ±SD.

FIGURE 8.11: (**A**) Flow cytometric analysis of DNA content in A549 cells exposed to *Alexandrium andersoni n*-butanol extract for 8 h at 200 µg ml^{-1} concentration (empty red line) and untreated control cells (full blue line). (**B**) Distribution of A549 cells in different phases of the cell cycle after 8 h of exposure to 100 and 200 µg ml^{-1} of *A. andersonii* extract, respectively. Percentage of cells in each phase was obtained with the ModFit LT Software. (**C**) Percentage of A549 cells in each cell cycle phase after 2, 4, 6 and 8 h treatment with *Alexandrium andersoni n*-butanol extract at 100 and 200 µg ml^{-1}concentrations.

FIGURE 8.12: Effect of SPE fractions of the dinoflagellate *Alexandrium andersoni* on lung adenocarcinoma (A549) and colorectal carcinoma (HT-29) cancer cell lines, and lung fibroblast (WI38) and brunch-lung epithelial (Beas-2B) normal cell lines. Percentage of viable cells for A549 (**A**), HT-29 (**B**) and control WI38 (**C**) and BEAS-2B (**D**) cell lines using the MTT viability assay. Same experiments performed on tumor cell lines in the presence of caspase inhibitor (**E**, **F**). Values are reported as mean ± S.D. compared to controls (100% viability). Concentrations tested were 1, 10 and 100 µg ml^{-1} for 48 h.

FIGURE 8.13: Histograms showing the effects of *Alexandrium andersoni* SPE fractions B and D on the expression levels of target genes in lung adenocarcinoma A549 (**A)** and in colorectal adenocarcinoma HT-29 (**B**) cell lines. Gene expression analysis was conducted after 2 h of treatment with 1 μg ml^{-1} of the two fractions; error bars represent ±S.D.

FIGURE 9.1: Schematic representation of the cellular response activated by H_2O_2 (A) and repairing effect induced by Tetraselmis suecica extract (B) after H_2O_2 pretreatment.

FIGURE 9.2: Schematic representation of pathways induced by *Alexandrium andersoni n*-butanol extract in lung adenocarcinoma A549 (A) and colorectal adenocarcinoma HT-29 (B) cell lines.

LIST OF TABLES

ABSTRACT

(English version)

The marine environment covers nearly the 70% of the earth surface. Furthermore, oceans contain a very rich and still unexplored biodiversity. Only the 10% of the total marine organisms living in the oceans are now identified and studied for various applications. Thus, the oceans represents one of most valuable natural resource. For this reason, the exploration of the marine ecosystem constitutes a European priority, within research strategies, in parallel with the creation of conservation and protection programs for keeping the ocean healthy for future generations, through an eco-friendly exploitation of marine resources. Starting from an ecological and holistic approach, all marine biodiversity will provide a sea of resources for biotechnological applications. In particular, marine organisms have several potential applications in the biotechnology field, for the discovery of new pharmaceuticals, nutraceuticals, cosmetics, food and feed, aquaculture methods and technologies, biomaterials, bioenergy, biomonitoring and bioremediation.

In this experimental study, I addressed two aspects of the use of marine resources for biotechnological applications: a) the development of marine model organisms as useful molecular tool for *in vitro* eco-toxicological studies and for *in situ* assessment of ocean health; b) the discovery of new marine natural products from marine microalgae for biomedical applications.

The sea urchin *Paracentrotus lividus* was studied as marine model organism in order to develop new tools to evaluate the effect of stressors in the marine environment. Using a bioinformatic approach, twelve genes involved in some of the main cell death pathways were identified from sea urchin *P. lividus* genome: Pl_Aifm1, Pl_Ripk, Pl_Tnfr16, Pl_Tnfr19/27, Pl_Bax, Pl_Bcl2, Pl_Parp, Pl_Becn, Pl_Pink, Pl_Ulk1/2 and Pl_Ulk3. Embryos treated with heptadienal, a bioactive compound from marine diatoms, activated programmed caspase-independent cell death (extrinsic apoptosis) with simultaneous involvement of selective autophagic mechanism (called mitophagy). These results are in accordance with molecular analysis obtained for human tumoral cell line treated with the same marine compound. In fact, A549 cells activated, after treatment with heptadienal, extrinsic apoptosis with the simultaneous trigger of autophagic pathway.

The study of the potential of marine microalgae for biotechnological applications focused on antiproliferative and antioxidant activities. In detail, the microalga *Alexandrium andersoni* showed anticancer effect against two tumour cell lines; the crude extract of *Tetraselmis suecica* posseshowed a strong scavenging and repairing effect after oxidative damage.

Results obtained demonstrated, from one hand, that the sea urchin *P. lividus* can represent a suitable model organism for the assessment of induction of cell death mechanisms by chemical extracts or pure compounds, but also as molecular tool for *in situ* studies of chemical contaminants or anthropogenic stressful factors that can interfere with the marine ecosystem. On the other hand, results obtained with two marine microalgae (*A. andersoni* and *T. suecica*) confirmed the enormous potential of marine microalgae for the identification of new natural products with possible applications for pharmaceutical and cosmeceutical industries.

ABSTRACT
(Italian version)

La superficie terrestre è ricoperta per quasi il 70% dall'ecosistema marino. Inoltre, gli oceani ospitano una ricca ed ancora poco esplorata biodiversità. Attualmente, solo il 10% degli organismi che vivono nell'ambiente marino sono stati identificati e studiati per varie applicazioni. Per queste ragioni, gli oceani rappresentano una tra le più preziose risorse naturali. La profonda esplorazione dei vari ecosistemi marini costituisce attualmente una priorità per l'Unione Europea, nel contesto delle nuove strategie di ricerca. L'obbiettivo principale riguarda la creazione di programmi di conservazione e protezione ambientale, utili a salvaguardare la salute dei nostri mari per le future generazioni, ma al contempo stabilire dei processi per un uso ecosostenibile delle risorse marine. Partendo da un approccio ecologico ed olistico, la biodiversità marina può offrire un mare di risorse per l'uomo e per le sue applicazioni biotecnologiche. In particolare, gli organismi marini hanno già dimostrato o posseggono enorme potenziale per applicazioni di tipo biotecnologico, nel settore della farmacologica, nutraceutica, cosmeceutica, cibo funzionale, nuove tecnologie per l'acquacoltura, biomateriali, bioenergia, biomonitoraggio e biorimediazione ambientale. Questo studio sperimentale prende in considerazione due aspetti fondamentali dell'uso di risorse marine per applicazioni biotecnologiche: a) lo sviluppo e la caratterizzazione di un organismo modello marino come strumento molecolare laboratoriale per studi eco-tossicologici *in vitro* e per monitoraggio *in situ* dello stato di salute degli ambienti marini costieri; b) l'identificazione di nuovi composti naturali con potenziali applicazioni biomediche, a partire dalle microalghe marine.

Un approccio bioinformatico è stato usato per identificare nel genoma del riccio di mare *Paracentrotus lividus* le sequenze codificanti per alcuni fattori chiave coinvolti nei principali pathway di morte cellulare programmata: apoptosi estrinseca, apoptosi intrinseca ed autofagia (compreso un meccanismo autofagico specifico, chiamato mitofagia). I geni identificati sono: Pl_Aifm1, Pl_Ripk, Pl_Tnfr16, Pl_Tnfr19/27, Pl_Bax, Pl_Bcl2, Pl_Parp, Pl_Becn, Pl_Pink, Pl_Ulk1/2 and Pl_Ulk3. Gli embrioni del riccio di mare *P. lividus* sono stati trattati con diverse concentrazioni di 2-*trans*,4-*trans* eptadienale e successivamente è stato analizzato l'effetto a livello molecolare. In particolare, l'eptadienale attiva una morte cellulare programmata (senza il coinvolgimento delle caspasi) ed un meccanismo mitofagico, i quali operano in sinergia. Questi risultati molecolari sono sovrapponibili con il pattern di attivazione genica ottenuto in seguito al trattamento di una linea cellulare umana con il medesimo composto puro. Infatti, la linea cellulare A549 attiva, in seguito al trattamento con eptadienale, un meccanismo di apoptosi estrinseca con la simultanea induzione della via autofagica.

Il lavoro sperimentale si è anche concentrato sullo studio del potenziale biotecnologico delle microalghe marine, quali fonti di nuovi composti naturali. In dettaglio, il dinoflagellato *Alexandrium andersoni* ha mostrato un potente effetto antiproliferativo su due linee tumorali umane, mentre un estratto crudo ottenuto dalla microalga *Tetraselmis suecica* possiede una forte attività di radical-scavenging ed è responsabile dell'attivazione dei meccanismi di riparo dal danno ossidativo. I risultati ottenuti, descritti in questo lavoro di tesi, dimostrano da un lato che il riccio di mare *P. lividus* può rappresentare un valido organismo modello per la valutazione dei meccanismi molecolari di morte indotti da estratti chimici o molecole pure, ed inoltre può essere utilizzato come tool molecolare per studi *in situ* atti alla valutazione dell'impatto sugli ecosistemi marini di contaminanti chimici o di

fattori antropocentrici in grado di interferire con i processi biologici ed ecologici dei nostri mari. Dall'altro lato, i risultati ottenuti dai due microorganismi marini (*A. andersoni* e *T. suecica*) rivelano l'enorme potenziale delle microalghe marine nell'identificazione di nuovi composti naturali dalla maggiore efficacia, con applicazioni per le industrie farmaceutiche e cosmeceutiche.

GENERAL INTRODUCTION

I. Resources from the sea for a sea of resources

The marine environment covers the major part of the earth's surface (71%). Europe has a 70.000 km coastline along two oceans and four seas: the Atlantic and Arctic Oceans, the Baltic, the North Sea, the Mediterranean, and the Black Sea. European population lives for about 40% in maritime regions. Oceans contain a very rich and still unexplored biodiversity. Only the 10% of the total marine organisms (including deep-sea organisms) living in the oceans are now identified and studied for various applications. The ocean is one of Earth's most valuable natural resource. It provides food in the form of fish and shellfish, moving a great portion of European economy each year. It serves for transportation, both travel and shipping. It provides a treasured source of recreation for humans. It is mined for minerals (salt, sand, gravel, and some manganese, copper, nickel, iron, and cobalt can be found in the deep sea) and drilled for crude oil.

The ocean plays a critical role in removing carbon from the atmosphere and providing oxygen, covering an essential role in regulating Earth's climate. The ocean is an increasingly important source of organisms with enormous biomedical potential for fighting diseases. These are just a few examples of the importance of the ocean for human wellbeing. The exploration of the marine ecosystems should constitute an essential research program to allow at each nation to activate conservation and protection strategies for keeping the ocean healthy for future generations. European States push for holistic and integrated approaches to sustainable development that will guide humanity to live in harmony with nature and lead to efforts to restore the health and integrity of the Earth's ecosystem.

In this context, a relevant issue is represented by the conservation and sustainable use of the oceans and seas and of their resources for sustainable development, including through their contributions to poverty eradication, sustained economic growth, food security and creation of sustainable livelihoods. Starting from an ecological and holistic approach all marine biodiversity will provide a sea of resources for biotechnological applications. The study of biology and physiology of unexplored marine organisms could be associated with a potential exploitation in marine biotechnology field, for the discovery of new pharmaceuticals, nutraceuticals, cosmetics, food and feed, aquaculture methods and technologies, biomaterials, bioenergy and so on. A goal of the VII Framework Programme for Research and Technological Development in marine biotechnology ERA-NET- MBT (European Research Area - NET - Marine Biotech) has been to support the development of marine biotechnology research and innovation. The Blue Growth strategy incorporates European marine biotechnology in the bio-economic strategy for Europe, recognizing a dominant role in the impact and socio-economic challenges faced by Europe. ERA - NET - MBT has set guidelines for marine biotechnology so that through the sustainable use of marine biological resources, there is the creation of new markets, thereby generating, new revenues and boosting employment. In this study I tried to address two aspects of the use of marine biological resources for biotechnological applications:

1. Development of marine model organisms as useful tool for eco-toxicological studies and for the assessment of ocean health;

2. Discovery of new marine natural products for biomedical applications.

II. European strategies and Marine Biotechnology

Seas have always represented for humans a fundamental source of products and services, becoming a predominant factor for the increase of population density around coastal areas. Ocean ecosystems influence consistently the good status of human populations, through the salubrious air along coasts, high quality of food offered and enhance psychophysical wellness (figure I). On the other hand, there are several factors acting as anthropic pressure on marine environment such as industrial productions, maritime transport, agriculture and organic wastewater. Changes and degradation of marine environments produce direct but also indirect effects on human health and wellbeing; it is still not well characterized and described how human pressure in a specific place affect other regions of the marine ecosystem, with a long-term repercussions. The evaluation and relative management of the impacts derived from this pressure on both human health and marine environment itself have extensively been studied, but as two separate phenomena so far.

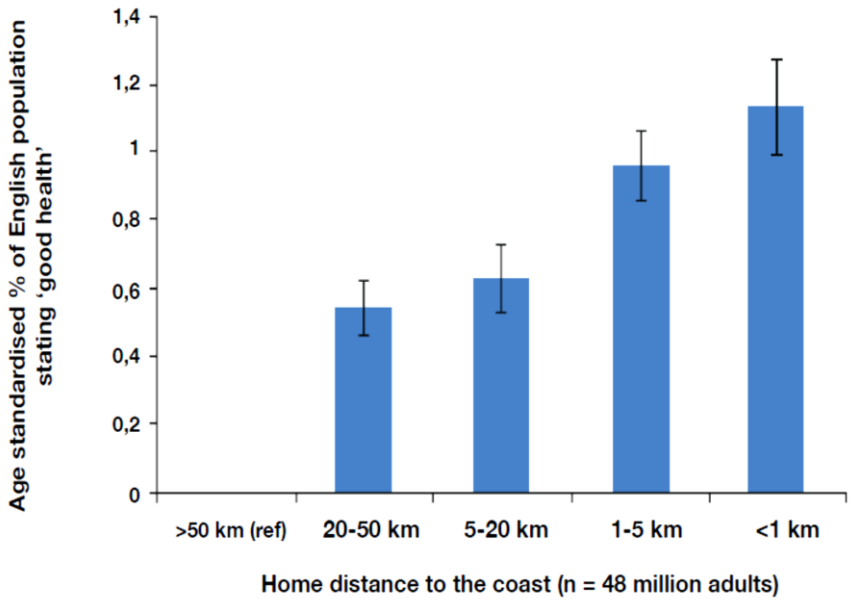

FIGURE I: English census data on the direct relationship between coastal proximity and stated health status (adapted from Wheeler et al., 2012).

The scientific community has recognizing the strong need for a more holistic approach to study and understanding the complex relationship between ocean environments on one hand, and human health and well-being on the other.

An interdisciplinary approach could be used to study the complexity of this effects and interactions by the formation of complex network across a wide range of scientific disciplines, within

medicine, public health and natural, social and economic sciences. The complex and mutual interactions between human health and marine environment requires a systems approach addressing all levels of organization from bottom (at gene level) to ecosystems.

In this direction, USA has already invested economic resources in the last decade, creating a multidisciplinary oceans and human health research programs. This program include the establishment of seven Centers for Oceans and Human Health (COHH) and a complementary National Oceanic and Atmospheric Administration (NOAA) Oceans and Human Health Initiative (OHHI) to conduct, coordinate and communicate research in this new integrative field.

Europe currently do not provide a similar oceans and human health research framework and the European Marine Board has recently published paper as a first step to raise priorities to encourage the development of a coherent transnational oceans and human health research effort in Europe (Position Paper 19, European Marine Board, 2013). This position paper identify the most important research needs and priorities to study ocean heath, that is intrinsically interconnected and impacted by humans and their well-being. To manage this relationship, European research need an efficient polity framework, linking maritime and public health policies.

Hence, the European research effort explained in this paper is not just an attempt to create new interesting scientific challenges, but could represent the starting point to ensure an improvement of public health and good environmental status of European seas, which are mutually linked.

Marine biotechnology is widely recognized as an outstanding research area that can contribute significantly to the well-being of the society and the European bio-economy. The definition of biotechnology is: "The application of science and technology to living organisms, as well as parts, products and models thereof, to alter living or non-living materials for the production of knowledge, goods and services" (www.oecd.org). In the case of marine biotechnology, the living organisms are derived from marine sources.

Marine biotechnology (called also blue biotechnology) is representing a relative new research field, which is creating new opportunities to explore and successively exploit marine resources, with sustainable development and approach. This scientific area raise great interest by European policies, able to build and contribute to an eco-sustainable and highly efficient economy and society. The strong point of marine biotechnology is represented by the high biodiversity of marine environments. So huge potential is still poorly exploited and marine resources could play a central role for many industrial activities and for bioprocesses used for the maintenance of ecosystem integrity. This will lead to new application in fields such as drug discovery, novel functional foods and food ingredients, bio-remediation, biomaterials, aquaculture, environmental biomonitoring, diagnostics, production processes, bioenergy etc. European policies focus attention and conspicuous part of its economic effort in the area of marine biotechnology in order to find competitive niches. Sufficient attention is given to sustainable exploitation of the uniqueness of Europe's marine biosphere and the understanding of its biodiversity and natural heritages.

AIM OF THE THESIS

The purpose of the experimental activities was the identification of new marine resources for biotechnological applications. First part (Section 1) of the thesis describes the attempt to redesign a new role for an "old" marine model organism, the sea urchin *Paracentrotus lividus*. This work aimed to develop useful molecular tools for the *in vitro* eco-toxicological or antiproliferative assays, with possible application for *in situ* assessment of marine environment health.
With a bioinformatic approach twelve key genes involved in some of the principal death cell signaling pathways were annotated in *P. lividus* genome, using orthologous relationship with well-studied *Homo sapiens* cell-death genes. Sea urchin embryos and human cell lines were treated with the same marine pure compound (heptadienal), in order to characterize the molecular pathways activated after the treatment and to compare the response between two such evolutionary distant organisms. This will help in understanding the degree of conservation of relevant pathways involved in the response of cell and organisms to stress induced by toxicants.

Second part (Section 2) of the thesis focuses on the discovery and characterization of new natural products from marine microalgae using different approaches. In particular, *Alexandrium andersoni* was studied for the potential antiproliferative activity of this dinoflagellate on two very resistant cancer cell lines, lung adenocarcinoma (A549) and colorectal carcinoma (HT-29). Absence of *in vitro* cytotoxicity on normal cell lines was also evaluated to verify the specificity of the anti-proliferative activity against tumour cell lines. Using a molecular biology approach, extracts and SPE fractions of this species were used to investigate the activation of different cell death signaling pathways in the two tumor cell lines tested. Cell cycle analysis was also carried out to better characterize the phase in which the block of proliferation occurs.

Tetraselmis suecica was the object of a study for the identification and characterization of compounds with antioxidant property and activation of repairing mechanisms following oxidative damage. To this end, *in vitro* human cell line and *ex vivo* human skin model were used. Viability assays were performed for the assessment of the desirable recovery effect of the ethanol/water crude extract of *T. suecica* after decrease of cell and tissue viability induced by well know oxidizing agent (H_2O_2). The interesting effect detected, was further analysed at the gene level in order to demonstrate the involvement of anti-inflammatory and repairing key molecular factors, and results corroborated at biochemical level.

This thesis intend to strongly demonstrate the wide range of opportunity that could offer the marine environment. The diversified marine world can take advantage from human research activities addressed to the identification of new biomonitoring tools and innovative techniques for the conservation, protection and bioremediation of the seas, but also humans can identify and exploit new natural marine resource for an ecosustainable concept of economy for pharmacological industries and healthcare sector.

SECTION 1

The marine model organism *Paracentrotus lividus*: an established marine model organism for new biotechnological applications

CHAPTER 1.

Introduction

1.1 The sea urchin model *Paracentrotus lividus*: an overview

Sea urchin represented for more than 150 years an ideal marine model system for a wide range of experimental purposes, trying to answer to fundamental biological questions. For well over a century, a huge number of seminal discoveries have provided insights that dramatically influenced several fields of biology. Their relative abundance along coasts, the large size of adults, clarity and large size of their eggs (and relative embryos) and the simplicity with which experiments can be set up on gametes and embryos and the ease of perturbation of embryo development made the sea urchins a favourite target for early works in many investigations. For these reasons, sea urchins have been one of the most popular marine organisms utilised for studies in a wide range of scientific disciplines, such as reproductive biology (Vacquier, Swanson, and Hellberg 1995), embryology (Davidson, Cameron, and Ransick 1998; Lee et al. 1999), toxicology (Dinnel et al. 1989), gene regulation (Davidson et al. 2002), as well as evolutionary biology (Peterson, Cameron, and Davidson 2000).

The adult body is characterized by pentamerous symmetry, having a central plate with five regions arranged around it. The typical size of adult animals ranging from 6 to 12 cm, but exist also larger sea urchin species that can reach up to 36 cm (for some Indo-Pacific sea urchin species). The entire body can be divided equatorially into upper part called aboral hemisphere and bottom part called oral hemisphere (figure 1.1).

FIGURE 1.1: Sea urchin *Paracentrotus lividus* in the marine environment. (modified from www.marinespecies.org)

A ring with 10 plates characterizes aboral hemisphere, which contains periprocto, the anal region of the animal. The madreporite (or madreporic) plate constitutes another important structure present in aboral hemisphere, having the role of connection between the liquid of the aquifer system and external environment. The madreporite plate is connected to the ring canal, which in turn is joined with the radial canals. This apparatus allow the sea urchin movements, using sea water brought from the external environment and canalized into the tube feet.

The oral hemisphere is the side facing the substrate, containing a mouth in the middle of this area. The mouth can be easily identify by the typical presence of the apparatus used to chew, composed by 5 teeth, operated by a complex system of plates and muscles called Aristotle's lantern; this structure is surrounded by peristomal membrane (a membranous layer).

Respiration occurs through the ambulacral pedicels, which allow gas exchange and the entrance of oxygen into the boby. Most animals possess five pairs of external gills, distributed all around the mouth. When the animal is low on oxygen, fluid can be pumped through the gills interiors, using muscles associated with the lantern. Tube feet could also function as additional respiratory organs, creating secondary sites of gas exchange.

At the end of sea urchin spines there are the pedicellariae, with different morphologies and relative different functions. Pedicellaria can be with suction-cup at the end, used for locomotion and for holding stones and snails through which some species of sea urchins use to cover their body, and pedicellaria with a small hollow spindle at the end used as defense against enemies, by injection of toxic poison (some examples are *Diatema* sp., and *Echinotrix* sp.).

Sea urchins are able to rapidly regenerate all these external appendages described (pedicellariae, tube foot and spines), as well as the wounds or lesions of the shell, by a regeneration process of the skeleton.

The reproductive system is organized in five separate gonads connected together by mesenteric filaments at the inner surface of the inter-ambulacral areas. When gonads are mature, they appear orange and swollen. Once mature, gonads extend from the aboral hemisphere, where they can communicate with the external marine environment, almost to the lantern of Aristotele (Lawrence, 2013).

Among several species of sea urchins with applications in science as model organisms, *Paracentrotus lividus* have gained a dominant presence in many European research institutes. Geographically, it is largely distributed throughout the Mediterranean Sea and in the Atlantic northeast, from Scotland and Ireland to southern Morocco and Canary islands, including the Azores. This species of sea urchin is particularly common in coastal habitat where winter water temperatures range from 10 to 15°C, and summer water temperatures range from 18 to 25°C. In fact, its temperature limits correspond to around 8°C winter and 28°C summer isotherms, respectively. A seasonal reproductive annual cycle that varies among species characterize the adult animals. Depending on the variation of specific temperatures every years, the reproductive period of *P. lividus* could be considered from December to May.

P. lividus belong to the Parachinidae, a family of the phylum Echinodermata (table 1.1). Due to their position in the phylogenetic tree, Echinoderms are considered a phylum in the direct evolutionary line leading to the vertebrates. In fact, it is important to remark that sea urchins, Hemichordates and other echinoderms, occupy a key phylogenetic position as the only non-cordate deuterostomes. For this reason, sea urchin has been broadly utilized to better describe molecular, embryonal and morphological repercussion of many stress factors able to induce diseases and disorders in marine environment and humans.

TABLE 1.1: Scientific classification of the sea urchin *Paracentrotus lividus*

Kingdom	Animalia
Phylum	Echinodermata
Subphylum	Echinozea
Class	Echinoidea
Subclass	Euechinoidea
Infraclass	Carinacea
Superorder	Echinacea
Order	Camarodonta
Infraorder	Echinidea
Family	Parechinidae
Genus	*Paracentrotus*
Species	*Paracentrotus lividus*

As deuterostomes, sea urchins have developed the anus from the blastopore and the mouth origin from the opposite cavity. A comparison between two so different organisms as humans and sea urchins could seems, at first glance, awkward. The sea urchin body has radial symmetry and a globose form with no proof of a head, whereas humans are bilaterally symmetrical with a complex head containing sensory structures. However, sea urchins lie on the same major branch of the tree of life (the deuterostomes) to which humans belong. Even though the sea urchin form differs radically from that of vertebrates, they share many of the same gene families. Echinoderms diverged very early from the major lineage of the deuterostomes; for this reason their genomes reflect the basic qualities

of this lineage and inform to a deep reach of time the evolutionary changes leading to the human genome.

P. lividus is typically a subtidal species, living from the mean water mark down to 70-80 meters (Harmelin et al. 1980; Crook et al., 2000); these animals live in contact with the seabed or otherwise fixed to a solid substrates. It is an herbivore with a variable impact on surrounding environment that might depends by population density in that specific area. Likely to other rock burrowing species, *P. lividus* can switch from mobile (grazing) to sedentary (drift-feeding) feeding when in burrows (Granville, 2008).

P. lividus, similarly to many sea urchin species, have a globular and regular shapes and all body is covered with robust spines. This external defensive structure is formed by calcium carbonate mixed with organic matter; the length of spines differs according to the genus (Smith 1999; Su et al., 2000).

The developmental process of sea urchins is characteristic of many marine invertebrates. Sea urchins are gonochoristic; individual adult animals aggregate in marine environment before spawning and then, after appropriate stimulations, they release eggs and sperm into the surround water column for an external fertilization.

The sea urchin eggs are typically spherical and very large (with a diameter of about 0.1 mm) and non-motile, containing a small amount of yolk. The eggs are internally homogeneous, containing uniformly distributed yolk granules and other intracellular organelles. The external region of the ovum cytoplasm, referred to as the cortex, includes numerous cortical granules underlying the egg plasma membrane, or oolema. The sea urchin eggs include two egg envelopes. The vitelline envelope is the primary egg envelope (an extended glycocalyx) and it is located just outside the oolema. The secondary egg envelope, the jelly coat, is a thicker coat around the ovum. It consists of several glycoprotein components, some of which have important roles in the pre-fusion fertilization processes. Once eggs are in contact with external sea water, jelly coat undergoes a swelling phenomenon.

Sea urchin sperms are very small gametes, with a head and a tail. The head appears ovoid and contains a pair of centrioles, the acrosome and the nucleus. The acrosome plays several important roles in fertilization, providing hydrolytic enzymes for penetration of the egg envelopes and for gamete fusion. The nucleus contains highly condensed chromosomes. The tail contains mitochondria and microtubules, essential for the movement. Under concentrated conditions (inside the adult animal), sea urchin sperms are immobile, probably due to the high carbon dioxide concentration. When dispersed in sea water (in diluted conditions), sperms become extremely motile. Once sperms are activated, their ability to participate in fertilization is rapidly lost after few minutes.

Fertilization, the union of a male and female gamete producing a zygote, consists of two fusion events. The first event is the gamete fusion, that consists in the fusion of the sperm and egg plasma membranes. The second event is represented by the pronuclear fusion, that is the fusion of the male and female haploid pronuclei. Gamete fusion results in the activation of the eggs. As a result, the metabolically quiescent eggs are stimulated to organise its developmental blueprint. Pronuclear fusion restores diploid condition and produces a genetically unique entity.

When sperms contact eggs they become bound to the jelly coat. This sperm-egg binding represent the first step and it is due to the interaction of fertilizin, one of the components of the egg jelly, and antifertilizin, associated with the sperm plasma membrane. The first two processes, activation of the sperm and sperm egg binding, are easily observed with light microscope. Following sperm egg binding, the acrosome reaction occurs; hydrolytic enzymes are released allowing the sperm

to penetrate the jelly coat and make contact with the vitelline envelope. At this point the first fusion event of fertilization, plasma-membrane fusion or gamete fusion, takes place.

Soon after the fusion process of the gametes, the creation of the fertilization envelope and the entrance of the sperm head into the ovum cytoplasm occur as simultaneous event. Moreover, the cortical granules exocytose and liberate their contents. This secretion causes a characteristic wrinkling of the egg surface (figure 1.2) and allow to the vitelline envelope to be lifted away from the oolema. The vitelline envelope and some of the cortical granule contents join and form the fertilization envelope. The fertilization envelope has an important role serving as barrier blocking the polyspermy process. The formation of the fertilization envelope is easy to observe in many sea urchins species by microscope, since this envelope is elevated a considerable distance from the egg surface. After gamete fusion, the second fusion event of fertilization occurs within 30 to 45 minutes and consists in the pronuclear fusion.

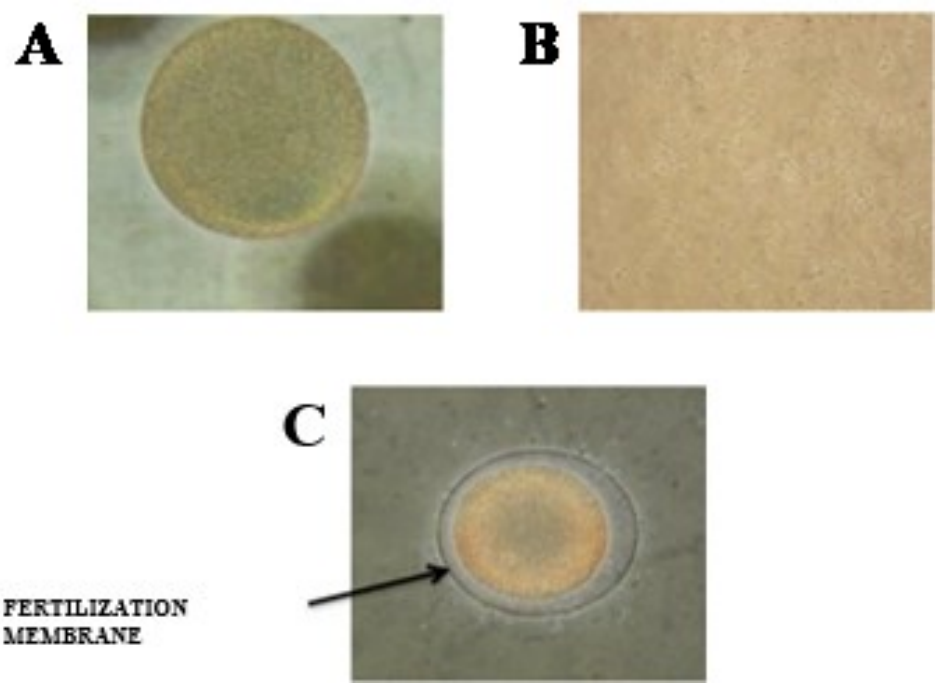

FIGURE 1.2: Pictures taken with inverted microscope. (**A**) Mature egg of the sea urchin *Paracentrotus lividus*. (**B**) Motile sperms of the sea urchin *Paracentrotus lividus*. (**C**) Egg of the sea urchin *Paracentrotus lividus* 4 minutes after fertilization event.

During the following cleavage processes, the single-celled zygote is converted into a multicellular embryo through rapid and repeated mitotic cell divisions. During this phase of development, there is no growth in term of size of the embryo. As the single cell is divided into many cells, the ratio of cytoplasmatic to nuclear volume of the blastomeres is increased, allowing for more effective nuclear-cytoplasmic interactions. In addition, the cytoplasmic areas containing specific developmental information are segregated into different cells of the embryo. This segregation of developmental potential is a fundamental finely regulated process for later cell differentiation. Cleavage of sea urchin embryos is radial holoblastic, since the cleavage furrow cuts through the entire dividing cell. Moreover, the cleavage occurs radial, the cleaving embryo is radially symmetrical, and with one exception equal, since the cells produced at each cytokinesis are equal in term of size.

The two-cell stage is the first cleavage event and (figure 1.3) occurs 60 to 90 minutes after gamete fusion, depending on the sea urchin species and on the experimental conditions. The plane of the cleavage furrow is meridional or longitudinal, passing along the animal-vegetal pole axis. The second cleavage is meridional and produces the four-cell stage (figure 1.3); the first and the second mitotic division are perpendicular to each other. The third cleavage is equatorial or horizontal, cut perpendicularly across the polar axis, dividing animal and vegetal hemisphere, and result in the eight-cell stage (figure 1.3).

However, the fourth mitotic division is completely different respect to the previous three. The eight cells previously formed become sixtheen blastomeres, with two meridional divisions. The animal half is represented by eight cells, with the same volume, called mesomeres. The vegetal hemisphere undergoes an unequal equatorial cleavage, producing four larger cells, called macromeres, and four smaller cells, called micromeres (figure 1.3). Soon after the 16-cell embryo cleaves, the eight mesomeres divide to create two animal tiers, "an_1" and "an_2", one staggered above the other. The macromeres go through a meridional division, forming a tier of eight cells below an_2. The micromeres also divide, albeit somewhat later, producing a small cluster below the larger tier. All the cleavage furrows of the sixth division are on equatorial plane. The seventh division event produces the 128-cell stage and occurs on meridional plane, bringing the embryo to the blastula stage.

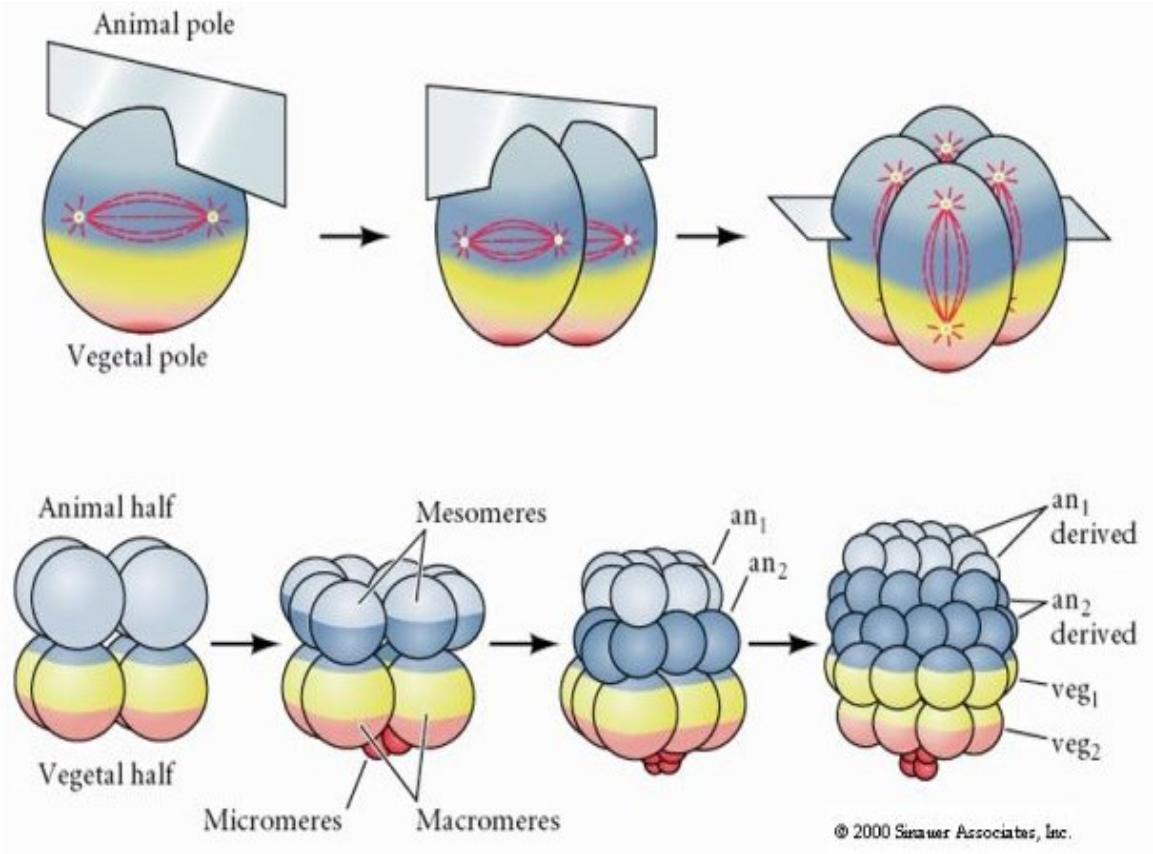

FIGURE 1.3: Cleavage in the sea urchin. Planes of cleavage in the first three divisions and the formation of tiers of cells in divisions 4–7. From: The Early Development of Sea Urchins. (modified from 'Developmental Biology'. 6th edition. Gilbert SF. Sunderland, MA; 2000)

The blastula stage is characterized by cells forming a sphere surrounding a central cavity fluid filled, called blastocoel. Starting from this stage, all cells have same size, rate of cell division declines and all are in contact on the inside with the proteinaceous fluid of the blastocoel and with the lyaline layer on the outside (figure 1.4).

Approximately six to seven hours after fertilization, the sea urchin embryo enters the blastula stage. The blastomeres develop cilia on their outer surface. As a result of the beating of these cilia, the embryo will rotate within the fertilization envelope. Approximately ten to twelve hours after fertilization, the mid-blastula is composed of about 600 cells and hatches out of the fertilization envelope. The hatching process is facilitated by the blastula releases of a "hatching enzyme", which is able to weaken and dissolve the membrane sufficiently for the blastula to break through. A small portion of long cilia, the apical tuft, develops at the animal pole of the blastula. In the late blastula stage the embryo becomes thicker at the vegetal pole, forming the vegetal plate.

Gastrulation begins when the primary mesenchyme cells, which are derived from the micromeres and located in the approximate center of the vegetal plate region, migrate as individual

cells into the blastocoel. This cell movement is called ingression. During gastrulation, extensive cellular rearrangements occurs, usually at morphogenetic level, converting the spherical and hollow blastula into a multi-layered gastrula. These deep rearrangements are due to changes in cell shape and in some cases changes in cell affinity, and are responsible of the creation of the three germ layers: ectoderm, mesoderm, and endoderm.

Following the ingression process, cells of the vegetal plate region invaginate, forming a depression called blastopore. As invagination of the vegetal plate region continues a blind-ended tube, the archenteron, is formed. The elongation of archenteron continues, due to continued cell movement from the surface of the embryo through the blastopore. The tip of the archenteron makes contact with the ectoderm opposite the blastopore. The gastrula stage (figure 1.4) and specific invagination of the vegetal plate region occur 20 to 24 hours after fertilization (the early process of gastrulation start 12 hours post fertilization). Approximately six hours are required for the archenteron to move across the blastocoel and make contact with the ectoderm at the animal pole of the embryo. At the gastrula stage, embryos contain approximately 1000 cells.

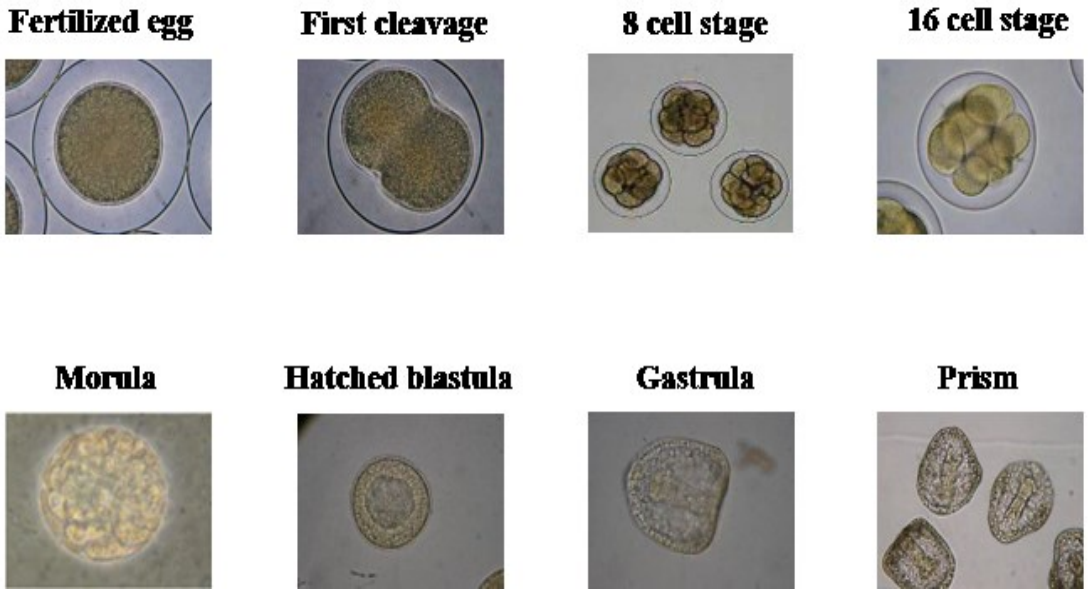

FIGURE 1.4: Pictures taken with inverted microscope of several developmental stage of the *Paracentrotus lividus* embryos.

The prism stage is characterized by a change in the overall shape of the embryos and the beginning of differentiation of larval structures (figure 1.4). During the prism stage, the embryo takes on the shape of a rounded, truncated pyramid. At the point of contact between the archenteron tip and

the overlying ectoderm, the ectoderm invaginates slightly to form the future stomodaeum. At the stomodaeum level, embryos develop the mouth and the anterior opening of the digestive tract will. The anal opening of the digestive tract develops from the blastopore. Two constrictions appear in the archenteron subdividing it into three regions-esophagus, stomach, and intestine. The side of the embryo containing the stomodaeum becomes flattened forming the oral surface (referred to as the ventral side) of the developing larva. The blastoporal side of the embryo also becomes flattened and forms the anal surface (referred to as the posterior side) of the developing larva. A band of cilia develops around the stomodaeum. As this occurs, the apical tuft disappears and the embryo elongates slightly along what classically has been called the dorso-ventral axis. As a result of these changes in shape, the direction of movement changes so that the prism (and later the pluteus) usually moves with the oral surface forward. The primary mesenchyme cells begin to aggregate and differentiate into the triradiate spicules, forming the rudiments of the larval skeleton. The secondary mesenchyme cells begin to differentiate into pigment cells.

FIGURE 1.5: Pictures taken with inverted microscope of pluteus larva of the *Paracentrotus lividus*.

The fully developed pluteus larva is somewhat elongated (figure 1.5). The oral lobe appears as an outgrowth on the oral surface above the stomodaeum. In this developmental stage appears also two arms, the preoral arms that extend out from the oral lobe (also called the oral arms). Two additional arms, the postoral arms, appear at the larval stage and extend out from the junction of the oral and anal surfaces (also called the anal arms); the postoral arms are longer than the preoral arms. Due to changes in the shape, the developing digestive tract is bent into a J-shape and the stomach enlarges and fills a large part of the body of the pluteus. The sea urchin embryos reach the larval stage 48

hours after the fertilization event and form part of the zooplankton. A period of extensive feeding and continued larval development is required (about 28 days) before metamorphosis process to a miniature sea urchin occurs (the most important developmental stages of *P. lividus* are summarised in table 1.2)

TABLE 1.2: schematic description of sea urchin *Paracentrotus lividus* embryo developmental stages

Chronological development of Sea Urchin *Paracentrotus lividus* embryos at 19°C	
TIME (hours)	**Developmental stages**
0 h	Fertilization event
1 h	2 blastomeres
2 h	4 blastomeres
3 h	8 blastomeres
4 h	Morula (32/64 blatomeres)
5-6 h	Blastula
10 h	Swimming blastula
12 h	Early gastrula
21-24 h	Late gastrula/Prism
48 h	Pluteus

Sea urchin is one of the few model organisms considered promising by the European Centre for the Validation of Alternative Models (ECVAM). In addition, early and late developmental stages of sea urchins, and echinoderms in general, represent since long time a principal experimental model to investigate the mechanisms driving the developmental and differentiation processes, the ecotoxicological implication of chemical compounds found as environmental and food contaminants and also an useful marine model organisms for the study of apoptotic mechanisms of new marine natural compounds with antiproliferative effect. This marine model organism fully respect the 3Rs objectives (Reduction, Refinement, Replacement of animal experiments), that will lead to the reduction of vertebrate use for toxicity tests (Passantino, 2008).

This is also support by the fact that in the last years results of the project "Sea Urchin Genome", carried out by California Institute of Technology were published, making available for the scientific community *Strongylocentrotus purpuratus* genome (Sea Urchin Genome Sequencing Consortium). Moreover, a consortium formed by European Research Institutes is working on the complete sequencing of the Mediterranean sea urchin (*P. lividus*). All this genomic information gives

new impulse at the sea urchin as marine model. In the last decade, molecular studies and bioinformatic investigations have gained a central role in many research institute, since genome contains all information regulating physiological cellular process and responsible of insurgence of many diseases. This new genomic knowledge support the reasonable scientific effort to validate sea urchin as molecular tool, *in vitro* and *in situ*, for the assessment and conservation of ocean health.

1.2 The sea urchin *Paracentrotus lividus* as model organisms to study the effect of diatom secondary metabolites

Diatoms have traditionally been regarded as providing the bulk of the marine food chain to top consumers and predominant fisheries. In the past, they have been considered as beneficial factor for the survival and growth of primary consumers such as benthic filter feeders (e.g. bivalves) and zooplankton (e.g. copepods). However, researchers have recently opened to doubt of the theory of beneficial role of diatoms in the marine food web. In the last 20 years, researchers studying the interactions between diatoms and copepods demonstrated a strong reduction of fertilization process and/or hatching success when herbivorous copepods species were fed with diatom diets. (Ianora and Poulet 1993; Poulet et al., 1994; Chaudron et al., 1996; Buttino et al., 1999; Ianora and Miralto 2010 for a review). All the evidences obtained are known as the paradox of the diatoms-copepods interaction. The term paradox is justified by the unique negative effect induced when copepods feed with diatoms. In fact, the most commons negative pant-animal interactions known in the marine environment are related to poisoning or repellent mechanisms, but a reproductive failure induction was never observed before.

Ianora and Poulet (1993) carried out the pioneer study in this new direction, demonstrating the blockage of the reproductive system of copepod *Temora stylifera* fed with mono-algal diet of diatom *Thalassiosira rotula*. More in detail, copepods kept unvaried the high eggs production for more than 15 days, but algal diet was able to strongly compromised the hatching success; control experiments were represented by same copepod species fed with the dinoflagellate *Prorocentrum minimum*. Poulet et al., (1994) hypothesized that the reduction of hatching rates in the copepod *Calanus helgolandicus* was a direct effect of unknown anti-mitotic compounds derived from diatoms, which arrested embryogenesis. The embryonic development of copepods was blocked when eggs were exposed to diatom extracts in a dose-dependent manner (Poulet et al., 1994; Ianora et al., 1995; Miralto et al., 1995).

Miralto et al. (1999) carried out in field experiments, demonstrating that the hatching success of copepods during a diatom dominated bloom in the Northern Adriatic Sea was strongly reduced. They observed only 12 % of the eggs hatching respect with 90 % measured at the end of algal bloom condition. In the same study, Miralto et al. (1999) isolated from the bloom of diatoms (*Thalassiosira rotula*, *Skeletonema marinoi* and *Pseudo-nitzschia delicatissima*) and then characterized two C10 short chain polyunsaturated aldehydes: 2E,4E/Z-decadienal and 2E,4E/Z,7Z-decatrienal.

In a more recent study, Ianora et al. (2004) have also assessed the effect of maternal diatom-diet on the fitness of copepod offspring. The study showed a blockage of the development in all larvae of *C. helgolandicus* females fed with the diatom *Skeletonema marinoi*. In addition, larvae, generated by females fed with *Skeletonema marinoi*, conserved high mortality rate even if the larvae were recovered with control diet of the dinoflagellates *Prorocentrum minimum*. On the other hand, when the females were fed with the dinoflagellates *Prorocentrum minimum* and the relative nauplii were grown with *Skeletonema marinoi*, the mortality rate decreased significantly. Considering all these experimental results, maternal-feeding quality was demonstrated to be even more important than nauplia sustenance for progeny survival.

These surprising findings have driven researchers to concentrate the attention on chemical studies in order to characterize the molecules responsible for these toxic effects. Thus, first biochemical evidences demonstrated that these uncharacterized compounds were the final products of a lipoxygenase-hydroperoxide lyase metabolic pathway (figure 1.6). This biochemical cascade is activated after mechanical breakage of algal cells, occurring during grazing by predators or senescence processes, and the production of secondary metabolites increases dramatically after few seconds. Lipoxygenases (LOXs) represent a key point involved in this biosynthetic pathway; they are enzymes able to catalyse insertion of oxygen to double bonds of polyunsaturated fatty acids (PUFAs). More in detail, lipase enzymes are activate by cell damages, which release PUFAs from cell membranes. These undergo immediately an oxidation and cleavage process with the consequent formation of polyunsaturated aldehydes (PUAs) and many other secondary metabolites, collectively termed oxylipins (Fontana e al., 2007a and 2007b)

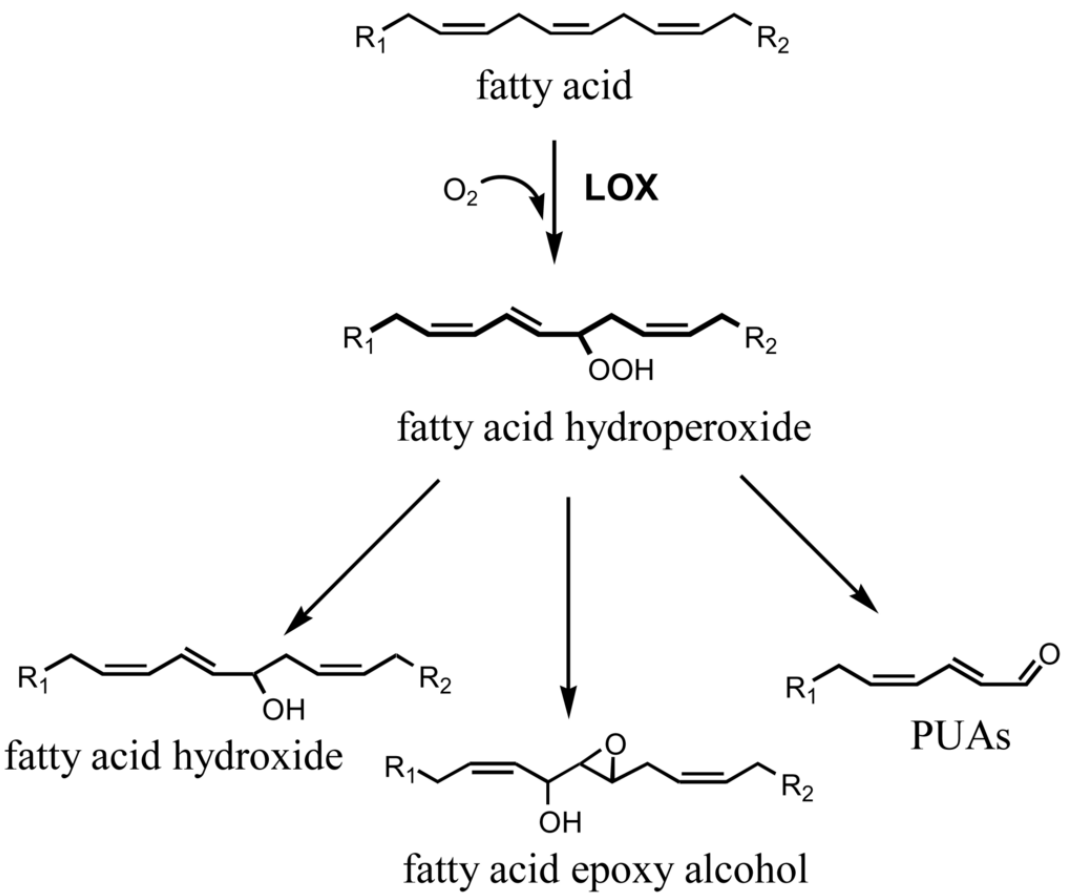

FIGURE 1.6: Biosynthetic pathway of oxylipins, starting from fatty acids. The biochemical mechanism involve the lipoxygenase enzimes (LOXs) in marine diatoms. R_1 represents the methyl terminal part and R_1 the carboxylic end of C16 or C20 fatty acid precursors (modified from Fontana et al., 2007b).

Diatom species and strains are able to produce specific type and different quantity of oxylipins (Pohnert et al., 2002, Taylor et al., 2009); these high specificity produce variable effects on zooplankton grazers (Ianora and Miralto 2010) (figure 1.7).

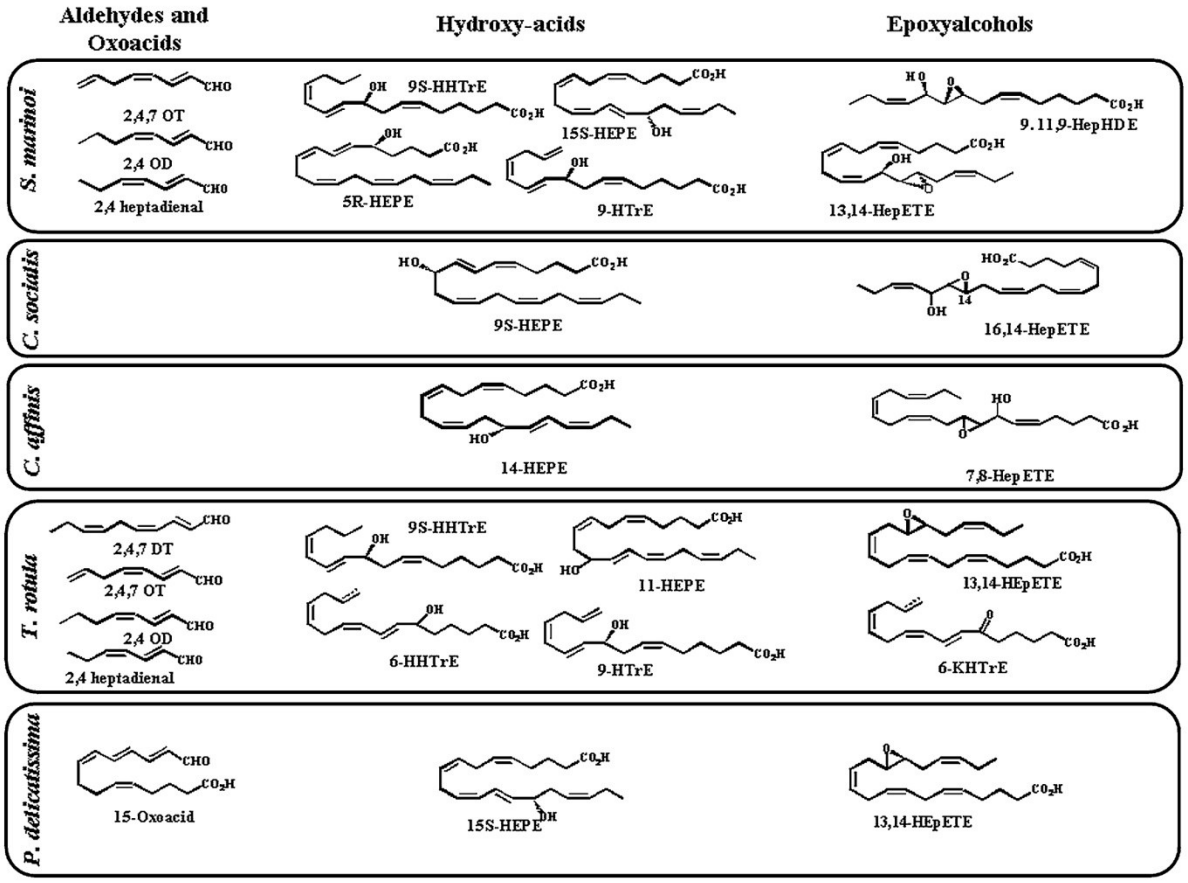

FIGURE 1.7: An overview of oxylipins synthetized in the marine diatom species *Skeletonema marinoi, Chaetoceros socialis, Chaetoceros affinis, Thalassiosira rotula and Pseudo-nitzschia delicatissima* (from Ianora and Miralto, 2010).

Plants produce a plethora of secondary metabolites with signalling functions. In particular, terrestrial plants are able to produce compounds belonging to oxylipin family. This mechanism is finely regulated, in fact when the production of oxylipins overtake a threshold, lipoxygenase activity is inhibited (Spiteller 2003), suggesting that the process reaches a balance between consumption of precursors (Polyunsaturated Fatty Acids, PUFAs) and synthesis of oxylipins.

In marine environment the regulation of oxylipin production is slightly different. Diatoms, after mechanical damage, produce continuously oxylipins such as Polyunsaturated Aldehydes (PUAs), because, at the sea level, the effect and relative efficacy of released compounds are constantly interfered by the dilution occurred in seawater. In this way, PUAs, as soon as produced by diatoms, are carried away and the production process continues until precursors are available. This specific regulation of the defence strategy in marine environment allows maintaining a high local concentration around diatoms (46.9, 4.7 and 0.5 μmol PUA L^{-1} at a distance of 1, 10 and 100 μm from the cell surface, respectively). Thus, high local concentration contrasts the potent dilution effect created by the sea, avoiding decline of secondary metabolites efficiency (Ribalet et al., 2007b).

At this important study, followed further chemical methodology able to identify a larger amount of PUAs from diatoms, expecially from *Skeletonema marinoi* and *Thalassiosira rotula*. Subsequently an expanded range of PUAs were identified (figure 1.8), including 2E,4E heptadienal; 2E,4Z-octadienal; 2E,4E-octadienal; 2E,4E-2,4,7-octatrienal and 2E,4Z decadienal (Pohnert 2000, 2002; Pohnert and Boland, 2002; d'Ippolito et al., 2002a, 2002b, 2003).

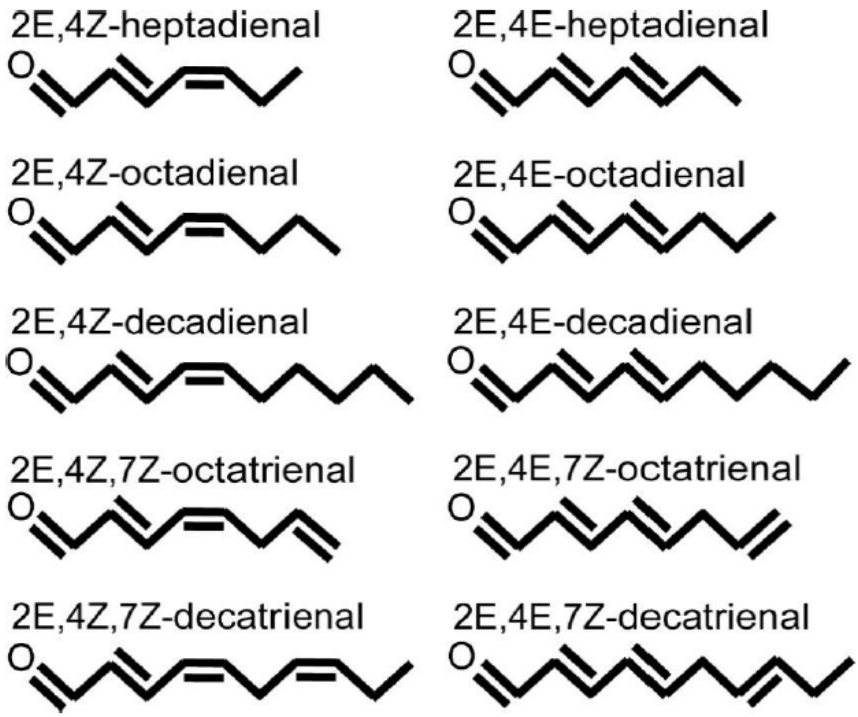

FIGURE 1.8: Chemical structures of diatom-derived polyunsaturated aldehydes (From Ribalet, 2007)

The metabolic pathway and all enzymes involved in the PUAs biosynthesis, as said before, seem to be induced soon after membrane damage and for this reason PUAs are, as principal function, the direct responsible of anti-predator signalling. However, researchers have also identified other PUAs related functions, each specific of certain concentration of the signalling molecules. In fact , Spiteller (2003) hypothesized three different types of physiological responses induced by PUAs and their precursors. The nanomolar levels or lower amounts of oxylipins constitute the cell division and cell proliferation signalling, while larger amounts of oxylipins induce death signalling. In particular, micromolar concentrations of signalling molecules are able to induce specifically necrosis, while very large amounts of oxylipins activate apoptotic cell death.

A confirmation at this thesis coming from the study of Casotti et al., (2005), where the marine diatom *Thalassosira weissflogii* treated with very large amounts of decadienal (up to 6.4 μM) exhibited a clear growth inhibition due to activation of the programmed cell death. Recent study assigned at PUAs two separate roles when they acting on their direct producers or on other species. In fact, Gallina et al., (2014) described that *Skeletonema marionoi*, a PUAs producing species, recognizes itself PUAs signal as intra-population infochemicals, as a chemical that transmits information in an interaction between two individuals, inducing in the receiver a behavioural or physiological response (Vet and Dicke, 1992). On the other hand, *Pheodactylum tricornutum*, a no-PUAs producing species, transduces PUAs input as allelochemical mechanism, as process involving secondary metabolites that influences the growth and development of biological systems (Roger et al., 2006).

At the end, PUAs could be synthetized and released even if there is not a cell damage or grazing activity. Watson and Satchwill (2003) detected PUAs in culture medium of the freshwater chrysophytes, growth as mono-species culture in normal conditions; thus, they confirmed that these oxylipins may play a role not only in the chemical defence mechanisms against grazers, but also as signalling molecules within diatom populations. The same role of the PUAs was confirmed by more recent studies with marine diatoms. Vidoudez et al. (2011) have quantified the release of PUAs in the Adriatic Sea in order to study its critical roles in chemically mediated plankton interactions, acting as dissolved infochemicals. *In situ*, PUAs are produced at the end of bloom as effect of cell disintegration.

All these studied described above had shed light on PUAs, their chemical characterization and molecular effects and ecological roles. Moreover, PUAs are commercially available, relatively cheap and enough stable to be used for laboratory experiments.

Few studies are carried out about the deleterious effects of algal toxic compounds on gametogenesis, gamete functionality, fertilization, embryonic mitosis, and larval fitness. By the way, the effects of oxylipins, produced by diatoms, on fertilization and development processes are the most comprehensively explored among marine natural products. First studies demonstrated that diatoms producing oxylipins were able to interfere with pronuclear fusion process. In fact, Poulet et al. (1995) studied the effect of diatom diet (*Phaeodactylum tricornutum*) on eggs of copedod *Calanus finmarchicus* and Buttino et al. (1999) treated *P. lividus* eggs with different diatom extracts. In both studies has been observed a failure of the pronuclear fusion. Some year later, Hansen et al. (2003) demonstrated that extracts of *Phaeocystis pouchetii* were able to reduce drastically the fertilization success of the sea urchin (*Sphaerechinus granularis*) eggs. In addition, interference with sperm functions and its fertilization potential was investigated. Ianora et al. (1999) fed the copepod *Temora stylifera* with different diets of dinoflagellates, which were able to induce a strong decrease of sperm quality. Tosti et al. (2003) investigated the effect of PUAs on first stages of fertilization processes in *Ciona intestinalis*. They demonstrated the inhibitory effect of decadienal and decatrienal on the fertilization-current generated when sperm-egg binding event occurs and on the plasma membrane voltage-gated calcium currents.

Many studies have largely demonstrate also the arrest of embryogenic process induced by diatom-derived oxylipins. Poulet et al. (1994) gave the first contribution in this field, studying the *Calanus helgolandicus* embryos exposed to *Thalassiosira rotula* extracts. Poulet et al. described in his study that the point of cell division arrest could change, but occur, depending on the age of the eggs before exposure, either prior to fusion of male and female pronuclei, or during mitosis. However, embryos underwent stonkingly abnormal development. The abnormality included a dark brown,

opaque outer membrane, globular cytoplasm, blockage of pronuclei, or dispersed chromatin scattered in the egg matrix of non-hatched eggs. In the same decade, Buttino et al. (1999) investigated the effect of extracts of *Thalassiosira rotula* on sea urchin and ascidian development. The study report a hatching inhibition with consequent blockage of tubulin organization, and inhibition of chromatin condensation. The cell division process is arrested due to an activation of microtubule depolymerisation, observed from pronuclear fusion to telophase. All these effects induced by diatom-derived oxylipins were directly connected with the activation of programmed cell death, although has been observed in the studies reported above different responses in copepods and sea urchins (Romano et al. 2003).

To date, only few studies are present in literature on the biological and chemical characterization of the other oxylipins. Fontana et al. (2007b) investigated the chemical compounds produce by two diatoms, which did not produce PUAs, but which, similarly to PUA-producing diatom *Skeletonema marinoi*, interfere with hatching success. Fontana et al., studying *Chaetoceros socialis* and *Chaetoceros affinis* better explained all a series of past laboratory and field results showing how diatoms damage zooplankton grazers even in the absence of polyunsaturated aldehydes production. More in detail, they showed that copepod dysfunctions can be also induced by highly reactive oxygen species (hROS) and a blended mixture pf secondary metabolites produced by diatoms, including fatty acid hydroperoxides (FAHs) and oxylipins such as Hydroxy-EicosaPentaEnoic acids (HEPEs) and epoxyalcohols (HepETEs); these molecules displayed teratogenic and proapoptotic activities agaist zooplankton grazers. All these finding are sufficient to assign to oxylipns a crucial role in plant defence mechanisms, because they are able to induce the activation of dangerous signalling against herbivore. Moreover, oxylipins are though as protective compounds, with antibacterial and wound healing functions.

In the marine ecosystem, not only diatoms produce oxylipins. In particular, the red alga *Rhodymenia pertusa* produce four oxylipins including 5-HEPE, suggesting that this specie contains a unique 5R-lipoxygenase system (Jiang et al., 2000). Moreover, the brown kelp *Laminaria digitata* synthetize the 15-HEPE and its production is triggered soon after copper-induced stress (Gerwick, 1994; Ritter et al., 2008); the same molecule was found in the microalga *Nannochloropsis gaditana* (Iqbal et al., 2013). The 15-HEPE was study also for its anti-inflammatory activity. In fact, Iqbal et al. (2013) demonstrated the inhibition of the Tumor necrosis factor-α (TNF-α) induced by the 15-HEPE. Other investigation in this research line can lead to the identification of novel oxylipins or secondary metabolites with crucial role in the chemical communication and defence mechanisms. The study of chemical structure and ecological role of these secondary metabolites should be followed by the investigation of their biological effect on other species, included human and animals. Therefore, more studied and efforts are still essential to better understand the role and the effects of these chemical mediators in the marine environment. These potential results can be utilized for pharmaceutical applications, investigating the bioactivity of marine compounds on mammalian cells and responding to the strong demand of new drug from emerging and established disease.

1.3 PUAs: morphological and molecular effects on *Paracentrotus lividus* and human cell lines

The morphological studies of the effect of PUAs has been carried out mainly using decadienal, as the first oxylipins chemically characterized that is also commercially available. More than a decade ago, one of the first study on the mechanisms underlying the effect of decadienal (Romano et al. 2003) described the pro-apoptotic effect induced by decadienal on sea urchin embryos. In this early study, researchers assessed the ability of the decadienal to specifically activate enzyme with caspase-like function in sea urchin embryos, using commercially available kit developed for vertebrate model organisms. This kit contains a fluorescent substrate, the acetylated peptideAc-DEVD-AFC (carbobenzoxy-Asp-Glu-Val-Asp-7-amino-4-trifluoromethyl coumarin), which releases the fluorescent AFC moiety after enzymatic hydrolysis (figure 1.9).

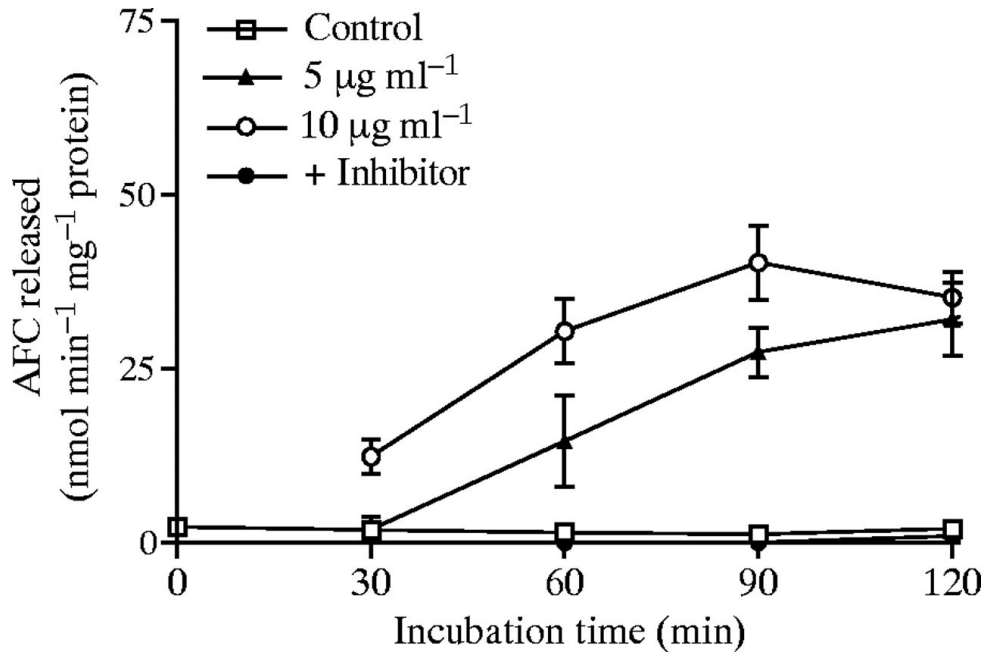

FIGURE 1.9: Caspase-3-like activity in *Paracentrotus lividus* embryos. Values represented (means ± S.D.) originate from three different biological experiment (modified from Romano et al., 2003)

Sea urchin embryos treated with 5 μg ml^{-1} of decadienal showed caspase-3-like activity already after 60 minutes of exposure, with maximum activity after 120 minutes of incubation (figure

1.9). In order to demonstrate that proteolytic activity measured was attributable univocally to the sea urchin caspase-3-like enzymes, researcher performed the same experiment in the presence of a caspase-3 specific inhibitor (Z-VAD-FMK). In this case, the release of AFC moiety drastically decrease to zero. Moreover, the activation of caspase-like enzymes was dose-dependent, because was more evident and occurred earlier if embryos were treated with higher concentration of decadienal (10 μg ml^{-1}).

Other PUAs, such as decatrienal, octadienal, octatrienal, tridecanal and heptadienal were investigated for their deleterious effects on early and later developmental stages of sea urchin embryos (Romano et al., 2010). All these secondary metabolites were able to block cell cleavage in *P. lividus*. Heptadienal arrests the cell cleavage at 27.27 μM, octadienal at 16.13 μM, octatrienal at 11.46 μM and decadienal was the most active among these compounds blocking cell division at 5.26 μM. The saturated aldehyde tridecanal, also found in diatoms, did not interfere with first cleavage up to 25 μM. These data demonstrate a direct proportion between the chain length of PUAs (from C7 to C10) and blockage effect of the cell cleavage. Moreover, researchers analysed the effect of decadienal, heptadienal and octadienal on sea urchin hatching success. They clearly showed that the three PUAs exerted a very strong dose-dependent effect, with decadienal showing somewhat stronger effect than the other two aldehydes. In fact, 3.0 μM of decadienal reduced hatching viability to <50%, whereas the other two aldehydes induced a slight reduction at the same concentration (>90% of hatching viability). The three PUAs induced a total inhibition of hatching viability at different concentrations: 3.95 μM for decadienal, 8.08 μM for octadienal and 11.36 μM for heptadienal. This confirm that longer-chained aldehydes had somewhat stronger effects than shorter-chained aldehydes (figure 1.10). Another interesting finding in Romano et al. (2010) was to observe that when decadienal, octadienal and heptadienal were added as a mixture to the medium containing a 1:1:1 ratio did not occur inhibition effect on cell cleavage and only a slightly increased effect on egg hatching viability, demonstrating a total absence of synergistic effects.

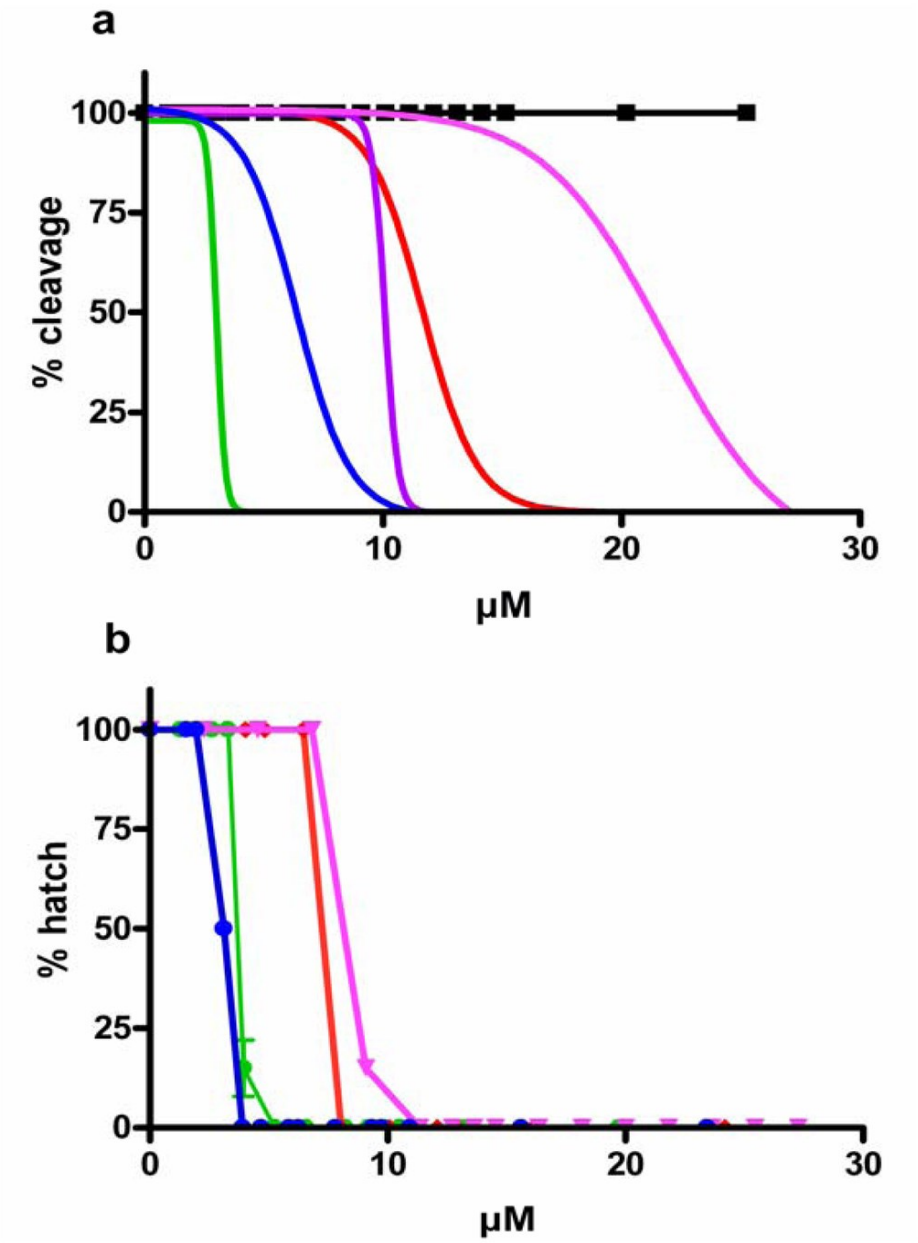

FIGURE 1.10: (**A**) Percentage of cleavage inhibition in sea urchin embryos following PUAs treatment. (**B**) Percentage of hatched sea urchin larvae. 2-*trans*,4-*trans*-decadienal (●), aldehyde mix (●), 2-*trans*,4-*trans*-octadienal (♦), 2-*trans,*4-*trans*,7-octatrienal (□), 2-*trans*,4-*trans*-heptadienal (▼) and tridecanal (■). Values (means ± S.D.; N = 600) are the results of three different biological experiments (modified from Romano et al., 2010).

Romano et al. (2010) tested also the effect of decadienal at lower concentration (than 6.58 µM that induce the arrest of cleavage) on arrest of cell division. From 1.32 to 5.26 µM of decadienal were used to treat sea urchin embryos soon after elevation of fertilization envelope. These decadienal

concentrations increased the number of abnormal sea urchin plutei and delayed the development of larvae or embryos, which showed various degrees of malformations with the increasing of concentrations tested (figure 1.11). At lower concentrations (1.32-2.63 µM), malformations were less severe with a shortening of spicules and arms. At higher concentrations (3.95-5.26 µM), larvae were similar to blastula and gastrula stages, showing severe abnormalities or blebbing associated with apoptosis.

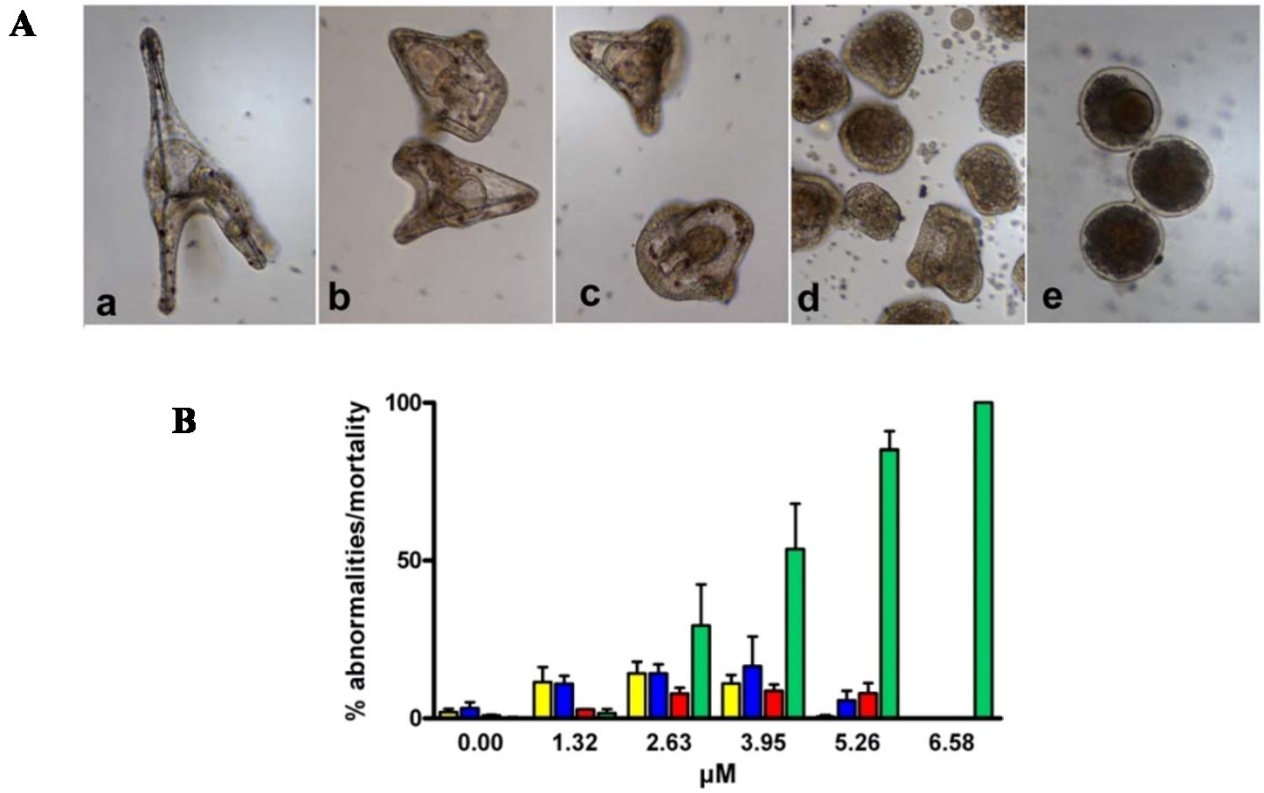

FIGURE 1.11: (**A**) *Paracentrotus lividus* 48 hours plutei after incubation in decadienal at 1.32 µM (b), 2.63 µM (c), 3.95 µM (d) and 5.26 µM (e) compared to control embryo (a). (**B**) Percentage of abnormal sea urchin larvae after 48 hours of treatment with several decadienal concentration ranging from 1.32 µM to 6.58 µM. Control is reported as 0 µM decadienal concentration. Yellow bars = retarded larvae; blue bars = abnormal pluteus larvae; red bar = abnormal gastrulae and blastulae; green = dead pre-hatched embryos. Values (means ± S.D.; N = 600) are the results of three different experiments (modified from Romano et al., 2010).

In a more recent study, Romano et al. (2011) assessed the effect of decadienal on the mitochondrial functionality of the *P. lividus* embryos. Mito tracker was used in this work, a dye staining mitochondria in live cells, which accumulates inside the organelle, depending on membrane potential. Sea urchin eggs, before to be fertilized, were treated with 5 μg ml^{-1} of decadienal in filter seawater and, 20 minute post fertilization, Mito Tracker was added to marks specifically active mitochondria. The figure 1.12 shows the fluorescence due to the Mito Tracker that dramatically decreased with respect to the control, indicating that decadienal impairs mitochondrial functionality.

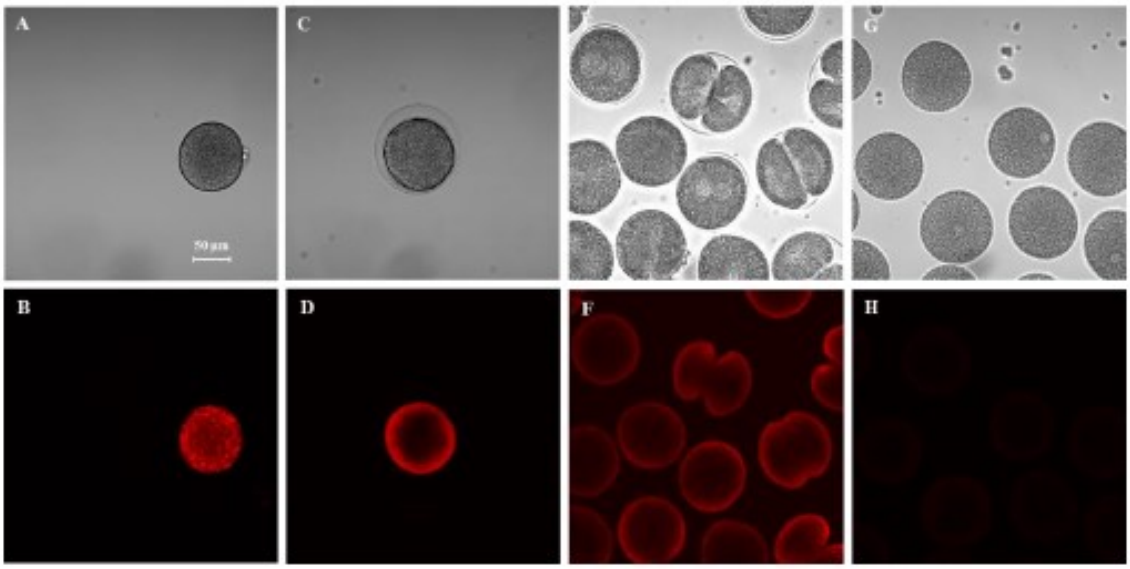

FIGURE 1.12: Active mitochondria visualised by the mitochondrial-specific fluorescent dye Mito tracker within *Paracentrotus lividus* egg before the fertilization (**A** and **B**); egg 10 minutes after the elevation of the fertilization envelope (**C** and **D**); embryos at 50 min post fertilization (**E** and **F**); embryos at 50 min post fertilization incubated with 5 μg ml^{-1} decadienal (**G** and **H**). Upper panels are images in transmitted light; lower panels are the same images in fluorescent light. (Modified from Romano et al., 2011).

P. lividus sea urchin embryos has recently been used as model organism to study the ecotoxicological effect at molecular level of marine natural compounds. Marrone et al. (2012) exposed sea urchin embryos at low concentration of decadienal (0.25 μg ml^{-1}) and analysed the variation of expression levels of sixteen genes by Real Time qPCR. These genes are implicated in a broad range of functional responses, such as stress, skeletogenesis and development. The low

decadienal concentration was able to activate different class of genes in the sea urchin *P. lividus*. The activation of this machinery is fundamental to defend sea urchin against the toxic aldehyde, inducing the upregulation of heat shock protein 60 and two proteases, (hat and BP10), at the blastula stage, and heat shock protein 56 and several other genes (14-3-3ε, p38 MAPK, MTase, and GS) at the prism stage. Moreover, sea urchin embryos treated with increasing concentrations of decadienal revealed a dose-dependent response of activated target genes. The researchers hypothesized a specific defence mechanism activate against decadienal, that *Paracentrotus lividus* place in motion as protection strategy from environmental toxicants. This mechanism represents a defensome, which is a complex network of genes involved in many cellular response related to toxicity injuries.

Recent molecular study carried out at Stazione Zoologica "Anton Dohrn" gave further insight in the molecular response induced by diatom-derived aldehydes on *P. lividus* (Varrella et al., 2014). This study investigated the variation of gene expression induced by other two ecologically relevant aldehydes, heptadienal and octadienal, allowing a comparison among the molecular effect of the three principal aldehydes. Varrella et al. (2014) described the activation of gene mechanisms induced by increasing concentrations of heptadienal and octadienal, hypothesising the molecular pathways responsible for the teratogenic effect. In fact, they analysed 31 genes that could be potential target of PUAs, having a key roles in a broad range of cellular response such as stress, skeletogenesis, detoxification, development and differentiation. More in detail, the three aldehydes were able to activate stress response in sea urchin *Paracentrotus lividus* whyle genes related to detoxification process were downregulated. Moreover, they found an upregulation of some gene involved in the development and differentiation process. Only the genes involved in the skeletogenic processes were differently activated by the three PUAs. Decadienal induced a downregulation of the skeletogenesis, but heptadienal and octadienal produced an upregulation of some gene involved in the same mechanism.

Following study used interactomic Ingenuity Pathway Analysis to show how the genes targeted by PUAs are correlated with four HUB genes, NF-κB, p53, δ-2-catenin and HIF1A. These four genes represent crucial nodes within the network, having a large number of interactions (Varrella et al., 2016). This study better described how the sea urchin *P. lividus* can use its defensome, the integrated network of genes, to mount a defence mechanism against environmental toxic compounds. The study suggests that sea urchin can be also used as sentinel organism and bioindicator for the early signals of stressful conditions in the marine ecosystem

Successively to these morphological and molecular evidences, in which was clear that PUAs were able to exert an antiproliferative effect on actively proliferating cells and target specific molecular pathway, drug discovery experiments were performed using this class of chemical compounds. Sansone et al. (2014) examined the effects of the three PUAs on different human cell lines. They studied the molecular mechanisms activated by the treatment at different concentrations of decadienal, octadienal and heptadienal on the lung adenocarcinoma cell line (A549), colorectal adenocarcinoma cell line (COLO 205) and the normal lung/brunch epithelial BEAS-2B cell line. The viability results revealed that PUAs have strong cytotoxic effects on both A549 and COLO 205 cancer cells, but the same compounds did not affect BEAS-2B normal cells. Decadienal was the strongest among the three PUAs tested, at all times and concentrations considered, but surprisingly, heptadienal was as strong as decadienal after 48 hours. On the contrary, octadienal was not able to reduce cell viability at levels similar to the other PUAs. More in detail, decadienal reduced the cell viability of A549 at about 25% with 2 μM and at 0 % with 5 and 10 μM, after 72 hours. Moreover, the same compound induced a strong reduction of cell viability also in COLO205, reducing viable cell to 30%,

20% and 10% when treated with 2, 5 and 10 µM respectively. The heptadienal induced a reduction of cell viability at 70%, 50% and 0% when A549 were treated with 2, 5 and 10 µM respectively. The same effect was observed on COLO205, where 2, 5 and 10 µM of heptadienal induced a decrease of percentage in cell viability of 70%, 60% and 35% respectively.

Sansone et al. (2014) characterized in the same study the molecular death signaling pathways activated by the three PUAs in A549 cells (figure 1.13). Cells treated with decadienal activated Tumor Necrosis Factor Receptor 1 (TNFR1) and Fas Associated Death Domain (FADD) leading to necroptosis via caspase-3 without activating the survival pathway Receptor-Interacting Protein (RIP). The same death signalling pathway, TNFR1/FADD/caspase pathway, was also activated by octadienal, but only after 48 hours. In the case of octadienal, researchers observed also an upregulation of RIP gene that probably is able to activate a survival pathway, in accordance with the results obtained, where octadienal caused less damage to the cells compared to the other two PUAs. In contrast, cells treated with heptadienal activated the receptor protein Fas that is a key factor able to induce early apoptosis mechanism without involvement of survival signals. Fas in turn activated FADD, which then triggers the same caspase molecular pathway induced by decadienal and octadienal, without the activation of RIP.

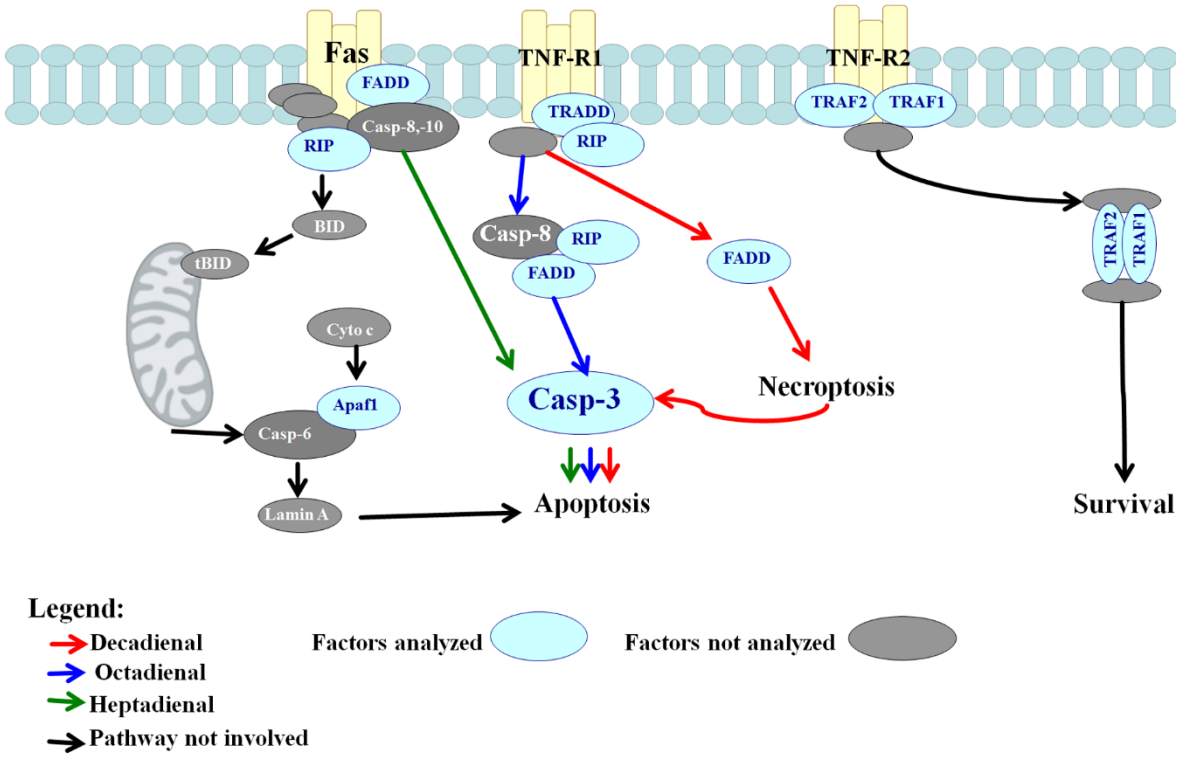

FIGURE 1.13: Schematic representation of molecular cell death pathways activated by the three different PUAs in lung adenocarcinoma cell lines A549. Red arrows indicate signal transduction via activated by decadienal; blue arrows indicate signal transduction via activated by octadienal; green arrows indicate signal transduction via activated by heptadienal (from Sansone et al., 2014).

CHAPTER 2.

Materials and Methods

2.1 Ethics Statement

All animals were collected in the Gulf of Naples, from non protected or private areas, according to Italian legislation of the Marina Mercantile (Decreto del Presidente della Repubblica DPR 1639/68, 09/19/1980 confirmed on 01/10/2000). The study involves only sea urchin *P. lividus*, not involving any protected or endangered species. All animal procedures were in compliance with the guidelines of the European Union (Directive 609/86), on the protection of animals used for scientific purposes.

2.2 *Paracentrotus lividus* collection, stimulation of spawning and fertilization test

Sea urchins *P. lividus* were collected by dive operators (Gianluca Zazo and Marco Cannavacciuolo), operating for the RIMAR department of the Stazione Zoologica "Anton Dohrn" of Naples. Animals were collected from a specific site of the Gulf of Naples, called Rocce Verdi (coordinates of sampling point are: 40°47'50.5"N 14°12'05.8"E). Sea urchins were transported in a refrigerated box and brought to the research institute; animals were maintained in large tanks with circulating sea water, at least for 3 days to allow to sea urchin to recover from stress conditions due to sampling and carriage, before to use them for experimental activities.

To obtain gametes from animals to carry out experiments, sea urchins were shaken vigorously and observed on the apical portion of the animal shell, where are released both eggs (that appear orange in colour) or sperms (that are white). If the only shaking was not efficacious, sea urchins were injected with a solution 2M of potassium chloride (KCl); this method generates definitely spawning through the contraction of muscles around the gonads. Sea urchins, soon after shaking or injection, were placed with the anal pole face down on a beaker containing filtered sea water (FSW) to collect eggs. Sperm was collected with a plastic disposable pipettes, transferred in a 1.5 ml Eppendorf tube and maintained dry and concentrated at 4°C until fertilization.

At the end of the spawning, eggs where washed and separated from macro-impurity (e.g. macroalgae and spines) using a cotton lint and washed for three times with FSW. During all manipulation steps eggs were maintained in a beaker with large surface, in order to contain eggs in monolayer, allowing gas exchange.

Before to start any experiment with sea urchin embryos, a fertilization test was carried out, in order to evaluate eggs and sperm quality and analyse the fertilization efficiency. Test was performed in a multiwell plate (12 well), where in 1 ml of FSW was added a drop containing eggs. The dry sperm was diluted 1:1000 with FSW and a drop of dilution was added to eggs; 2 minutes after fertilization was possible to evaluate if biological material was suitable for further *in vitro* experiments. An observation with optical microscope was enough to understand if the sperm has been

able to elevate the fertilization membrane and later to observe the first mitotic division. These basic biological processes are crucial to identify if eggs are suitable for *in vitro* experiments, showing absence of previous stress factors, which could alter the following step of experimentation and relative result quality.

2.3 Setting up the *in vitro* experiment for the incubation of sea urchin embryos with the Oxylipin

The purpose of this experiment was to collect samples treated with the heptadienal to analyse the effect of this aldehyde on target genes and proteins. In detail, Pyrex crystallizing dishes with 50 ml of FSW were used to incubate 8000 eggs (about 150/160 eggs/ml).

After the washing step and successfully passed the fertilization test, eggs were maintained in a backer with exactly 100 ml of FSW. In a multiwell plate, 3 wells were filled with 1 ml of FSW, and 10 µL of homogeneous suspension of eggs was added in each well. These three samples were counted under an inverted microscope (Zeiss Axiovert 135TV microscope), in order to evaluate the number of eggs contained in each well. The mean of the three values represents the number of eggs present in 10 µL of suspension. Using a proportion formula, has been possible to calculate the volume of eggs suspension containing 8000 eggs to set up the incubation step.

The oxylipin 2E,4E-heptadienal (Sigma-Aldrich, Milan, Italy) was diluted in 10 ml methanol in a graduated flask . The effect of methanol on sea urchin development has been already tested in a previous studies (Romano et al 2003). The maximum percentage of methanol concentration that do not interfere with sea urchin embryo development is 10%.

The solution was then diluted in order to obtain heptadienal concentrations of 200 µM, 250 µM, 300 µM, 550 µM and 600 µM; these concentrations were 100 time more concentrated than those to be tested, in order to reach the desired concentrations after the final dilution in the crystallizing dish containing FSW.

The figure 2.1 shows the set up created for the 18 different *in vitro* incubations to obtain biological samples in order to study variation of gene expression after heptadienal treatment. In this case, 5 different concentrations were tested (2 µM, 2,5 µM, 3 µM, 5,5 µM and 6 µM), at three incubation times (5 hours, 21 hours, and 48 hours), with relative controls.

FIGURE 2.1: Schematic representation of *in vitro* experiment for the treatment of sea urchin *Paracentrotus lividus* embryos with different concentrations of heptadienal (2 µM, 2,5 µM, 3 µM, 5,5 µM and 6 µM) for 5 hours, 21 hours and 48 hours.

In each crystallizing containing FSW was added the right amount of unfertilized eggs. 500 µL of the different stock solutions of heptadienal (100 time more concentrate) were added to crystallizing containing 50 ml of FSW to obtain 2 µM, 2,5 µM, 3 µM, 5,5 µM and 6 µM. Eggs were incubated for 10 minutes with oxylipin at room temperature, before to proceed with the fertilization.

Dry sperm was diluted 1:1000 (5 µL of sperm in 15 ml of FSW) and added to each crystallizing, in accord to previous study (Romano et al., 2010). In detail, 180 µL of diluted sperm was added to each crystallizing containing 50 ml of FSW and 8000 eggs. Sea urchin eggs, soon after treatment with heptadienal and fertilization, were maintained in a thermostatic chamber with 12-12 hours light:dark cycle at 19-20°C.

2.4 Samples collection for gene expression analysis in *Paracentrotus lividus*

To stop the incubation of sea urchin embryos, 50 ml of embryo culture for gene expression experiments were centrifuge in Falcon tube at 3600 x g, for 15 minutes, at 4°C. Supernatants were discard and pellets were transferred in 2 ml Eppendorf tube and centrifuge again at 3600 x g, for 15 minutes, at 4°C to remove all residual FSW. Pellets obtained were quickly frozen in liquid nitrogen and then stored at -80°C for further experimental steps.

These *in vitro* incubation experiments were conducted in 5 replicates, collecting eggs from 5 different females each fertilized with a mix of sperm from different males. Each replicate experiment was carried out in different working days.

At the end of incubation time (48 hours), 1 ml from each crystallizing dish were fixed using 2% formalin to evaluate, though a morphological analysis, the entity of malformations generated after incubation of sea urchin embryos with the oxylipin (see 4.1 paragraph, in chapter 3, Results).

More in detail, about 120-140 fixed plutei were evaluated using a microscope and considered normal or abnormal larvae following the classification of malformations reported in Carballeira et al. (2012). The number of malformed plutei at 48 hours after fertilization, incubated with different oxylipin concentrations, was compared to the control, in order to obtain the percentage of malformation generated by heptadienal exposure.

2.5 A bioinformatic approach for identifying coding DNA and aminoacid sequences of a set of human proteins involved in cell death pathways

The purpose of the thesis was the investigation of death cell signaling pathways activated when sea urchin embryos were incubated with a pure marine compound, analysing the effects of heptadienal at specific developmental stages. For this reason, twelve key genes were selected in order, never studied before, to understand which specific cell death mechanism was activated by the oxylipin.

The thesis project focused its attention on searching, with several bioinformatic tools, coding regions for proteins playing key role in three of the principal cell death signaling pathways, in order to understand how sea urchin organizes, at molecular level, cell death response. These genes are listed in the Table 2.1 and are classified in 3 clusters:

- **Extrinsic apoptotic pathway**:
  Apoptosis Inducing Factor, Mitochondria Associated 1 (AIFM1);

Receptor Interacting Serine/Threonine Kinase 4 (RIPK4);
Tumor Necrosis Factor Receptor 16 (TNFR16);
Tumor Necrosis Factor Receptor 27 (TNFR27);
Nuclear Factor Kappa B (NF-*k*B)

- **Intrinsic apoptotic pathway:**
  BCL2 Associated X Protein (BAX);
  B-Cell CLL/Lymphoma 2 (BCL2);
  Poly ADP-Ribose Polymerase 1 (PARP1)

- **Autophagic pathway:**
  Beclin 1 (BECN1);
  PTEN Induced Putative Kinase 1 (PINK1);
  Unc-51 Like Autophagy Activating Kinase 1 (UKL1);
  Unc-51 Like Autophagy Activating Kinase 3 (UKL3);

These genes, with the exception of NF-*k*B, have not a nucleotide sequence available online. The sequences annotated using several bioinformatics tools available online: the algorithm BLAST (Basic Local Alignment Search Tool, available at www.ncbi.nih.nlm.gov; Altschul et al., 1997); GenScan (available at http://genes.mit.edu/GENSCAN.html); Reverse and Complement (available at http://www.bioinformatics.org/sms/rev_comp.html); EMBOSS Transeq (available at http://www.ebi.ac.uk/Tools/st/emboss_transeq/).

The National Center for Biotechnology Information (NCBI) was used as preferential bioinformatic database to search nucleotide and aminoacid sequences with relative annotations already available online.

Bioinformatic analysis started searching the *Homo sapiens* proteins listed above. Each sequence was used to find the relative orthologous protein from *Strongylocentrotus purpuratus* running a Blastp search, when it was not possible to directly identify the *P. lividus* candidate. For this purpose, SpBase (http://www.spbase.org/SpBase/search/) represented the genome sequencing database used for the purple sea urchin (*S. purpuratus*).

Therefore, once obtained human protein of interest and its clear orthologs from *S. purpuratus*, they were used to run a tBlastn search against the *P. lividus* genome database (http://octopus.obs-vlfr.fr/blast/oursin/blast_oursin.php), in order to identify the genomic region coding for the ortholog protein. The identified contig or scaffold were processed with GenScan (Burge and Karlin, 1997) for predicting the genomic locus and exon-intron structure of genes of interest. This step allowed to obtain *in silico*, starting from contig/scaffold without any annotations, all possible coding DNA sequences (CDSs) and the relative aminoacid sequences prediction, with a good approximation.

The following step required a multiple protein alignment, performed by using ClustalW of all possible with those of *H. sapiens* and *S. purpuratus*. The only one aminoacid sequence predicted with high homology with *H. sapiens* and *S. purpuratus* was expected result and was validated running a Blastp of the aminoacid sequences prediction and a Blastn of the CDS selected against all sequences of NCBI database. This last check level of the analysis was essential to confirm that our *in silico*

prediction, obtained by bioinformatic tools and criteria, was highly conserved in phylogenetically close organisms and therefore reliable.

At the end of this bioinformatic analysis, ClustalW was used to align contig/scaffold of *P. lividus* and relative CDS prediction, in order to design the exon-intron structure (see flowchart in figure 2.2).

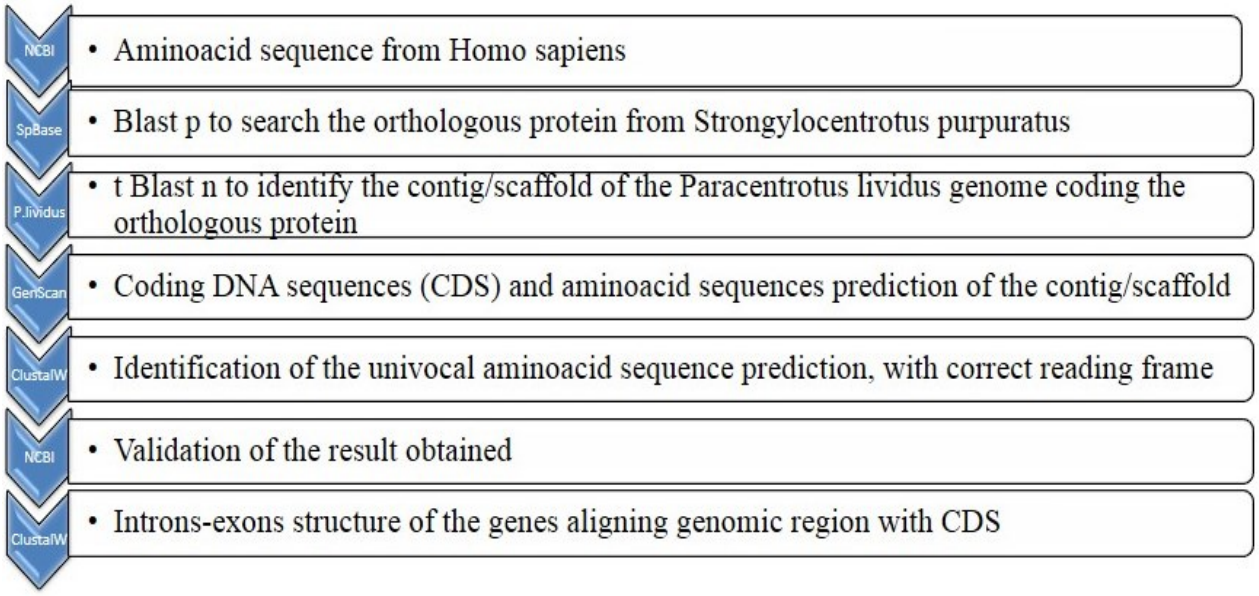

FIGURE 2.2: the flowchart show the several steps needed for the bioinformatic study of *Paracentrotus lividus* database. This analysis started from aminoacid sequences from *Homo sapiens*, and, passing though *Strongylocentrotus purpuratus*, identified and annotated ortholog protein and nucleotide sequences from our model organism.

2.6 RNA extraction and cDNA synthesis from sea urchin embryos

Frozen pellets of *P. lividus* embryos were dissolved in Trisure Reagent (adopting a ratio of 100µl reagent:10 mg embryos) for RNA extraction, promoting tissue desegregation (Bioline, cat. BIO-38033). Direct-zol^{TM} RNA MiniPrep (Zimo Research, cat. R2052) was used to purify, by spin column, total RNA directly from biological samples lysed with Trisure Reagent. RNA concentration was assessed by the aborbance at 260 nm, using the nanophotomer NanodroP (ND-1000 UV-Vis Spectrophotometer; NanoDrop Technologies). The purity of extracted RNA was evaluated by 260 nm/280 nm and 260 nm/230 nm ratios, indicative of presence of protein and phenolic residues,

respectively (samples with ratios comprised between 1.8<A260/A280<2 and 1.6<A260/230<2.2 were considered high purity RNA). Contaminating DNA was removed by treating each sample with DNase RNase-free kit (Roche), in order to degrade DNA trace still present in the RNA samples, according to the manufacturer's instructions. Extracted RNA samples, resuspended in H_2O plus DEPC (diethylpyrocarbonate, potent inhibitor of RNase), were stored at -80°C until the reverse transcription step.

The samples were then loaded and resolved on a 1% agarose gel in TAE 1x buffer (40 mM Tris Acetate and 1 mM EDTA) with pH 8, in order to assess the integrity of extracted RNA (Sambrook et al., 1989). Agarose gels showed intact rRNA subunits (28S and 18S), indicating slight or absent degradation of RNA samples.

Each sample was retrotranscribed (600 ng of total RNA extracted) with iScriptTM cDNA Synthesis kit (Biorad), following the manufacturer's instructions. Synthetized cDNA was stored at -20°C and later used in Real-Time qPCR experiments without dilution.

Once all cDNA have been synthetized, several PCR (Polymerase Chain Reaction) was performed using primers previously designed for the zinc-finger transcription factor *Pl-Z*12–1. PCR performed with well studied gene were carried out, before the Real Time qPCR, as checkpoint control assessing efficiency of previous steps, in order to establish the high quality of the RNA samples.

C1000 Touch Thermal Cycler (Bio-Rad) was used to carry out all PCR reactions. In each sample was mixed 1x PCR reaction buffer (Roche), 0.2 mM dNTP, 5 units of Taq (Roche), 100 ng/µL of each oligo, 2 µL of template cDNA and nuclease-free water to reach 30 µl final volume. The machine run a PCR program consisting of a initial denaturation phase at 95° C for 2 minutes, followed by 35 cycles (single cycle is formed by 3 step: 95° C for 45 seconds, 60° C for 1 minute and 72° C for 30 seconds) and a final elongation phase at 72° C for 10 minutes. At the end of PCR process, all samples were run on 1% agarose gel (containing ethidium bromide) to observe the presence of specific bands. Size marker was used for fragment size determination.

2.7 Primer design and validation

In order to verify the reliability of primer pairs of the twelve selected genes identified by bioinformatic analysis (designed for the following Real-Time qPCR experiments), a PCR experiment was performed for amplifying the relative coding sequences (Table 2.1). It was strongly preferred those primers able to amplify regions that anneal to genomic sequences on intron-to-exon boundary. With such primers, any products amplified from genomic DNA would be much larger than the product amplified from intron-less cDNA. Primers were designed to amplify region from 90 to 200 bp size and Gene Runner program, V3.05 (Hasting Software) was used to predict primer melting temperature (Tm) and check if they formed dimers, hairpin, bulge and internal loops.

The amplification of fragments were carried out using Taq High Fidelity PCR System (Roche, Milan, Italy). PCR conditions were optimized on a C1000 Touch Thermal Cycler (Bio-Rad). In each reaction was mixed 1x PCR reaction buffer (Roche), 0.2 mM dNTP, 5 units of Taq (Roche), 100

ng/µL of specific primers, 2 µL of template cDNA and nuclease-free water to reach 30 µl final volume. The machine run a PCR program consisting of an initial denaturation phase at 95° C for 2 minutes, followed by 35 cycles. Each cycle is formed by a first step at 95° C for 45 seconds, temperature and time of annealing evaluated for every pair of primers (from 56°C to 65°C) and 72° C for 30 seconds. At the end of 35 cycles, a final elongation phase is set at 72° C for 10 minutes.

Amplified PCR products were separated by 1% agarose gel in TAE 1x buffer (40 mM Tris Acetate and 1 mM EDTA) with pH 8 and ethidium bromide staining at the final concentration of 0.5 µg/ml. The resulting bands were excised from the gel and extracted according to the procedure reported in QIAquick Gel Extraction kit (Qiagen, Milan, Italy). The specificity of the PCR products were checked at the SZN-Molecular Biology Service by DNA sequencing, using 15 femtomoles of purified PCR product and 4.5 picomoles of each primers in the Beckman CEQ 2000 Automated Sequencer. The results obtained were aligned, through algorithm BLAST, with the relative nucleotide sequence used for the primer design.

TABLE 2.1: schematic representation of genes analysed in different developmental stages of sea urchin *Paracentrotus lividus*

Gene	Accession number	Primer	Sequence (5'=>3')	PCR fragment (bp)
REFERENCE GENE				
Pl-Z12-1			5′-AGCGCCACACCAAAAGAAGTC-3′	93
			5′-GGATGATAGACAGGGCTGTTTGGA-3′	
EXTRINSIC APOPTOSIS				
AIFM1		Pl_Aifm1_F3	5′- 3′: TAGTGGCAGTGGGTCTGGAA	163
		Pl_Aifm1_R3	5′- 3′: CGCCCTAGCTTGATGTCGTA	
RIPK_4		Pl_Ripk4_F1	5′- 3′: GGAGGCTCTTTTGGAGACG	151
		Pl_Ripk4_R1	5′- 3′: CCTCACGTCTGAGTTCATCG	
TNFR_16		Pl_Tnfr16_F3	5′- 3′: TGGAACCTACTCGGATCTCGT	155
		Pl_Tnfr16_R3	5′- 3′: CATTGGCTGGTTGGGAAGTC	
TNFR_27		Pl_Tnfr27_F1	5′- 3′: CAACTGAAGAGCCTTCTCC	202
		Pl_Tnfr27_R2	5′- 3′: GATCAAGCTCAGTACAACGC	
Pl_NF-kB:	HE574572		5′- 3′: TCCCATGGAGGACTGCCGTGTCA	116
			5′- 3′: TCGTTGGTTACCAAGGAGACCACA	
INTRINSIC APOPTOSIS				
BAX		Pl_Bax_F1	5′- 3′: CGTATCGAGCAGACACGGTT	100
		Pl_Bax_R1	5′- 3′: GCTGGAAACGCTCCACAATG	
BCL_2		Pl_Bcl2_F2	5′- 3′: TAGGGGTATAGCGGCAGTCA	91
		Pl_Bcl2_R2	5′- 3′: GGCATCCCATCCTCCTTGTT	
PARP_1		Pl_Parp_F2	5′- 3′: CCAAGAACCCAATCAAACGCC	97
		Pl_Parp_R1	5′- 3′: CTAGTAAAGAACGTGCAGG	
AUTOPHAGY				
BECN_1		Pl_Becn1_F2	5′- 3′: TCCACTCCTCCAGTGCAAAC	113
		Pl_Becn1_R2	5′- 3′: ACAAGAGCACGGGGAGGATA	
PINK		Pl_Pink_F1	5′- 3′: GCAGTTGGTTACCTTGGC	137
		Pl_Pink_R1	5′- 3′:GGATGTGCGATTTCATTGCG	
ULK1		Pl_Ulk1_F3	5′- 3′: TTGAAGGCTAGGACACTGGAC	176
		Pl_Ulk1_R3	5′- 3′: ACTGGCATTGGGGAAGTTGAG	
ULK_3		Pl_Ulk3_F1	5′- 3′: GTAATGGAAGCTGTGAAGGC	160
		Pl_Ulk3_R2	5′- 3′: GCCTAGAGTACATGAGGAGAG	

2.8 Analysis of variation of gene expression of *Paracentrotus lividus* samples, by Real Time qPCR

Real Time qPCR experiments were run with all cDNA samples to study the quantitative variations of gene expression along five developmental stages of *P. lividus* incubated with five increasing concentrations of heptadienal.

Prior to conduct Real Time qPCR experiments, the efficiency and specificity of amplification reactions was assess for all primer pairs, through melting curve analysis. The efficiency (E) of each primer pair was calculated according to standard methods curves, in accord with the equation:

$$E = 10^{-1/slope}$$

Starting from a cDNA obtained from control embryos (about 200ng/µl), five serial dilutuions were generated: 1:1, 1:5, 1:10, 1:50 and 1:100. Using the cycle threshold (Ct) values obtained versus the logarithm of each dilution factor, standard curves were designed for each oligonucleotide pair. PCR efficiencies were found to be 2 for endogenous control and target genes.

Real Time qPCR experiments were set up using not diluted cDNA as template for the reaction mix containing 0.3 mM for each of the two primers (final concentration) and 1x FastStart SYBR Green master mix (total volume of 10 µl; Applied Biosystems).

All data obtained from Real Time qPCR experiments with cDNA sample were normalized using the zinc-finger transcription factor *Pl-Z*12–1 mRNA as endogenous control, the expression of which remained relatively constant in all the developmental stages examined, according to Costa et al. (2012). Each assay included a no-template control for each primer pair. To capture intra-assay variability all Real Time qPCR reactions were carried out in triplicate.

Real Time qPCR amplifications were run in a ViiATM7 Real Time PCR System (Applied Biosystems) thermal cycler, using a specific thermal profile composed by four steps. The fist cycle, for cDNA denaturation, was at 95°C for 10 min. Second step was characterized by 40 cycles for amplification at 95°C for 15 sec and 60°C for 1 min. Following step was for final elongation at 72°C for 5 min. Last cycle, for melting curve analysis (from 60°C to 95°C), was set to verify the presence of a single product. Fluorescence was measured using ViiATM7 Software (Applied Biosystems). The expression of each gene was analysed and internally normalized against *Pl-Z*12–1 endogenous control using REST software (Relative Expression Software Tool) based on the Pfaffl method (Pfaffl 2001; Pfaffl et al., 2002). Evaluation of the relative expression ratio (*R*) of a target gene took into consideration *E* value and the CP deviation of an unknown sample versus a control; *R* was expressed in comparison to a reference gene:

$$R = \frac{(E_{target})^{\Delta CP_{target}(control - sample)}}{(E_{ref})^{\Delta CP_{ref}(control - sample)}}$$

The equation shows the most convenient mathematical model, because considers an efficiency correction for real time PCR efficiency of the individual transcripts (Pfaffl 2001). The ratio of a target gene is expressed in a sample versus a control in comparison to a reference gene. E_{target} is the Real Time PCR efficiency of target gene transcript; E_{ref} is the Real Time PCR efficiency of a reference gene transcript; ΔCP_{target} is the CP deviation of control – sample of the target gene transcript; ΔCP_{ref} is the CP deviation of control – sample of the reference gene transcript. Only expression values greater than a 2.00-fold difference with respect to the controls were considered a significant variation of gene expression.

2.9 Maintenance and treatment of A549 with heptadienal

A549 (ATCC CCL185) human lung adenocarcinoma cells were cultured in DMEM medium (Dulbecco's modified Eagle's medium) supplemented with 10% (v/v) fetal bovine serum (FBS), 100 units ml-1 penicillin and 100 μg ml^{-1} streptomycin. Cells were seeded in flasks and incubated in a 5% CO_2 humidified chamber at 37 °C for growth. Medium renewal occurred every 3 days, and cells were detached via trypsinization before they reached confluence. A549, (20 x 10^6 cells $well^{-1}$) were seeded in Petri dishes (100 mm diameter) and kept overnight for attachment. The next day, the medium was replaced with fresh medium containing 5μM of heptadienal. The experiment was performed in triplicate and cells collected after 2 hours for RNA extraction and gene expression analysis.

2.10 RNA Extraction and Real-Time PCR of the cell samples

After 2 hours of treatment, A549 cells were washed directly in the Petri dish by adding cold PBS and rocking gently. Cells were lysed in the Petri dish by adding 1 ml of Trisure Reagent (Bioline, cat. BIO-38033) per 100 mm diameter dish. RNA was isolated according to the manufacturer's protocol of the extraction reagent. RNA concentration and purity was assessed using the nanophotomer NanodroP (Euroclone). RNA concentration was measured for each sample by the aborbance at 260 nm, using the nanophotomer NanodroP (ND-1000 UV-Vis Spectrophotometer; NanoDrop Technologies). The purity of the RNA samples were evaluated by 260 nm/280 nm and 260 nm/230 nm ratios, indicative of presence of protein and phenolic residues, respectively. 200 ng of RNA was subjected to reverse transcription reaction using the RT2 first strand kit (Qiagen, cat.330401) according to the manufacturer's instructions. Real-Time quantitative reverse

transcription PCR (qRT-PCR) was performed in triplicate using the RT^2 Profiler PCR Arrays kit (Qiagen, cat.330231) to analyze the expression of death cell signaling genes in the human cell lines. Plates were run on a ViiA7 (Applied Biosystems 384 well blocks), Standard Fast PCR Cycling protocol with 10 µl reaction volumes. Cycling conditions used were: 1 cycle initiation at 95.0 °C for 10 min followed by amplification for 40 cycles at 95.0°C for 15 s and 60.0 °C for 1 min. Amplification data were collected via ViiA 7 RUO Software (Applied Biosystems). Ct-values were analyzed with PCR array data analysis online software (http://pcrdataanalysis.sabiosciences.com/pcr/arrayanalysis.php, Qiagen).

CHAPTER 3.

Results

3.1 Morphological analysis of the effects of Heptadienal on *Paracentrotus lividus* embryos development

The present study intends to evaluate the effect, at morphological and molecular level, of the aldehyde heptadienal on sea urchin *P. lividus* embryos development. Sea urchin eggs were exposed to increasing concentrations of the pure compound: 2.0 μM, 2.5 μM, 3.0 μM, 5.5 μM and 6 μM. After 10 minutes from the treatment, sea urchin eggs were fertilized with diluted sperm mix and let to develop in standardised conditions.

The morphological analysis was carried out at 48 hours after fertilization (larva stage, pluteus), comparing the normal embryo body structures of controls with sea urchin embryos treated with different concentrations of heptadienal. Only three biological replicate were considered suitable for further experiment because they showed similar morphological response to the heptadienal.

The observation of plutei by microscope revealed strong morphological differences between control and treatment experiments. The percentage of abnormal plutei increased proportionally with heptadienal concentrations. As shown in figure 3.1, 2.0 μM of the aldehyde induced malformations in 15% of sea urchin embryos treated. Around 24% of total embryos treated with 2.5 μM of the aldehyde showed significant abnormality. 3.0 μM of heptadienal caused malformations in 37% of plutei exposed to the treatment. 61% of total sea urchin embryos treated with 5.5 μM of pure compound showed developmental abnormalities. 6.0 μM of the aldehyde induced malformations in around 74% of treated plutei.

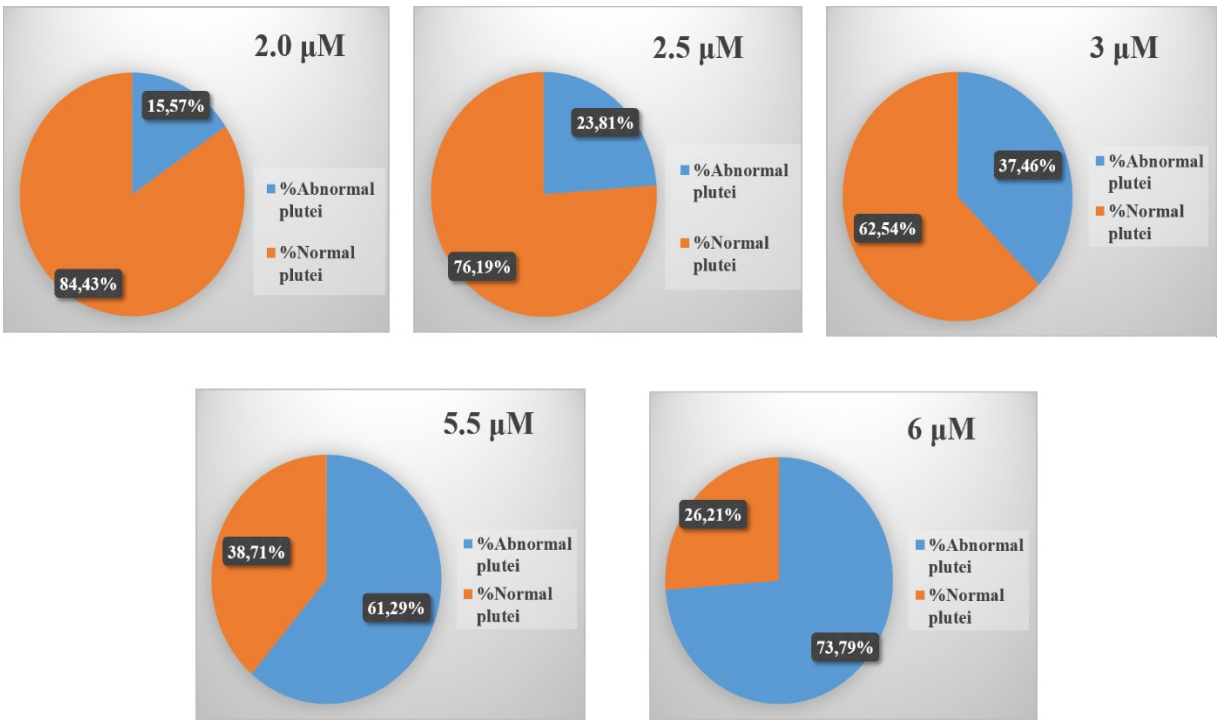

FIGURE 3.1: Morphological effects of five different heptadienal concentrations (2.0 µM, 2.5 µM, 3.0 µM, 5.5 µM and 6.0 µM) on sea urchin *Paracentrotus lividus* embryo development. For each concentration of pure compound, embryos at the pluteus stage were analysed under the microscope and divided in 'Normal plutei' and 'Abnormal plutei'. The ratio between the two different morphological groups is expressed as percentage respect to the entire number of embryos examined.

More in detail, heptadienal was able to cause significant malformations along entire body of sea urchins and delay of embryo development. In particular, each pluteus was classified as abnormal when entire body was malformed, but also when malformations occurred in specific structures and appendices of the larva, such us spicules, arms and apex (figure 3.2). Sometimes arms asymmetrical crooked or degraded; they could be found longer and broader than in the negative control. Spicules development was another important parameter for evaluation of abnormality. Microscopic observation revealed poorly formed and parallel spicules in plutei treated with heptadienal. Spicules were also found to be unattached at the tip and/or with crooked apex.

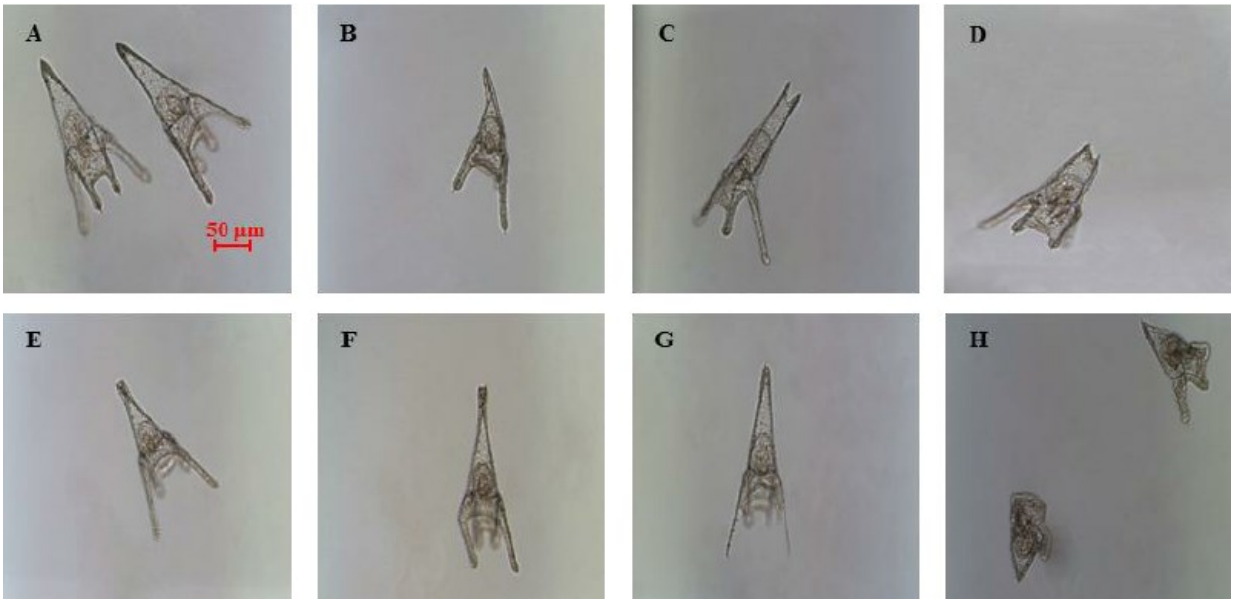

FIGURE 3.2: Pictures obtained by inverted microscope showing some examples of different types of malformations induced in Paracentrotus lividus plutei at 48 hours post fertilization (hpf) after incubation with the three polyunsaturated aldehydes (**B**, **C**, **D**, **E**, **F**, **G** and **H**) in comparison with the normal conformation (**A**) of the control. Embryos were fixed with 4% of paraformaldehyde (modified from Varrella et al.,2014).

3.2 Gene structures and aminoacid sequences of *Paracentrotus lividus* identify by bioinformatic study

The annotation of the gene structure was instrumental to design primers able to amplify coding regions that anneal to genomic sequences on intron to exons boundary.

The genes Apoptosis Inducing Factor, Mitochondria Associated 1 (Aifm1), Receptor Interacting Serine/Threonine Kinase (Ripk), Tumor Necrosis Factor Receptors 16 (Tnfr16) and Tumor Necrosis Factor Receptors 19/27 (Tnfr19/27) are considered key factors involved in the extrinsic apoptosis death signaling pathway (figure 3.3).

A

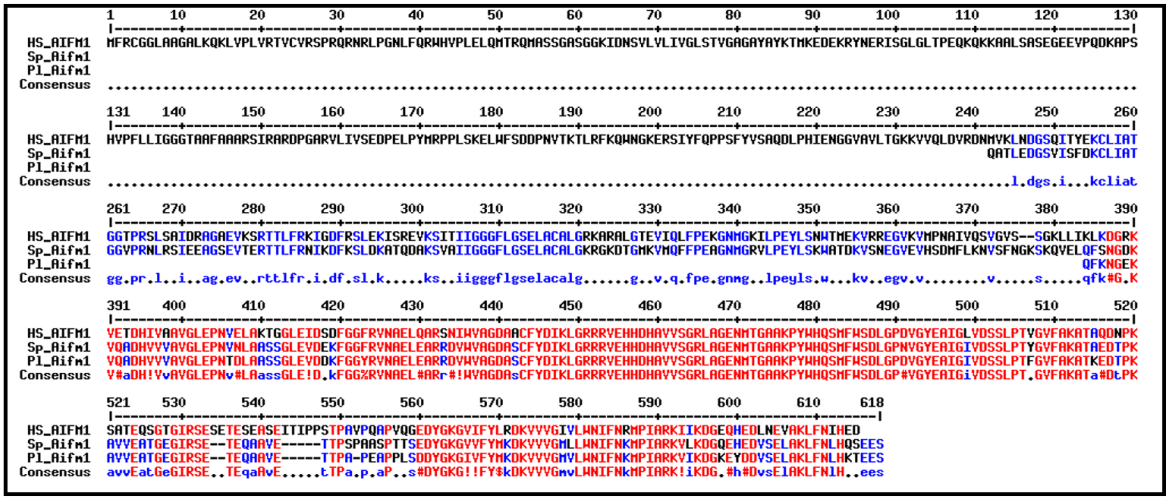
HS_AIFM1 MFRCGGLAAGALKQKLVPLVRTVCVRSPRQRNRLPGNLFQRWHVPLELQMTRQMASSGASGGKIDNSVLVLIVGLSTVGAGAYAYKTHKEDEKRYNERISGLGLTPEQKQKKAALSASEGEEVPQDKAPS
HS_AIFM1 HVPFLLIGGGTAAFAAARSIRARDPGARVLIVSEDPELPYMRPPLSKELWFSDDPNVTKTLRFKQWNGKERSIYFQPPSFYVSAQDLPHIENGGVAVLTGKKVVQLDVRDNMVKLNDGSQITYEKCLIAT
HS_AIFM1 GGTPRSLSAIDRAGAEVKSRTTLFRKIGDFRSLEKISREVKSITTIGGGFLGSELACALGRKARALGTEVIQLFPEKGNMGKILPEYLSNWTMEKVRREGVKVMPNAIVQSVGVS--SGKLLIKLKDGRK
HS_AIFM1 VETDHIVAAVGLEPNVELAKTGGLEIDSDFGGFRVNAELQARSNIWVAGDAACFYDIKLGRRVEHHDHAVVSGRLAGENMTGAAKPYWHQSMFWSDLGPDVGYEAIGLVDSSLPTVGVFAKATAQDNPK
HS_AIFM1 VQADHVVVAVGLEPNVLAASSGLEVDEKFGGFRVNAELEARRDVWVAGDASCFYDIKLGRRVEHHDHAVVSGRLAGENMTGAAKPYWHQSMFWSDLGPNVGYEAIGIVDSSLPTYGVFAKATAEDTPK
HS_AIFM1 VQADHVVVAVGLEPNTDLAASSGLEVDDKFGGYRVNAELEARRDVWVAGDASCFYDIKLGRRVEHHDHAVVSGRLAGENMTGAAKPYWHQSMFWSDLGPDVGYEAIGIVDSSLPTFGVFAKATKEDTPK
HS_AIFM1 SATEQSGTGIRSESETESEASEITIPPSTPAVPQAPVQGEDYGKGVIFYLRDKVVVGIVLWNIFNRMPIARKIIKDGEQHEDLNEVAKLFNIHED
HS_AIFM1 AVYERTGEGIRSE--TEQAAVE-----TTPSPAASPTTSEDYGKGVVFYMKDKVVVGHLLWNIFNKMPIARKVLKDGQEHEDVSELAKLFNLHQSEES
HS_AIFM1 AVYERTGEGIRSE--TEQAAVE-----TTPA-PEAPPLSDDYGKGIVFYMKDKVVVGMVLWNIFNKMPIARKVIKDGKEYDDVSELAKLFNLHKTEES

B

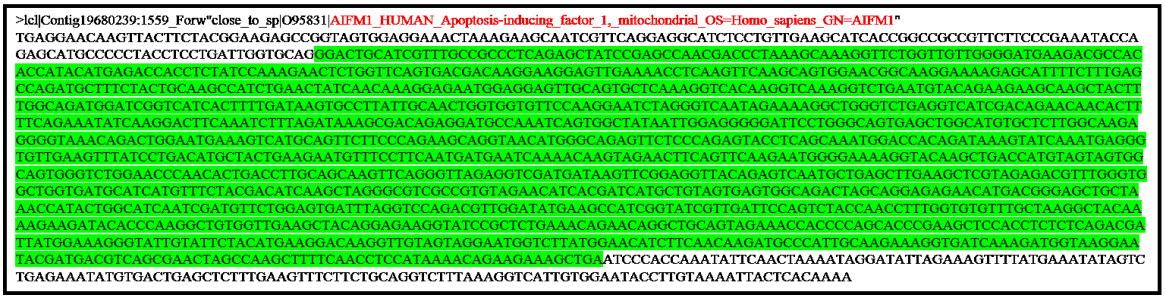
>lcl|Contig19680239:1559_Forw"close_to_sp|O95831|AIFM1_HUMAN_Apoptosis-inducing_factor_1,_mitochondrial_OS=Homo_sapiens_GN=AIFM1"

C

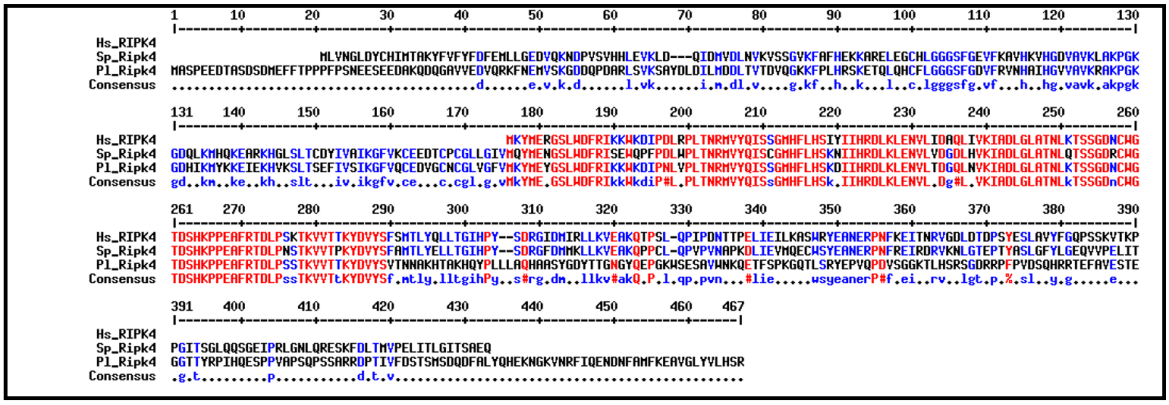
Hs_RIPK4
Sp_Ripk4 MLVNGLDYCHIMTAKYFVFYFDFEMLLGEDVQKNDPVSVHHLEVKLD---QIDMVDLNVKVSSGVKFAFHEKKARELEGCHLGGGSFGEVFKAVHKVHGDVAVKLAKPGK
Pl_Ripk4 MASPEEDTASDSDMEFFTPPPFPSNEESEEDAKQDQGAVVEDVQRKFNEMVSKGDDQPDARLSVKSAYDLDILMDDLTVTDVQGKKFPLHRSKETQLQHCFLGGGSFGDVFRVNHAIHGVVAVKRAKPGK
Hs_RIPK4 MKYMERGSLHDFRIKKWKDIPDLRPLTNRMVYQISSGMHFLHSIYIIHRDLKLENVLIDAQLIVKIADLGLATNLKTSSGDNCWG
Sp_Ripk4 GDQLKMHQKEARKHGLSLTCDYIVAIKGFVKCEEDTCPCGLLGIVHQYMENGSLHDFRISEWQPFPDLWPLTNRMVYQISCGMHFLHSKNIIHRDLKLENVLVDGDLHVKIADLGLATNLQTSSGDRCWG
Pl_Ripk4 GDHIKMYKKEIEKHVKSLTSEFIVSIKGFVQCEDVGCNCGLVGFVMKYMEYGSLHDFRIKKWKDIPNLVPLTNRMVYQISSGMHFLHSKDIIHRDLKLENVLTDGQLNVKIADLGLATNLKTSSGDNCWG
Consensus gd..km..ke..kh..slt...iv.ikgfv.ce...c.cgl.g.vMKYME.GSLHDFRIKkWkdiP#L.PLTNRMVYQISsGMHFLHSk.IIHRDLKLENVL.Dg#L.VKIADLGLATNLKTSSGDnCWG
Hs_RIPK4 TDSHKPPEAFRTDLPSKTKVVTTKYDVYSFSMTLYQLLTGIHPY--SDRGIDMIRLLKVEAKQTPSL-QPIPDNTTPELIEILKASWRYEANERPNFKEITNRVGDLDTDPSYESLAYYFGQPSSKVTKP
Sp_Ripk4 TDSHKPPEAFRTDLPNSTKVVTPKYDVYSFAMTLYELLTGIHPY--SDRGFDMMKLLKVEAKQPPCL-QPVPVNAPKDLIEVMQECWSYEANERPNFREIRDRVKNLGTEPTYASLGFYLGEQVVPELIT
Pl_Ripk4 TDSHKPPEAFRTDLPSSTKVVTTKYDVYSVTNNAKHTAKHQYPLLLAQHAASYGDYTTGNGYQEPGKWSESAVWNKQETFSPKGQTLSRYEPVQPDVSGGKTLHSRSGDRRPFPVDSQHRRTEFAVESTE
Consensus TDSHKPPEAFRTDLPssTKVVTsKYDVYSf.mtLy.lltgiHPy..s#rg.dm..llkv#akQ.P.l.qp.pvn...#lie.....wsyeanerP#f.ei..rv..lgt.p.%.sl..y.g.....e...
Hs_RIPK4
Sp_Ripk4 PGITSGLQQSGEIPRLGNLQRESKFDLTMVPELITLGITSAEQ
Pl_Ripk4 GGTTYRPIHQESPPVAPSQPSSARRDPTIVFDSTSMSDQDFALYQHEKNGKVNRFIQENDNFAMFKEAVGLYVLHSR
Consensus .g.t.....p.....d.t.v.....

D


>lcl|scaffold10601length=40299
[...]
[...]

E

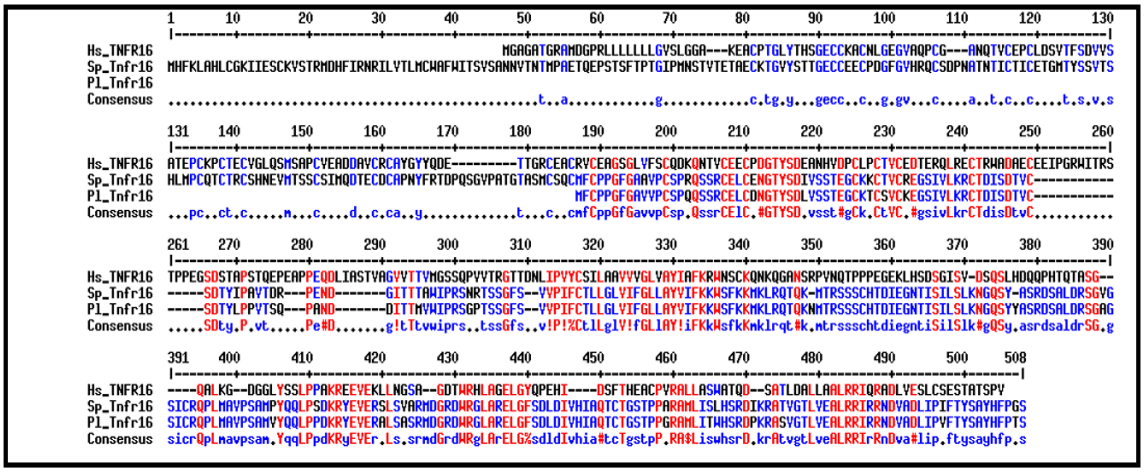

F

>lcl|scaffold20496 length=5837 (Reverse and complement)

[...]TCATTTCATTTTCTGTTGCAGAGCACCATGCCCGCTGAAACCCAAGAGCCTCTGACGTCTTTGACACCACCAACGGATAAACCAATGAATGCAACAGCCG
AATGCCCGACAGGAGTCCTTTCCACCACCGGTGAATGTTGCGAGGAGTGTCCGGTTGGCTTCGGCGTTCATCGGAAATGTTCGGACCCTAATGGCACCAACA
CGATCTGTACCATCTGCGAACCGGGTATGACATACTCTTCCATCACAAGTCACGTAGCGTCATGCCAAACCTGCTCTCGATGTAGCCACACTGAGGTGATGA
CGTCAGCCTGCAGCATCATGCAAGACACTGTGTGCGAGTGCGCGCCAAACTATTTCCGGACGGACGCGCAGCCGAGTGGCACTTCGGCGGTGGGGACCGCC
TCAACGTGCAGCCAGTGTATGTTCTGTCCTCCTGGGTTCGGTGCGGTAGTTCCTTGTTCGCCTCAACAGAGTTCTAGATGCGAACTGTGTGACAATGGAACCT
ACTCGGATCTCGTCAGTTCAACGGAAGGATGTAAAACATGTTCAGTCTGCAAGGAGGGTAGCATTGTACTCAAGAGATGCACTGATATCTCAGATACAGTAT
GCTCAGGTAAGTGATATACATGTAAAAGTAATTTAATCTCAATTAACAAGCGCCTTGGACAGTTGAGATAATTCAGAATTATTT[...]CCCTCATTAATTGGTA
ATCATTAATACACTGCACTTAAATAAATCATAAATCGATATCCCCTAATCCCTTTACTTGATACTTCTCTACACAGATACCTACCTACCACCAGTGACTTCCC
AACCAGCCAATGATGACATCACGACGATGGTATGGATTCCGAGGTCGGGCCCGACATCGTCCGGTTTCAGCGTCGTGCCCATCTTCTGTACCCTCCTTGGAC
TCGTCATCTTTGGTCTGCTTGCTTACGTCATCTTCAAAAAATGGTCCTTCAAGAAAATGAAGCTGAGGCAGACACAGAAGAACATGACCAGGTTGGTAGGCT
TGGCATGTTTTCAAAGAAGAGCCAATCATTATTGGCCAATGGCTATATGCCACAGGGGTCGCAGTCACATTT[...]CTAAATGTAAAATAACATATTTTCTATG
TTTCTTTCACAAACCAGGTCGAGTTCGTGCCATACCGATATTGAAGGAAACACAATATCAATCCTTTCACTGAAGAATGGTCAGAGCTATTATGCATCCAGG
GATTCAGCCCTAGATCGATCAGGTGCCGGCAGTATCTGCAGACAACCTCTTATGGCAGGTGATTATGCATGCACAGAACTAGCAAAAGTTTAATTGTTAC[...]
GAATACTGGCTACTTTACTAAAGTCCTTCGGCAAGACATTGATCTGCTACACTCGACCCAGGTGAAAATAATGGGCACTATGAGAAATTGGGATGTTATATA
TGATGGTGAAATGCGCTATTACAATGTTGTCATCTGTCTTTTTCCCCCTCCCAGTTCCCAGTGCGATGGTGTATCAGCAACTGCCTCCAGACAAACGTTACGA
GGTGGAACGCGCCCTCTCCGCTTCCAGGATGGATGGCCGTGACTGGCGGGGTCTGGCCCGGGAACTAGGATTCTCCGATCTAGATATTGTCCACATCGCTCA
GACGTGTACAGGCTCAACGCCTCCAGGTAGAGCAATGCTCATTTCCTGGCACAGCAGAGACCCCAAACGCGCATCTGTCGGGACGCTCGTCGAAGCGCTGC
GGAGGATACGACGAAATGATGTTGCCGATTTAATACCAGTTTTCACCTATAGTGCTTATCATTTTCCTACTTCATGATGTCAGCTGCAAAAATATCAAAATGT
TTTACTAAAAATGGACTACTTGTAA[...]

G

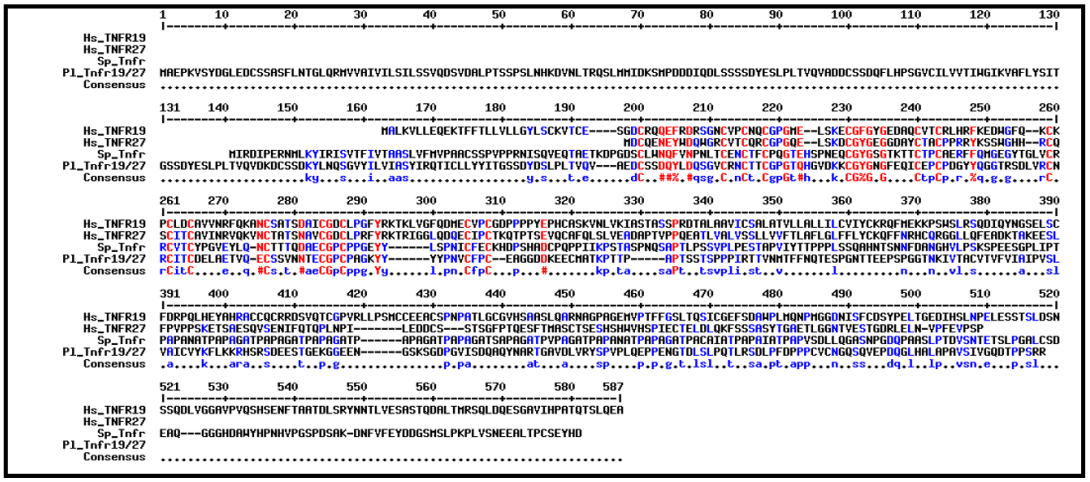

H

FIGURE 3.3: Extrinsic apoptotic pathway: (**A**, **C**, **E** and **G**) Multialignment of aminoacid sequences AIFM1, RIPK4, TNFR16 and TNFR27 from *Homo sapiens*, *Strongylocentrotus purpuratus* and *Paracentrotus lividus*. (**B**, **D**, **F** and **H**) Complex intron-exon structure of the *P. lividus* genes involved in extrinsic apoptosis.

In particular, Pl_Aifm1 was found to be the ortholog of human Apoptosis Inducing Factor, Mitochondria Associated 1 (Hs_AIFM1), in *P. lividus*. As shown in figure 3.3, this gene is intron-less, since the CDS is contained in a single exon. On the other hand, bioinformatic analysis of Pl_Ripk did not conduct to a clear orthology with a specific human gene belonging to the Receptor Interacting Serine/Threonine Kinase (RIPK) superfamily. Nevertheless, Pl_Ripk represented the only element found in *P. lividus* with nucleotide and aminoacid sequence having the highest similarity to queries used (Hs_RIPK1 and Sp_Ripk), and characterized by a CDS derived from eight exons. To obtain this result was necessary annotation for the scaffold found in *P. lividus* database and phylogenetic study

among members of this Receptor superfamily from *H. sapiens*, *S. purpuratus* and *P. lividus* (figure 3.4).

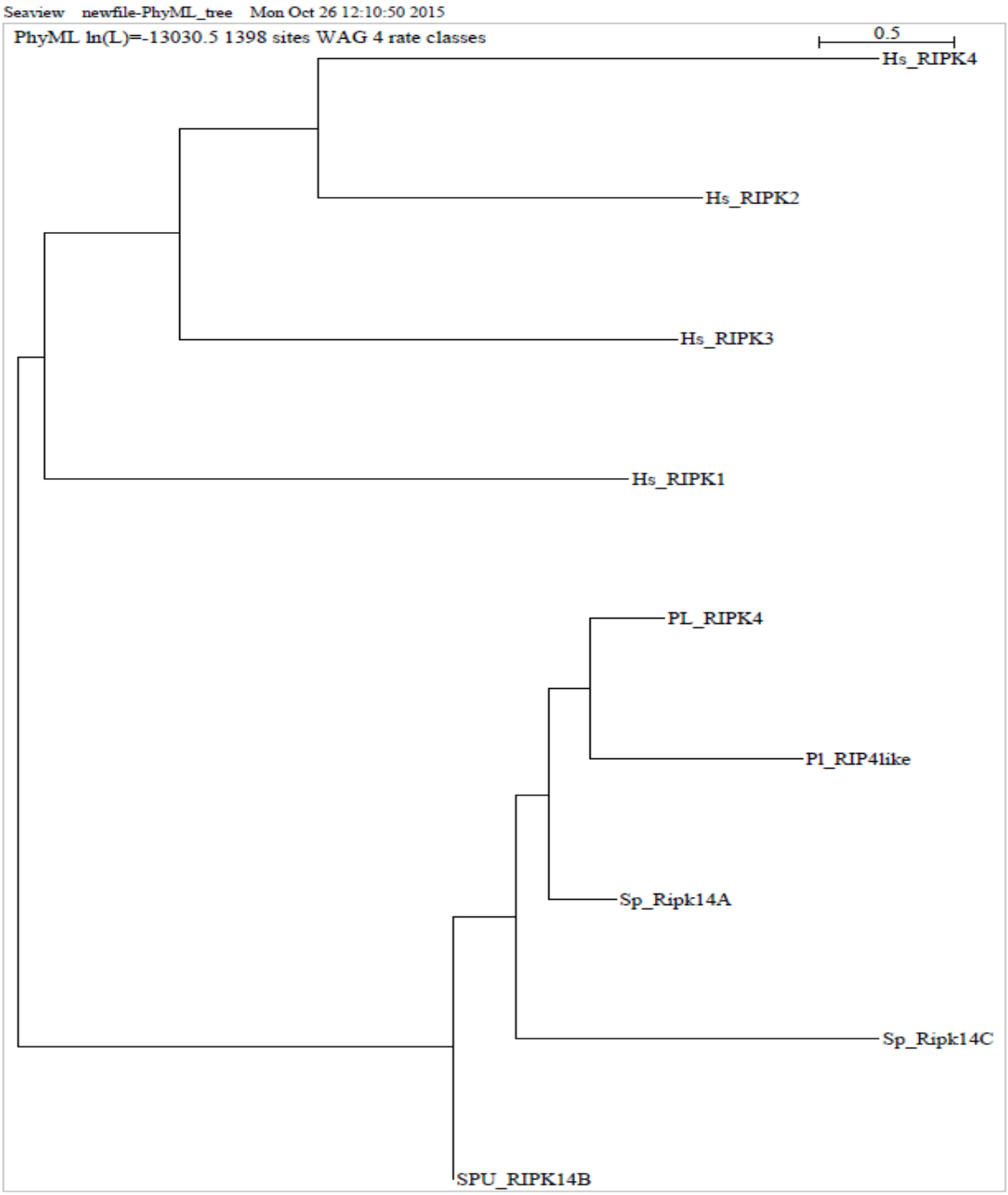

FIGURE 3.4: Phylogenetic tree showing the inferred evolutionary relationship among various members of the Receptor Interacting Serine/Threonine Kinase (RIPK) superfamily from *Homo sapiens*, *Strongylocentrotus purpuratus* and *Paracentrotus lividus*.

The only two genes belonging to the Tumor Necrosis Factor Receptors (TNFR) superfamily identified in *P. lividus* were Pl_Tnfr16 and Pl_Tnfr19/27. Annotation and phylogeny were necessary to establish orthologous relationship between TNF receptors superfamily members from *H. sapiens* and *P. lividus*. As it is possible to deduce from the phylogenetic analysis (figure 3.5), Pl_Tnfr16 is the clear ortholog of human gene Hs_TNFR16 and *S. purpuratus* gene Sp_Tnfr16; Pl_Tnfr19/27 seem to be the single correspondent gene of human onhologs Hs_TNFR19 and Hs_TNFR27. Both genes are characterized by a complex intron-exon structure, being multi-exon genes. The primary transcript contains 4 exons from Pl_Tnfr16 and 7 exons from Pl_Tnfr19/27.

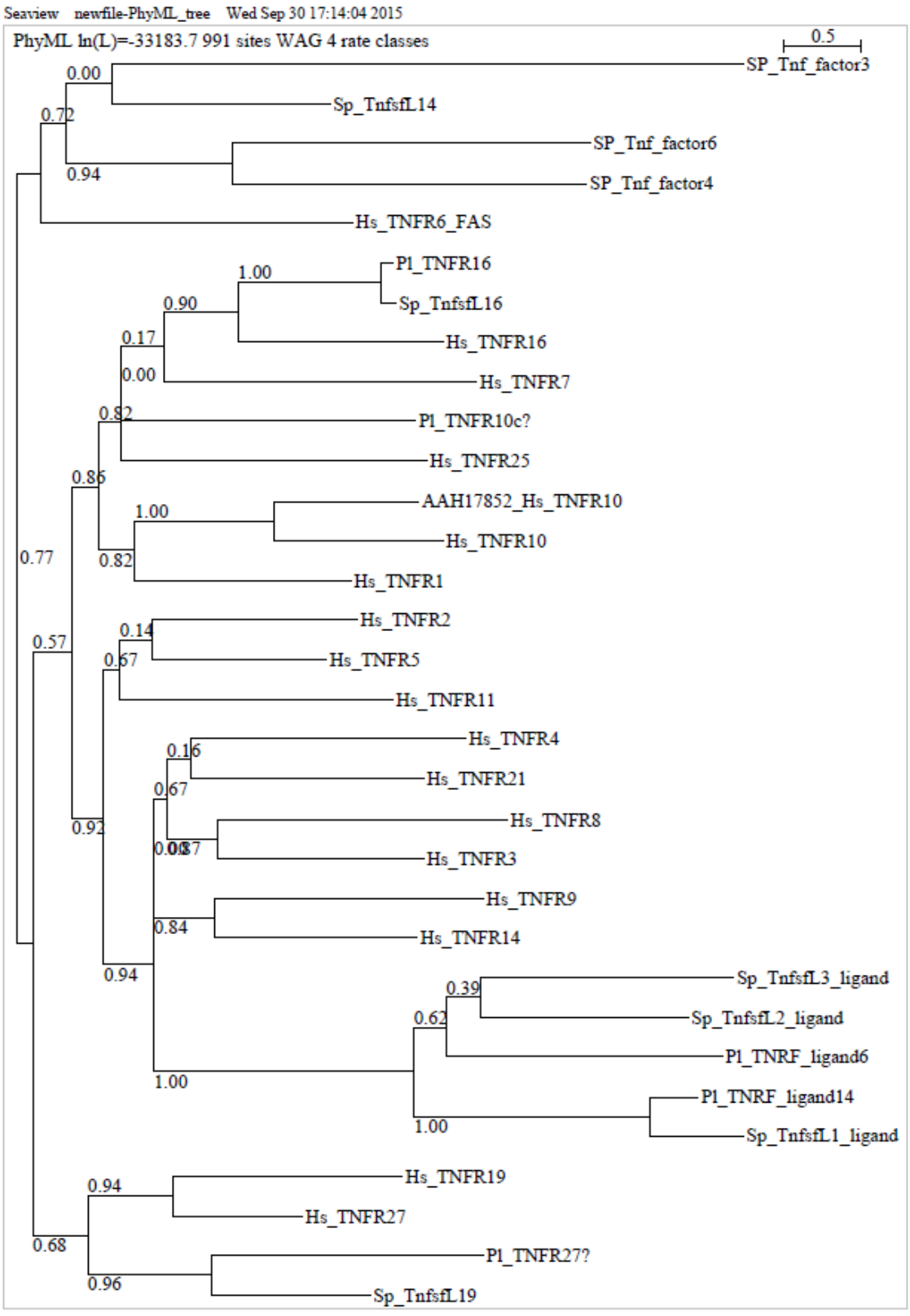

FIGURE 3.5: Phylogenetic analysis showing the inferred evolutionary relationship among various members of the Tumor Necrosis Factor Receptor (TNFR) superfamily from *Homo sapiens*, *Strongylocentrotus purpuratus* and *Paracentrotus lividus*.

The genes BCL2 Associated X Protein (BAX), B-Cell CLL/Lymphoma 2 (BCL_2) and Poly ADP-Ribose Polymerase 1 (PARP1) are considered key factor involved in the intrinsic apoptosis death signaling pathway. In more detail, Pl_Bax was found to be a clear ortholog of human gene Hs_BAX and, as shown in figure 3.6, this sea urchin gene is characterized by a single exon (intronless). On the contrary, the others two genes possess a complex intron-exon structure. Pl_Bcl2 primary transcript contains 6 exons and this gene is a clear ortholog of the human Hs_BCL2. Pl_Parp is the ortholog of the human gene Hs_PARP1 and the relative primary transcript contains 13 exons.

A

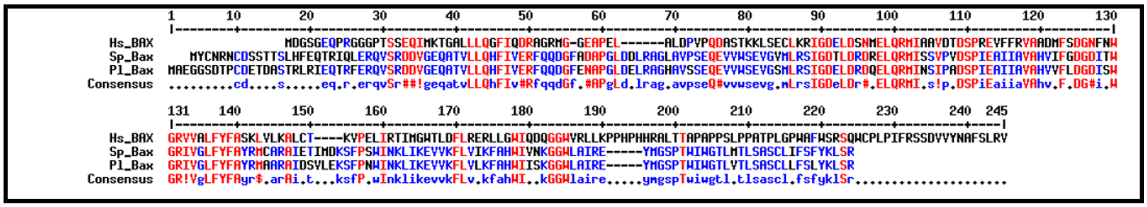

B

>lcl|ATILLocus_3927_Transcript_8/8_Confidence_0.680_Length_2685

[…]AGATCGATCAGCGAGTAGAGGAAACAAGAAAGGACAATATCTCGTCAGTATTACCCCTACCCATTCCATTCAACAATCAAATAGACCCAAACAATGGCT
GAAGGGGGCTCGGATACTCCTTGTGATGAAACTGATGCATCAACCCGTTTGCGTATCGAGCAGACACGGTTTGAGCGTCAGGTGAGCCGCGATGATGTTGGG
GAGCAGGCCACTGTTCTCCTTCAACATTTCATTGTGGAGCGTTTCCAGCAGGACGGCTTTGAGAATGCCCCAGGTTTAGATGAACTGAGGGCGGGGCATGCTG
TGTCGAGTGAGCAGGAGGTCGTCTGGTCAGAGGTCGGGTCAATGCTGAGGTCAATCGGGGACGAGTTGGACAGAGATCAGGAGCTGCAGAGAATGATAAAC
TCCATACCAGCCGACTCTCCAATCGAGGCTATCATAGCAGTGGCCCATGTGGTCTTTCTTGATGGTGATATCTCATGGGGCAGGATAGTAGGTCTATTCTACTT
CGCTTACAGAATGGCTGCCAGGGCAATAGACTCTGTATTGGAGAAGAGCTTTCCAAACTGGATCAACAAACTGATCAAAGAAGTCGTCAAGTTTCTCGTCCT
CAAGTTTGCTCACTGGATCATCAGCAAGGGTGGATGGCTGGCCATCCGAGAATACATGGGCTCACCCACATGGATATGGGGCACTCTGGTAA[…]

C

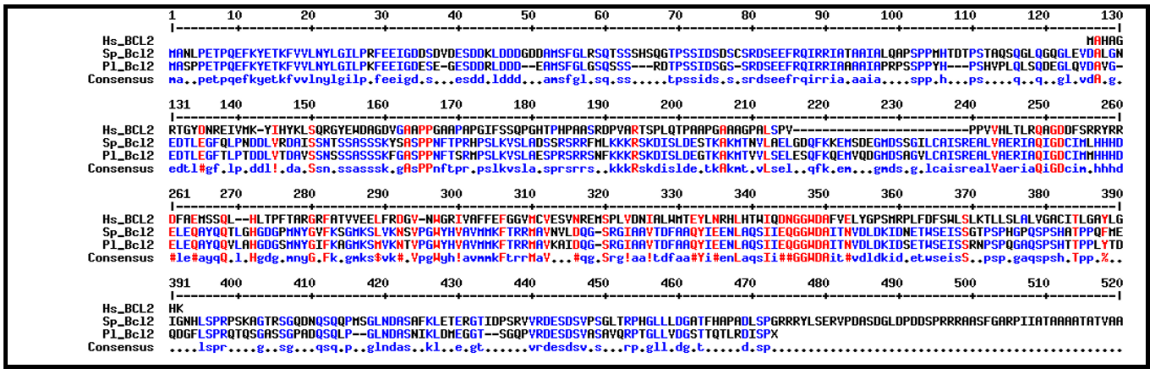

D

>lcl|scaffold12593 length=31907 (Reverse and Complement)

[…]AATCTACTCGTGCATGATGTTAACCTTATAATTTAAACTTTAATTATTAAAGAATTGGTATTTTCAAATTATTACTGCTTCATCTTTGTACCTCTTCTTTCA
TGACATTAGATCAGGCATGGCAAGCCCTCCGGAGACACCCCAGGAGTTCAAGTATGAGACCAAGTTTGTCGTCCTCAACTACCTTGGTATCCTGCCTAAGTTT
GAGGAGATCGGGGATGAGTCTGAAGGAGAGAGTGATGATAGGCTTGATGATGATGAGGCAATGAGCTTCGGATTGGGAAGTCAATCCAGCTCAAGAGGTTA
GTCGGAGTTGGCATGTGCCTTGTAGTTAGAATTTTTTTTTCTCCATTGGATGCAAAATGTTGATGGTTAACTATATGTACAT[…]TTATAATTTATTATCTTATTT
ATTAAAAACAGATGCTTTACACCATCAAAAAATGTTTATTGACCAAATATATTTTTTGTTTGTTAAAATTCCATGTGACAGATACCCCCTCTAGTATAGACAGT
GGCAGTAGCAGAGATAGTGAAGAATTCCGTCAGATCAGGCGAATCGCTGCAGCGGCAATCGCTCCTCGACCAAGCTCTCCTCCTTATCATCCCTCCCACGTCC
CTCTCCAGCTATCGCAAGATGAGGGGCTCCAGGTGGATGCAGTCGGTGAGGACACCCTCGAGGGATTTACGTTACCGACCGACGATTTGGTGACCGATGCCG
TCTCGTCTAATTCTTCATCAGCATCCAGTTCCAAGTTTGGTGCATCACCACCTAATTTCACCTCGAGAATGCCTTCTCTGAAAGTTTGTAAGTTTACCAGTTTTA
CTGATTTCATTTGCAATTTCAAGAATTAATCGAACTTTAGATATTTCTTGCGTCAGTATACAATTCATGATACATGCTTCTCTTCTATCCAATTTTCCCCCATTG
TACTGCAAAAATTAAAAAGTAAGACTCAATGTATATGAGGTAATA[…]AAAATGAGATAAAGAATAGAGAAACGATGACAAGAAATATGAGTGGTAATATT
CATAAGAGCATACATTAATTTTTATTATCACTCTTCTGTCTCCAGCTTTAGCTGAGTCTCCCAGATCCCGAAGATCGAATTTCAAGAAGAAGAGGAGCAAGGA
TATTTCACTTGATGAAGGGACCAAAGCCAAGATGACCGTGGTCCTCTCAGAACTAGAATCACAGTTCAAACAAGGTATCCATATTGTTTTATTATCAGAATAT
GAGAAGTGCAAATTCAAGATGTTTTGTTACAA[…]ATATGAACATTTAGAGAAGGTGTGTAATGTGTAGTTCTTTGTGTGATTTTTTTATGGATCTAAATTAA
TTGGATATTTTATTAAAAATGTAAATAAAATTGTTTTCGCTAATCACTTTCCAGAAATGGTACAGGATGGCATGGACTCGGCAGGGGTACTGTGTGCCATCAG
TCGGGAGGCTCTCGTCGCAGAGAGGATTGCCCAGATCGGAGACTGTATCATGATGCACCATCATGACGAATTGGAACAAGCCTACCAGCAGGTCCTAGCCCA
TGGGGATGGGTCTATGAACTATGGTATCTTCAAAGCGGGCATGAAAAGCATGGTTAAAAACACTGTTCCAGGATGGTACCATGTAAGAAGAGAATTTCCTTC
ATTCTTTTCGTTCTTATAGTTGCCAAAAGGCAATAAGCTCATGGTAATAGTGTCATGGGATGTGTTTCCTAATAATTGATATCACCTCTCAGTGGTATGCAAGA
ACTAGGT[…]GTAATTTCTGAAGGTTGTATACCCTTAGTGGTAAGAAAAGAGGTTTACAAAATGTGTGTGATCTTGATCAATGCTATCATTTTGCTGTTTTCAG
GTTGCAGTAATGATGAAATTCACCAGACGGATGGCAGTCAAAGCGATAGATCAAGGGAGTAGGGGTATAGCGGCAGTCACTGATTTTGCAGCACAGTACATT
GAGGAAAACCTAGCCCAATCTATTATAGAACAAGGAGGATGGGTGAGTATTGAGGCTTGAAGGGGAATTCACCCTGGAATTGAATTTGTTGTTAAAATTGCC
TCATTATCATTAAAGTTTGGCAGAAGTTAAACCCCAGGATATGATTGTAAAAACTATTTCTGTATCAGCTTGAAGAAAGTTTAAGAAAATAAGTGAAGTTGGT
TAAATGCTCTTTAAATAAGTGAAGTTGGTTAAATGAACTTAAATTCATATGGCTATGGATTATTTTTTTTACAGGATGCCATAACCAACGTTGATTTAGACAAG
ATAGACAGCGAGACATGGTCTGAGATATCATCCAGGAACCCTTCACCTCAAGGAGCCCAGTCACCATCACACACTACTCCACCCCTCTACACGGACCAAGAT
GGTTTCCTCTCTCCTAGGCAGACCCAATCAGGTGCGAGCTCTGGGCCAGCCGACCAATCACAGTTGCCCGGTTTAAACGATGCCTCCAACATCAAATTAGATA
TGGAGGGTGGGACGTCAGGACAGCCTGTAAGGGACGAATCGGATTCAGTTGCGTCCGCCGTACAAAGACCTACTGGACTACTTGTGGATGGATCAACGACTC
AGACCCTGAGAGACATCAGTCCTGGTTC[…]

E

F

FIGURE 3.6: Intrinsic apoptoc pathway: (**A**, **C** and **E**) Multialignment of aminoacid sequences of BAX, BCL2 and PARP from *Homo sapiens*, *Strongylocentrotus purpuratus* and *Paracentrotus lividus*. (**B**, **D** and **F**) Complex intron-exon structure of the *P. lividus* genes involved in intrinsic apoptosis.

The genes Beclin 1 (BECN1), PTEN Induced Putative Kinase 1 (PINK1), Unc-51 Like Autophagy Activating Kinase 1 (UKL1) and Unc-51 Like Autophagy Activating Kinase 3 (UKL3) are involved in the molecular pathway of autophagy. This set of genes contributes to induction of the mechanism,

formation of characteristic autophagosomes and activation of selective autophagic process as mitophagy, designed for the removal of damaged mitochondria (figure 3.7).

A

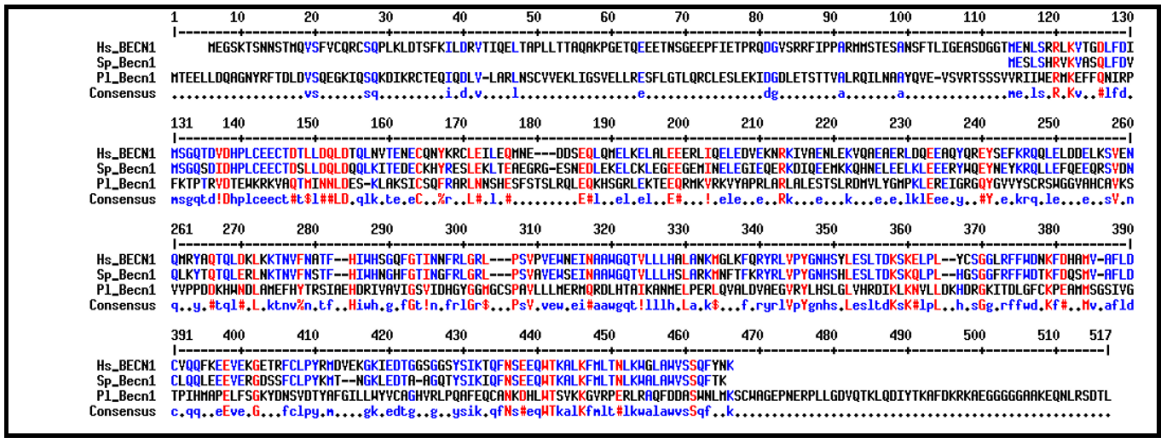

B

>lcl|scaffold46192 length=3508

[…]TACAGACGATGCTAAGCATTCTGCTGAACATGAGTAAATTAACTACCGCTCAATTGCAAGCTCAGCAGCCCGGTAGGGACGGGGACTACACGACTGGAA
ATGCTTGGTTTGCTGTGCTGCGTCGAAACGCACATGGTTTTCAAACCCATTCCAGAATGGGTTTGAAAATATGAGTATGAAATCATTGATATCTCGAAAGTAA
AGCAAGCAATTAGCTTGCAATTTTGAAGAGATGCCAGACTGACCTACCCGGTATGTGTTTATAATCATGTTTGCAAAATGAGCTAAATCGAATAAATTGTCAT
TTGAATATCATTCAATGTTAGTGCATCCCTTTAAATATTAAATTTTAAAATTCTGAAGTGGTGAAGTTATTCTGATGTTCCAATTGGCTAGCCATGCATCCTTC
AGACTTGCCTTCCATCAGTAATTACCAGCTCCATTGTTGAGAAATTGATGACCCTTTCAATCAATTTATATGTATCTGTTACATACACATGTACATGTATGTAT
GACAGTATGGGAGATCGACAGCATATGGTTCCCCTATGCTATACTTTGTTTTAAAGATTAATTTTCTTGTCTGACCTTTATCTTTTTAGATATCATATCAACTCT
TGTGTTGCCACCAGAGGCTGATGAAGTTGTTGGGAAGGTAACAAAGAATCCACCAGCTCTAGTCATCTTTGGTCAAACCTACACAAGTAAAGCAACCCTGGT
CAACAAAATCTTCAGGGAGGACCTCTTCCAGATTGTTGATGATTCGGATAACAATAAGACATGGCGAGCTGTACACCTGAAATACGGTTCCCAGCGGAACAC
GAGGTTGACCCTGACTAACAGTTTTGAGCTGGTCAATGGGGAGCCAGGATCTCCGGTAATGAGGAATTCTTGGACAGGGATTCCTAGAGTGGACATGCTTGT
GAAGGAGGAAGATCAGAAGGATGCATGTATGCTAAGTGCAACCACTGAGGCAACGCTGAATCATCCACTCCTCCAGTGCAAACTTCAAATTCTTGTCACTCC
GCATAACTGTCCTGGAATATCCATATCTCAAGCTTACAATGTGTGCACTCACAATATCCTCCCCGTGCTCTTGTACTGTTTCGATAAGGATCAATTATCGGAGG
AGAACCTTGGAAATTTGGATGAACTTCAGAATTGTGCTGGAACACTTCCCATCTTATTTGTAGACTGCAGGGAGCCGAGCGAACCGGTTGCGGCCCCCAGGG
AGAGGCATCTGGTCGAGGACGCCCATGAAGACTTTGATGAAGATTCTGCGTATGACACCGACGAGCGGATAGAAGGAGAGCGTGAAAGGCACAATGGGCTG
GGTGCTAGGTTGCGTCGCAGGTGCAGACCAGGGCTCAACGACAGGCCGAGTGTAATGGACCAGTTAGGCAGGGCAGGCTTTATCAACATTCCCGAAGAGAA
TGGTAGAATACGTGGTGTCCTTGACGCATTCACCATCGTCAACCAGTTGGAGGACATTCAAAACTCTATATCTATCGTGCAATTCATACGTCGTTCCTTGCAAT
ATTACCTGATCAGATGCTGTACTGCCATGCATGATCTCCATCAGCACTGCATGAATCTGTTCATTACGACAGCTTTCGACATGCAGCGGGATATCATGGTGAC
CCCAAAGCGCATTGAATATGCAAGACAGAGAGAGAATGAACTCTTTGACTCCTTGAAAGACCTAACTAATCAAAAGCAGGAGCAGCTTCGGACCTTGATTCA
AAGTACAGTTGCAGACATGACGGAGGAATTGCTTGATCAGGCTGGAAATTACAGATTTACAGGTTCGTAATATTTAT

C

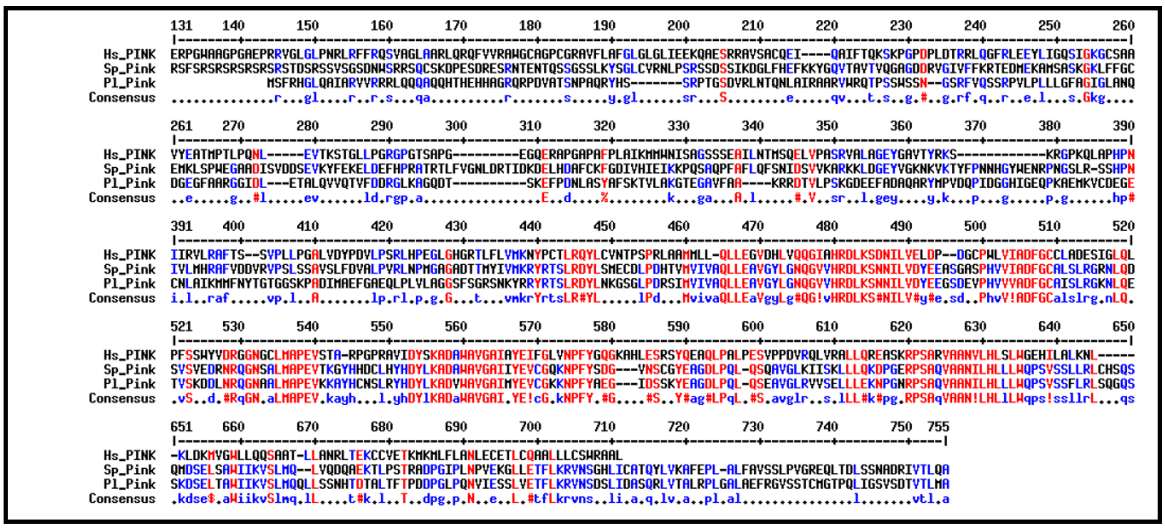

```
            131       140       150       160       170       180       190       200       210       220       230       240       250       260
            |---------+---------+---------+---------+---------+---------+---------+---------+---------+---------+---------+---------+---------|
Hs_PINK     ERPGWAAGPGAEPRRVGLGLPNRLRFFRQSVAGLAARLQRQFVVRAWGCAGPCGRAVFLAFGLGLIEEKQAESRRAVSACQEI----QAIFTQKSKPGPDPLDTRRLQGFRLEEYLIGQSIGKGCSAA
Sp_Pink     RSFSRSRSRSRSRSRSTDSRSSVSGSDNWSRRSQCSKDPESDRESRNTENTQSSGSSLKYSGLCVRNLPSRSSDSSIKDGLFHEFKKYGQVTAVTVQGAGDDRVGIVFFKRTEDMEKAMSASKGKLFFGC
Pl_Pink                 MSFRHGLQAIARVVRRRLQQQAQQHTHEHHAGRQRPDVATSNPAQRYHS-------SRPTGSDVRLNTQNLAIRAARVVRQTPSSWSSN--GSRFVQSSRPVLPLLGFAGIGLANQ
Consensus   .............r...gl....r..r.s...qa.........r.......s.....y.gl.....sr...S........e....qv...t.s..g.#..g.rf.q..r..e.l...s.Gkg....

            261       270       280       290       300       310       320       330       340       350       360       370       380       390
            |---------+---------+---------+---------+---------+---------+---------+---------+---------+---------+---------+---------+---------|
Hs_PINK     VYEATMPTLPQNL-----EVTKSTGLLPGRGPGTSAPG---------EGQERAPGAPAFPLAIKMMWNISAGSSSEAILNTMSQELVPASRVALAGEYGAVTYRKS----------KRGPKQLAPHPN
Sp_Pink     EMKLSPWEGAADISVDDSEVKYFEKELDEFHPRATRTLFVGNLDRTIDKDELHDAFCKFGDIVHIEIKKPQSAQPFAFLQFSNIDSVVKARKKLDGEYVGKNKVKTYFPNNHGYWENRPNGSLR-SSHPN
Pl_Pink     DGEGFAARGGIDL---ETALQVVQTVFDDRGLKAGQDT----------SKEFPDNLASYAFSKTVLAKGTEGAVFAA----KRRDTVLPSKGDEEFADAQARYMPVDQPIDGGHIGEQPKAEMKVCDEGE
Consensus   ..e.....g..#l.....ev......ld.rgp.a.................E..d....%.......k...ga...A.l.....#.V..sr..l.gey....y.k...p...g.....p.g.....hp#

            391       400       410       420       430       440       450       460       470       480       490       500       510       520
            |---------+---------+---------+---------+---------+---------+---------+---------+---------+---------+---------+---------+---------|
Hs_PINK     IIRVLRAFTS--SYPLLPGALVDYPDVLPSRLHPEGLGHGRTLFLVMKNYPCTLRQYLCVNTPSPRLAAMMLL-QLLEGVDHLVQQGIAHRDLKSDNILVELDP--DGCPWLVIADFGCCLADESIGLQL
Sp_Pink     IVLMHRAFVDDVRYPSLSSAVSLFDVALPVRLNPMGAGADTTMYIVMKRYRTSLRDYLSMECDLPDHTVMVIVAQLLEAVGYLGNQGVVHRDLKSNNILVDYEEASGASPHVVIADFGCALSLRGRNLQD
Pl_Pink     CNLAIKMMFNYTGTGSKPADIMAEFGAEQLPLVLAGGSFSGRSNKYRRYRTSLRDYLNKGSGLPDRSIMVIVAQLLEAVGYLGNQGVVHRDLKSNNILVDYEEGSDEVPHVVVADFGCAISLRGKNLQE
Consensus   i.l..raf.....vp.l..A.......lp.rl.p.g.G...t...vmkrYrtsLR#YL.....lPd...MvivaQLLEaVgyLg#QG!vHRDLKS#NILV#y#e.sd..PhvV!ADFGCalslrg.nLQ.

            521       530       540       550       560       570       580       590       600       610       620       630       640       650
            |---------+---------+---------+---------+---------+---------+---------+---------+---------+---------+---------+---------+---------|
Hs_PINK     PFSSWYVDRGGNGCLMAPEVSTA-RPGPRAVIDYSKADAWAVGAIAYEIFGLVNPFYGQGKAHLESRSYQEAQLPALPESVPPDVRQLVRALLQREASKRPSARVAANVLHLSLWGEHILALKNL-----
Sp_Pink     SVSVEDRNRQGNSALMAPEVTKGYHHDCLHYHDYLKADAWAVGAIIYEVCGQKNPFYSDG---VNSCGYEAGDLPQL-QSQAVGLKTISKLLLQKDPGERPSAQVAANILHLLLWQPSVSSLLRLCHSQS
Pl_Pink     TVSKDDLNRQGNAALMAPEVKKAYHCNSLRYHDYLKADVWAVGAIMYEVCGKKNPFYAEG---IDSSKYEAGDLPQL-QSEAVGLRVVSELLLEKNPGNRPSAQVAANILHLLLWQPSVSSFLRLSQGQS
Consensus   .vS..d.#RqGN.aLMAPEV.kayh...l.yhDYlKADaWAVGAI.YE!cG.kNPFY.#G....#S..Y#ag#LPqL.#S.avglr..s.lLL#k#pg.RPSAqVAAN!LHLlLWqps!ssllrL...qs

            651       660       670       680       690       700       710       720       730       740       750  755
            |---------+---------+---------+---------+---------+---------+---------+---------+---------+---------+----|
Hs_PINK     -KLDKMVGWLLQQSAAT-LLANRLTEKCCVETKMKMLFLANLECETLCQAALLLCSWRAAL
Sp_Pink     QMDSELSAWIIKVSLMQ--LVQDQAEKTLPSTRADPGIPLNPVEKGLLETFLKRVNSGHLICATQYLVKAFEPL-ALFAVSSLPVGREQLTDLSSNADRIVTLQA
Pl_Pink     SKDSELTAWIIKVSLMQQLLSSNHTDTALTFTPDDPGLPQNVIESSLVETFLKRVNSDSLIDASQRLVTALRPLGALAEFRGVSSTCMGTPQLIGSVSDTVTLMA
Consensus   .kdse$.aWiikvSlmq.lL....t#k.l..T..dpg.p.N..e..L.#tFLkrvns..li.a.q.lv.a..pl.al..............l.......vtl.a
```

D

>lcl|scaffold08146 length=37601

[…]GTTCTTGTATTACAAATTCAAACTCTTAGACACATTATTTTTTATAGATCTGGGGAAGAGACTGTAAAACATGTCGTTCCGGCATGGCTTGCAAGCCATCG
CTCGAGTGGTGCGACGAAGGCTGCAGCAGCAGGCACAACAACACACCCACGAACATCATGCAGGCCGACAGAGGCCCGATGTAGCGACATCGAATCCCGCT
CAACGCTACCATAGCAGTAGACCAACTGGATCCGATGTTCGTCTAAATACTCAAAATCTTGCGATTAGGGCGGCACGGGTTTGGAGGCAGACTCCTTCATCAT
GGTCATCAAATGGTAGTAGATTTGTTCAATCATCACGTCCGGTATTGCCACTCTTACTAGGATTTGCAGGAATTGGACTTGCCAATCAGGATGGAGAAGGTTT
TGCAGCAAGAGGTGGCATTGATCTTGAGACAGCTCTGCAGGTTGTACAGGTATGTTTTTTTTTTTATTTTTT[…]ATATTGAGCAGAATTTTCCTGCCAATACCG
CTCCTAATCAACATTTAGGCCTGTAATTGGATGAGTGTTATAATGTATACAATTGCCAAACAATCCCCCCCCCCCCTTGTCTTACAGACTGTCTTCGATGACCG
GGGCTTGAAAGCAGGTCAGGACACATCTAAAGAGTTCCCCGACAACCTAGCTAGTTACGCATTCTCAAAAACTGTCCTGGCGAAAGGCACAGAGGGCGCAG
TCTTTGCTGCCAAGAGGAGAGACACGGTTCTTCCATCAAAGGGGGATGAAGAGTTTGCTGATGCCCAAGCTAGGTACATGCCTGTGGATCAGCCAATAGATG
GAGGGCATATCGGAGAGCAGCCAAAGGCAGAGATGAAAGTTTGTGATGAGGGAGAGTGCAATCTAGCCATTAAGGTTTGTAGATCATTTCAAAAGACTTTTG
TAGCGTGGTTACTCGAATGTAAATATGTAGATAATAGACAAAAC[…]ATAATTGTACTATTTAAAAAAATGCAGACTGCAGAATCTAATTTTTTTCTCCCAAA
AAATTCATATTAACTTTAACAACACCAATATGTTGTATCTTGATCTTGTAGATGATGTTTAATTACACTGGCACTGGGGGATCCAAACCAGCTGACATCATGG
CAGAATTTGGGGCTGAACAGCTCCCCCTAGTGTTGGCTGGAGGGTCATTCTCTGGTCGATCCAATAAATATAGGAGGTACGTACCTGCAGATTTACGTCTATG
GTACCAGTTTCTAGGACTGATTTTAAAATTGTTTTTACTTTTCCTGATATCTATGTACTCC[…]GTAGAGTTCGCATGTATAAATAATAAAATTACCTGTTTATA
AACCTTTTGATATACATTGTAACCATTTACTGGTAATTCTTTGGTCTAATTTGCAGGTACAGAACATCCCTCAGGGATTATCTCAACAAGGGGTCTGGCCTTCC
AGATAGAAGTATCATGGTCATCGTTGCCCAGTTGCTGGAAGCAGTTGGTTACCTTGGCAACCAGGGTGTGGTCCATCGTGACCTCAAGAGTAACAACATCCTC
GTTGACTACGAGGAAGGTGAGTGAATGACGTGTTAAAGCAGCAACTAGCAAATGTGCGCAGACTTCCCAAGTCAC[…]ATCAATGGTCAACTCTGTCACCTA
AAGAGAACCAGCGAGATTCCACCCATGTTAGATTTTCAACTGTAAATGGGCCTGTCCCATCATGGATGTTGTAACATTTATCATTTATCTTTTCTGTTTTTCCC
TGTCTTTTGACCAGGCTCTGATGAGGTACCCCACGTGGTGGTCGCAGACTTTGGATGTGCGATTTCATTGCGAGGTAAAAAACCTGCAGGAGACTGTGAGCAA
AGATGACCTGAACAGGCAAGGCAATGCTGCCCTTATGGCCCCTGAGGTGAGAATGTAAAGTTGACTGTGACTTTATAGCTTTTCACAGTCAAA[…]TTATTCT
AATCATTTAATCATGGAACTACTGAAAATTTTATTTTTGTTTCTTTTAATTGCACGTAGGTTAAGAAGGCATATCATTGTAACTCTCTGCGCTACCATGACTAC
CTAAAGGCAGATGTCTGGGCGGTGGGAGCCATTATGTATGAGGTTTGCGGTAAAAAAAATCCATTCTATGCTGAAGGAATCGACAGCAGCAAGTATGAAGCT
GGTGACCTTCCCCAGCTCCAAAGTGAAGCAGTGGGACTGAGGGTAGTGTCAGAGCTCCTGCTGGAGAAAAACCCTGGAAATGTAAGTACATGTATGATCGGT
TTATTCAT[…]GAAAAAGGGGCAAAAAGACTATCAATTCACCTTTGTTTCGGACAATAATATTTGGAGCATTTTTTTTTCTCATTGTAGCGACCATCTGCTCAA
GTAGCTGCAAACATTCTTCATCTATTACTGTGGCAACCATCAGTCAGCAGTTTCCTGCGTCTGTCCCAGGGTCAGTCGTCGAAAGATAGCGAGCTTACCGCCT
GGATTATTAAGGTTTGTACTTCAAAATGAATTATAACAATAATACTC[…]TTAAAGTGGGTTTAGACCAATTGGCAATTTACCATTACCTGTTGATCTCTACAT
TCACTCTTTCAAGGAAATACAATAAATGAAAGTTGAAGCCCACTATTTCCATTTGCCTTCACATCCAGGTATCTCTCATGCAACAGCTCTTGTCATCGAACCA
TACCGATACGGCGCTAACCTTCACCCCCGACGACCCTGGGCTTCCCCAGAACGTTATAGAGAGCAGTCTTGTGGAGACGTTCTTGAAGCGTGTCAATTCAGAC
AGTCTGATCGATGCCTCTCAACGCCTCGTCACAGCTCTTCGCCCACTCGGAGCGTTGGCGGAATTCAGAGGGGTGTCGTCCACGTGCATGGGAACGCCACAG
CTGATAGGCAGTGTCTCTGACACAGTGACACTTATGGCCTAACTCCCTCTATGCTATACAGATCTAAAATGGGCTAGTTGTGCATCTAATATCCCAACTCCAC
CCCGAAAATAAAATAATGATAACTTTTAGTAGTTGAATGCAAAAAAAAAGAAAAGAAAAGAGAGAACTCCTGAAACTGTTTTATCCAATAAAAGAGA[…]

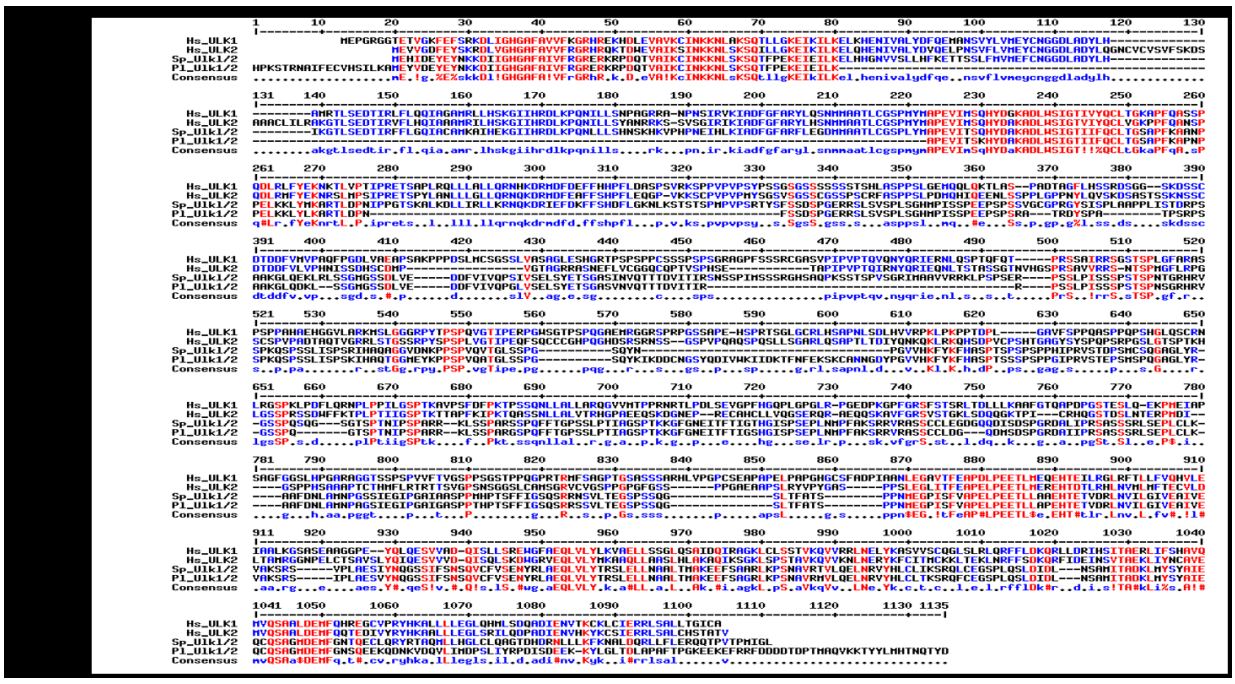

F

>lcl|scaffold02681
length=95983[…]TAGAGCTGCGGATCCCAGCTCGTGAGAACAATAACTCCATTTGCATTTGCCATTGCATTGGGATACGTCGCGAACGAACCTCATGACATGCTTTGTCATCCGCATTTTTAG
CATCCGAAATCAACTAGAAATGCTATTTTTGAATGTGTTCACAGTATCTTGAAGGCCATGGAGTACGTTGACGAGTACGAATATAACAAGAAGGATATAATTGGGCATGGAGCTTTCGCCA
TTGTGTTCAGAGGAAGGGAGCGAAAGGTGAGTTCCCGAGCCAGCCGTCCGTGCGCCAGGCGGATGAGCCTGAAGCAAGCATG[…]AGAGAAAATATTTTAATTGTGTTTAATGT
TAGCTTTAAAAATTTGACTTGTTTAACTCAACAGAGACCTGACCAAACAGTTGCCATTAAGTGCATCAATAAGAAGAATCTGTCTAAATCGCAGACTTTCCCAGAAAAGGAGATTGAAATA
TTGAAGGTATGTGT[…]GTTTGTATAGATATTTTAGATATGTAATTCTCTGATGATTTTTTTCTTCCAACCCCAGGCCCCTGAAGTGATCACATCAAAGCATTATGATGCAAAGGCTGACTTGT
GGAGTATAGGAACAATTATATTCCAATGTCTGACTGGTAGTGCACCCTTCAAAGCTCCTAATCCTCCTGAACTCAAGAAGCTTTACTTGAAGGCTAGGACACTGGACCCTAAGTAAGTAA
CATTACC[…]GAATTTCTTGTGAATACAGAACTGTGAATGATATTTTCAAATGTGTCACCTTTATATGTGATTGTCATTTTTATATCTTTGTTTGATTTCACTCTCAGTATACCACCTGGTACAT
CAAGGGCCCTCAAAGACTTGCTCATAAGACTTCTCAAAAGAAACCAGAAGACAGGATAGAATTTGGTATGATTTATGTAATTTCCAATATTCAACTTATTCATAGAATAAAATGTGCTGA
TTTT[…]TAATTTTAATGTGAAGTTTCACTTAATTTCTTTTTCTTTTTTCTTTTCATCTGCAGATGAATTTTTCAATCATGACTTTCTATCAAAGACCCTGAAATCTACCTCAAGTAAGTGTGTCT
CTTAAAAAAAAAAAAAACCTACAATATTTTTATAGGATTGTTTTTGTTGATTAAATTCCGACCATTCATAGCATGATCAATTCTAGTTTAGAGGTCTTGAGAAAACAAAGACATTAAATCCT[
…]AAATAACCAGAAATGGAATATATTTGCTACTGTACAGCTTCCCCAATGCCAGTTCCCGGCCGTACATACAGCTTCAGTTCTGATTCTCCTGGCGAGAGGCGATCCCTGTCAGTATCACCT
CTCTCAGGGCATATGCCTATCTCATCCCCAGAGGAACCTTCTCCTAGTAGGGCTACCAGAGACTACAGTCCAGCAACACCATCTAGACCTTCAGCAGCTAAGGGATTGCAGGATAAACTAT
CATCAGGAATGGGCTCTTCAGATTTAGTTGAAGATGTATGTTTACAATCCTTATCAAAAATGAAGAAAGATCATTCTCTAAAGTGTAGAVTGAGTCGGTTTAACTTTAAATTATTTTCTAT
ATTTCTGTTTC[…]TTAAATGCATTATGAGCATCTTTTCATTGTAGGACTTTGTAATAGTACAGCCGGGCCTTGTCTC[…]TGGGAAAGTGTTTTAGGCAATGGTGTCTTTTCAACTTTGTATGT
TATGTATATTTGGGATTCGATATCATGATAAGGAATGAATCTAATCACACATTTTAATCTTGTTTGTTCATTCAGATGAAACCAGTGGTGCTAGTGTAAATGTGCAAACTACAACCGATGTA
ATAACGATACGAAGGTGAGTCAAAATTTTACCATTATCCAGTTTTAATGTTTGAAGACAAATGTTGGAACGAGGTTTGCATTAAAAGAATTGAAAAGAAAAAAAGCGACAAAAGGAAGAT
GAAAAAACAGTATAACAACTAAAATCATCTCATC[…]ACCATTATTATTATTATTGCTTTGTTCTTTCTTTGTTCTTTCAGGCCAAGCAGCTTGCCAATCTCTTCTAGTCCATCAACCAGTCCT
AATAGTGGTAGACATCGAGTCAGTCCTAAGCAATCTCCATCATCACTTATATCACCAAGCAAGATACATCGCACAGGTAACATGAAGTCCACTCCTCTTATCATGAGAATGGACATCAAAAG
GAGTTTGGTATAATGAGGCAATTCACCCTAGTCCC[…]CTTATTATTTGTAAGTCTTGCAGCCTTAATATTTCCTCTTGACGTGTTTCCACTTTTAGACAGGAGGAATGGAGTATAAGCCAC
CTAGTCCTGTTCAAGCTACTGGACTTTCTTCACCGGGCAGTCAATACAGTAAGTATACAGTCATTAACAAAAGTTGTATAGATCTACACATTAATGTCCTTTTAATTGTTTACATTGATAGA
AATAAAGGATGATTGTAATGGAAGCTATCAAGATATTGTTTGGAAAATAATTGATAAGACATTTAACTTTGAAAAGTCAAAGTGTGCCAACAATGGGGATTGTAAGTGGGAATCATTTAAA
ATCACACATCACACAACTTTCTTTTGTCACACAACTTTTTTATGCCTCCGCGACGAAGTTTCGTTTTATCGACGTAACTGACAAAAAGTTGCAGTTACCACAGATTAAAAATTAATTATCAA
ATTATTATCTCTTTTTCTGTTTACCTTTGTAGATCCGGGTGTAGTACACAAGTTCTACAAGTTCCATGCATCTCCTACGTCTTCTTCCCCCTCCCCTCCCGGTATACCTAGGGTATCAACAGAA
CCCAGTATGTCCCCTCAGGGGGCGGGACTCTATAGAGGATCATCACCTCAAGGGACATCACCTACTAACATTCCATCTCCAGCAAGAAGGAAATGTAAGTTTAAGATCATCGAAGTACAGT
GTGTCCCAGAAAAAAAAAAAGTATACCCAATTTTGAGAGCCTCTTATTACAAGTTTATACATTAATTTTTATTTACATTATAGAGTAACTCTATCCAGTGATATGAAATTTAGAGATA[…]GC
ATGTATTATCTTTGTCATGACAGTATCATCACCAGCTAGAGGATCACCTCAGTTCTTCACAGGACCATCCTCCCTACCCACAATCGCTGGCTCACCAACCAAGAAAGGTTTTGGGAATGAGA
TTACATTCACTATAGGATCTCATGGTATCAGTCCATCAGAGGTAAGACATCTCATTGTTATTAATAAATAATGAGAGATTAATTCTAGTGATGAATAAAAAAAAATAATTACATGAA[…]AT
TTTCATATTTGTGTTTGTTTTGAATAGCCTCTGAACATGCCATTCGTCGTGTAAGGGCATCATCGTGTTGCCTAGATGGTCAGGACATGTCTGATTCACCAGGACGGGATGCT
ATCATACCAAGGAGTGCTAGCTCTAGTAGATTATCTGAACCACTGTGTTTGAAGGCTGCCTTTGATAACCTGGCTATGAATCCTGCAGGAAGCATTGAGGGTATCCCAGGTAAGATAA[…]A
GCGATTTTCATATTTTTTTACTCACTTCACTCTTAATTAGCATTGACTTTAATAAAAATTGTTTTGTGTTAACATTTCTCTTCTTTTCTTTATCAGGTGCTATCGGTGCTAGTCCCCCAACGC
ACCCTACCAGTTTCTTTATCGGTAGCCAATCACGTCGCAGCTCAGTGCTGACGGAGGGGTCACCGTCGAGTCAAGGGTCATTAACCTTTGCCACCTCACCTCCAAATATGGAAGGACCCAT
CTCGTTTGTGGCTCCTGAACTTCCTGAGGAAACTCTATTAGCAGTAAGTTTAGTTGCATCTGCTAACAAGCTAACT[…]GTGCATGTATTACAGTGAAATTATTACAGAATTATAAAATATAT
TTTTCCTTCTCTCTTTCTCTTTTCATGCACATGTAGCCTGAGCACTGAGACTGTAGATAGATTGAATGTTATCCTGGGTATTGTGAGGTAGCCAAGTCAAGAAGCATA
CCTTTAGCTGAATCTGTATACAACCAAGGATCGTCTATCTTCAGTAATTCACAAGTCTGCTTCGTCAGTGAGAACTATAGGTAAGTGGAGGGACAAGGCTGAAAGAAAGGAAAGAAAATG
GTTACTTGAAAAAAGAAAA[…]CCTGATAAGACAGGGCCCAGCTCTCCTAACTTAAAATAATTGGTATGATGATATCCATGTATTAAATCTCACAATGATCTTGTCTCTTACAGGTTAGCTG
AGCAGCTTGTACTATACACACGATCCCTTGAGTTACTTAATGCTGCACTTACTATGGCCAAAGAGGAGTTCAGTGCTGGAAGGTTAAAACCTTCAAATGCAGTCAGAATGGGTAAGAAACA
TCACAGCCACATCAACTTAAAG[…]TCTTCCAAGAAAAGATTGATATTTTTTAGCCTTATTIGTCTTACGAATTTTGACGATTTGTAATGTGTTACCTTCCATTTTAATGAAGTAATGATTAAT
GAAATGAACATTGTATGTCTTGCATTGGTAGTCCTTCAGGAGCTGAACCGTGTCTACCATCTCTGCCTGACAAAGAGCCGTCAATTCTGTGAAGGGAGCCCTCTACAGTCCTTAGATATTGA
TCTAAACTCTGCTATGATCACTGCTGATAAGCTCATGTATAGCTATGCCATTGAGCAATGTCAGTCTGCTGGTATGGACGAGATGTTTGGCAACTCACAGGAGGTAATAATAATAGTTCTTT
ATTTTTATTCTGCGCTTTTCCCATTAGGCCTTTAAAGTGCTTAATGTCTTATAAGTGATCAGATTTCACAGTTACATTCCACTGCGGGGTTTGTATGG[…]AAAAAG
ATTAATTTTGCATTTTGGGATTTTTTTTTCCTCCATTCTTTGAAAGGAGAAGCAGGACAACAAGGTTGACCAGGTCCTAATAATGGATCCATCACTAATCTATCGGCCTGACATCTCAGATG
AAGAGAAGAAGTACTTGGGCTTGACTGACCTAGCACCAGCCTTCACCCCTGGAAAGGAGGAGAAAGAATTCCGCAGATTTGATGTAAGGTGTAAAATAATCCAATGTGTCCAGGGAAAAA
AAGAGGACGTGCACAGGTATTGTTATCTGGTTATGCCTCTCAGTGATG[…]TAGCTAAGACAGATCATTTCTGTGAGAATCAATAACTTGACCAAACTTATTGTTGTCAGAACTCATAATAT
CTTTAAATTTAAAAAAACAGTTGTTGAAATGTACTCTTGTGATTTGATATAATTTATTCGTGTACAGGATGATGATACTGATCCAACTATGGCACAAGTAAAGAAGACTTACTACCTCATGC
ATACCAACCAAACATATGACTATGTTATGAAACGAGGTGGGTAGGAACTGGCCCATATTCTCAAAGGTGGCCTAAAGTTAAGCCTAACTTAAATCTGTCGGTTTAACTATGACTAGCAAAATG
GGATACAATCTCAAAAAGTACATGTAAGTATTTAAATTCAATTTATGATTGGAATGATAAGT[…]GGTGTAGGGTCACCATGACCCGGTGTCCTAGGACTATCAGGCTGTAACTGTTTTG
CATTACCTTGCAAGAAAGAGTTACCTTTATATTATCATTTCAACCTGTTCAACTTCCTTCCATTTTCATTTGTTTTTCCTCGTTTTCTCAGTGGTCAACTGTAGGTGACACGTTTGTTGTTGGAT
GTCTCCCTCCTCCAAGTCTTCCTTACGGTATGAAGAGCTTCACTGATAACCCTGACCTCAACGACCCTCGATATAACACTCGCCTCGGTATCTACAAGGAAAACTGCGGCCTTAGTCATGTG
ACTATGTCATGGGGTCATGATGAATATCTCTATCATGTTCTCTTAAAGAACAAGACAACTTTACCTGAGGAGGGTCTGTACATGGTACGATATCATTCCTTCTATCCATGGCACAGAGGGGA
TGAATACACCTTCCTTACTGATAATAAAGATAGAGAGATGCTCAAATGGATCCACGAATTCAAGTAAGTCTACATTCTTTTTCATTCTCTCTTTTTATCTCAGACGTGTTCTGTTTATCAAGG
TGTATGTTCCGAGTTGCTTTTCTATGTCTTTCA[…]

G

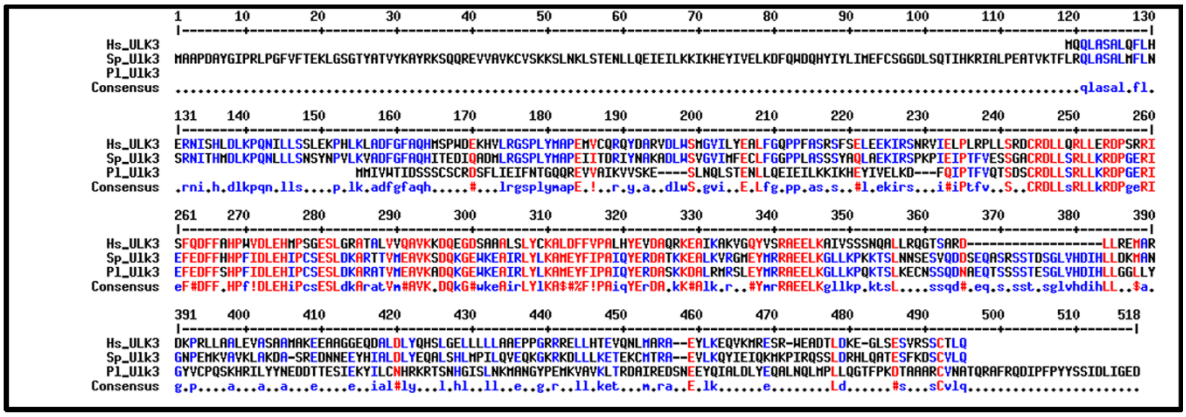

H

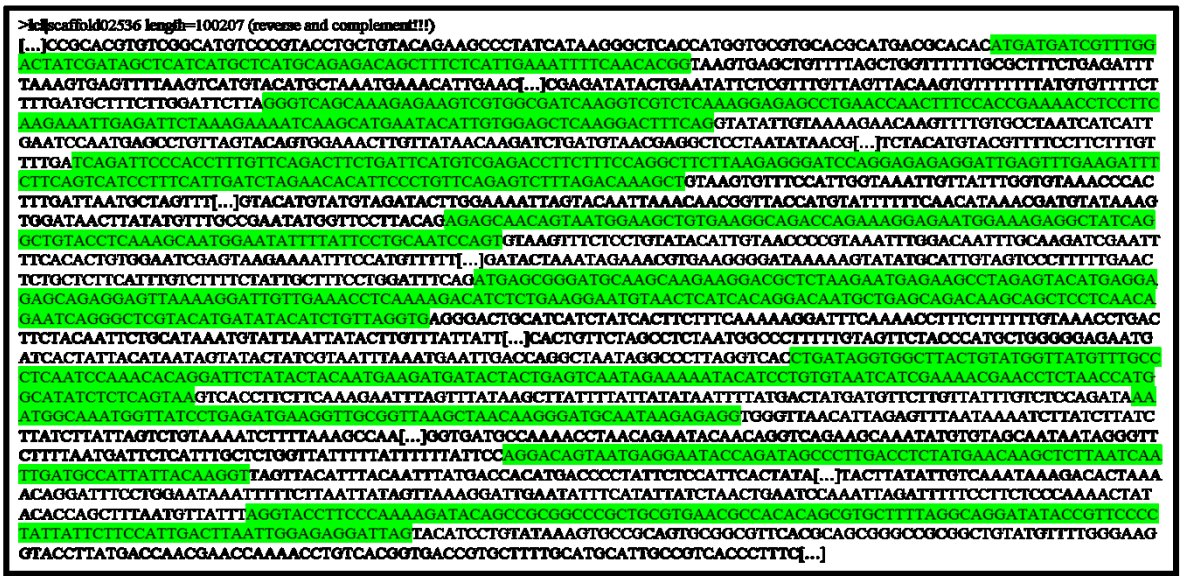

FIGURE 3.7: Autophagy: (**A**, **C**, **E** and **G**) Multialignment of aminoacid sequences of BECN, PINK, ULK1 and ULK3 from *Homo sapiens*, *Strongylocentrotus purpuratus* and *Paracentrotus lividus*. (**B**, **D**, **F** and **H**) Complex intron-exon structure of the *P. lividus* genes involved in intrinsic apoptosis.

In particular, both Pl_Becn and Pl_Pink were found to be clear orthologs of human Hs_BECN1 and Hs_PINK1. The complex intron-exon of these genes were also annotated (Pl_Becn presents 2 exons and Pl_Pink 8 exons). A different analysis was carried out for members 1 and 3 of the Unc-51 Like Autophagy Activating Kinase family, where a phylogenetic analysis was performed.

Sea urchin *P. lividus* seem to code only for 2 members of Unc-51 Like Autophagy Activating Kinase (ULK) superfamily: Pl_Ulk1/2 and Pl_Ulk3. As shown in figure 3.8, Pl_Ulk1/2 is a clear ortholog of equivalent protein in *S. purpuratus* (Sp_Ulk1); these two proteins are grouped in the phylogenetic tree with Hs_ULK1 and Hs_ULK2 from *H. sapiens*. For this reason, Pl_Ulk1/2 was considered the ortholog of human proteins HS_ULK1 and Hs_ULK2. On the other hand, the analysis for Pl_Ulk3 conducted to a clear orthology with proteins from *S. purpuratus* and *H. sapiens* (Sp_Ulk3 and Hs_ULK3).

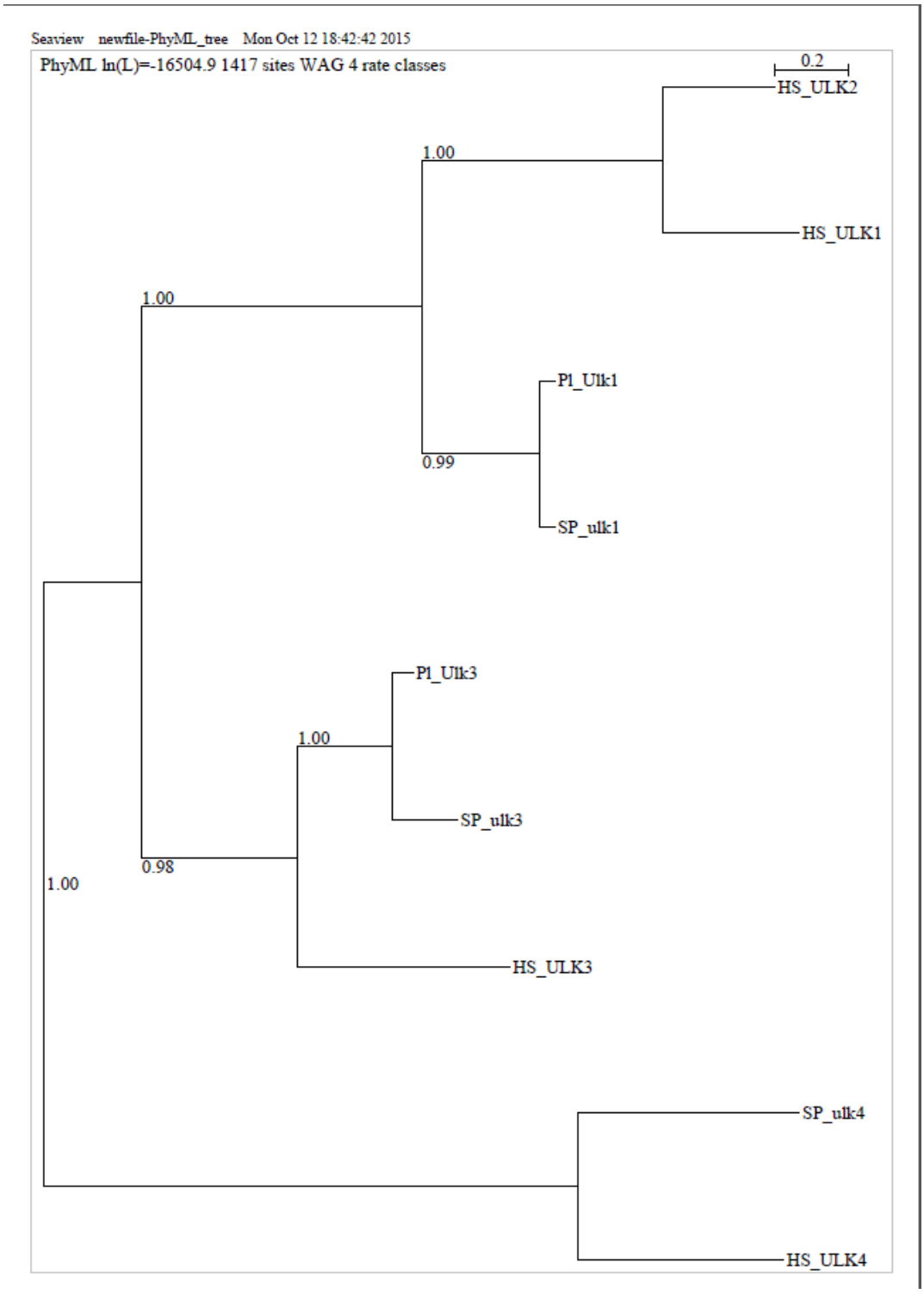

FIGURE 3.8: Phylogenetic tree that represents the evolutionary relationship among various members of the Unc-51 Like Autophagy Activating Kinase (ULK) superfamily from *Homo sapiens*, *Strongylocentrotus purpuratus* and *Paracentrotus lividus*.

3.3 Primers validation

The primers specificity and relative efficiency was tested in order to study the expression level of the twelve selected genes. The ability of each primer pair designed to amplify genes of interest was at first instance tested by standard PCR. Amplification was verified on 1.5% agarose gel and subsequently sequenced. The specificity was also confirmed by the presence of a single peak in the melting curve analysis performed by qPCR. The linear regression coefficients (R^2) of each standard curve for PCR efficiency (figure 3.9), which was determined for each gene using 10-fold serial dilutions of the cDNA, ranged from 0,9282 to 0.9983.

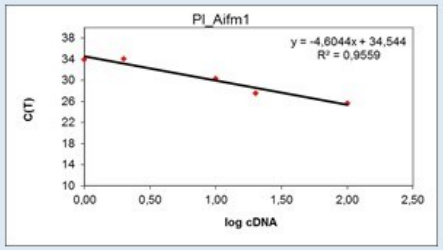
Pl_Aifm1
y = -4,6044x + 34,544
R² = 0,9559
C(T)
log cDNA

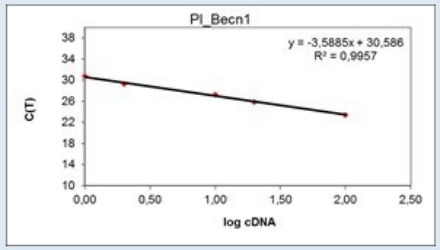
Pl_Becn1
y = -3,5885x + 30,586
R² = 0,9957
C(T)
log cDNA

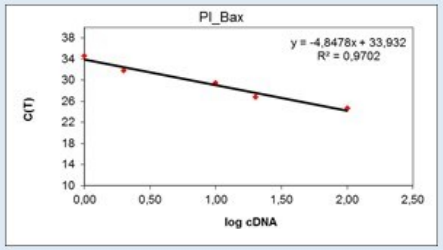
Pl_Bax
y = -4,8478x + 33,932
R² = 0,9702
C(T)
log cDNA

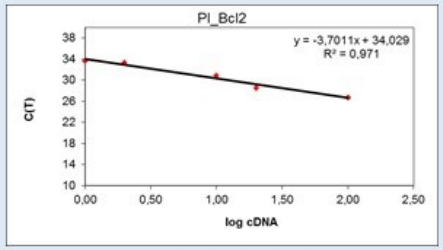
Pl_Bcl2
y = -3,7011x + 34,029
R² = 0,971
C(T)
log cDNA

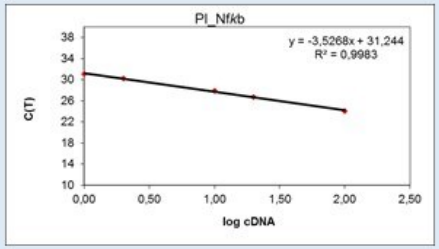
Pl_Nfkb
y = -3,5268x + 31,244
R² = 0,9983
C(T)
log cDNA

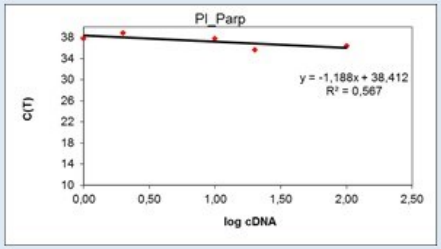
Pl_Parp
y = -1,188x + 38,412
R² = 0,567
C(T)
log cDNA

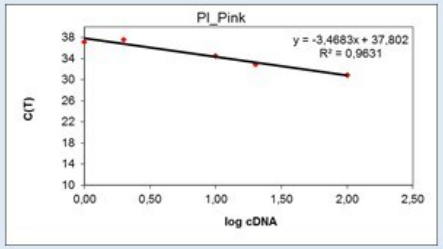
Pl_Pink
y = -3,4683x + 37,802
R² = 0,9631
C(T)
log cDNA

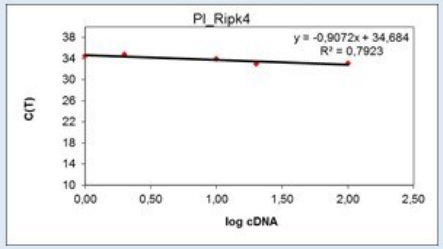
Pl_Ripk4
y = -0,9072x + 34,684
R² = 0,7923
C(T)
log cDNA

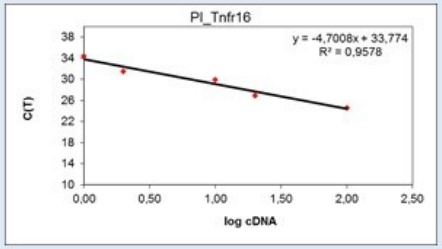
Pl_Tnfr16
y = -4,7008x + 33,774
R² = 0,9578
C(T)
log cDNA

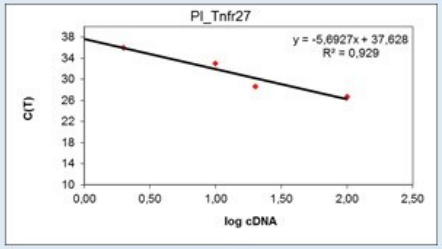
Pl_Tnfr27
y = -5,6927x + 37,628
R² = 0,929
C(T)
log cDNA

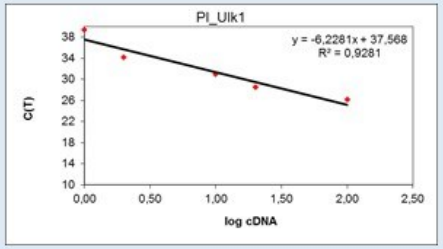
Pl_Ulk1
y = -6,2281x + 37,568
R² = 0,9281
C(T)
log cDNA

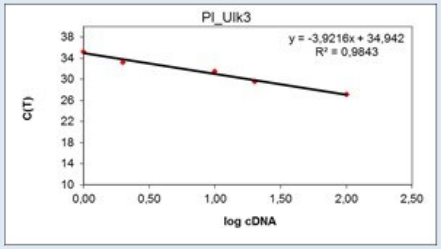
Pl_Ulk3
y = -3,9216x + 34,942
R² = 0,9843
C(T)
log cDNA

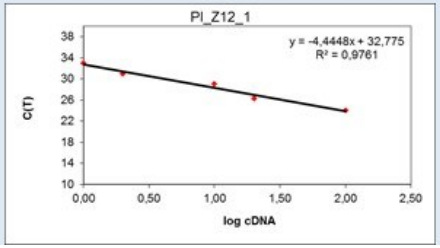
Pl_Z12_1
y = -4,4448x + 32,775
R² = 0,9761
C(T)
log cDNA

FIGURE 3.9: Efficiency amplification was calculated for each primer pair, generating a standard curves with serial 10-fold dilutions of the calibrator's cDNA sample by using the cycle threshold (Ct) value versus the logarithm of each dilution factor and using the equation $E=10^{-1}/slope$.

The PCR efficiency was excellent for the majority of genes examined (Aifm1, 0.9559; Bax, 0.9702; Bcl2, 0.9710; Becn1, 0.9957; Nfkb, 0.9983; Pink, 0.9631; Tnfr16, 0.9578; Tnfr27, 0.9290; Ulk1, 0.9281; Ulk3, 0.9843; Z12-1, 0.9761). Two other genes showed not perfect efficiency (Parp, 0.5670 and Ripk4, 0.7923), but in these cases the cycle threshold (Ct) values observed were higher of 30 (Table 3.1).

TABLE 3.1: Efficiency and linear regression coefficients (R^2) values of the twelve genes.

Gene	Efficiency	R^2 Value
Aifm1	1.65	0.9559
Bax	1.61	0.9702
Bcl2	1.86	0.9710
Becn1	1.90	0.9957
Nf*k*b	1.92	0.9983
Parp	6.95	0.5670
Pink	1.94	0.9631
Ripk4	12.66	0.7923
Tnfr16	1.63	0.9578
Tnfr27	1.50	0.9290
Ulk1	1.45	0.9281
Ulk3	1.80	0.9843
Z12-1	1.68	0.9761

3.4 Analysis of the variation of gene expression of sea urchin *Paracentrotus lividus* exposed to heptadienal

Sea urchin eggs were treated 10 minutes before fertilization and the following embryos developed were collected at three different times, stopping the incubation at specific developmental stages. The incubation times were: 5 hours post fertilization (hpf) corresponding to early blastula stage, 21 hpf corresponding to early prism and 48 hpf where embryos reach the larva stage called pluteus stage. Genes were grouped for their involvement in the specific cell death signaling pathway.

As shown in figure 3.10 A, the treatment of sea urchin embryos with heptadienal at different concentrations (2 μM, 2.5 μM, 3 μM, 5.5 μM and 6 μM) for 5 huors did not produce significant variation of expression for all genes analysed, involved in extrinsic apoptotic death pathway.

Among genes involved in intrinsic apoptotic pathway (figure 3.10 B), only PARP showed a variation of gene expression at the same incubation time, since BAX e BCL_2 have fold-change values comparable to the control. Treatment of sea urchin embryos with 2 μM of heptadienal produced down-regulation of the Parp gene (-2.35 fold change).

No genes belonging to the autophagic molecular mechanism showed a significant variation of gene expression level, since Ulk1, Ulk3, Pink and Becn1 showed fold-change values into basal expression levels (figure 3.10 C).

A

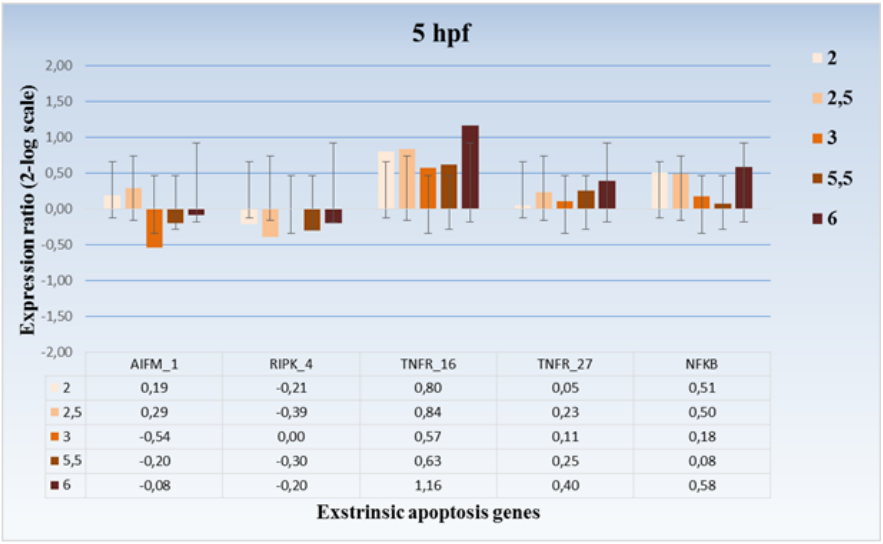

	AIFM_1	RIPK_4	TNFR_16	TNFR_27	NFKB
2	0,19	-0,21	0,80	0,05	0,51
2,5	0,29	-0,39	0,84	0,23	0,50
3	-0,54	0,00	0,57	0,11	0,18
5,5	-0,20	-0,30	0,63	0,25	0,08
6	-0,08	-0,20	1,16	0,40	0,58

B

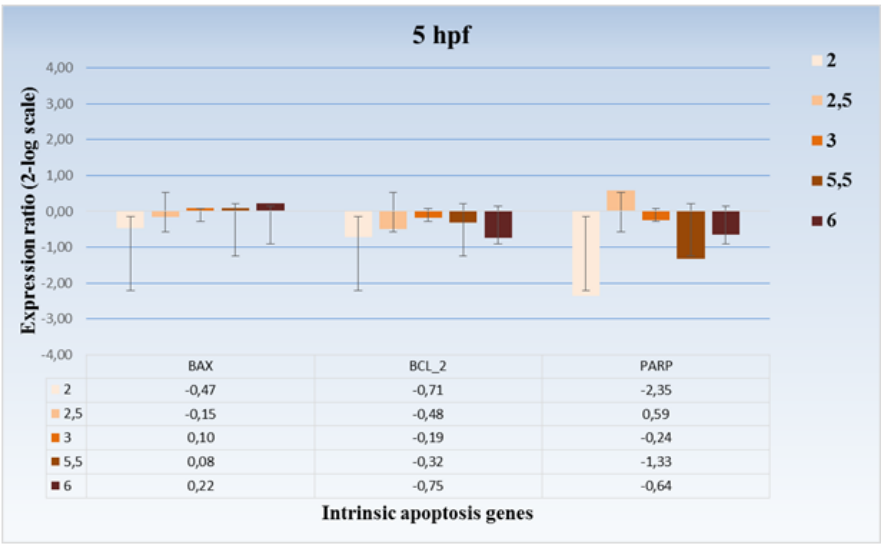

	BAX	BCL_2	PARP
2	-0,47	-0,71	-2,35
2,5	-0,15	-0,48	0,59
3	0,10	-0,19	-0,24
5,5	0,08	-0,32	-1,33
6	0,22	-0,75	-0,64

C

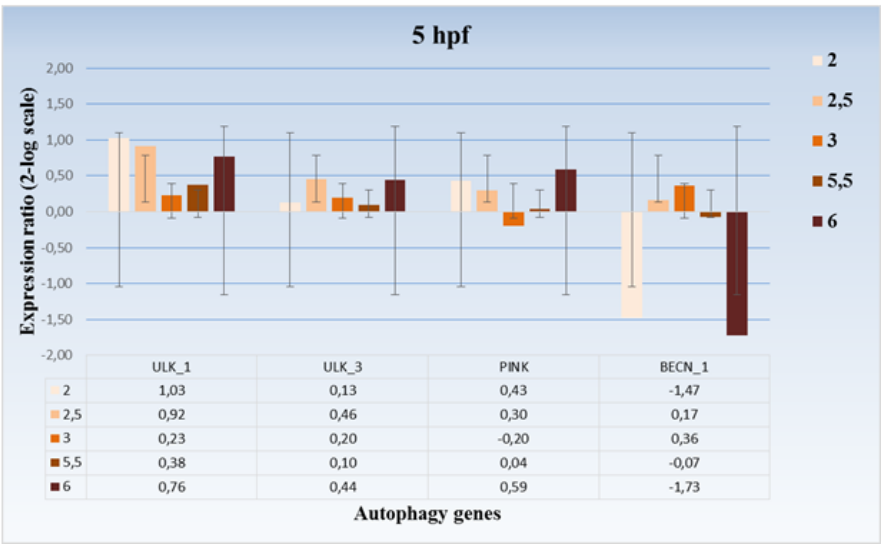

	ULK_1	ULK_3	PINK	BECN_1
2	1,03	0,13	0,43	-1,47
2,5	0,92	0,46	0,30	0,17
3	0,23	0,20	-0,20	0,36
5,5	0,38	0,10	0,04	-0,07
6	0,76	0,44	0,59	-1,73

FIGURE 3.10: Gene expression study by Real Time q-PCR of twelve genes involved in three different death cell signaling pathway in embryos incubated with increasing heptadienal concentrations (2 µM, 2.5 µM, 3 µM, 5.5 µM and 6 µM) and collected at a specific developmental stage of *P. lividus*: early blastula (5 hpf). (**A**) Gene expression levels of Aifm1, Ripk, Tnfr16, Tnfr27 and N*f*kB (involved in extrinsic apoptosis). (**B)** Gene expression levels of Bax, Bcl2 and Parp (involved in intrinsic apoptosis). (**C**) Gene expression levels of Ulk1, Ulk3, Pink and Becn1 (involved in autophagy). Data are reported as a fold difference (mean ± SD), compared to control embryos in sea water without heptadienal. Fold differences greater than ±2 were considered to be significant.

In figure 3.11 (A, B and C) is shown the variation of gene expression levels of all genes examined when *P. lividus* embryos were incubated for 21 hpf with different concentrations of heptadienal (2 µM, 2.5 µM, 3 µM, 5.5 µM and 6 µM). At this developmental stage, 2.5 µM of heptadienal was the most active concentration, creating a down-regulation of all genes involved in the extrinsic apoptotic pathway. In particular, Aifm1 was down-regulated with 4.13-fold change decrease, Ripk showed a 4.20-fold change decrease, Tnfr16 and Tnfr27 was down-regulated with 5.35-fold change and 3.86-fold change decrease respectively and N*f*kB exhibited 4.68-fold change decrease. Moreover, 2 µM of heptadienal showed a downregulation effect on Aifm1 and 6 µM was able to downregulated the Ripk4 gene.

A different response pattern was found for genes involved in intrinsic apoptotic pathway, when embryos were treated with the five concentrations of heptadienal for 21 hpf. Bax and Bcl2 genes were not affected at this developmental stage for all concentrations tested. The only gene responsive was Parp at two specific concentrations. In particular, 2.5 and 5.5 µM of heptadienal decrease the expression level of the Parp gene, -6.82-fold change and -3.13-fold change respectively. All the others concentrations, even if created negative values of fold change of the Parp gene, did not show a significant reduction of gene expression levels (2 µM -1.39-fold change, 3 µM -1.33-fold change and 6 µM -1,83-fold change)

In regard to autophagy, the most active concentration of heptadienal was again 2.5 µM. More in detail, Ulk1, Ulk3 and Pink genes were down-regulated when embryos was treated with the specific concentration of 2,5 µM (-4.10-fold change, -4.38-fold change and -4.50-fold change, respectively). At lower concentration (2 µM), only Ulk1 was down-regulated (-2.57-fold change), while at higher concentrations no genes were affected by the treatment, showing fold differences values inside the range of non-significance. Becn1 did not showed significant variation of gene expression levels at all concentrations tested of heptadienal.

A

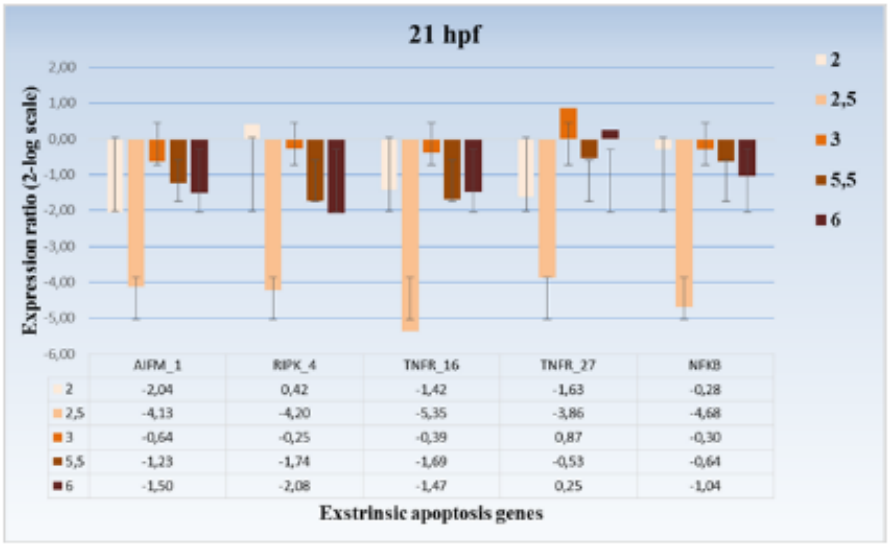

	AIFM_1	BIPK_4	TNFR_16	TNFR_27	NFKB
2	-2,04	0,42	-1,42	-1,63	-0,28
2,5	-4,13	-4,20	-5,35	-3,86	-4,68
3	-0,64	-0,25	-0,39	0,87	-0,30
5,5	-1,23	-1,74	-1,69	-0,53	-0,64
6	-1,50	-2,08	-1,47	0,25	-1,04

Exstrinsic apoptosis genes

B

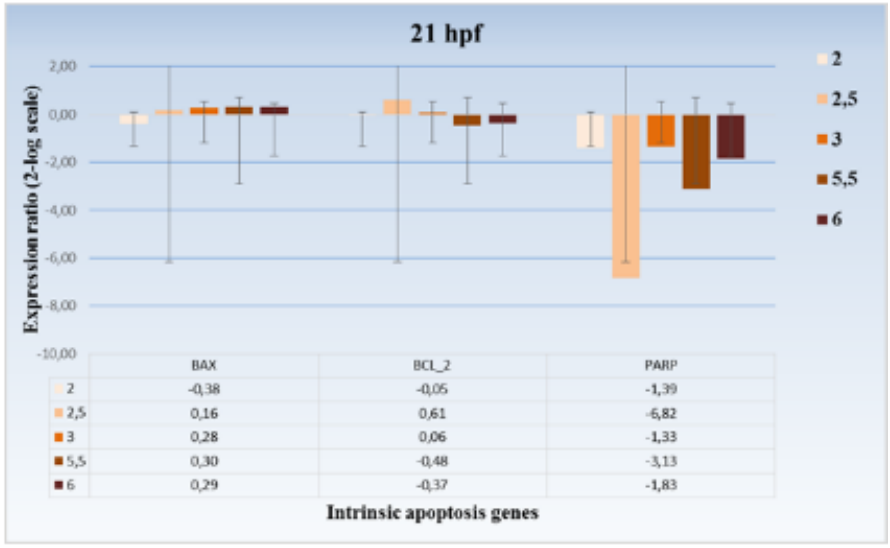

	BAX	BCL_2	PARP
2	-0,38	-0,05	-1,39
2,5	0,16	0,61	-6,82
3	0,28	0,06	-1,33
5,5	0,30	-0,48	-3,13
6	0,29	-0,37	-1,83

Intrinsic apoptosis genes

C

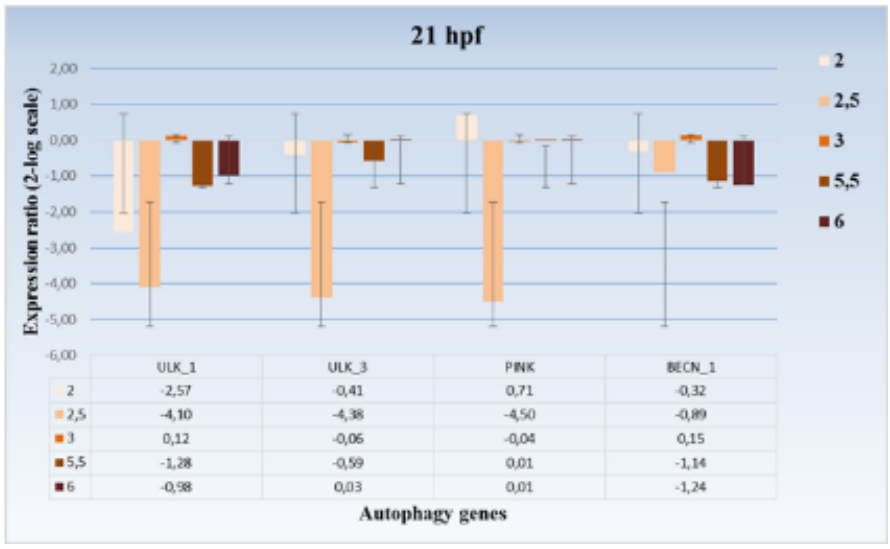

	ULK_1	ULK_3	PINK	BECN_1
2	-2,57	-0,41	0,71	-0,32
2,5	-4,10	-4,38	-4,50	-0,89
3	0,12	-0,06	-0,04	0,15
5,5	-1,28	-0,59	0,01	-1,14
6	-0,98	0,03	0,01	-1,24

Autophagy genes

FIGURE 3.11: Gene expression study by Real Time q-PCR of twelve genes involved in three different death cell signaling pathway in embryos incubated with increasing heptadienal concentrations (2 µM, 2.5 µM, 3 µM, 5.5 µM and 6 µM) and collected at a specific developmental stage of *P. lividus*: early prisma (21 hpf). (**A**) Gene expression levels of Aifm1, Ripk4, Tnfr16, Tnfr27 and Nf*k*B (involved in extrinsic apoptosis). (**B**) Gene expression levels of Bax, Bcl2 and Parp (involved in intrinsic apoptosis). (**C**) Gene expression levels of Ulk1, Ulk3, Pink and Becn1 (involved in autophagy). Data are reported as a fold difference (mean ± SD), compared to control embryos in sea water without heptadienal. Fold differences greater than ±2 were considered to be significant.

The figure 3.12 show the variation of expression levels of all genes studied at the larval stage (pluteus stage, 48 hpf) of sea urchin *P. lividus* embryos treated with five concentrations (2 µM, 2.5 µM, 3 µM, 5.5 µM and 6 µM). At this specific developmental stage, several concentrations produced a significant upregulation of all the five genes involved in the extrinsic apoptotic pathway.

In particular (figure 3.12 A), Aifm1 was upregulated (3.55-fold change) at lowest concentration of heptadienal (2 µM), but also at highest concentrations, such as 5.5 µM and 6 µM (3.67-fold change and 2.48-fold change, respectively). Surprisingly, 2.5 µM and 3 µM did not produce a significant variation of gene expression level. 2 µM, 5.5 µM and 6 µM of heptadienal were also responsible of the upregulation of Ripk (4.26-fold change, 4.08-fold change and 3.24-fold change, respectively), the expression of which remained unaltered with the other two concentrations (2.5 µM and 3 µM). The same expression pattern was observed for the two tumor necrosis factor receptors studied. More in detail, Tnfr16 was upregulated with 2 µM, 5.5 µM and 6 µM of heptadienal (4.81-fold change, 4.66-fold change and 4.42-fold change, respectively), but the other treatments did not produce a significant variation of gene expression level. The same occurs for Tnfr27, which was upregulated with only 2 µM, 5.5 µM and 6 µM of heptadienal (3.33-fold change, 3.24-fold change and 2.91-fold change respectively). Also in this case, 2.5 µM and 3 µM did not produce a significant variation of gene expression level. The last gene analysed, belonging to extrinsic apoptosis, was Nf*k*B, which showed 4.15-fold change, 4.29-fold change and 3.58-fold change when treated with 2 µM, 5.5 µM and 6 µM of heptadienal, respectively. Nf*k*B, similarly to the other genes, was not affected by the other two heptadienal concentrations tested.

A different response pattern was found for genes involved in intrinsic apoptotic pathway, when embryos were treated with the five concentrations of heptadienal for 48 hpf (figure 3.12 B). Bax and Bcl2 genes did not modify their expression levels when treated with heptadienal, as observed for the previous developmental stages. Heptadienal induced an upregulation at 2 µM, 5.5 µM and 6 µM of the gene Parp (6.19-fold change, 5.43-fold change and 4.10-fold change, respectively). On the contrary, 2.5 µM and 3 µM did not produce a significant variation of gene expression level.

Results related to autophagy showed that, also in this case, the most active concentrations of heptadienal were 2 µM, 5.5 µM and 6 µM of heptadienal (figure 3.12C). More in detail, Ulk1 showed 3.67-fold change, 3.40-fold change and 2.69-fold change, when treat with 2 µM, 5.5 µM and 6 µM of heptadienal. Similarly, Ulk3 was upregulate at the same concentrations (3.67-fold change, 3.40-fold change and 2.69-fold change, respectively). Pink, the function of which is strictly related to

mitophagic mechanism, was significantly upregulated with the same three active concentrations of heptadienal (4.34-fold change, 4.41-fold change and 3.82-fold change, respectively). Becn1 did not showed, after 48 hours of heptadienal exposure, significant variation of gene expression levels at all concentrations tested.

A

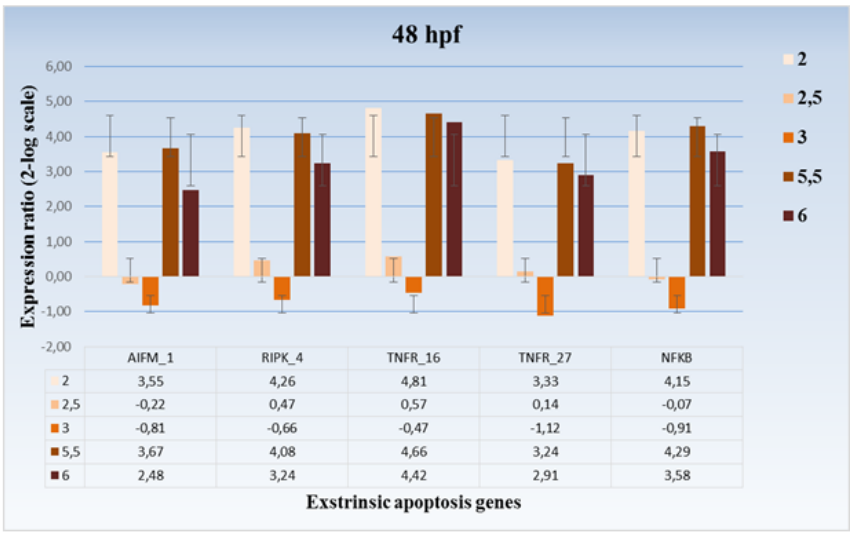

	AIFM_1	RIPK_4	TNFR_16	TNFR_27	NFKB
2	3,55	4,26	4,81	3,33	4,15
2,5	-0,22	0,47	0,57	0,14	-0,07
3	-0,81	-0,66	-0,47	-1,12	-0,91
5,5	3,67	4,08	4,66	3,24	4,29
6	2,48	3,24	4,42	2,91	3,58

B

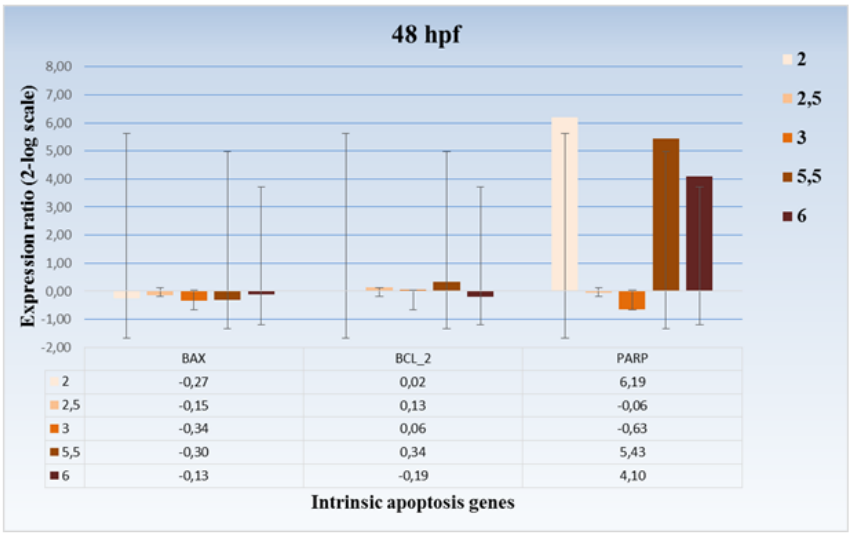

	BAX	BCL_2	PARP
2	-0,27	0,02	6,19
2,5	-0,15	0,13	-0,06
3	-0,34	0,06	-0,63
5,5	-0,30	0,34	5,43
6	-0,13	-0,19	4,10

C

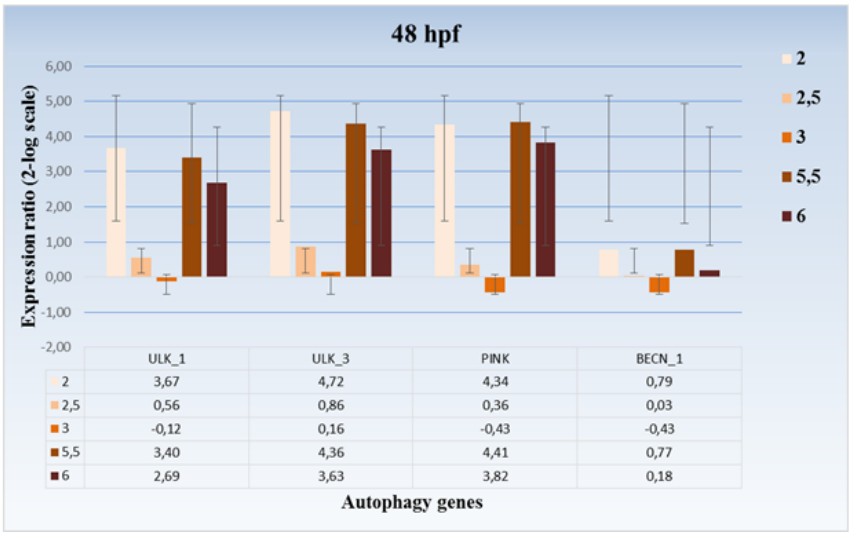

	ULK_1	ULK_3	PINK	BECN_1
2	3,67	4,72	4,34	0,79
2,5	0,56	0,86	0,36	0,03
3	-0,12	0,16	-0,43	-0,43
5,5	3,40	4,36	4,41	0,77
6	2,69	3,63	3,82	0,18

FIGURE 3.12: Gene expression study by Real Time q-PCR of twelve genes involved in three different death cell signaling pathway in embryos incubated with increasing heptadienal

concentrations (2 μM, 2.5 μM, 3 μM, 5.5 μM and 6 μM) and collected at a specific developmental stage of *P. lividus*: pluteus stage (48 hpf). (**A**) Gene expression levels of Aifm1, Ripk, Tnfr16, Tnfr27 and Nf*k*B (involved in extrinsic apoptosis). (**B**) Gene expression levels of Bax, Bcl2 and Parp (involved in intrinsic apoptosis). (**C**) Gene expression levels of Ulk1, Ulk3, Pink and Becn1 (involved in autophagy). Data are reported as a fold difference (mean ± SD), compared to control embryos in sea water without heptadienal. Fold differences greater than ±2 were considered to be significant.

3.5 Analysis of the variation of gene expression of A549 cell line exposed to heptadienal

To understand better cytotoxic effects of the heptadienal at the gene level on human cells, A549 cell line was used to carry out the analysis of the variation of gene expression levels by Real-Time qPCR. Gene expression results are here reported after 2 h of treatment with 5 μM of heptadienal, since many factors implicated in the cell death signaling pathways were already expressed and activated after 2 h and also because at lower concentrations of pure compounds transcriptional effects were less evident. The treatment concentration was chosen following the IC50 results obtained by Sansone et al. (2014) for viability experiments. Control genes used for Real-Time qPCR were actin-beta (ACTB), beta-2-microglobulin (B2M), hypoxanthine phosphoribosyltransferase (HPRT1) and large ribosomal protein P0 (RPLP0), the expression of which remained constant in A549 cell line. The histograms reported in figure 3.13 (A, B and C panels) show the relative expression ratios of the analysed genes with respect to controls without treatment. Only expression values greater or lower than a two-fold difference with respect to the controls were considered significant for up and downregulation results.

As showed in figure 3.13 A, all genes examined belonging to the extrinsic pathway are significantly upregulated. When A549 cells were treated with 5 μM of heptadienal for 2 hours, death receptors, such as TNF Receptor Superfamily Member 10a (TRAIL_R1, 10.12-fold change), TNF Receptor Superfamily Member 1A (TNF_R1, 8.11-fold change), TNF Receptor Superfamily Member 1B (TNF_R2, 4.49-fold change) were upregulated. Moreover, upstream and downstream death factors, such as Apoptosis-Inducing Factor Mitochondria Associated 1 (AIFM1, 6.19-fold change), Homeodomain Interacting Protein Kinase 2 (RIPK_2, 3.11-fold change and Nuclear Factor Kappa B Subunit 1 (Nf*k*B, 3.41-fold change) were significantly upregulated.

For whom concern genes belonging to the intrinsic pathway, only the anti-apoptotic factor B-Cell CLL/Lymphoma 2 (BCL_2, 18.53-fold change) and the enzyme Poly ADP-Ribose Polymerase 1 (PARP, 21.69-fold change) were found to be upregulated, when treated with 5 μM of heptadienal. On the contrary, BCL2 Associated X Protein (BAX, 1.61-fold change) did not affected by heptadienal after 2 hours of treatment (figure 3.13 B).

The figure 3.13 C shows the expression level of genes involved in the autophagic mechanisms. Heptadienal induced after 2 hours an upregulation of Unc-51 Like Autophagy Activating Kinase 1 (ULK1, 4,81-fold change). The other genes examined did not show a significant variation of expression level (ULK3, 1.89-fold change; BECN1, 1.67-fold change; PINK, 0.04-fold change).

A

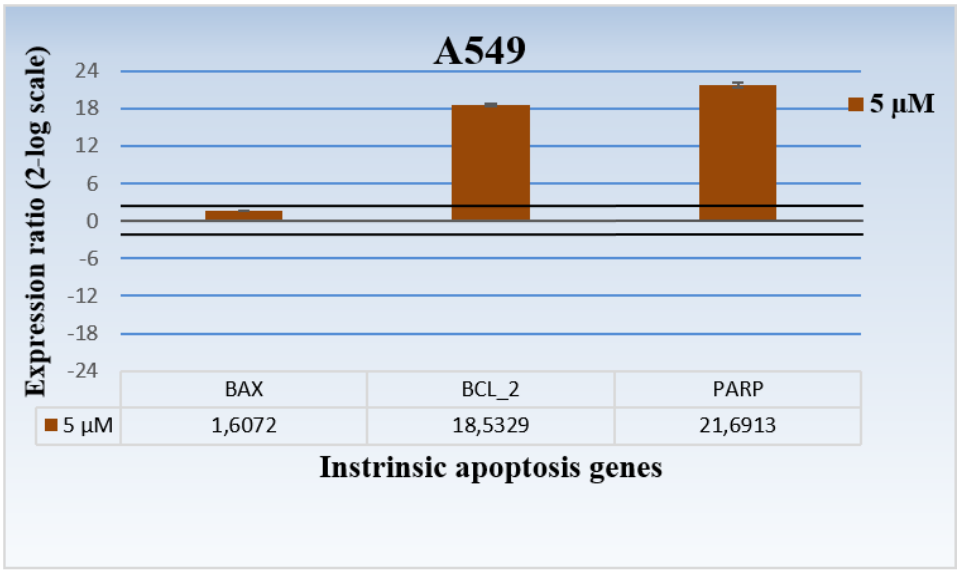
A549
Expression ratio (2-log scale)
24
18
12
6
0
-6
-12
-18
-24
5 µM
BAX
BCL_2
PARP
5 µM
1,6072
18,5329
21,6913
Instrinsic apoptosis genes

B

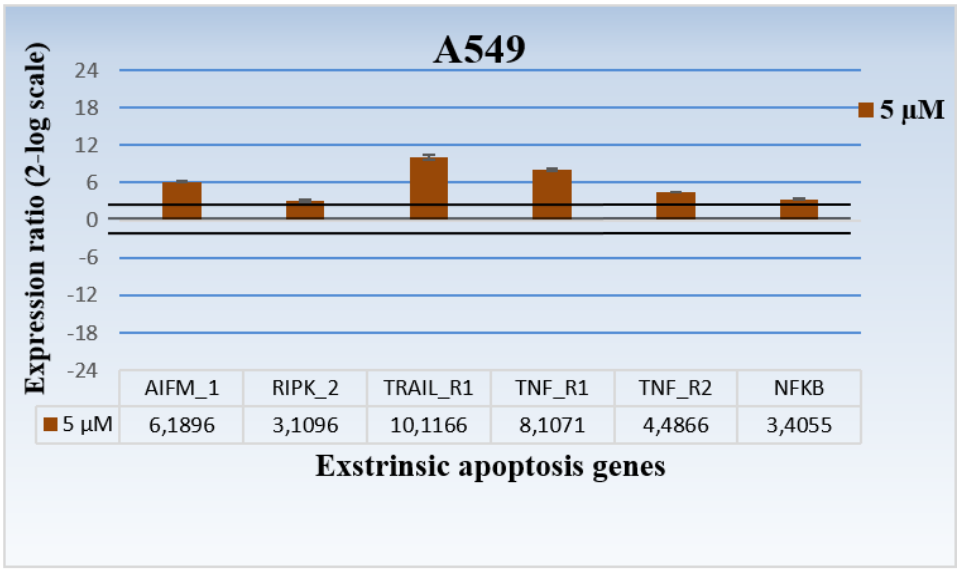
A549
Expression ratio (2-log scale)
24
18
12
6
0
-6
-12
-18
-24
5 µM
AIFM_1
RIPK_2
TRAIL_R1
TNF_R1
TNF_R2
NFKB
5 µM
6,1896
3,1096
10,1166
8,1071
4,4866
3,4055
Exstrinsic apoptosis genes

C

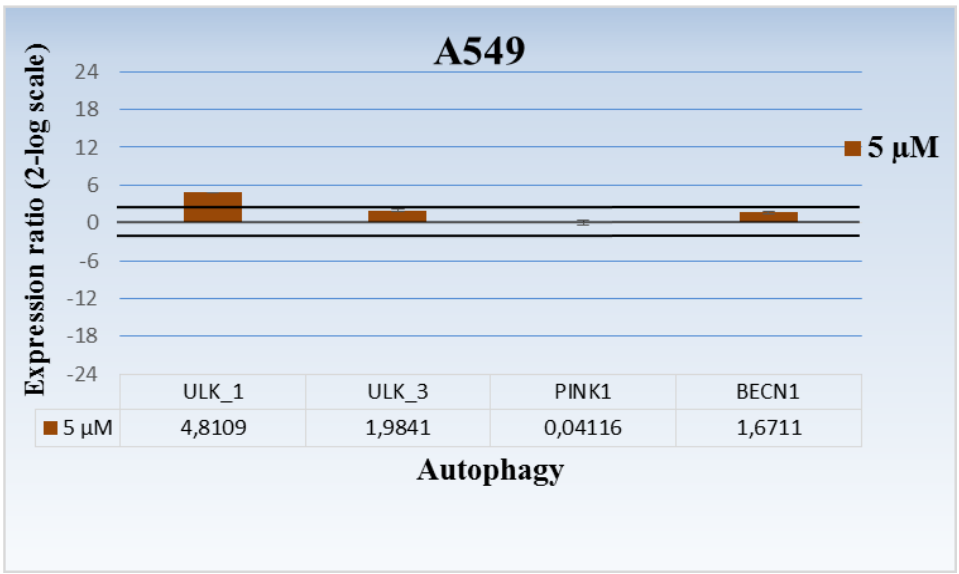
A549
Expression ratio (2-log scale)
24
18
12
6
0
-6
-12
-18
-24
5 µM
ULK_1
ULK_3
PINK1
BECN1
5 µM
4,8109
1,9841
0,04116
1,6711
Autophagy

FIGURE 3.13: Gene expression study by Real-Time qPCR of thirteen genes involved in three different death cell signaling pathways in A549 cell line treated with 5 μM of heptadienal for 2 hours. (**A**) Gene expression levels of AIFM_1, RIPK_2, TRAIL_R1, TNF_R1, TNF_R2 and Nf*k*B (involved in extrinsic apoptosis). (**B**) Gene expression levels of BAX, BCL_2 and PARP (involved in intrinsic apoptosis). (**C**) Gene expression levels of ULK_1, ULK_3, PINK and BECN_1 (involved in autophagy). Data are reported as a fold difference (mean ± SD), compared to control A549 cells without heptadienal. Fold differences greater than ±2 were considered significant.

CHAPTER 4.

Discussion

Bioinformatic approach and molecular analysis to study programmed cell death in sea urchin *Paracentrotus lividus*

The present study describes the morphological and molecular effect of the aldehyde heptadienal on sea urchin *P. lividus* embryo development. Results were obtained applying a propaedeutic bioinformatic approach, fundamental to find and annotate several genes involved in specific death cell signalling pathways. The information deriving from molecular experiments was compared with gene expression results obtained when a human tumour cell line was exposed to the marine compound heptadienal.

Researchers showed in previous studies morphological results at several concentrations of PUAs, which are able to induce teratogenesis and different degrees and types of malformations in sea urchin embryos. By definition, teratogens are agents that cause birth defects in the offspring of organisms exposed to them during gestation (Ianora and Miralto 2010).

Results reported in this study significantly expand previous studies (Romano et al., 2011; Marrone et al., 2012; Varrella et al., 2014 and Varrella et al., 2016) about the molecular response of the sea urchin *P. lividus* embryo to the ecologically relevant PUA heptadienal. The study investigates more deeply into the effect induced by the toxic PUA heptadienal on many genes belonging to death cell signalling pathways. Moreover, the study offers a bioinformatic approach useful to identify genes in *P. lividus* genome, for which there are not already annotation available.

To date, only few scientific research groups have study the effects induced by PUAs on marine organisms, which live in close contact or interact with these secondary metabolites produced by marine microorganisms. In fact, very few studies are present in literature on the morphological and molecular effects of pure marine compounds PUAs on copepods (Ceballos and Ianora, 2003; Taylor et al., 2007; Buttino et al., 2008; Kâ et al., 2014; Lauritano et al., 2011 and Lauritano et al., 2012). More recent study investigated the effect of decadienal on the tunicate *Ciona intestinalis*. Lettieri et al. (2015) and described the induction of specific developmental malformations in *C. intestinalis* larvae in a dose-dependent manner, studying also the variation of gene expression of those factors involved in stress response and developmental processes.

Moreover, sea urchin embryos showed, in the studies cited above, comparable malformations when they were treated with decadienal, heptadienal and octadienal, with the apex or arms being strongly compromised. All the aldehydes studied induce a dose-dependent effect on sea urchin embryos, but they differed for the concentration able to cause teratogenesis. In fact, as illustrated in the introduction section, decadienal represents the strongest of the three PUAs, since it can affect embryo development at low concentrations (Varrella et al., 2014). For the other two PUAs higher concentrations are necessary to perturb significantly the sea urchin embryo development. In particular, heptadienal act in the range of 3.0 μM and 6.0 μM to reach the same effect of decadienal, and octadienal required the highest concentrations (from 4.5 μM to 8.0 μM).

In this thesis project we chose heptadienal as chemical model as it represents the most abundant polyunsaturated aldehyde in the marine ecosystem (Wichard et al., 2005). Bartual and collaborators (2014) analysed the natural amount of PUAs released principally when phytoplanktonic cells are wounded during grazing or lysed for senescence processes. This study shows the ubiquitous presence of PUAs in the open ocean environment, including upwelling areas, as well as oligotrophic gyres. The total concentration ranged from zero to 4.18 pmol from cells in 1 L of sea water. Three

PUAs were detected: heptadienal, octadienal and decadienal. Among these aldehydes, heptadienal represented the most common compounds in marine environment (result obtained in 79% of total stations sampled).

Heptadienal is well known to induce perturbations and delay of the cell cycle in organisms ecologically related with diatoms. For this reason, in this study a wide range of concentrations was used to treat sea urchin *P. lividus* embryos. Sea urchin eggs were exposed to five increasing concentrations of the aldehyde: 2.0 µM, 2.5 µM, 3.0 µM, 5.5 µM and 6 µM (figure 3.1, see results chapter 3). This range of concentrations is able to produce several degree of embryo malformations. In fact, morphological data showed a wide range of percentage of abnormal embryos, from 15% up to 75%. The main result that comes out from morphological analysis is the strong direct proportion between heptadienal concentrations and percentage of abnormal embryos, which accumulate several malformations on the entire body at the larval stage.

With the efforts of the European research community for the complete characterization of sea urchin *P. lividus* genome, the molecular studies utilising this marine model organism are becoming more facilitated. Using this new knowledge, it has been possible to adopt a bioinformatic strategy to identify and annotate nucleotide and aminoacid sequences from *P. lividus*. In particular, the aim of this thesis, is the study of molecular targets of the marine compound heptadienal, in order to better clarify the cell death signalling pathways activated in sea urchin *P. lividus* and to compare the results with variation of gene expression study carried out with the same compound on human cell line (A549, human lung adenocarcinoma cells).

The selection of these two model organisms found a reason in the similarity of some their features. Both models possess a high rate of proliferation and they are composed of cells with different degree of differentiation. Sea urchin embryos covered a relevant role in many studies on fundamental biological processes and it is still largely used to study cell death mechanisms , since possess morphological and biochemical characteristics suitable for this experimental applications (clarity and large size of eggs, the ease of perturbation of embryo development, etc.; see introduction section). On the other hand, tumor cell lines represent the ideal *in vitro* model to assess the potential antiproliferative effects of chemical compounds and to investigate their relative ability to induce a programmed cell death in human cells. A comparison of the molecular effect activated by a pure marine compound on two model organisms having so distant phylogenetic relationship, with sea urchin occupying a key phylogenetic position as the only non-cordate deuterostomes, may give some insight in the evolutionary conservation on fundamental cellular processes.

A first important outcome of this experimental work was the finding that many key factors involved in various death mechanisms in human are indeed strongly conserved in the *P. lividus*. In fact, many key genes involved in the extrinsic apoptosis, intrinsic apoptosis and autophagy were identified and annotated from the new genome data bank (http://octopus.obs-vlfr.fr/blast/oursin/blast_oursin.php, a consortium of marine research institutes, which are still working on *P. lividus* genome).

For the extrinsic cell death pathway, the nucleotide sequences of the genes Aifm1, Ripk, Tnfr16 and Tnfr27 were found and annotated (figure 3.3, see results chapter 3), starting from the corresponding well-known death genes in humans. In particular, Aifm1 gene product is a mitochondrial effector of apoptotic cell death, synthetized and released, in response to apoptotic signals, from the mitochondrion intermembrane space into the cytosol and to the nucleus, where it act as a proapoptotic factor, starting the cascade for a caspase-independent pathway (Susin et al., 1999). In *P. lividus* genome a single gene was found with high homology with the human AIFM1.

The genes belonging to the Serine-threonine kinase receptors (RIPK) family are implicated in specific caspase-independent cell death mechanism. Members of this family are involved in the transduction of inflammation and cell death signals (programmed necrosis) following death receptors ligation and DNA damage (Hsu et al., 1996). In our study, only a single gene was found with high homology with the human members of the RIPK family. No a clear orthology was found for the sea urchin Pl_Ripk with one of the human gene family, probably due to vertebrate-specific duplications.

The signaling that initiate extrinsic apoptotic pathways involve several transmembrane receptor-mediated interactions. The Tumor Necrosis Factor Receptors (TNFR) superfamily cover an important role in these interactions (Locksley et al., 2001; Wang and El-Deiry, 2003). Members of the TNF receptor superfamily share similar cysteine-rich extracellular domains and are characterized by a cytoplasmic domain of about 80 aminoacids called the "death domain" (Ashkenazi and Dixit, 1998). This death domain plays a critical role in transmitting the death signal from the extracellular space to the intracellular signalling pathways. In this study, only two genes in *P. lividus* showed high similarity with members of the human TNFR superfamily. In particular, Pl_Tnfr16 was identified as a clear ortholog of the human member Hs_TNFR16, since sea urchin gene showed the highest similarity univocally with only that human receptor. On the other hand, Pl_Tnfr19/27 showed strong similarity with two members of the human TNFR superfamily: Hs_TNFR19 and Hs_TNFR27. These could originate from a vertebrate genome duplication (onhology relationship), therefore we can hypothesize that a unique ancestral Tnfr gene, still present in sea urchins, evolved in two independent members as observable in humans.

Referring always to well-known death genes in human, the bioinformatic strategy was useful also for the individuation and annotation of three genes involved in the intrinsic apoptotic pathway: BCL2 Associated X Protein (Bax), B-Cell CLL/Lymphoma 2 (Bcl2) and Poly ADP-Ribose Polymerase 1 (Parp1) (figure 3.6, see results chapter 3). The genes Bax and Bcl2 are the principal antagonists for the regulation of intrinsic apoptotic machinery. More in detail (Guo et al., 2003), in humans Bax is responsible of the activation of programmed cell death undergoing a conformation change that lead to translocation to the mitochondrion membrane, with consequent release of cytochrome c that then is able to triggers intrinsic apoptosis (with the involvement of Caspase 3). In this study, Bax showed a high conservation along the evolution, due to crucial role for the regulation of programmed cell death. In fact, Pl_Bax was found to be the only clear ortholog of human gene Hs_BAX.

The same phylogenetic result was obtained for the antiapoptotic factor BCL2, where Pl_Bcl2 is a clear ortholog of the human Hs_BCL2. This gene regulate cell death mechanisms by a tight physiological control of the mitochondrial membrane permeability. In particular, the apoptosis-activating factor (APAF-1) requires Cytochrome C (Cyt C) to activate Caspase 9 and BCL2 prevents mitochondrial cytochrome c release. For this reason, BCL2 is widely believed to inhibit intrinsic programmed cell death (Yip and Reed, 2008).

Different results were obtained for Parp annotation in *P. lividus* genome. Parp genes are involved in many processes, such as modulation of chromatin structure, assembly of DNA repair machinery, promotion of the release of Apoptosis-Inducing Factor (AIF) from mitochondria and transport to nucleus (Luo and Krause, 2012). Pl_Parp, the only Poly ADP-Ribose Polymerase found in *P. lividus*, is the clear ortholog of the human gene Hs_PARP1.

Autophagy is an essential process for the lysosomal turnover of cellular macromolecules and organelles. The genes Beclin 1 (BECN_1), PTEN Induced Putative Kinase 1 (PINK_1), Unc-51 Like

Autophagy Activating Kinase 1 (UKL_1) and Unc-51 Like Autophagy Activating Kinase 3 (UKL_3) are involved in the molecular pathway of autophagy (figure 3.7, see results chapter 3).

Beclin 1 is part of the PI(3) kinase class III (PI(3)KC3) lipid kinase complex that plays a central role in the induction of autophagy (Levine et al., 2008)). In addition to the activity in inhibiting apoptosis, Bcl-2 also inhibits autophagy through its ability in binding to the Beclin 1-PI(3)KC3 complex, an example of the interaction between two major pathways of cell death (Pattingre., 2005). Pl_Becn was found in *P. lividus* as the only possible ortholog of human Hs_BECN1.

Interesting evolutionary aspects were found for *P. lividus* Ulk genes. These class of molecular factors regulate the entire autophagic process, from upstream activation to the downstream factors (Klionsky, 2009). Main role of the serine/threonine-protein kinase involved in autophagy is the upstream regulation of phosphatidylinositol 3-kinase (PIK3C3) that regulate the formation of autophagophores, the precursors of autophagosomes (Chan et al., 2009). Pl_Ulk3 showed the highest similarity with unique member of human family (Hs_ULK3). On the other hand, Pl_Ulk1/2 exhibited an equal high similarity with two member of Autophagy Activating Kinase family: Hs_ULK1 and Hs_ULK2. As for the bioinformatic result obtained for Tnfr superfamily, this preliminary evidence need further detailed study and could be due to onhology relationship between sea urchin and human genes, since the ancestral Ulk gene generated two members with more specific functions.

The gene Pink is involved in the protection against mitochondrial dysfunction during cellular stress and in the following clearance of damaged mitochondria via selective autophagy. In fact, Pink acts upstream of Parkin in a sort of mitochondrial quality control pathway, able to remove damaged mitochondria in a specific autophagic process called mitophagy (Voigt et al.,2016). Similarly to Pl_Becn, the sea urchin gene Pl_Pink is highly conserved in evolution, and it resulted to be the only clear ortholog of human Hs_PINK1.

Once obtained these results, specific primer pairs were designed for each *P. lividus* gene and later validated for their specificity and relative efficiency (figure 3.9 and table 3.1, see results chapter 3). As described in the results section, the majority of the genes studied showed an excellent PCR efficiency with a single peak in the melting curve analysis, related to selected amplicon. The R^2 values were higher of 0.9, with the exception of Pl_Parp and Pl_Ripk. In these cases, the efficiency was not optimal even if there was a single pick generated by melting curve analysis. This result is probably due to the low expression of these transcripts in normal conditions (in control embryos). In fact, the Ct values for not diluted samples was already up to 30 and reach the value 40 after two or three serial dilutions, making not possible the generation of standard curves on wide range of values.

Analysing the molecular data, this study clearly demonstrate that none death gene, belonging to the intrinsic apoptosis were activated in both *P. lividus* and human A549 cell line, when treated with heptadienal (figures 3.10 B, 3.11 B, 3.12 B and 3.13 B, see results chapter 3). In detail, intrinsic apoptosis is not activated by heptadienal treatment in *P. lividus* embryos (early blastula stage), with the only exception of Pl_Parp gene. In fact, the only lowest concentrations of heptadienal (2 μM and 2.5 μM) were able to induce a significant downregulation of Pl_Parp in the first two developmental stages examined. This gene is implicated, in human, in many functions essential in stress response pathways (Luo and Lee Kraus, 2012). Our result is in complete agreement with previous studies, where is demonstrate that sea urchin *P. lividus* activate stress response pathways at the swimming blastula stage (after 9 hours post fertilization). Varrella et al. (2014) showed that PUAs (decadienal, heptadienal and octadienal) induced upregulation of heat shock protein 70 (hsp70) at the same developmental stage (swimming blastula stage). In fact, only at the pluteus stage, heptadienal is able to induce upregulation of Pl_Parp gene. The intrinsic apoptotic mechanism remain inactivated due to

the basal expression of Bax, principal responsible of the activation of this type of programmed cell death. Without this protein, the mechanism that leads to the release of cytochrome c is not triggered.

A similar result was observed for the molecular study carried out with the same pure compound on A549. After 2 hours of treatment with heptadienal, Hs_BAX is comparable to the untreated control, while Hs_BCL2 is strongly upregulated. These data confirm that heptadienal can not preferentially activate intrinsic apoptosis in both sea urchin and human. Also in the case of A549, Hs_PARP result upregulated, since heptadienal can induce stress signals in different biological model, through PARP stress response pathway.

Completely different results were found for genes involved in extrinsic cell death pathway (figures 3.10 A, 3.11 A, 3.12 A and 3.13 A, see results chapter 3). In the early blastula and early prism stages, heptadienal did not induce activation of Pl_Aifm1, Pl_Ripk, Pl_Tnfr16, Pl_Tnfr19/27 and Pl_Nf*k*b. These genes were found all downregulated after 21 hpf. This represent an interesting outcome of this study, since heptadienal seems to not target any gene involved in canonical programmed cell death. In particular, lower concentrations (especially 2.5 μM) are responsible of the downregulation of many genes involved in extrinsic apoptosis and, as previously described, one belonging to the intrinsic pathway. This effect is probably due to the fact that heptadienal, at this developmental stage (prism), targeted other genes (not studied here) involved in specific death mechanisms. Moreover, interferences with pathways involved in the differentiation or development occur, as it is evident with morphological experiments, where embryos increase death and malformations when proportional increase dose and time of exposure (see result section and Varrella et al., 2014). At the prism stage, SRY-related HMG-box 9 (Sox9) gene was upregulated by heptadienal, suggesting an interference effect on development and in particular on left-right asymmetry processes (Duboc et al., 2005). When *P. lividus* embryos were treated for 48 hours with the aldehyde all genes involved in the extrinsic apoptosis were upregulated. The Pl_Tnfr16 and Pl_Tnfr19/27 demonstrated to be target genes of the aldehyde. The recruitment of death receptors produce the activation of Pl_Aifm1 (mitochondrial effector), which is a proapoptotic factor that initiates the cascade for a caspase-independent pathway. Moreover, death receptors are responsible also for the activation of Pl_Ripk that in turn is able to upregulated the transcription of the Nuclear Factor Kappa B (Pl_Nf*k*b).

The same pathway activated was observed also in A549 cells treated with heptadienal. In the human *in vitro* model, all receptors containing an intracellular death domain resulted upregulated (Hs_TRAILR1, Hs_TNFR1 and Hs_TNFR2) and, as consequence, downstream effectors of extrinsic apoptosis were also activated (Hs_AIFM1, Hs_RIPK2 and Hs_NF*k*B). These results obtained on human cell line concord with those described by Sansone et al. (2014). In fact, the authors identified a cell death signalling pathway caspase-independent activated by heptadienal, through the upregulation of TNFR2 that lead to direct suicide program without any survival mechanisms with the involvement of (AIFM1, FADD, FAS and FASL).

Another relevant outcome of this work is represented by the involvement of autophagy in the molecular mechanism activated by heptadienal(figures 3.10 C, 3.11 C, 3.12 C and 3.13 C, see results chapter 3). The genes examined are not activated by the aldehyde before the pluteus stage. In fact, low concentration of heptadienal (especially 2.5 μM) induce a downregulation of Pl_Ulk1, Pl_Ulk3 and Pl_Pink, without the involvement of Pl_Becn1, after 5 and 21 hours. Only when treatment reaches 48 hours of incubation, heptadienal induce an autophagic response, though the activation of the same genes resulting downregulated at the previous developmental stage. A similar result was obtained

from expression analysis of autophagic genes of A549 treated with 5 μM. In this specific case, only the gene Hs_ULK1 was found upregulated, demonstrating an initial activation of the autophagy. This pattern of gene response could be explained by the high specialization typical of the autophagy. More in detail, after treatment with heptadienal, sea urchin embryos and human cell line undergo a programmed cell death process, caspase independent, with the attempt to remove the intracellular damage compartments, by autophagy. Autophagy regulates the intracellular turnover of the organelles and proteins within cells, whereas the apoptosis controls the turnover of cells within tissues and organs. Many stress factors are able to induce sequentially autophagy and apoptosis within the same cell, by common upstream molecular signals. In fact, autophagy and autophagy related proteins may help the trigger of apoptosis and necrosis. In addition, autophagy can also lead an autophagic cell death, apoptosis independent, by the completely degradation of the cytoplasm. A dialogue between autophagy and programmed cell death pathway is crucial and strongly influences the normal clearance of damage and dying cells. In fact, the interruption and alteration of this functional relationship between autophagy ('self-eating') and apoptosis ('self-killing') has important pathophysiological consequences.

CHAPTER 5.

Conclusions and future implications

New molecular and environmental applications for the marine model organism *Paracentrotus lividus*

Per definition, model species are organisms that are chosen by scientists and then recognised by all scientific community for their useful applications for in-depth studies. They are normally chosen in function of a certain characteristics of the organism, or their potential to provide easily answers to universal biological questions. Working with these organisms can produce information and knowledge transferable to other living organisms on which it is unfeasible to perform in-depth studies (e.g. human). Model organisms have to meet certain criteria such as a short generation time, the possibility to cultivate them and to reproduce fertilization and development in lab, low associated costs, the possibility to easily manipulate their genome and therefor to have a feasible genome size, and not less important, an interesting evolutionary position. Only a few model organisms that are currently investigated in biological Institutes around the world are of marine origin. Among eukaryotes, most of them are animals (e.g. sea urchin, sea squirt, lamprey, polychaete, platyneris) and few marine microorganisms.

In particular, sea urchin demonstrated along many decades its validity as good model for embryology, ecotoxicology, developmental biology studies and also for cancer research and neurodegenerative disorders. Sea urchins embryos, for their specific characteristic, provide a unique opportunity to study patterns in developmental processes, cell cycle regulation and tumorigenesis events. All these biological processes need even now a well explanation for all their aspects, being fundamentals and at the basis of many human disorders. Using sea urchins as a model is important since these organisms occupy a key evolutionary position with respect to vertebrates. Indeed, the echinoderms and their sister group, the hemichordates are the only other deuterostome animals besides the chordates. The sea urchin is thus more closely related to humans than other major invertebrate models in use. Almost everything we today know about the chromosomal basis of development, maternal determinants, fertilization, maternal messenger RNA and the main regulatory mechanisms associated with cell cycle progression originates from research where sea urchin has had a central role .

At the present, a huge group of researches forms a consortium working on the complete sequencing of the Mediterranean sea urchin *Paracentrotus lividus* genome. All this effort is producing a considerable amount of genomic information that will gives new impulse and a new light to the *P. lividus* as crucial marine model organisms for many European research Institutes. In fact, in the last decade, molecular studies and bioinformatic investigations have gained a central role in many research institute, since genome contains all information regulating cellular process and responsible of insurgence of many serious diseases. This new genomic knowledge support the reasonable scientific effort to validate sea urchin as a new molecular tool, *in vitro* and *in situ*, for the assessment and conservation of ocean health.

The work of this experimental thesis is strictly related with this scenario with important future implications. The molecular investigation using sea urchin *P. lividus* and the preliminary knowledge about its genomic information described in this thesis has been a first attempt to validate an innovative molecular tool. In particular, sea urchin embryos could be used to evaluate in depth the effect of certain chemical compounds on a fundamental response activation: survival or death. For

this reason, the thesis describes a direct evolutionary relationship between sea urchin and human in relation to the conservation at gene level of the key factors involved in some of the main cell death signaling pathways. In addition, experimental work focused the attention on the analysis of gene expression of key genes involved in programmed cell death mechanisms after treatment with a pure marine compound (heptadienal), at three different sea urchin embryo developmental stages. These results were associated with expression level of the orthologous genes of the *Homo sapiens* after *in vitro* treatment of human cell line with the same marine pure compound (heptadienal). Comparing the bioinformatic and molecular results obtained working with the two experimental models, it is clear that *P. lividus* and *H. sapiens*, two evolutionarily distant organisms, show identity of the genomic information about key death factors and the gene network involved in programmed cell death seems to act in both organisms with conserved mechanism and regulation.

Further information should be added to this study, in order to completely validate sea urchin *P. lividus* as molecular tool for the *in vitro* assessment of the activation of survival or death signals after treatment of embryos with chemical crude extracts, relative fractions or pure compounds, but also as environmental molecular tool for *in situ* studies of chemical contaminants or anthropocentric stressful factors that can interfere with the marine ecosystem. In fact, sea urchin naturally constitutes a sentinel organism able to reveal the health conditions of the seas. They are very sensitive to small environmental changes or stressful agents, modifying especially their reproductive fitness with alterations of developmental process at morphological and gene level, with consequence at the expense of future generations. For this reason, areas of naturalistic interest or marine environments with contamination rate to be evaluated, could benefit from these results and future additional molecular knowledge about sea urchin *P. lividus* death cell mechanisms, in order to assess the presence in the surround of chemical, physical and biological factors that are able to induce death or survival, acting on crucial natural switch (on/off).

SECTION 2

Drug Discovery from marine microorganism:
Microalgae as source of new natural products for application in pharmacology

CHAPTER 6.

Introduction

6.1 Drug from the sea: current research and market

Diseases affecting humans and all animals involved with human life are evolving their patterns, and new and poorly characterized diseases are emerging due to environmental changes and dysregulated lifestyle. The enormous increase of world population is representing a pressure factor on the existing resources for new drugs. As consequence, there is a continuous research of new natural sources to obtain innovative solution for human and animal health. In first instance, the drug industries research new and renewable resources to develop efficacious and safe drugs as answer to the increasing demands of the world population. Oceans represent a large source of a variety of organisms with high biodiversity due to the diversified environment generated by diverse external conditions with high chemical and physical variations. The enormous resources of the seas have been exploited by humans since ancient times, but the human activities include mainly the use of marine macroorganisms and plants, like fish and preparations from algae as natural medicine remediation.

Despite the abundance and variety of marine environments and the huge biodiversity they host, researchers and pharmacology industries have payed scarce attention to marine organisms, that still remain an underexplored natural source for biotechnological purposes. For this reason, marine ecosystems could represent a promising resource that can be exploited for the identification of new lead compounds and the development of new drugs to combat major diseases of our era, such as cancer or neurodegenerative diseases.

To date, scientists have identified 33 animal phyla, 32 of which are embodied in the marine environment. Among them, 15 phyla are exclusively present in the marine ecosistems (Margulis and Schwartz, 1998). Marine organisms such as sponges, tunicates, soft corals, nudibranchs, sea hares, opisthobranch molluscs, echinoderms, bryozoans, prawns, shells, sea slugs, and marine microorganisms have showed potential application in the field of drug discovery and development. The marine organisms are in the last two decades object of studies and they are screened for antibacterial, anti-inflammatory, immunomodulatory, anti-fungal, antimicrobial, neuroprotective, anticancer, analgesic, and antimalarial properties. Up to now, 15,000 marine molecules have been described, out of which 3000 having interesting biological properties (Vignash et al., 2011).

Marine natural products are generally secondary metabolites. In fact, they are not synthetized by primary metabolic pathways and do not cover main functions responsible for development, growth, or reproduction and propagation of species (Martins et al., 2014).

Bergmann (1957) formally reported the first biologically active marine natural product in late 1950. As previously stated, around 15,000 such unique natural compounds have been described and out of them 30% products have been isolated from sponges (Murti and Agarwal, 2010).

The following molecules represent some examples of success of marine pharmacology research moving to the global market. Linington and colleagues (2006) discovered that the novel caminosides B and D glycolipids, isolated from the Caribbean marine sponge *Caminus sphaeroconia,* were inhibitors of pathogenic *Escherichia coli* type III secretion system. Of particular interest for its anti-inflammatory properties is the Mediterranean sponge species *Spongia officinalis*, chemical extract of which was object of the *in vivo* study on rat model of carrageenan-induced paw edema assay (Dellai et al., 2010). Another chemical extract from green seaweed *Ulva*

reticulata prompted a strong interest for its neuroprotective effect. This marine plant is able to inhibit acetyl-and butyryl-cholinesterases, with an effect and efficacy comparable to molecules currently approved for Alzheimer's disease treatment (Suganthy et al., 2010). Also antiparasitic activity was observed for marine compounds. In particular, a chemical extract, prepared using dichloromethane, of *Sarcotragus* sp. (known as Tunisian sponge) has demonstrated *in-vitro* anti-leishmanial activity by demonstrating the associated morphological alterations in promastigotes of leishmania major (Ben Kahla-Nakbi et al., 2016). Antiviral agents from marine source was also found. For instance, high molecular weight exo-polysaccharides extracted from the *Celtodoryx girardae* (French marine sponge) possess anti-herpes simplex virus-1 (HSV) activity (Roshid et al., 2009).

Another sponge species, *Acanthella* sp. (Japanese species), received attention for drug discovery for its antimalarial activity. The invertebrate was chemically studied and molecules belonging to kalihinane diterpenoids class were found, which also contains antifungal, anthelmintic, and antifouling compounds (Miyaoka et al., 1998).

Cancer research has obtained important results in term of new therapeutic approaches with marine derived drugs. Bryostatin was obtained from the Bryozoan, *Bugula neritina*; some analogues have been extracted from sponges and tunicates. Sorbicillactone-B has been purified from a culture of the bacterial strain *Penicillium chrysogenum*, which has been isolated from a Mediterranean sponge *Ircinia fasciculata* (Bringmann et al., 2007). This marine compound has shown activity against leukemia cells.

Another anticancer drug, with promising applications for tumor treatments, is keyhole limpet hemocyanin (KLH) that is present in *Megathura crenulata*, a marine gastropod species found abundantly in the Pacific coast of California and Mexico (Harris and Markl, 1999). KLH has been investigated for its remarkable immunostimulatory properties in experimental animals and also in human; it is finding application in experimental immunology and also clinically as an immunotherapeutic agent (Curtis et al., 1971).

The first compound of marine origin to obtain approval from the U.S. Food and Drug Administration (USFDA) in 2004 was ziconotide, an analgesic drug for the treatment of pain. This marine compound derived from the marine snail *Conus magus*. Studies with animal models suggested the role of ziconotide in blocking of N-type calcium channels on the primary nociceptive nerves of the spinal cord (Skov et al., 2007).

Antimicrobial properties were also found in marine compounds. For instance, the antimicrobial agents cephalosporins. In particular, cephalosporin C was purified and characterized from a marine fungus, *Cephalosporium acremonium* (Murti and Agarwal, 2010).

Even though the potentiality of marine environment are largely recognized, there are certain major challenges and obstacles to the identification and characterization of new drugs from marine organisms. One of this is represented by the variability of environmental conditions, which could produce different metabolites from the same organism, for the effect of rapid adaptation. Isolation and identification of new marine lead compounds could also have some limit, because the natural molecules often are present only in low quantity and it becomes very difficult to isolate such compounds (Molinski et al., 2009). The quantity needed for chemical and activity studies can vary depending on the step in the drug discovery pipeline and the typology of study. The amount of compound may range from few grams needed for preclinical drug development and safety analysis to quantities as much as kilograms required for clinical study in different phases and many of tons for cosmetics (Martins et al., 2014).

Many scientific attempts have been performed to overcome this hurdle by increased development of synthetic or hemisynthetic analogues derivatives with desired properties, or designing a pharmacophore of lower complexity with easier synthesis method (Radjasa et al., 2011). The major results are coming from biotechnology applications trying to design and develop a pipeline for the marine cultures of organisms with pharmacological and nutraceutical interest. Natural resources should be cultured for obtaining a sustainable approach for marine drug discovery and marine natural compounds production. There are already several applied research lines in this direction,for instance, the growth of marine organisms in their natural environment by farming, which is also known as "mariculture", and the cultivation of the marine organisms under artificial conditions by the process called as "aquaculture" (Maier, 20109; Gerwick and Moore, 2012).

6.2 Biotechnological potential of marine microalgae

Marine microalgae are still unexplored resource for biotechnological applications with more than 25,000 species of which only 16 are actually in use for their economical interest. In recent years, microalgal culture technology is a new business area which is developing innovative technologies for different practical applications. Innovative processes and products have been introduced in microalgal biotechnology to produce vitamins, proteins, cosmetics, and healthy foods. For most of these applications, the market is still developing new sectors and the biotechnological use of microalgae will extend into new business areas. With the development of sophisticated culture and screening techniques, microalgal biotechnology can meet the challenging demands of both the food and pharmaceutical industries (Raja et al., 2008)

At present, in nutraceutical field, due to their high nutritional value, mainly freshwater microalgae such as *Spirulina* and *Chlorella* are being massively cultured as ingredient of healthy food. A variety of high value products including polyunsaturated fatty acids (PUFAs), pigments such as carotenoids and phycobiliproteins, and bioactive compounds are useful as nutraceuticals and pharmaceuticals, as well as for industrial applications (Cardozo et al., 2007).

Pharmaceutical applications of microalgae are still underexploited, although they produce a multitude of compounds that microalgae use as chemical defence against stress conditions or predators (Chu, 2011). Many important research programs are exploring and demonstrating the advantage of the microalgae exploitation for bioactive molecules because they represent a high renewable resource, since they can be cultured on a large scale for production of the desired chemicals. The advent of molecular biology has led to a better understanding of the biosynthesis and physiological functions of these bioactive molecules in microalgae. Efforts have also been invested to develop transgenic microalgae as "green cell factories" to produce new pharmaceuticals using genetic transformation techniques.

In terms of applications in drug discovery and medical biotechnology, microalgae represent thus a potential sources of high value products and bioactive molecules that may produce new lead compounds for further pharmacological and industrial studies and development (Chu, 2012).

The use of microalgae as a biological tool for monitoring and assessment of environmental toxicants is another application that has attracted much interest. For environmental biotechnology, microalgae are founding many applications, especially for bioremediation, bioassay and biomonitoring of environmental toxicants. Actually, several studies have demonstrated that a combination of various microalgae species are efficient in wastewater treatment. In addition to suspended cultures, immobilised microalgae system can further enhance the efficiency in the removal of environmental toxicants. While microalgae that are tolerant to toxicants are useful in bioremediation, sensitive species are useful tools for bioassay and biomonitoring of environmental pollutants. Microalgae have been used as bioassay organisms to assess the toxicity of pollutants such as heavy metals, pesticides and pharmaceuticals. The common microalgae used for bioassays of toxicants include *Pseudokirchneriella subcapitata*, *Dunaliella tertiolecta*, *Isochrysis galbana*, *Chlorella* spp. (Garcia et al., 200; Phang et al., 2000; Lim et al., 2010; Mustafa et al., 2012; De Bashan and Bashan, 2010). Microalgae have thus found a wide range of applications, but still remain to characterize their huge potential for larger applications in the biotechnology field.

6.3 The green microalga *Tetraselmis suecica*

Reactive oxygen species (ROS) have been linked to the pathogenesis of several human diseases such as atherosclerosis, diabetes mellitus, chronic inflammation, neurodegenerative disorders and many types of cancers. ROS can be partially neutralized by antioxidant compounds that can reduce the risk of many diseases related to oxidative stress (Fiedor and Burda, 2014). Hence, consumer preference for natural products is increasing the interest in finding new antioxidants from natural sources because synthetic products can cause potential long term toxic effects (Edge and Truscott, 2010). Most, if not all, commercially available natural antioxidants are derived from terrestrial plants (e.g. rosemary, tea, coffee, grape seeds, tomato and cocoa). Many of these antioxidants are carotenoids that are a class of more than 700 naturally occurring pigments synthesized by plants, algae, and photosynthetic bacteria. Carotenoids are known to be potent physical and chemical quenchers of singlet oxygen ($^1O_2$) and scavengers of other reactive oxygen species. However, the exact mechanisms underlying the protective function and specific molecular targets of carotenoids *in vivo* and *in vitro* are still poorly understood (Maiani et al.,, 2009).

Tetraselmis suecica is a marine green microalga belonging to the class Chlorophyceae, widely used in aquaculture for the feeding of mollusks and crustacean larvae (Chini Zittelli et al.,, 2006) and as a probiotic in fish (Irianto and Austin, 2014). *T. suecica* is rich in vitamin E, carotenoids, chlorophyll, and tocopherols (Perez-Lopez et al.,, 2014) and has been suggested as a food supplement in human and animal diets[7]. The total pigment extract from *T. suecica* has been patented for its ability to enhance dermal pigmentation, reduce psoriasis lesions and increase hair growth (Carballo-Cárdenas et al., 2003). In this study the potential biotechnological application of this species was investigated, analysing the protective role at molecular level on human anaplastic cells and tissues.

To this aim, the pigment content of an ethanol/water extract of *T. suecica* was characterized. Moreover, the study represents an attempt to better understand the antioxidant and protective effects of this extract against oxidative damage, at gene and protein level.

6.4 The dinoflagellate *Alexandrium andersoni*

Marine dinoflagellates are a large group of eukaryotic microalgae with approximately 2000 living species (Taylor et al., 2008). While eukaryotic, they possess many characteristics not seen in typical eukaryotes, such as a fifth base replacing uracil in their DNA (Hackett et al., 2004; Rizzo, 2003), unusually large genomes and greatly reduced chloroplast genomes (Zhang et al., 1999), permanently condensed chromosomes lacking in histones (Hackett et al., 2004), and complex organelle structures such as eyespots (Hoppenrath et al., 2009; Murray et al., 2012). Several species of this group are potentially toxic, causing economic losses such as death of fish and shellfish, and human health problems due to consumption of contaminated organisms (Glibert et al., 2005). Toxic dinoflagellates include the species *Alexandrium tamarense* (gonyautoxins), *Amphidinium carterae* (haemolysins), *Prorocentum lima* (okaidic acid and dinophysistoxins), *Prorocentrum rhathymum* (water-soluble fast-acting toxins and hemolytic effects), *Coolia monotis* (cooliatoxin) and *Ostreopsis sp*. (toxic butanol-soluble compound, palytoxin analogue) (Kita et al., 2005; Kobayashi and Tsuda, 2004; Onodera et al., 2005). Recently, a few studies have also evaluated the specific cytotoxic, antitumor, antibiotic, antifungal, immunosuppressant and neurotoxic activity of cultured dinoflagellates as potential sources for novel drug discovery (Camacho et al., 2007; Dragunow et al., 2005; Wright and Cembella, 1998). For instance, okadaic acid from Dinophysis is a potent neurotoxin used in studies on the therapeutic effects of atypical antipsychotic drugs in the treatment of cognitive impairment and schizophrenia (He et al., 2005); whereas the compound 13-desmethyl spirolide C (polyketide-derived), that can be synthesized by the dinoflagellate *Alexandrium ostenfeldii* (MacKinnon et al., 2006), has shown to have beneficial effects in a transgenic mouse model of Alzheimer's disease (Alonso et al., 2013). In addition, pectentoxins from Dinophysis show cytotoxic activity against several human cancer cell lines (Jung et al., 1995) and brevetoxin exposure may elicit important cellular effects, including apoptosis, cell metabolism and proliferation, and cytotoxicity, in an immune-derived transformed cell line following in vitro exposure (Walsh et al., 2008). Amphidinolides isolated from the dinoflagellate *Amphidinium carterae* also exhibit remarkably potent cytotoxicity against human tumor cell lines and are expected to be hopeful lead compounds for new anticancer drugs (Kobayashi et al., 2003).

This study evaluates the potential cytotoxic activity of a strain of the dinoflagellate *Alexandrium andersoni* against two very resistant cancer cell lines, lung adenocarcinoma (A549) and colorectal carcinoma (HT-29). Using a molecular approach, it was demonstrate that extracts of this species are able to activate two different cell death signalling pathways in the two tumor cell lines tested. We show that both signaling pathways are caspase-independent as opposed to many

therapeutic agents that induce caspase-dependent apoptosis (Debatin 2004), often targeting all proliferating cells without distinguishing between tumor and somatic cells.

CHAPTER 7.

Materials and Methods

7.1 Microalgae biomass production

The prasinophyte *Tetraselmis suecica* (strain CCMP 906) was purchased from the culture collection at the National Center for Marine Algae and Microbiota (NCMA – formerly "CCMP", Bigelow Laboratory for Ocean Sciences, Maine, USA) and was grown in Guillard's f/2 (Guillard, 1975) medium in two-liter polycarbonate bottles, constantly bubbled with air filtered through 0.2 µm membrane filters. The dinoflagellate *Alexandrium andersoni* (strain FE 108 from the microalgal collection maintained at the Stazione Zoologica Anton Dohrn) was grown in 10 liter carboys, with Guillard's f/2 medium; also this species required bubbling with air filtered through 0.2 µm membrane. Cultures were grown at 19°C, under a photon-flux density of about 150 µmol photons m^{-2} s^{-1}, and a photoperiod of 12:12 h light:dark (12L:12D) cycle. Initial cell concentrations were about 5 x 10^3 cells ml^{-1}. Microalgal biomass was collected by centrifugation after 9 days (~8 x 10^3 cells ml^{-1}).

7.2 Chemical extractions and fractionation

The ethanol/water *T. suecica* crude extract was obtained according to Goiris et al. (2011). Extraction procedure was conducted under dark conditions, at room temperature and under nitrogen atmosphere, in order to avoid oxidation of the samples. Freeze-dried biomass (~100 mg) was extracted with 1 ml ethanol/water (3/1, v/v) mixture for 30 min. The mixture was separated by centrifugation at 4500 x g, for 10 min, at 20°C, and the upper layer was transferred to a clean tube. The pellet was resuspended in 1 ml of the ethanol/water mixture and extracted for a second time. The ethanolic extract was dried in a rotary vacuum evaporator (Buchi rotavapor R-114). Dry extract was stored under nitrogen atmosphere at -20°C prior to analysis.

An aliquot of the wet pellet obtained (1.3 g) from the *A. andersoni* cultures was frozen and stored at -80 °C until use for Solid Phase Extraction, whereas 10 g were lyophilized to yield 1.4 g of dried material that was extracted with methanol (3×150 ml) at room temperature. An aliquot of this methanol extract (30 mg) was subjected to a modified Kupchan's partitioning procedure as follows (Kupchan et al., 1973). The methanol extract was dissolved in a mixture of MeOH/H_2O containing 10% H_2O and partitioned against n-hexane (2.1 mg of extract). The water content (%, v/v) of the MeOH extract was adjusted to 30% and partitioned against $CHCl_3$ (11.4 mg of extract). The aqueous phase was concentrated to remove MeOH and then extracted with *n*-BuOH (2.0 mg of extract).

For solid phase extraction (SPE) of *A. andersoni*, the wet microalgal cell pellet (1.3 g) was extracted directly with MeOH (3x7 ml). After evaporation of the solvent, 20 mg of this organic extract (82 mg) was subject to SPE on a GX-271 ASPEC Gilson apparatus by using CHROMABOND® HR-X cartridges (6 ml/500 mg) as reported by Cutignano et al. (2015). This extraction yielded 4 fractions that were tested on A549, HT-29, WI38 and BEAS-2B human cell lines.

7.3 HPLC and LC-MS/MS analysis

For the ethanol/water *T. suecica* crude extract was carried out chemical characterization in order to describe more in detail the content of this pool of molecules (chemical analysis were performed by Bio-Organic Chemistry Unit, Institute of Biomolecular Chemistry-CNR, Pozzuoli). Pigment measurements were conducted by High Performance Liquid Chromatography (HPLC), according to methods described in Brunet et al. (2014). Prior to injection into the HPLC, 250 µL of an Ion Pairing Agent (ammonium acetate 1 mol L^{-1}, final concentration of 0.33 mol L^{-1}) was added to 0.5 mL of the pigment extract and incubated for 5 minutes in the dark at 4°C. This extract was then injected in the 50 µL loop of the Hewlett Packard series 1100 HPLC (Hewlett Packard, Wilmington, NC, USA), equipped with a reversed-phase column (C8 Kinetex column; 50 mm×4.6 mm; 2.6 µm particle size, Phenomenex®, USA). The temperature of the column was steadily maintained at 20°C, and the flow rate of the mobile phase was set up at 1.7 mL min^{-1}. The mobile phase was composed of two solvent mixtures: A, methanol/aqueous ammonium acetate (70/30, v/v) and B, methanol. During the 12 minutes elution, the gradient between the solvents was programmed: 75% A (0 min), 50% A (1 min), 0% A (8 min) isocratic for 3 min.

Chlorophylls and carotenoids were detected by diode-array spectroscopy (spectrum data collected in the range 350 - 750 nm) using a Hewlett Packard photodiode array detector, model DAD series 1100 and absorbance chromatogram was reported at 440 nm. Chlorophylls were also detected by fluorescence using a Hewlett Packard standard FLD cell series 1100 with excitation and emission wavelengths set at 407 nm and 665 nm, respectively. Identification and quantification of pigments were carried out using pigment standards from the D.H.I. Water & Environment (Horsholm, Denmark). Pigment standards derived primarily from phytoplankton. The standards are flushed with 100% N2 and supplied in sealed vials with 2.5 mL, together with a certificate of analysis. All information regarding the accuracy of the preparation of the standards and reference numbers of all standards are available at the following address: http://c14.dhigroup.com/productdescriptions/phytoplanktonpigmentstandards. Moreover, spectral information was compared with a library of chlorophyll and carotenoid spectra of pigments prepared from standard phytoplankton cultures (Jeffrey and Wright, 1997).

To better characterize chemically the ethanol/water *T. suecica* crude extract, LC-MS/MS analysis was carried out on a Waters Alliance HPLC with a Waters 996 PDA detector on line with a Q-Tof mass spectrometer (Waters) featured by an ESI source in positive ionization mode. Column: Phenomenex Luna C8 250 x 4.6 mm, 5µm, 100A. Eluent A: Water, B: MeOH. Gradient: 90% B to 100% B in 15 mins, holding for 20 mins. Flow: 0.7 ml min-1. PDA: 400-700 nm. Full Mass range: 450-1000 m/z.

7.4 Scavenging activity against DPPH radical

2,2-Di(4-tert-octylphenyl)-1-picrylhydrazyl (DPPH) was used to perform the radical scavenger assay (Sigma Aldrich, cat. 257621) of the ethanol/water *T. suecica* crude extract. Various concentrations of extract were mixed with a final concentration of DPPH of 0.1 mM in methanol, allowed to react for 30 min in the dark. At the end of incubation time, absorbance was measured at 517 nm using a microplate reader (Multiskan FC, THERMO SCIENTIFIC).

7.5 Maintenance, treatment of human cell lines and cell viability

The adenocarcinomic human alveolar basal epithelial cell line A549 was used to perform the *in vitro* experiments with the ethanol/water *T. suecica* crude extract.

The lung/brunch epithelial cell line (BEAS-2B), the normal diploid human lung fibroblasts (WI-38), the human colorectal adenocarcinoma cells (HT-29) and A549 were used for *in vitro* experiments with *A. andersoni* extract and relative fractions.

A549 cells (ATCC CCL185) were cultured in DMEM medium (Dulbecco's modified Eagle's medium) supplemented with 10% (v/v) fetal bovine serum (FBS), 100 units ml^{-1} penicillin and 100 µg ml^{-1} streptomycin. HT-29 cells (ATCC HTB38) were maintained in McCoy's 5A medium supplemented with 10% (v/v) FBS, 2 mM L-glutamine, 100 units ml^{-1} penicillin and 100 µg ml^{-1} streptomycin. WI-38 cells were purchased from the American Type Culture Collection (ATCC® CCL-75™) and grown in MEM supplemented with 10% of FBS, 100 units ml^{-1} penicillin and 100 µg ml^{-1} streptomycin, 2mM of L-glutamine and non-essential amino acids (NEAA, 2 mM). BEAS-2B cells (ATCC CRL-9609) were maintained in BEGM medium containing all the recommended supplements (Lonza). All cell lines were incubated in a 5% CO_2 humidified chamber at 37°C for growth. Medium renewal occurred every 3 days, and cells were detached via trypsinization before they reached confluence.

The effect of all chemical samples on cell viability was determined using the 3-(4,5-Dimethylthiazol-2-yl)-2,5-Diphenyltetrazolium Bromide (MTT) assay (Applichem A2231) in according to Gerlier and Thomasset (1986). All cell lines, seeded in 96-well plates (2 x 10^3 cells $well^{-1}$), after incubation times with specific samples, were treated with 10 µl (5 mg ml^{-1}) of MTT and incubated for 3 h. The absorbance was recorded on a microplate reader at a wavelength of 570 nm (Multiskan FC, THERMO SCIENTIFIC). The effect of the samples on cell viability was evaluated as percent of cell viability calculated as the ratio between mean absorbance of each sample and mean absorbance of control.

The ethanol/water *T. suecica* crude extract was tested at eight increasing concentrations: 2, 5, 10, 25, 50, 100, 200 and 400 µg ml^{-1}, for 24 and 48 hours.

The *A. andersoni* extracts were tested at 10, 50, 100, 200 and 400 µg ml^{-1}, for 24 and 48 hours. At the same incubation time were also tested the *A. andersoni* SPE- fractions at 1, 10 and 100 µg ml^{-}

[1]. In an independent experiment, A549 and HT-29 cells (26 x 10^3 cells $well^{-1}$) were treated with three concentrations (1, 10 and 100 µg ml^{-1}) for each SPE fraction and with caspase-3 Inhibitor ($C_{30}H_{41}FN_4O_{12}$, sc-3075, Santa Cruz) at 9.7 mM. Cells were allowed to grow for 24 and 48 h and viability was then checked with the MTT assay, as described above.

7.6 RNA extraction, cDNA synthesis and Real-Time PCR of the cell samples

A549 cells (2 x 10^6), used for RNA extraction and analysis of the ethanol/water *T. suecica* crude extract, were seeded in Petri dishes (100 mm diameter) to obtain four types of samples: negative control without any treatment, positive control with 30 mM of H_2O_2, cells treated with ethanol/water extracts (100, 200 and 400 µg ml^{-1}), and cells recovered with extracts (100, 200 and 400 µg ml^{-1}) after pre-treatment for 1 h with 30 mM H_2O_2.

A549 and HT-29 cells were used for RNA extraction and analysis of the extracts and SPE fractions of *Alexandrium andersoni*.

After 2 h of exposure time, cells were washed directly in the Petri dish by adding cold Phosphate-Buffered Saline (PBS) and rocking gently. Cells were lysed in the Petri dish by adding 1 ml of Trisure Reagent (Bioline, cat. BIO-38033) per 100 mm dish diameter. RNA was isolated according to the manufacturer's protocol. RNA concentration and purity was assessed using the nanophotomer NanodroP (Euroclone).

About 200 ng RNA was subjected to reverse transcription reaction using the RT2 first strand kit (Qiagen, cat.330401) according to the manufacturer's instructions. The qRT-PCR analysis was performed in triplicate using the RT2 Profiler PCR Array kit (Qiagen, cat.330231), in order to analyze the expression of cell oxidative stress genes on A549 cells. Plates were run on a ViiA7 (Applied Biosystems 384 well blocks), Standard Fast PCR Cycling protocol with 10 µl reaction volumes. Cycling conditions used were: 1 cycle initiation at 95.0 °C for 10 min followed by amplification for 40 cycles at 95.0°C for 15 s and 60.0 °C for 1 min. Amplification data were collected via ViiA 7 RUO Software (Applied Biosystems). The cycle threshold (Ct)-values were analyzed with PCR array data analysis online software (http://pcrdataanalysis.sabiosciences.com/pcr/arrayanalysis.php, Qiagen).

7.7 Protein extraction and western blotting

A549 cells (2 x 10^6), used for protein extraction and analysis of the ethanol/water *T. suecica* crude extract, were seeded in Petri dishes (100 mm diameter) to obtain four types of samples: negative control without any treatment, positive control with cells treated with 30 mM H_2O_2, cells treated with 100, 200 and 400 μg ml^{-1}, and cells recovered with 100, 200 and 400 μg m^{-1} of extract after pre-treatment for 1 h with 30 mM H_2O_2. The same cell line was used to assess protein expression with *A. andersoni* extract.

A549 cell lysate was prepared after 24 h of treatment by scraping the cells of each Petri dish into 1 ml of Radio Immune Precipitation Assay buffer (RIPA, Cell Signaling, cat. 9806), supplemented with 1 μM of protease inhibitor PMSF (Cell Signaling, cat. 8553). The lysate was incubated on ice for 15 min and then clarified by centrifugation at 14000 x *g*, for 20 min. Total protein concentration was determined according to the Bradford method using a Protein Assay Reagent (Applichem, cat. A6932) with bovine serum albumin (BSA, Sigma Aldrich, cat. A2058) as a standard. The protein extract was stored at -20°C until use. Before electrophoresis, protein samples were incubated at 100°C for 5 min. Following 10% SDS-PAGE, gels were stained with Coomassie or blotted onto nitrocellulose membrane (Biorad, cat. 170-4159). Membranes were incubated for 1 h in blocking reagent (1X Tris Buffered Saline-TBS), with 0.1% Tween-20 with 5% w/v nonfat dry milk, and incubated overnight at 4°C with the primary antibodies diluted in 1X TBS, 0.1% Tween-20 with 5% BSA.

Three key proteins were investigated for the ethanol/water *T. suecica* crude extract: 24-dehydrocholesterol reductase (DHCR24, 1:1000, Sigma Aldrich SAB1405713), glutathione peroxidase 4 (GPX4, 1:1000, Sigma Aldrich SAB2500486), prostaglandin reductase 1 (PTGR1, 1:1000, Sigma Aldrich SAB4500918). Positive control was obtained by using anti-β-actin antibody (1:500, Novus Biological cat. NB600-501).

Primary antibodies used for *A. andersoni* extract were from the Death Receptor Antibody Sampler Kit (Cell Signaling, 8356S), including anti-TNFR1 (1:1000), anti-RIP-k1 (1:1000), anti-DR3/TNFRSF25 (1:1000). Positive control was obtained by using anti-β-actin antibody (1:500, Sigma cat. A2668).

After incubation, membranes were washed three times for 5 min each with 15 ml of TBS/Tween and then incubated with HRP-conjugated secondary antibody with gentle agitation for 1 h at room temperature. For β-actin and DHCR24 antibodies, we used HRP-conjugated secondary antibody anti-mouse (1:10000, Santa Cruz Biotechnology); for GPX4, PTGR1, TNFR, RIP-k1 and DR3/TNFRSF25 antibodies we used HRP-conjugated secondary antibody anti-rabbit (1:10000, Jackson ImmunoResearch).

After incubation, membranes were washed three times for 5 min each with 15 ml of TBS/Tween. Blotted membranes were immunodetected using clarity Western ECL (Biorad, cat. 170-5060). Proteins were visualized with Fuji medical X-ray film (cat. 47410). Densitometric analysis of immunopositive bands was performed using Image J software.

7.8 Elisa for prostaglandin E_2 (PGE_2)

Quantitative ELISA test was used to determine prostaglandin E_2 (PGE_2) levels secreted by A549 cells in cell culture medium before and after ethanol/water *T. suecica* crude extract treatment. Prostaglandins were quantified in the cell medium by ELISA kit (Life Technologies, cat. EHPGE2) according to standard manufacturer's recommendations. We quantified prostaglandins in four samples: A549 cells without treatment (control), A549 cells treated with 100, 200 and 400 µg ml^{-1} of extract, A549 cells treated with only 30 mM of H_2O_2 and A549 cells treated with 100, 200 and 400 µg ml^{-1} of the extract after pre-treatment for 1 h with 30 mM H_2O_2.

7.9 Treatment of human epidermis and tissue viability

The human epidermal tissue model EpiDerm EPI-200 (size 0.63 cm^2) was used as *in vitro* model to confirm the potential application of ethanol/water *T. suecica* crude extract as cosmeceutical. The effect of the extract on tissue viability was determined using the MTT assay. After 1 h treatment and 24 h of recovery time, tissues were transferred to 24-well plates containing MTT medium (1 mg ml^{-1}). After 3 h incubation in MTT, the blue formazan salt was extracted with 2 ml/tissue of isopropanol and the optical density of the extracted formazan was determined using a spectrophotometer at a wavelength of 570 nm. Relative tissue viability was calculated for each tissue as percentage of the mean of the negative control tissues. Skin irritation potential of the test extract was predicted if the remaining relative tissue viability was below 50% (MatTek Corporation-Protocol).

7.10 Cell cycle analysis

A549 cells (2 x 10^5) used for cell cycle analysis of the *A. andersoni* extract were seeded in 6-well plates and treated with 10, 50, 100, 200 and 400 µg ml^{-1} extract for 2, 4, 6, 8, 24 and 48 hours in order to verify dose response in time course experiments. After treatment times, A549 cells were collected from plates using 1 ml of Trypsin EDTA (Lonza, Italy), fixed in 70% ethanol and stored at

-20° C. Cells were then washed twice with PBS, re-suspended in PBS containing 1 mg ml^{-1}RNase A (Qiagen, Cat.19101), incubated at 37° C for 45 minutes and then stained with propidium iodide (10 µg ml^{-1}, Sigma cat. P4864) for 15 min. The percent distribution of cells in the different phases of the cell cycle was then estimated using a FACScalibur flow cytometer (BD Biosciences Immunocytometry Systems, San Jose, CA, USA), equipped with a 488 nm Ar laser and standard filter sets. The percentage of cells in the different phases of the cell cycle was calculated using ModFit LT (Verity Software House, Topsham, ME, USA).

7.11 Statistical analysis

Statistical significance of the DPPH assay was determined by Students-t test (*p values ≤ 0.05). Statistical differences between treated and control cells for cell viability counts were determined by One-way ANOVA and significant differences between the treated groups by Students-t test (*) and ANOVA followed by Dunnett's test (#) (p values ≤ 0.001) using Microsoft Excel software (365 version, 2013). Gene expression data were analyzed by PCR array data analysis online software (http://pcrdataanalysis.sabiosciences.com/pcr/arrayanalysis.php, Qiagen®). Only expression values greater than a 2.0-fold difference with respect to the controls were considered significant. Immunoblotting protein expression was calculated as the percentage of integral area of every single gel band with respect to total gel lane area, represented as pixels. Statistical differences between treated and controls were determined by Students-t test with significant p values ≤ 0.05. Data significantly different from controls, with p values < 0.001 are marked with two asterisks in the figures. Significant differences between treated groups, after epidermal human tissue experiments, were determined using Students-t test (*p ≤ 0.05) and ANOVA.

CHAPTER 8.

Results

Tetraselmis suecica

8.1 Chemical characterization

The high performance liquid chromatography (HPLC) pigment profile of the ethanol/water crude extract of *Tetraselmis suecica* was performed to better analysed the chemical contents (figure 8.1 A). The technique applied was able to reveal porphyrin pigments, chlorophyll *a* and *b*, α- and γ-carotene and xanthophyll pigments such as lutein, loroxanthin dodecenoate, loroxanthin decenoate, violaxanthin, neoxanthin, 9'-*cis*-neoxanthin and antheraxanthin (figure 8.1 B). The pigments were identified by diode array (DAD) spectroscopy and comparing their visible absorption spectra with authentic standard.

A

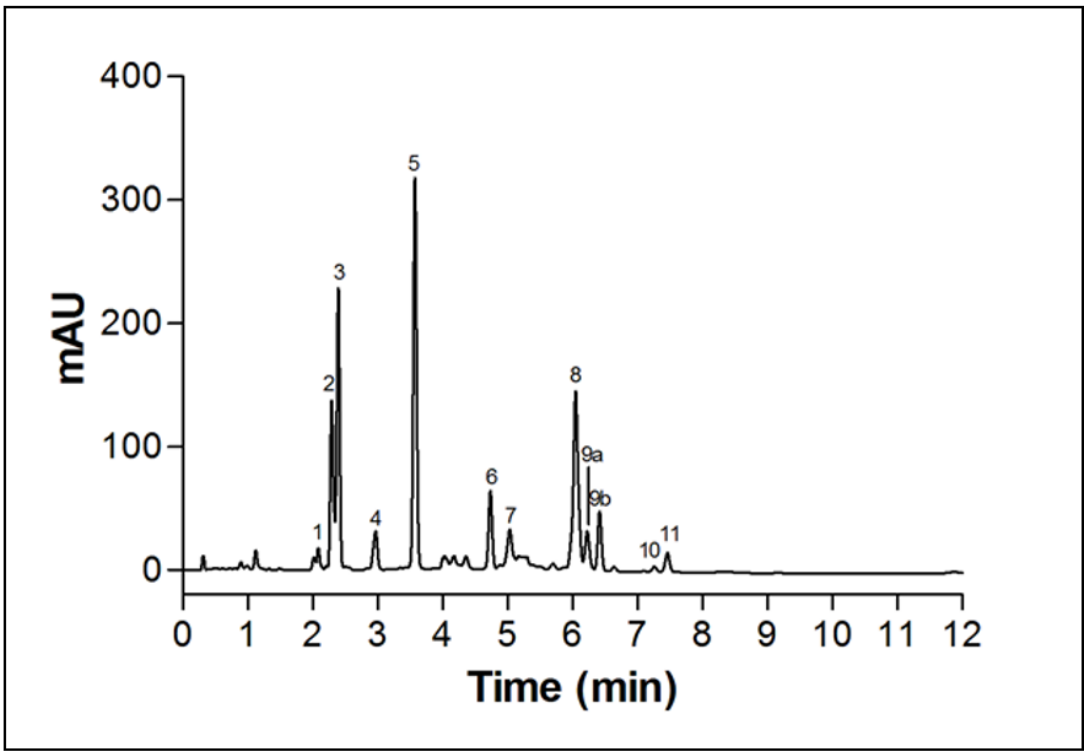

B

Peak	Retention time (min)	Pigment	Abbreviation	Absorbance maxima (nm)
1	2.08	Violaxanthin-like	Viola-like	415-440-469
2	**2.29**	**Neoxanthin**	**Neo**	**413-436-465**
3	2.39	Violaxanthin	Viola	415-440-469
4	**2.97**	**9'-*cis*-Neoxanthin + Antheraxanthin**	***c*-Neo Anth**	**413-436-465 422-447-472**
5	3.58	Lutein	Lut	418-444-474
6	**4.74**	**Loroxanthin dodecenoate**	**Loro-*d***	**420-448-473**
7	5.04	Chlorophyll *b*	Chl *b*	457-650
8	**6.05**	**Chlorophyll *a***	**Chl *a***	**430-618-665**
9a	6.23	Chlorophyll *a*'	Chl *a*'	430-618-665
9b	6.42			
10	**7.26**	**γ-Carotene**	**γ-Car**	**436-462-490**
11	7.46	α-Carotene	α-Car	425-449-476

FIGURE 8.1: Chemical characterization of ethanol/water crude extract. (**A**) HPLC chromatogram of pigments from the ethanol/water extract of the green microalga *Tetraselmis suecica*. (**B**) Table describes peak identification, retention time, abbreviations and online spectral characteristics of the ethanol/water extract of the green microalga *Tetraselmis suecica*.

Results were also supported by HPLC-PDA-MS/MS data (figure 8.2). Other xanthophyll pigments, such as loroxanthin and zeaxanthin, which are usually found in green algae, were not observed in this sample. Loroxanthin decenoate was tentatively identified only by LC-MS/MS

analysis. Xanthophylls constituted almost 79% of the total pigments identified, and, within the group, lutein was the most abundant, reaching concentrations comparable to that of chlorophyll b (Chl *b* 31% of Chl *a*, Lutein 33% of Chl *a*; see for more details figure 8.2, A and B). Neoxanthin and violaxanthin pigments showed a percentage over Chl *a* of about 16%, whereas loroxanthin dodecenoate a percentage of 8%.

A

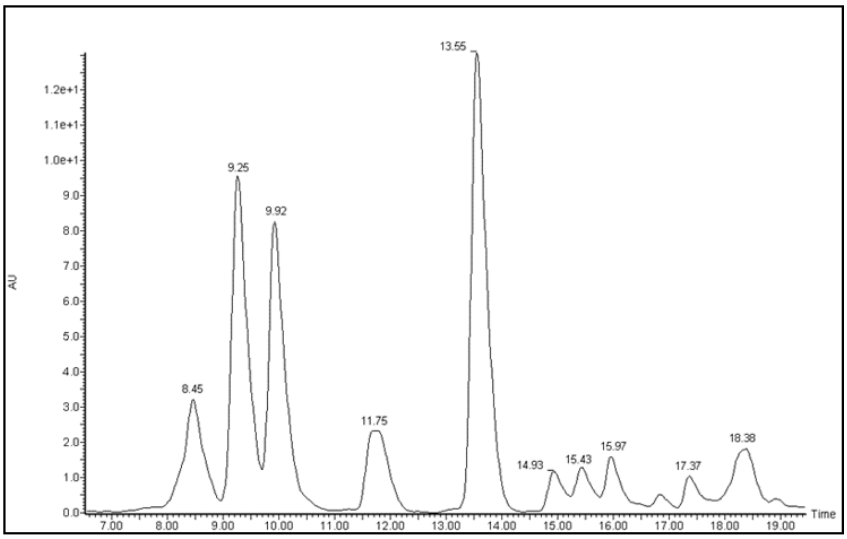

B

Tr	Abs max (nm)	ESI$^+$-MS *m/z*	ESI$^+$-MS/MS *m/z*	Name
8.45	439, 469	623.4 (M+Na$^+$)	605 (M-H$_2$0+Na$^+$), 587(M-2H$_2$0+Na$^+$), 531 (M-92+ Na$^+$)	Violaxanthin-lik
9.25	**413, 436, 464**	**623.4 (M+Na$^+$)**	**605 (M-H$_2$0+Na$^+$), 587(M-2H$_2$0+Na$^+$), 531 (M-92 +Na$^+$)**	**Neoxanthin**
9.92	416, 439, 469	623.4 (M+Na$^+$)	605 (M-H$_2$0+Na$^+$), 587(M-2H$_2$0+Na$^+$), 531 (M-92 +Na$^+$)	Violaxanthin
11.75	**440, 474**	**607.4 (M+Na$^+$) + 623.4 (M+Na$^+$)**	**589 (M-H$_2$0+Na$^+$), 515 (M-92+Na$^+$); 605 (M-H$_2$0+Na$^+$), 587(M-2H$_2$0+Na$^+$), 531 (M-92+ Na$^+$)**	**Antheraxanthin + *c*-Neoxanthin**
13.55	444, 472	591.4 (M+Na$^+$)	573 (M-H$_2$0+Na$^+$), 499 (M-92+ Na$^+$)	Lutein
14.93	**438, 465**			**Not identified**
15.43	440, 466			Not identified
15.97	**446, 473**	**759.5 (M+Na$^+$)**	**589 (M-170 +Na$^+$)**	**Loroxanthin decenoate**
17.37	446, 473	787.5 (M+Na$^+$)	589 (M-198 +Na$^+$)	Loroxanthin dodecenoate
18.38	**457, 633**	**975.5 (M+Na$^+$)**	**915, 697, 665**	**Chlorophyll-like**

FIGURE 8.2: Chemical characterization of ethanol/water crude extract. (**A**) LC-PDA-ESI+MS/MS analysis of the carotenoid pool in the ethanol/water extract of *Tetraselmis suecica*. (**B**) Table describes for each peak retention time, maximum of absorbance (expressed in nm), ESI$^+$-MS (expressed in *m/z*), ESI$^+$-MS/MS (expressed in *m/z*) and relative names of the chemical components of the ethanol/water extract of the green microalga *Tetraselmis suecica*.

8.2 Antioxidant activity assay

The ethanol/water extract of the *Tetraselmis suecica* exhibited marked reducing activity toward radical species. This property was demonstrate testing the ability of crude extract of the green microalga of scavenging the 2,2-diphenyl -1-picrylhydrazyl (DPPH) radical. Addition of extract concentrations of 50 µg ml^{-1}, 100 µg ml^{-1} and 200 µg ml^{-1} resulted in a dose-dependent reduction (21.5%, 52.0% and 97.7%, respectively) of the purple radical DPPH into the yellow reduced form. This activity was significantly stronger than the positive control, α-Tocopherol, tested at the same concentrations (Table 8.1).

TABLE 8.1: Radical scavenging capacity (RSC, %) of *Tetraselmis suecica* ethanol/water extract on DPPH free radical. Values are reported as percentage versus a blank and are the mean ±SD of three independent samples analyzed three times. Asterisks denote significant increases in measured radical scavenging activity *p≤0.05 versus control.

Extract concentration (µg/ml)		Optical density (OD517 nm)	Inhibition percentage (IP) of DPPH radical
		ODT0-ODTS	
	0	0.000±0.001	0.0±0.789
Tetraselmis suecica	50	0.0655±0.029	21.1±2.87*
	100	0.081125±0.034	52.00±3.44*
	200	0.111±0.051	97.72±5.09*
	0	0.000±0.001	0.0±0.789
α-Tocopherol	50	0.0125±0.052	5.98±5.21
	100	0.026±0.035	12.36±1.10*
	200	0.040±0.013	26.00±1.3*

8.3 Cell viability and recovery experiment

Lung adenocarcinoma (A549) cells treated with different concentrations of the extract for 24 and 48 h were not affected in the majority of the concentrations tested (2 μg ml^{-1}, 5 μg ml^{-1}, 10 μg ml^{-1}, 25 μg ml^{-1}, 50 μg ml^{-1}, 100 μg ml^{-1} and 200 μg ml^{-1}). An exception was represented by A549 cells at the highest concentration of 400 μg ml^{-1}, which induced a slight reduction in cell viability (80% and 81% cell viability, at 400 μg ml^{-1}, at the two incubation times, figure 8.3 A).

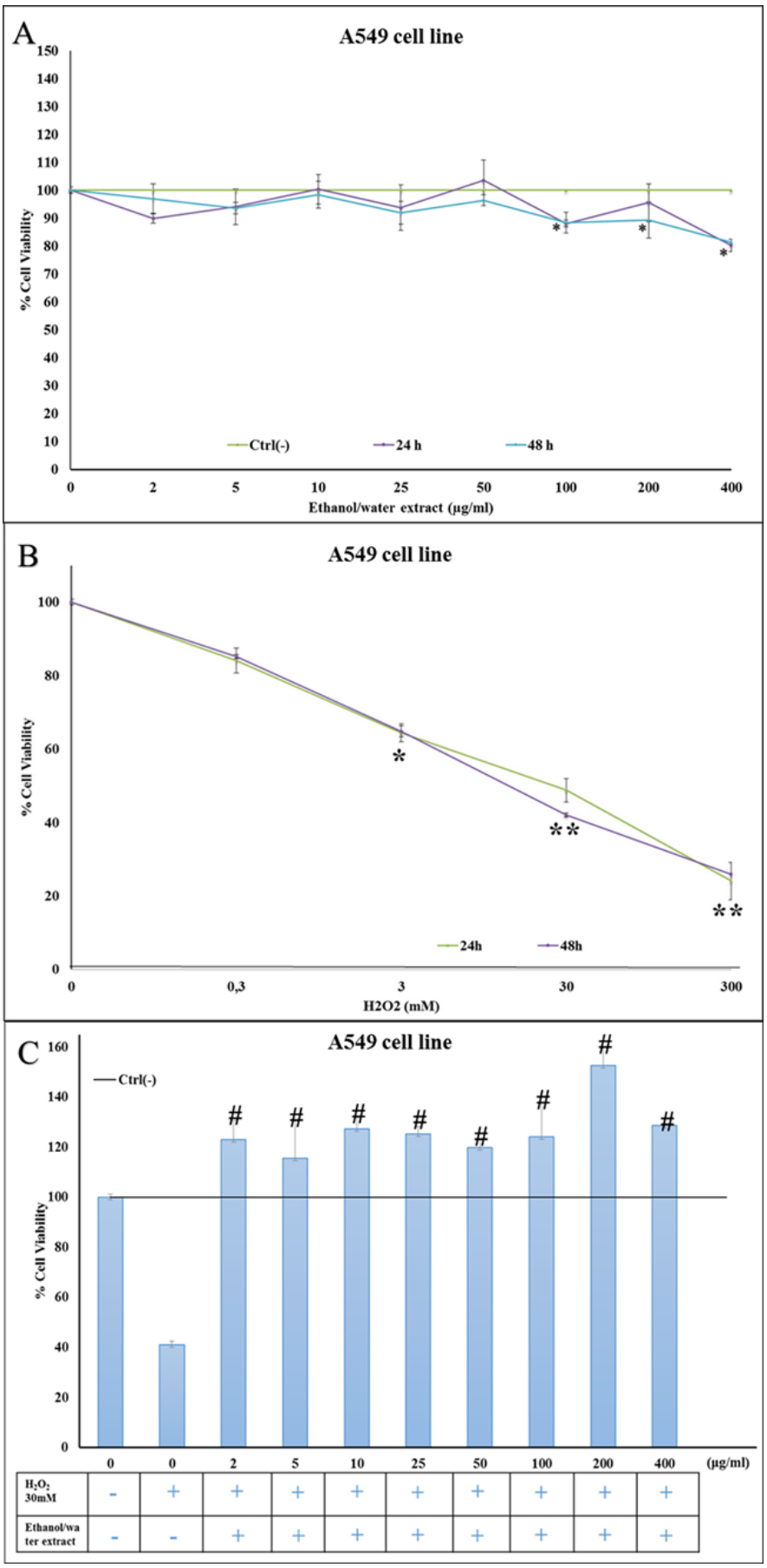

FIGURE 8.3: *In vitro* repairing activity of *Tetraselmis suecica* ethanol/water extract against H_2O_2 treatment. (**A**) Human lung adenocarcinoma cells (A549) treated with various concentrations of *T.*

suecica extracts for 24 and 48 h. Cell viability was determined using the MTT assay and expressed as the percentage of control growing cells. (**B**) Cell viability of lung adenocarcinoma cells (A549) treated with various concentrations of H_2O_2 (0.3 mM, 3 mM, 30 mM and 300 mM) for 24 and 48 h . (**C**) Effect of extract on cell viability of A549 cells following exposure to H_2O_2 prior to extract treatment at 2 μg ml^{-1}, 5 μg ml^{-1}, 10 μg ml^{-1}, 25 μg ml^{-1}, 50 μg ml^{-1}, 100 μg ml^{-1}, 200 μg ml^{-1} and 400 μg ml^{-1}. Three independent assays were performed in triplicate; data are shown as mean ±S.D. Significant differences between treated groups were determined using Students-t test (*) and ANOVA followed by Dunnett's test (#). Crosshatched symbols denote significant differences between treatments and control (#$p<0.05$).

In order to assess the antioxidant effects of the extract we induced an oxidative stress on A549 cells with hydrogen peroxide (H_2O_2). First, we treated A549 cells with a wide range of H_2O_2 concentrations (0.3, 3, 30 and 300 mM) to determine the half maximal Inhibitory Concentration (IC50) dose to be used for pretreatment of cells, before to perform recovery experiments with extract; the IC50 dose was established as 30 mM after 24 h and 48 h of treatment (Figure 8.3 B). We then treated A549 cells with 30 mM of H_2O_2 for 1 h, inducing H_2O_2 oxidative stress, and added the extract to cells. The extract induced a significant recovery effect on H_2O_2 stressed A549 cells after 48 h of treatment. Histograms in figure 8.3 C show the effect of treatment with H_2O_2 (injury treatment) and successive extract. Treatment with H_2O_2 resulted in 36% cell viability after 48 h, whereas addition of extract induced a proliferation of A549 cells, with a cell viability increase of 143, 114, 125, 112, 133, 126, 114 and 148% for all concentrations tested (2, 5, 10, 25, 50, 100, 200 and 400 μg ml^{-1}) with respect to the negative control. Within the experimental error, there was a plateau effect already at 2 μg ml^{-1} of the extract and a further increase of this concentration did not affect cell viability.

8.4Analysis of the variation in gene expression

The expression of genes involved in oxidative stress and repairing pathways were studied by Real-Time qPCR (Table 8.2).

TABLE 8.2: List of genes studied belonging to several oxidative stress response and detoxification and repairing mechanisms.

Unigene	Refseq	Symbol	Description	Gname
Oxidative Stress Responsive Genes				
Hs.125213	NM_004045	ATOX1	ATX1 antioxidant protein 1 homolog	ATX1/HAH1
Hs.514821	NM_002985	CCL5	Chemokine (C-C motif) ligand 5	D17S136E/RANTES/SCYA5 SIS-delta/SISd/TCP228/eoCP
Hs.498727	NM_014762	DHCR24	24-dehydrocholesterol reductase	DCE/Nbla03646/SELADIN1/ seladin-1
Hs.239	NM_021953	FOXM1	Forkhead box M1	FKHL16/FOXM1B/HFH-11/HFH11 HNF-3/INS-1/MPHOSPH2 MPP-2/MPP2/PIG29/TRIDENT
Hs.76686	NM_000581	GPX1	Glutathione peroxidase 1	GPXD/GSHPX1
Hs.433951	NM_002085	GPX4	Glutathione peroxidase 4	GPx-4/GSHPx-4/MCSP PHGPx/snGPx/snPHGPx
Hs.523836	NM_000852	GSTP1	Glutathione S-transferase pi 1	DFN7/FAEES3/GST3/GSTP HEL-S-22/PI
Hs.368525	NM_020992	PDLIM1	PDZ and LIM domain 1	CLIM1/CLP-36/CLP36/HEL-S-112 hCLIM1
Hs.502823	NM_181652	PRDX5	Peroxiredoxin 5	ACR1/AOEB166/B166/HEL-S-55/PLP/PMP20/PRDX6/PRXV/ SBBI10/prx-V
Hs.466693	NM_012237	SIRT2	Sirtuin 2	SIR2/SIR2L/SIR2L2
Hs.487046	NM_000636	SOD2	Superoxide dismutase 2, mitochondrial	IPOB/MNSOD/MVCD6
Peroxide metabolism genes				
Hs.460260	NM_001354	AKR1C2	Aldo-keto reductase family 1, member C2	AKR1C-pseudo/BABP/DD/DD-2 DD/BABP
Hs.525600	NM_001017963	HSP90AA1	Heat shock protein 90kDa alpha A	EL52/HSP86/HSP89A/HSP90A HSP90N/HSPC1/HSPCA/HSPCAL1
Hs.390594	NM_014331	SLC7A11	Solute carrier family 7 member 11	CCBR1/xCT
Antinflammatory pathway				
Hs.584864	NM_012212	PTGR1	Prostaglandin reductase 1	LTB4DH/PGR1/ZADH3

In particular, variation of gene expression analysis was performed for A549 cells treated with 100 µg ml^{-1}, 200 µg ml^{-1} and 400 µg ml^{-1} of extract alone (figure 8.4 D) and 100 µg ml^{-1}, 200 µg ml^{-1} and 400 µg ml^{-1} of extract after 1 h of exposure to 30 mM of H_2O_2 (figures 9.4 A, 9.4 B and 9.4 C, respectively).

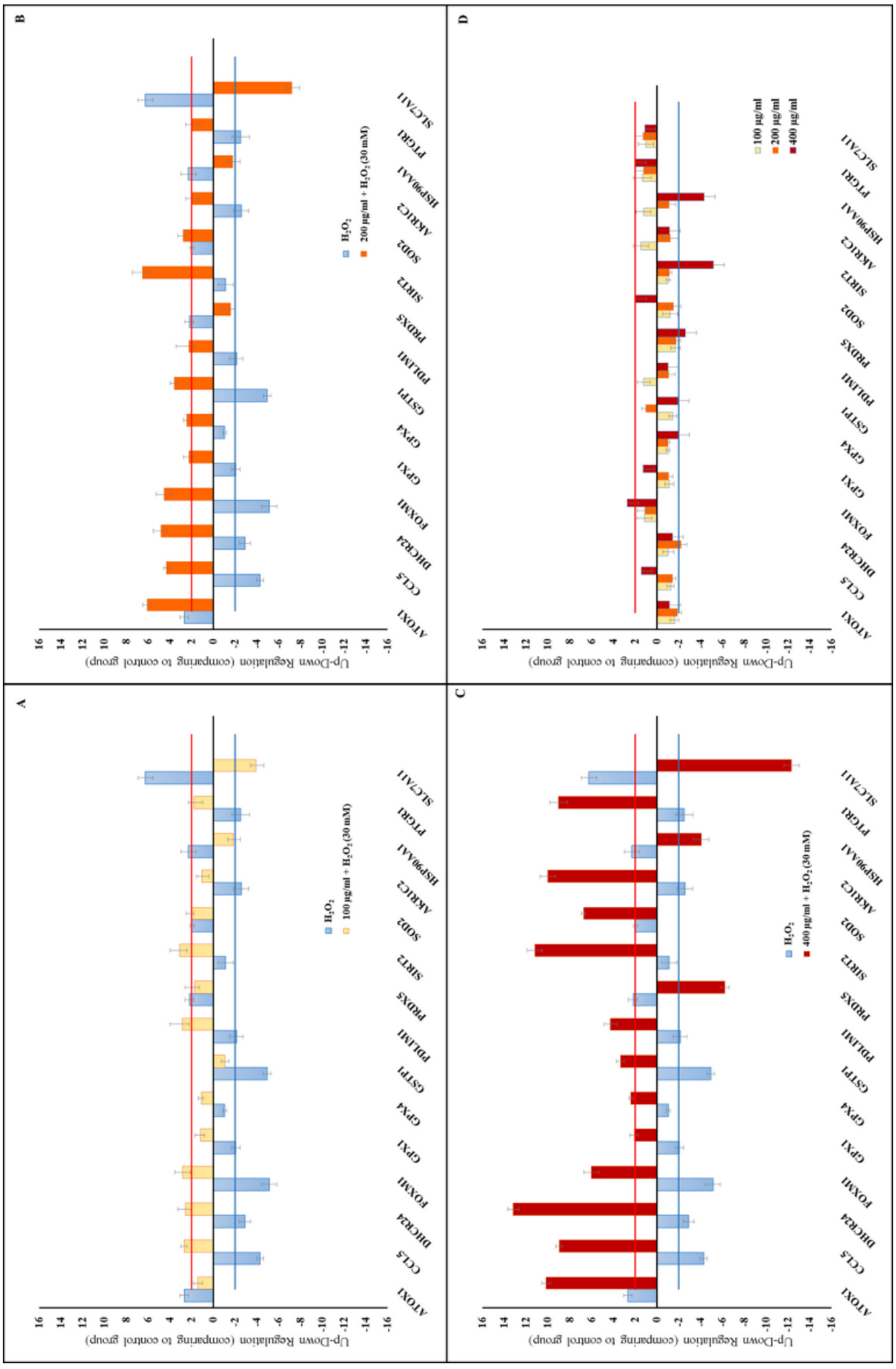
A
B
C
D
Up-Down Regulation (comparing to control group)
16
14
12
10
8
6
4
2
0
-2
-4
-6
-8
-10
-12
-14
-16
ATOX1
CCL5
DHCR24
FOXM1
GPX1
GPX4
GSTP1
PDLIM1
PRDX5
SIRT2
SOD2
AKR1C2
HSP90AA1
PTGR1
SLC7A11
H2O2
100 µg/ml + H2O2 (30 mM)
200 µg/ml + H2O2 (30 mM)
400 µg/ml + H2O2 (30 mM)
100 µg/ml
200 µg/ml
400 µg/ml

FIGURE 8.4: Histograms showing the results of gene expression analysis. **(A, B,** and **C)** Effect of *Tetraselmis suecica* ethanol/water extract at three different concentrations (100 μg ml^{-1}, 200 μg ml^{-1} and 400 μg ml^{-1}) on oxidative stress gene expression in H_2O_2-treated human lung adenocarcinoma cells (A549). A549 cells were pretreated with H_2O_2 (30 mM = 12 μg ml^{-1}) for 1 h prior to extract treatments (100, 200 and 400 μg ml^{-1}) and harvested 2 h later. **(D)** Negative control for the evaluation of the effect of *Tetraselmis suecica* ethanol/water extract (without any injury pre-treatment) at three different concentrations (100, 200 and 400 μg ml^{-1}) on oxidative stress gene expression in human lung adenocarcinoma cells (A549). Three independent assays were performed in triplicate and the data are expressed as mean ±S.D. Expression values greater or lower than a two-fold difference with respect to the controls were considered significant.

Only these three concentrations were chosen among that used for viability and recovery assays, since lower extract concentrations did not induce significant changes in gene and protein expression. Gene expression results are reported after 2 h of treatment since several factors implicated in oxidative damage repairing pathways were already expressed and activated after this time interval. Control genes for Real-Time qPCR were actin-beta (ACTB), beta-2-microglobulin (B2M), hypoxanthine phosphoribosyltransferase (HPRT1) and ribosomal protein large P_0 ($RPLP_0$), the expression of which remained constant. For gene expression studies, we chose the three highest concentrations (100, 200 and 400 μg ml^{-1}) that showed strong repairing activities even if we observed a slight cytotoxicity (about 20%) at the two highest concentrations (200 and 400 μg ml^{-1}).

Notwithstanding the toxicity observed at biochemical level, there was only a significant dose-dependent activation of specific oxidative stress response mechanisms without the involvement of those genes belonging to cell death programs with all three concentrations. This suggests that the slight cytotoxicity did not inhibit or interfere the repairing activity of the extract.

24-dehydrocholesterol reductase (DHCR24) was downregulated only at 200 μg ml^{-1} (2.2-fold change). Whereas at 400 μg ml^{-1} all the following genes were downregulated: glutathione peroxidase 4 (GPX4, 2.0-fold change), glutathione *S*-transferase pi 1 (GSTP1, 2.0– fold change), peroxiredoxin 5 (PRDX5, 2.6-fold change), Sirtuin 2 (SIRT2, 5.18-fold change) and heat shock protein alpha class A member 1 (HSP90AA1, 90 kDa, 4.3-fold change). At the same concentration, there was an upregulation of forkhead box M1 (FOXM1, 2.71-fold change), superoxide dismutase (SOD2, 2.0-fold change) and prostaglandin reductase 1 (PTGR1, 2.0-fold change). As shown in figures 8.4 A, 9.4 B and 9.4 C, the antioxidant protein 1 homolog gene (ATOX1) was upregulated after H_2O_2 treatment (2.7-fold change) and was highly upregulated after extract recovery treatment at 200 and 400 μg ml^{-1} (6.1 and 10.2-fold change, respectively). The small inducible cytokine subfamily A5 gene (CCL5) was downregulated with H_2O_2 (4.3-fold change) and was upregulated with the extract at all concentrations tested (2.7, 4.3 and 8.9-fold change, respectively). Opposing gene expression patterns between H_2O_2 and extract recovery treatment at all concentrations tested were recorded in: 24-dehydrocholesterol reductase (DHCR24, -2.9 vs 2.5, 4.8 and 13.2-fold change), forkhead box M1 (FOXM1, -5.1 vs 2.5, 4.5 and 6.0-fold change), glutathione peroxidase 1 (GPX1 -2.0 vs 1.2, 2.0 and 2.1-fold change) and glutathione peroxidase 4 (GPX4, -1.04 vs 1.0, 2.5 and 2.4-fold change,

respectively), glutathione *S*-transferase pi 1 (GSTP1, -4.9 vs -1.1, 3.6 and 3.4-fold change), C-terminal lim domain protein 1 (PDLIM1, -2.11 vs 2.8, 2.2 and 4.3-fold change) and aldo-keto reductase family 1, member C2 (AKR1C2, -2.6 vs 1.1, 2.03 and 10.0-fold change). On the contrary, peroxiredoxin 5 (PRDX5), solute carrier family 7 (SLC7A11) and heat shock protein alpha class A member 1 (HSP90AA1, 90 kDa) were upregulated with H_2O_2 (2.2, 6.2 and 2.3-fold change) and downregulated or poorly expressed at 100 µg ml^{-1} (1.7, -1.6 and 6.0-fold change), 200 µg ml^{-1} (-1.6, 7.2 and -1.8-fold change) and 400 µg ml^{-1} (-6.0, -12.3 and -4.1-fold change). Interestingly, prostaglandin reductase 1 (PTGR1) was downregulated after H_2O_2 injury (-2.5-fold change) and was even upregulated after extract treatment at all concentrations (1.8, 2.0 and 9.0-fold change). Gene expression of the Sirtuin 2 (SIRT2) and superoxide dismutase (SOD2) was enhanced by extract treatment after 1 h of exposure to H_2O_2 (from -1.1 to 3.1, 6.5 and 11.2, and from 1.9 to 2.0, 2.8 and 6.7-fold change, respectively).

8.5 Analysis of the variation in protein expression

Since DHCR24, GPX4 and PTGR1 genes play crucial roles in antioxidant/anti-inflammatory cell signaling pathways, A549 cells were treated with 200 and 400 µg ml^{-1} extract for 24 h in the presence and absence of 30 mM H_2O_2 and protein levels were analyzed by immunoblot. We chose the two most active concentrations used for PCR array analysis in order to compare the upregulation between gene and protein expression. Exposure time was 24 h since protein expression levels were too low before this time. Immunoblot analysis revealed a significant increase only in the expression of DHCR24 at the two concentrations tested with the only ethanol/water crude extract (figure 8.5 A), whereas the expression of GPX4 and PTGR1 significantly increased only after at 400 µg ml^{-1}, with H_2O_2 pretreatment (figures 8.5 B and 8.5 C).

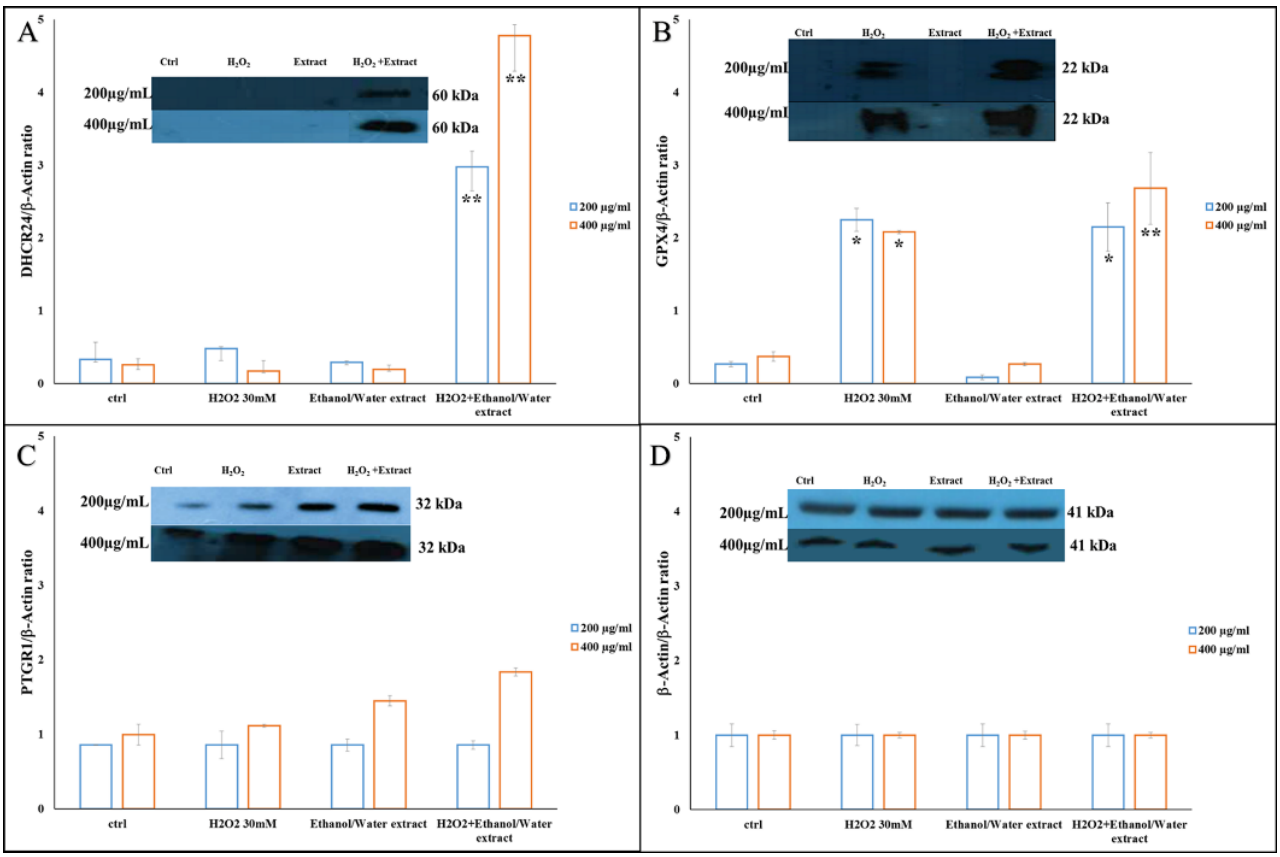

FIGURE 8.5: The effect of *Tetraselmis suecica* ethanol/water extract on oxidative stress protein expression in H_2O_2-treated human lung adenocarcinoma cells (A549). (**A**, **B** and **C**) Three independent assays were performed in triplicate and the data shown are mean ±S.D. The values above the blots represent the densitometric analysis of the photographic sheets measuring the variation in protein expression. The values of the bands are normalized versus actin and represented as ratio between the expression of single protein and actin. Asterisks denote significant differences compared to controls (*p≤0.05 and **p<0.005).

8.6 Assessment of prostaglandin E_2 release

In light of these results, we hypothesized that the extract was able to repair peroxidative cell damage by reducing the quantity of prostaglandins. Quantitative ELISA test was used to determine prostaglandin E_2 (PGE_2) levels secreted by A549 cells in cell culture medium before and after extract treatment. As shown in figure 8.6 A, A549 cells treated with extracts (100, 200 and 400 µg ml^{-1} concentrations) had the same levels of prostaglandin E_2 (29, 30 and 28 pg $µl^{-1}$, respectively) as the negative control (30 pg $µl^{-1}$). On the contrary, there was a significant dose-dependent decrease (90, 29 and 28 pg $µl^{-1}$) in prostaglandin E_2 levels with respect to the positive control (140 pg $µl^{-1}$) in A549 cells treated with extract (100, 200 and 400 µg ml^{-1}) after pretreatment with 30 mM of H_2O_2 (figure

8.6 B). Our data show that extract treatment results in a significant decrease in PGE_2 levels in cells damaged by H_2O_2.

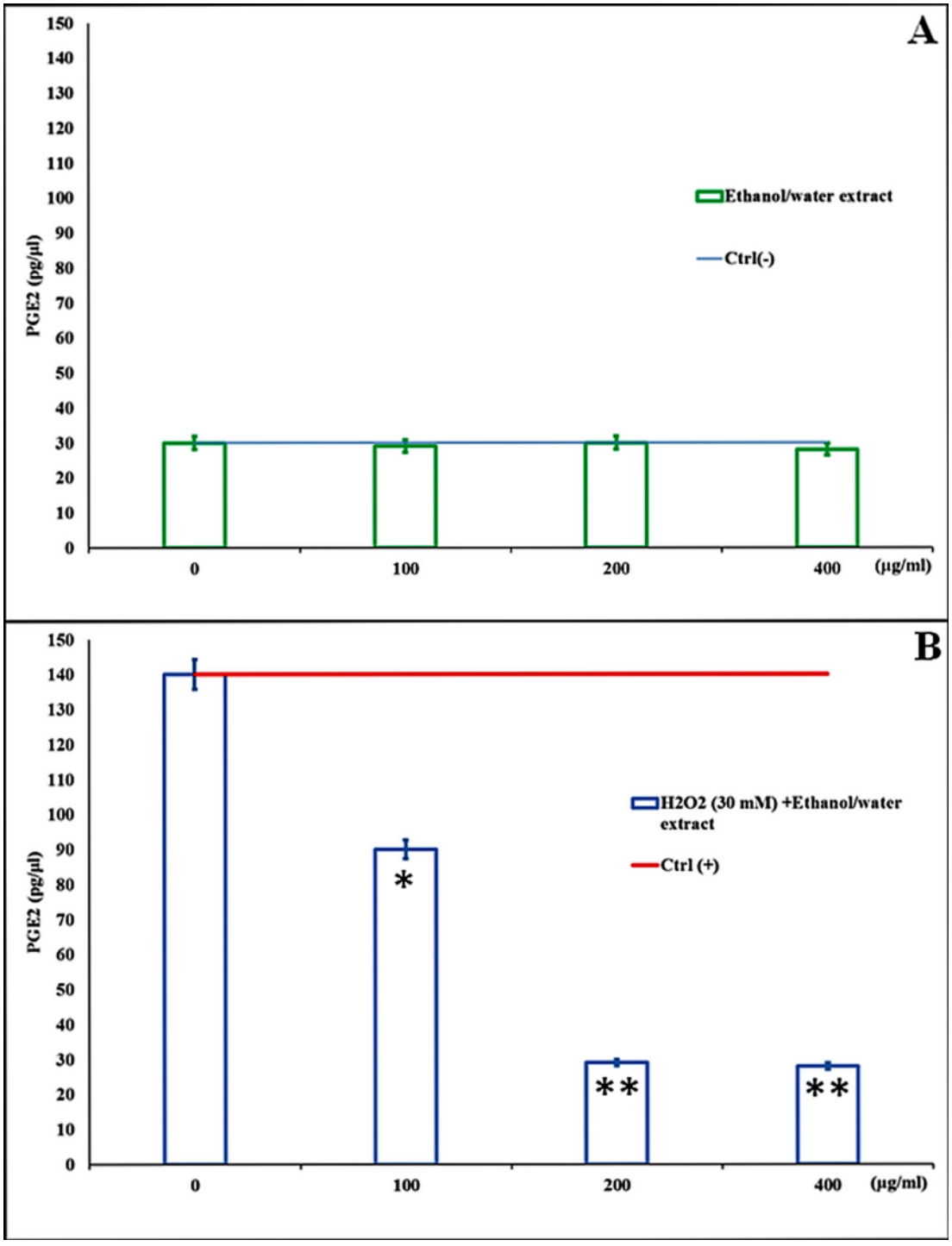

FIGURE 8.6: The effect of ethanol/water extract from *Tetraselmis suecica* on prostaglandin PGE_2 serum-release induced by H_2O_2 -treatment in human lung adenocarcinoma cells (A549). (**A**) Average PGE_2 concentration (pg μl^{-1}) determined by ELISA in culture medium of cells treated with 100, 200 and 400 µg ml^{-1} of the extract for 24 h. (**B**) Average of the PGE_2 concentration (pg μl^{-1}) determined by ELISA in culture medium of cells treated with 100, 200 and 400 µg ml^{-1} of extract for 24 h after

pretreatment with 30 mM (= 12 μg ml^{-1}) of H_2O_2 for 1 h. Asterisks denote significant differences compared to controls (*$p \leq 0.05$ and **$p < 0.005$) and determined using Students-t test.

8.7 Effect on *ex vivo* tissue

Finally, we used the reconstructed human epidermal tissue model EpiDerm EPI-200 (size 0.63 cm^2) as *ex vivo* model to confirm the potential topic application of this extract as cosmeceutical. In particular, we chose this tissue because *in vivo* oxidative stress frequently occurs in the epidermidis causing aging and other oxidative stress-related diseases. EPI-200 was treated with 30 mM H_2O_2 and with 200 μg ml^{-1} of the ethanol/water extract for 1 h, after injury with H_2O_2. The epidermal tissue model was treated with 200 μg ml^{-1} of the extract since this was the lowest concentration at which gene and protein expression data revealed a complete activation of all key factors in the antioxidant pathway. Treated medium was removed and replaced with extract, but without H_2O_2, to assess if the irritant effect persisted after 24 h of recovery (referred to as recovery time). Treatment with 200 μg ml^{-1} extract for 1 h significantly affected tissue viability after 24 h recovery time (85% viability) compared to the irritant effect of 1 h treatment with H_2O_2 (18% viability) (Figure 8.7). The repairing effect by the extract was even more evident 1 h later after treatment with 30 mM H_2O_2 and 200 μg ml^{-1} of the extract tissue, with viability increasing from about 20% to 108.5% with respect to the negative control.

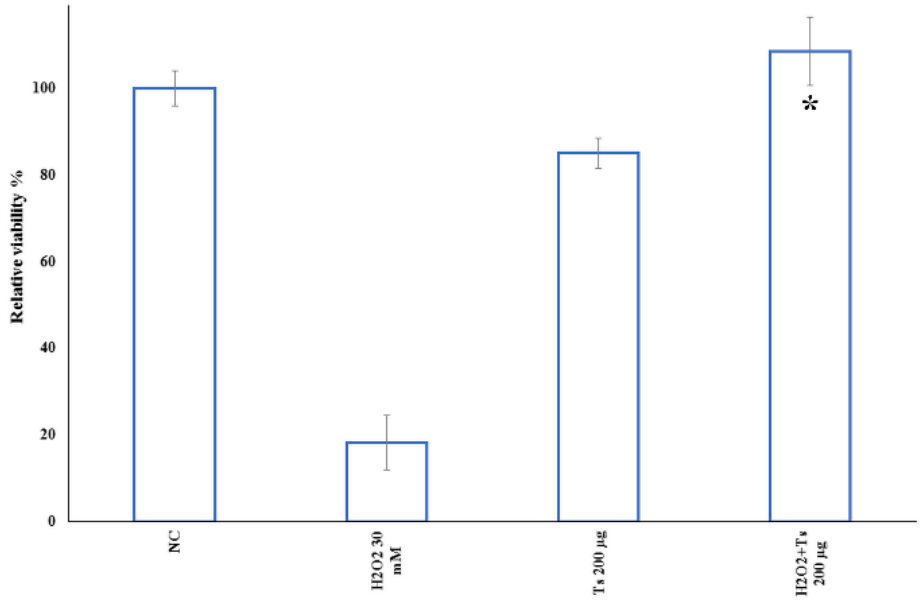

FIGURE 8.7: Response of EpiDerm^{TM} tissue cultures after topical application of 30 mM (= 12 µg ml^{-1}) H_2O_2 for 1 h prior to *Tetraselmis suecica* ethanol/water extract treatment (200 µg ml^{-1}) showing the repairing effect of the extract after H_2O_2 treatment. Three independent assays were performed in triplicate; data are shown as mean ±S.D. Significant differences between treated groups were determined using Students-t test (*p≤0.05) and ANOVA. NC = not treated. Ts 200 µg = 200 µg *T. suecica* extract; H_2O_2 + Ts 200 µg = epidermal tissue pretreated with H_2O_2 for 1 h and recovered with extract.

Alexandrium andersoni

8.8 Viability of tumor cell lines after treatment with *Alexandrium andersoni n*-butanol extract

Different concentrations (10 μg ml^{-1}, 50 μg ml^{-1}, 100 μg ml^{-1}, 200 μg ml^{-1} and 400 μg ml^{-1}) of *Alexandrium andersoni* chemical partitions were tested on A549 and HT-29 cell lines using the MTT assay to determine IC50 viability values after 24 and 48 h of treatment. Only the *n*-butanol extract significantly affected viability, whereas chloroform, hexane and aqueous chemical partitions had no effect.

The *n*-butanol extract induced a significant dose- and time-dependent reduction in cell viability compared to controls ($p < 0.0001$) in both cell lines. As shown in figure 8.8 A, there was a strong decrease in the percentage of viable A549 lung cancer cells after 24 and 48 h, especially at higher extract concentrations (100, 200 and 400 μg ml^{-1}). Cell viability after 24 h was reduced to 48, 21 and 8 % at these concentrations whereas after 48 h cell viability was reduced to 16, 5 and 3 %, respectively. IC50 value was calculated as 50 μg ml^{-1} after 48 h of treatment. A similar toxic effect was also observed in HT-29 colon cancer cells (figure 8.8 B), with a significant reduction in cell viability (57, 14 and 5 %) when exposed to highest concentrations (100, 200 and 400 μg ml^{-1}) of *n*-butanol extract after 24 h of treatment. After 48 h, cell viability was further reduced (14, 4 and 3 %) at these concentrations. IC50 value was about 52 μg ml^{-1} as calculated after 48 h of treatment.

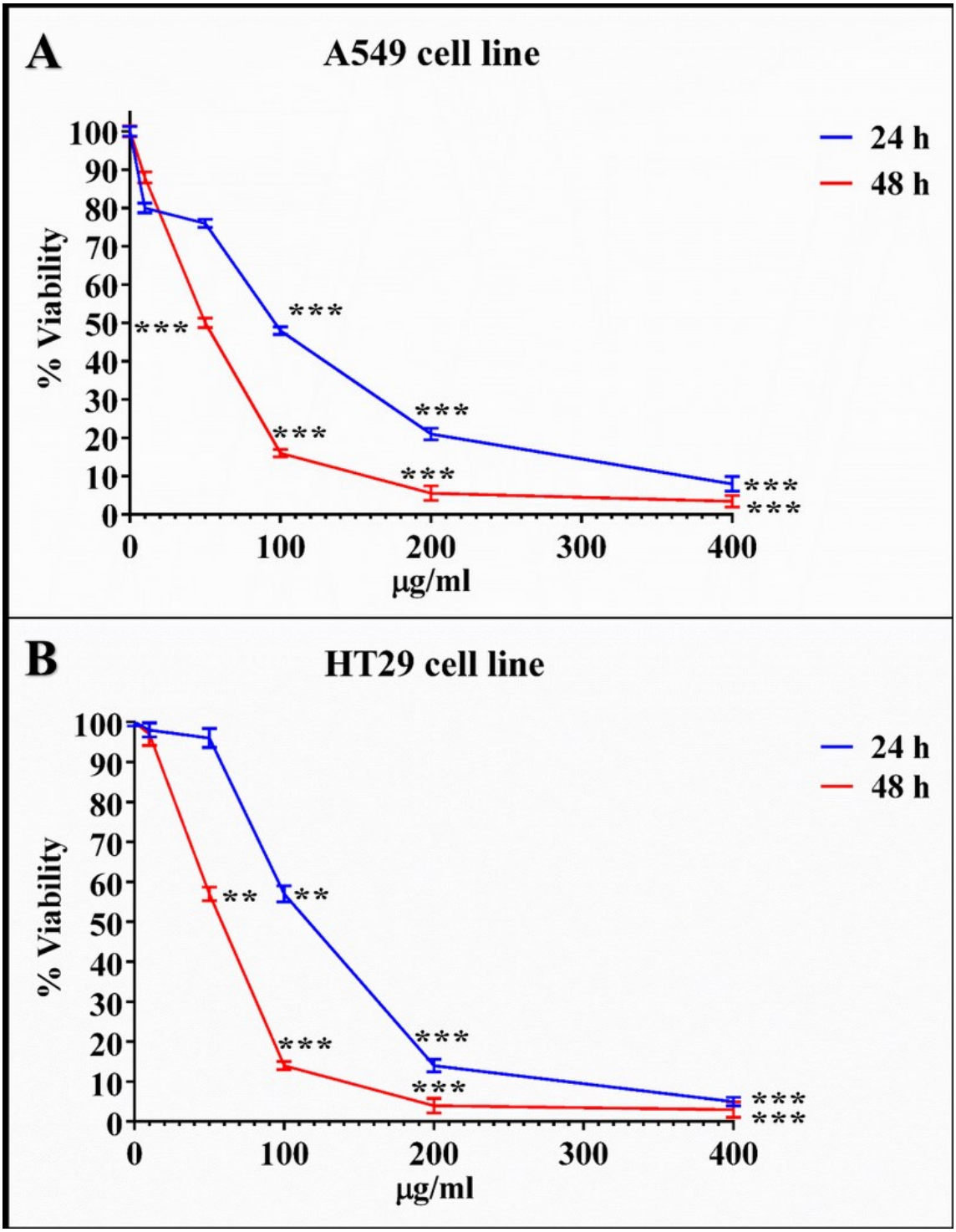

FIGURE 8.8: Effect of an *n*-butanol extract of the dinoflagellate *Alexandrium andersoni* on lung adenocarcinoma (A549) and colorectal carcinoma (HT-29) cancer cell lines. Percentage of viable cells for A549 (**A**) and HT-29 (**B**) were calculated with the MTT viability assay. Values are reported as mean ± S.D. compared to controls (100% viability). Concentrations tested were 10, 50, 100, 200 and 400 µg ml^{-1} for 24 and 48 h. Asterisks denote statistically significant differences with a p value ≤0.0001.

8.9 Analysis of the variation in gene expression after treatment with *Alexandrium andersoni n*-butanol extract

To better understand toxic effects of the *n*-butanol extract at the molecular level, A549 and HT-29 cells were analyzed for gene expression levels. Gene expression results are reported after 2 h of treatment with 400 μg ml^{-1} extract since many factors implicated in the cell death pathway were already expressed and activated after 2 h, and because at lower concentrations transcriptional effects were less evident. This concentration was tested to assess specific cell death signaling pathways thereby avoiding non-specific toxic responses of a "pool" of different molecules present in the chemical partition.

Control genes for real-time qPCR were actin-beta (ACTB), beta-2-microglobulin (B2M), hypoxanthine phosphoribosyltransferase (HPRT1) and large ribosomal protein P0 (RPLP0), the expression of which remained constant in A549 and HT-29 cells. The histograms reported in figure 8.9 show the relative expression ratios of the analyzed genes with respect to controls without treatment. Only expression values greater or lower than a two-fold difference with respect to the controls were considered significant for up- and downregulation results.

After 2 h of treatment with *A. andersoni n*-butanol extract on A549 cells line, there was an upregulation of the AIFM1 - apoptosis-inducing factor 1 (2.3 fold-change) with a consequent increase in BCL2 - like 10 apoptosis facilitator (6.6 fold-change) and BID - BH3 interacting domain death agonist (2.0 fold-change) (figure 8.9A). There was also a significant upregulation of four genes belonging to the tumor necrosis factor superfamily: CD27 - binding pro-apoptotic protein (SIVA) (16.1 fold-change), FASLG - Fas ligand (2.0 fold-change), TNF - tumor necrosis factor (2.1 fold-change), TNFSF8 - tumor necrosis factor ligand superfamily member 8 (2.5 fold-change) and DR3 - death receptor which is also known as TNFRSF25 - tumor necrosis factor ligand superfamily member 25 (19.0 fold-change). Other genes that were upregulated after 2 hours of treatment were CRADD - CASP2 and RIPK1 domain containing adaptor with death domain (2.3 fold-change) and CYCS - cytochrome c somatic (3.8 fold-change). In contrast, there was a downregulation of genes that encode for proteins that inhibit apoptosis: BIRC3 - baculoviral IAP repeat containing 3 (-2.2 fold-change), XIAP - X-linked inhibitor of apoptosis (-2.9 fold-change), IGF1R - insulin-like growth factor 1 receptor (-4.1 fold-change), NFKB1 - Nuclear Factor Kappa B Subunit 1 (-2.5 fold- change) and TRAF2 - TNF receptor-associated factor 2 (-2.8 fold-change). Three of the main caspases involved in the apoptotic cascade (caspases 2, 3 and 9) were not upregulated (figure 8.9 A).

Also in HT-29 cells, 2 h of extract treatment induced a significant upregulation of FASLG - Fas ligand (5.3 fold-change) and TNF - tumor necrosis factor (29.2 fold-change) (figure 8.9 B). Other genes such as GADD45 alpha - growth arrest and DNA-damage-inducible protein and Foxl1 - forkhead box L1 were also significantly upregulated (4.8 and 9.1 fold-change, respectively). Finally, there was an upregulation of apoptosis inductors such as Bcl-2-like protein 11 (BCL2L11) and induced myeloid leukemia cell differentiation protein-Mcl-1- isoform 2 (MCL1) (4.8 and 2.2 fold-change, respectively). The DPYSL4 - dihydropyrimidinase-related protein 4 gene increased its expression after *A. andersoni* extract treatment (21.8 in fold change). In contrast, there was a downregulation of the ATP6V1G2 - V-type proton ATPase subunit G 2 (-4.6 fold-change) with a consequent decrease of Kv channel-interacting protein 1, also known as KCNIP1 (-14.9 fold-change).

There was also a downregulation of two genes CD40 ligand (also known TNFSF5) belonging to the tumor necrosis factor ligand superfamily (-7.1 fold-change) and EIF5B - eukaryotic translation initiation factor 5B (-2.3 fold-change). As in the case of A549 cells, there was an early downregulation of the TRAF2 gene (-1.5 fold-change) also in HT-29 cells. Finally, no apoptotic caspase gene expression was recorded, with caspases 2, 3, and 9 genes showing fold-changes values comparable to the control (figure 8.9 B).

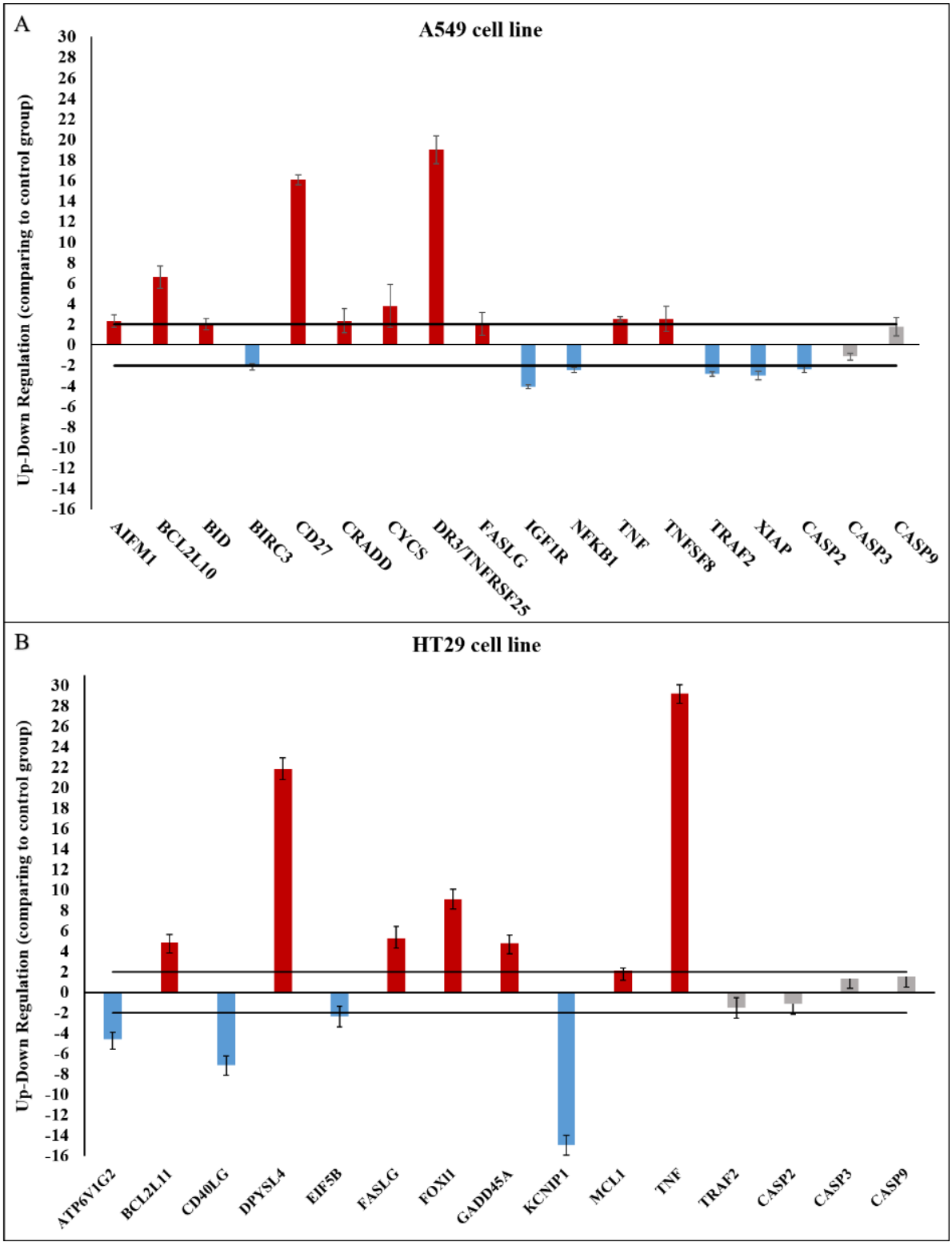

FIGURE 8.9: Histograms showing the effects of *Alexandrium andersoni n*-butanol extract on the expression levels of target genes in lung adenocarcinoma A549 (**A)** and in colorectal adenocarcinoma HT-29 (**B**) cell lines. Gene expression analysis was conducted after 2 h of treatment with 400 µg ml^{-1} of extract; error bars represent ±S.D.

8.10 Analysis of the variation in protein expression of death receptors after treatment of A549 with *Alexandrium andersoni n*-butanol extract

Protein expression results are reported after 48 h of treatment with 400 μg ml^{-1} extract concentrations (figure 8.10) since many genes implicated in the necroptosis cell death pathway were upregulated at this concentration. After 48 h, there was a significantly increase in the expression of tumor necrosis factor receptor 1 (TNFR1) compared to controls, as revealed by densitometric analysis of the photographic sheet of the immunoblotting membrane (figure 8.10 A). On the contrary, TNF receptor associated factors (TRAF1 and TRAF2) were not activated as also revealed in the gene expression analysis (figure 8.10 A), indicating the absence of a survival pathway. The receptor-interacting protein (RIP-k1) increased significantly (figure 8.10 B) indicating an early death-signaling pathway. This was confirmed by the downregulation of TNF receptor associated factors TRAF2 and by the upregulation of caspase and RIP adaptor with death domain-CRADD (figure 8.10 A). Another death receptor implicated in the extrinsic apoptotic pathway, death domain receptor 3-DR3 (also known as tumor necrosis factor receptor superfamily member 25-TNFRSF25) was strongly activated confirming death signal transduction mediated by death domain containing adaptor proteins such as CRADD in response to a cytotoxic effect (figure 8.10 C). β-actin protein was used as the positive control to normalize our experimental data (figure 8.10 D). None of the cleaved key caspases implicated in the apoptotic pathway were revealed by the immunoblot analysis.

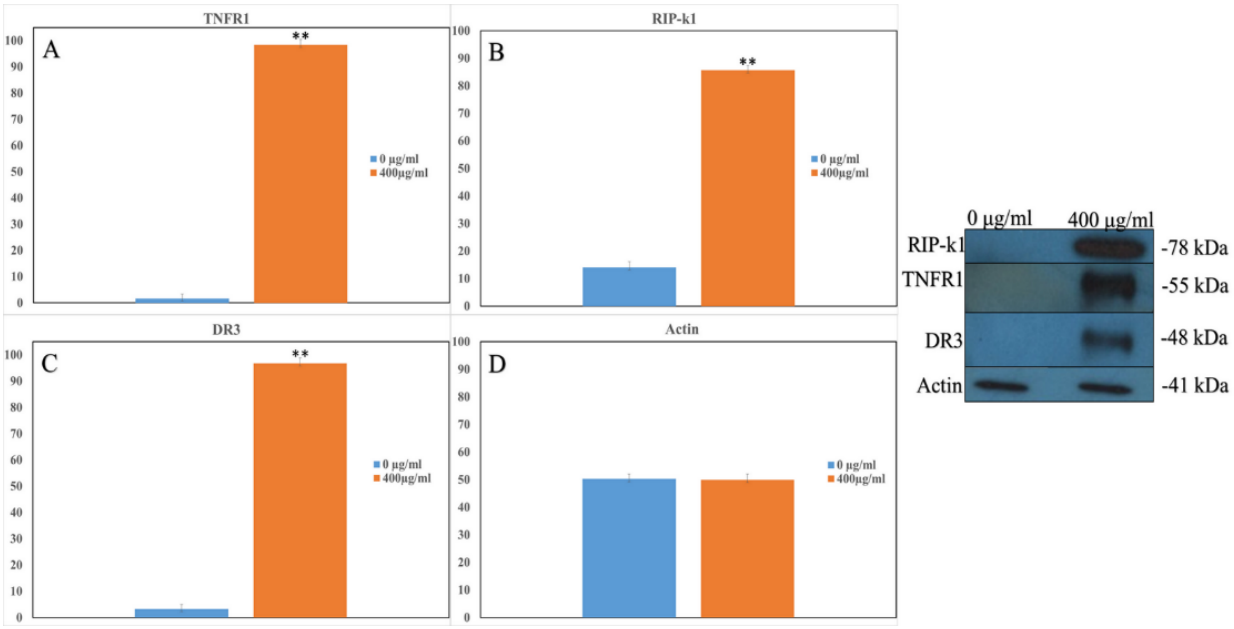

FIGURE 8.10: Histograms showing the effects of *Alexandrium andersoni n*-butanol extract on the expression levels of target proteins. (**A**) TNFR1, (**B**) RIP-k1, (**C**) DR3 and (**D**) control (actin) in lung adenocarcinoma A549 cells. Immunoblot analysis shows that the extract induced TNF signaling after 24 h. Asterisk denotes significant increase in protein levels. **$p \leq 0.05$ versus control; error bars represent ±SD.

8.11 Cell cycle arrest in A549 cell line

Flow cytometry was performed to analyze the effects of *A. andersoni* extract on the cell cycle of A549 cells in order to confirm the activation of the necroptotic cell death pathway revealed by gene expression. Cell cycle progression showed accumulation in the G2 phase with respect to G1, while percentages of cells in S phase were stable or similar to the untreated control (figures 8.11 A and 8.11 C). This accumulation suggests that the extract has a target in the late G2 phase of the cell cycle or first part of the M phase. The blockage was concentration dependent and highest after 8 h exposure to 200 µg ml^{-1} of extract (figures 8.11 B and 8.11 C).

A

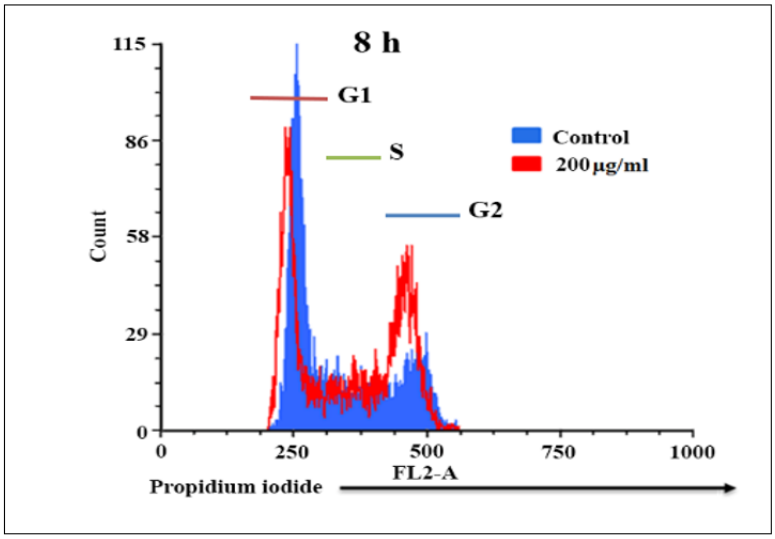

B

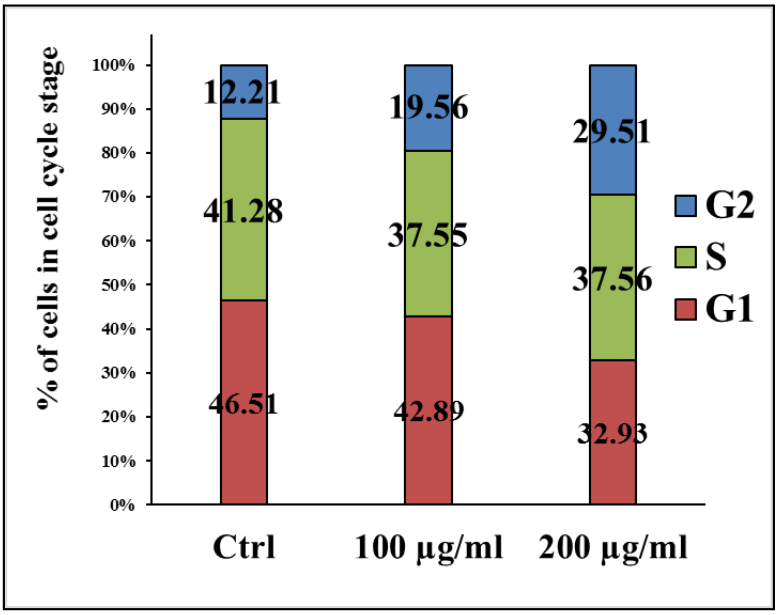

C

Time (h)	Cell cycle phase	*n*-butanol extract		
		0	100 µg/ml	200 µg/ml
0	G_1	46,79	/	/
	G_2	11,83	/	/
	S	41,38	/	/
	Sub G_1	/	/	/
2	G_1	49,45	41,71	40,71
	G_2	6,44	12,08	11,32
	S	44,1	46,21	47,97
	Sub G_1	/	/	/
4	G_1	45,66	41,65	40,21
	G_2	12,78	14,88	17,92
	S	41,57	43,47	41,87
	Sub G_1	/	/	/
6	G_1	40,51	36,47	32,71
	G_2	13,55	17,67	22,63
	S	45,94	45,87	44,66
	Sub G_1	/	/	/
8	G_1	46,51	42,89	32,93
	G_2	12,21	19,56	29,51
	S	41,28	37,55	37,56
	Sub G_1	/	/	/

FIGURE 8.11: (**A**) Flow cytometric analysis of DNA content in A549 cells exposed to *Alexandrium andersoni n*-butanol extract for 8 h at 200 μg ml^{-1} concentration (empty red line) and untreated control cells (full blue line). (**B**) Distribution of A549 cells in different phases of the cell cycle after 8 h of exposure to 100 and 200 μg ml^{-1} of *A. andersonii* extract, respectively. Percentage of cells in each phase was obtained with the ModFit LT Software. (**C**) Percentage of A549 cells in each cell cycle phase after 2, 4, 6 and 8 h treatment with *Alexandrium andersoni n*-butanol extract at 100 and 200 μg ml^{-1}concentrations.

8.12 Viability of tumor and normal cell lines after treatment with *Alexandrium andersoni* SPE-fractions and Caspase Inhibitor Assay

Different concentrations (1 μg ml^{-1}, 10 μg ml^{-1} and 100 μg ml^{-1}) of *A. andersoni* SPE- fractions were screened for their cytotoxicity on different cell lines using the MTT assay to determine IC50 values after 48 h of treatment (figure 8.12). Of the four fractions tested, fraction here named B, eluted with CH_3CN/H_2O, was the most active on A549 cell line, inducing a strong dose dependent decrease in cell viability (34, 29 and 5 % cell viability respectively, for all concentrations tested, figure 8.12 A). The IC50 value calculated was ≤1 μg ml^{-1}.

Interestingly, the same B fraction did not induce a strong cytotoxicity on HT-29 cells (figure 8.12 B). In this case, fraction identified as D, eluted with CH_2Cl_2/MeOH, significantly reduced cell viability of HT-29 in a dose dependent manner (43, 37 and 14 % cell viability respectively for all concentrations tested, Fig. 5B). The IC50 value calculated was about 1 μg ml^{-1}. None of the two fractions induced cytotoxicity on normal cell lines (WI38 and Beas-2B) at all concentrations tested (figures 8.12 C and 8.12 D).

To assess whether cell death induced by fractions B and D was caspase independent, we performed experiments in presence of caspase inhibitor. As shown in figures 8.12 E and 8.12 F, fractions B and D reduced viability in A549 and HT-29 cells respectively, also in the presence of the caspase inhibitor, indicating that cell death was not caspase-dependent.

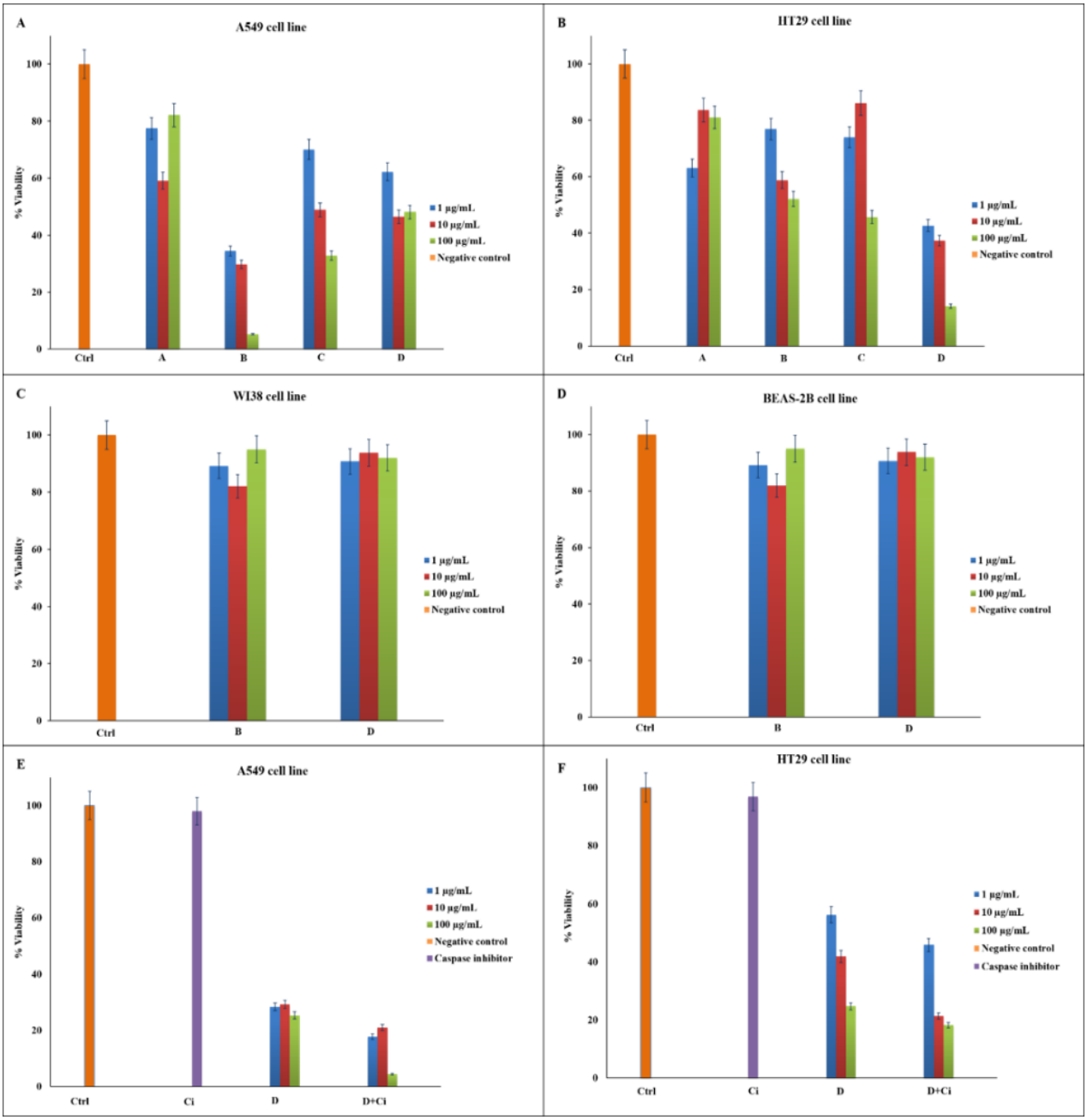

FIGURE 8.12: Effect of SPE fractions of the dinoflagellate *Alexandrium andersoni* on lung adenocarcinoma (A549) and colorectal carcinoma (HT-29) cancer cell lines, and lung fibroblast (WI38) and brunch-lung epithelial (Beas-2B) normal cell lines. Percentage of viable cells for A549 (**A**), HT-29 (**B**) and control WI38 (**C**) and BEAS-2B (**D**) cell lines using the MTT viability assay. Same experiments performed on tumor cell lines in the presence of caspase inhibitor (**E**, **F**). Values are reported as mean ± S.D. compared to controls (100% viability). Concentrations tested were 1, 10 and 100 µg ml^{-1} for 48 h.

8.13 Variation of gene expression analysis after treatment of A549 and HT-29 with Alexandrium andersoni SPE-fractions

In order to confirm that the active SPE-fractions B and D are the responsible for the activation of two different cell death signaling pathways, we analyzed the gene expression of A549 and HT-29 cells after treatment. Gene expression results are reported after 2 h of treatment with IC50 concentration (1 μg ml^{-1} for both fractions) of the B and D fraction. Control genes for real-time qPCR were actin-beta (ACTB), beta-2-microglobulin (B2M), hypoxanthine phosphoribosyltransferase (HPRT1) and large ribosomal protein P0 (RPLP0), the expression of which remained constant in A549 and HT-29 cells. The histograms reported in figure 8.13 show the relative expression ratios of the analyzed genes with respect to controls without treatment. Only expression values greater or lower than a two-fold difference with respect to the controls were considered significant for up- and downregulation results.

After 2 h of treatment with fraction B on A549 cells line there was an upregulation of BCL2-like 10 apoptosis facilitator (8.6 fold-change) and BID - BH3 interacting domain death agonist (2.1 fold-change) (figure 8.13 A). As well as observed for the *n*-butanol crude extract, there was also a significant upregulation of four genes belonging to the tumor necrosis factor superfamily: CD27 - binding pro-apoptotic protein (SIVA) (26.1 fold-change), FASLG - Fas ligand (9.0 fold-change), TNF - tumor necrosis factor (7.1 fold-change), TNFSF8 - tumor necrosis factor ligand superfamily member 8 (5.5 fold-change). The other key genes involved in the necroptosis pathway were upregulated after 2 hours of treatment: CRADD - CASP2 and RIPK1 domain containing adaptor with death domain (12.3 fold-change) and CYCS - cytochrome c somatic (13.8 fold-change). Confirming the signaling activated by the crude extract, there was a downregulation of genes that encode for proteins that inhibit apoptosis: BIRC3 - baculoviral IAP repeat containing 3 (-2.1 fold-change), IGF1R - insulin-like growth factor 1 receptor (-4.1 fold-change) and NFKB1 - Nuclear Factor Kappa B Subunit 1 (-6.5 fold- change). Two of the main caspases involved in the apoptotic cascade (caspases 3 and 9) were not activated (figure 8.13 A).

The SPE active fraction D induced in HT-29 cells, after 2 h of treatment a strong upregulation of FASLG - Fas ligand (12.1 fold-change) and TNF - tumor necrosis factor (12.3 fold-change), as shown in figure 8.13 B. Other genes such as growth arrest and DNA-damage-inducible protein GADD45 alpha and gamma together with forkhead box L1 (Foxl1) were also significantly upregulated (2.7, 8.0 and 8.7 fold-change, respectively). Finally, there was an upregulation of apoptosis inductors such as Bcl-2-like protein 11 (BCL2L11) and MCL1 - induced myeloid leukemia cell differentiation protein-Mcl-1- isoform 2 (2.7 and 2.6 fold-change, respectively). Dihydropyrimidinase-related protein 4 - DPYSL4 gene increased its expression after fraction D treatment (13.0 in fold change). The same result obtained with crude extract treatment was also found with fraction D regard the downregulation of the ATP6V1G2 - V-type proton ATPase subunit G 2 (-2.1 fold-change) with a consequent decrease of Kv channel-interacting protein 1, also known as KCNIP1 (-12.3 fold-change). There was also a downregulation of two genes CD40 ligand (also known TNFSF5) belonging to the tumor necrosis factor ligand superfamily (-2.4 fold-change) and EIF5B - eukaryotic translation initiation factor 5B (-2.0 fold-change). Finally, no apoptotic caspase gene expression was recorded, with caspases 3, and 9 genes showing fold-changes values not significantly changed respect to the control (figure 8.13 B).

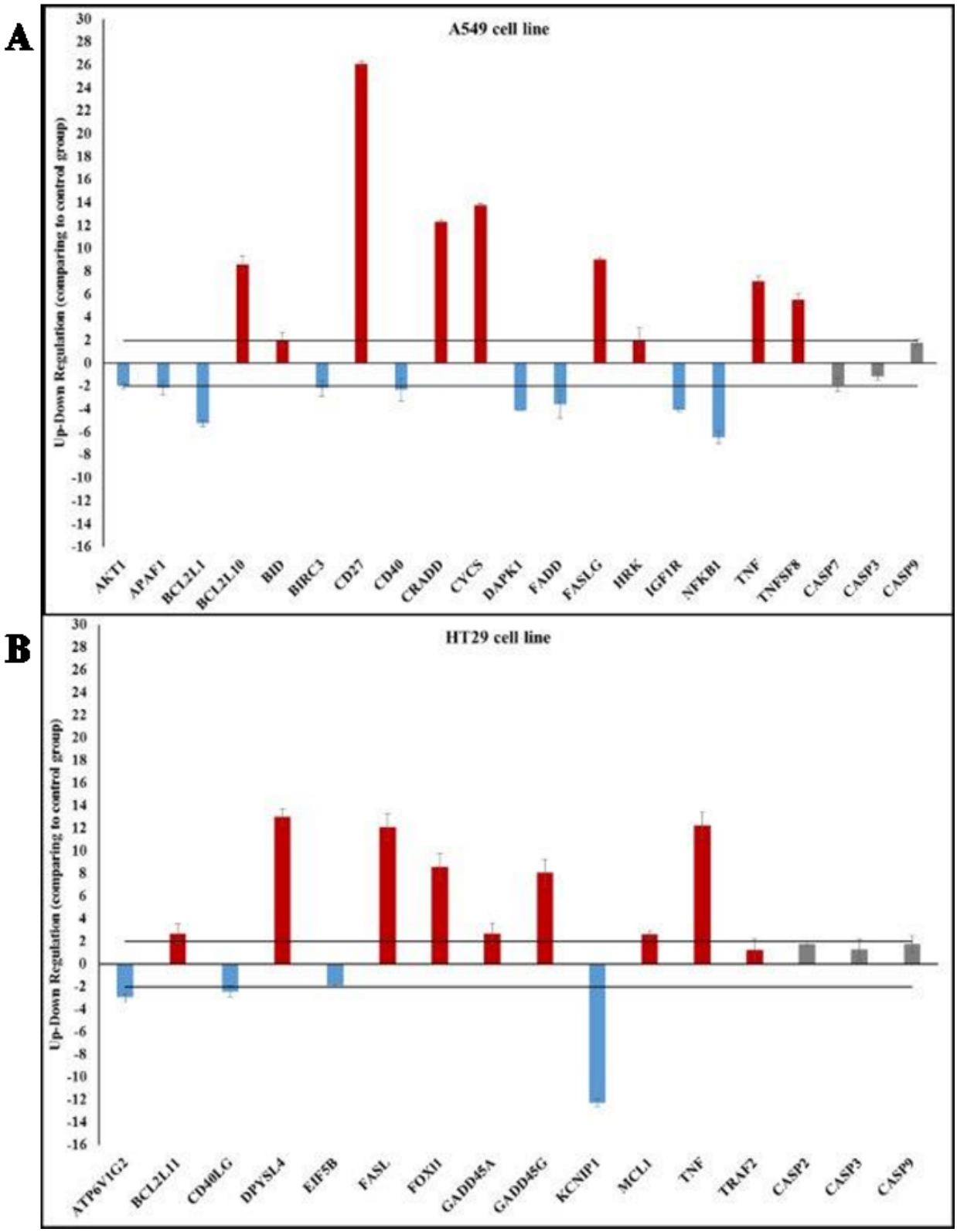

FIGURE 8.13: Histograms showing the effects of *Alexandrium andersoni* SPE fractions B and D on the expression levels of target genes in lung adenocarcinoma A549 (**A)** and in colorectal adenocarcinoma HT-29 (**B**) cell lines. Gene expression analysis was conducted after 2 h of treatment with 1 µg ml^{-1} of the two fractions; error bars represent ±S.D.

CHAPTER 9.

Discussion

9.1 *Tetraselmis suecica* reduces oxidative damage and induces repairing mechanisms in human cells

In this experimental work, the green marine microalga *Tetraselmis suecica* was thought to be an innovative natural source for many industrial sectors operating in the field of health care, since showed an interesting repairing mechanisms activator. Previous studies have shown that total extracts of *Tetraselmis* sp. have potential cosmetic and pharmaceutical applications for the human hair growth and pigmentation of the skin, and also for stimulating the increased production of skin structural proteins such as filaggrin and involucrin involved in dermal diseases as Psoriasis (Pertile et al., 2015). In a previous study, an ethanol/water extract of *Tetraselmis suecica* showed a strong scavenging activity against 2,2-difenyl-1-picrylhydrazyl (DPPH) and peroxyl radicals rather than against the superoxide anions from the xanthine/xanthine oxidase system (Jo et al., 2012).

In this work was obtained a similar type of crude extract from *T. suecica*, which was able to stimulate a strong response to cell damage and to activate, *in vitro*, a repairing mechanism in human epidermal cells. The crude extract contains high levels of xanthophylls (lutein, violaxanthin, neoxanthin, antheraxanthin and loroxanthin esters), pigments that are well known, singularly, for their biological activities as antioxidants and which are precursors of other pigments or vitamins (Dall'Osto et al., 2007). Lutein, which was particularly abundant in this extract, possesses pronounced free radical scavenging ability due to its polarity and number of conjugated double bonds (Sindhu et al., 2010). Moreover, the same molecule has been shown to significantly decrease neurogenic inflammatory response in the mouse skin (Horvath et al., 2015). The antioxidant activity of violaxanthin and neoxanthin is also well documented (McNulty et al., 2008), whereas the biological activity of antheraxanthin and loroxanthin esters recently characterized in *T. suecica* (Garrido et al., 2009) have not yet been investigated.

In our study, the ethanol/water crude extract, containing high levels of carotenoids, from *T. suecica* showed marked radical scavenging ability when tested with the DPPH assay. The addition of extract led to 98% reduction of the radical DPPH (purple) into its reduced (yellow) form at the highest concentrations. As reported in Table 8.1(see chapter 8, results), the radical scavenging activity of the extract was dose-dependent and its strength was 70% greater than α-Tocopherol at the highest concentrations. Moreover, the inhibition of DPPH free radicals induced by the extract was comparable to other well-known antioxidant molecules such as ascorbic acid where the percentage reduction of the free radical is about 95% (Garcia et al., 2012).

In order to evaluate this effect at the cellular level we challenged cells with H_2O_2 because a previous study showed that A549 lung cells have a multifaceted response when exposed to hydrogen peroxide (D'Andrea et al., 2004). D'Andrea et al. (2004) have shown that H_2O_2 induces damage to lipids, proteins, and nucleic acids due to the generation of reactive oxygen species (ROS). In our case, H_2O_2 caused a reduction in A549 cell viability to 36% after 48 h, but addition of the extract induced a strong recovery effect in cell viability, with up to 100% recovery in some cases. In order to clarify this effect at the molecular level, we studied the difference in oxidative stress gene expression patterns between cells treated only with 30 mM H_2O_2 and cells recovered with 100, 200 and 400 μg ml^{-1} of crude extract. The genes involved in ROS metabolism such as oxidative stress responsive genes ATOX1, CCL5 (RANTES), DHCR24, FOXM1, GPX1, GPX4, PDLIM1, PRDX5, SIRT2, SOD2

were all significantly upregulated in a dose dependent manner after extract recovery treatment for the highest concentrations tested.

In particular, antioxidant genes such as GPX1 and GPX4 showed a completely reversed expression after extract-induced recovery with respect to H_2O_2 injury for all concentrations tested. On the contrary, PRDX5 showed an upregulation with H_2O_2, because this gene codes for a mitochondrial peroxiredoxin (Gornicka et al., 2011) that decomposes hydrogen peroxide. However, after recovery treatment with extract, PRDX5 gene expression levels decreased in a dose dependent manner and were significantly downregulated at 400 μg ml^{-1}. This interesting finding is probably due to the ability of the extract to scavenge the effect induced by H_2O_2 thereby reducing PRDX5 gene expression levels.

The genes involved in ROS metabolism such as SOD2 were upregulated with H_2O_2. Recovery treatment with the extract caused an enhanced upregulation of this gene in a dose dependent manner. This is an important finding because, as demonstrated in previous studies, mitochondrial SOD2 plays a crucial role in protecting cells against oxidative stress (Culotta et al., 2006). Another important result regards the effect of the extract on upregulation of DHCR24 because this is a multifunctional enzyme, which exerts resistance against oxidative stress and prevents apoptotic cell death when it is expressed at high levels (Ivanov et al., 2013). The increase in expression levels of the inflammatory pathway gene PTGR1 suggests a potential anti-inflammatory activity because this enzyme is responsible for the biological inactivation of prostaglandins and related eicosanoids (Hybertson et al., 2011).

The downregulation of the GSTP1 gene after H_2O_2 treatment indicates that cells were unable to defend themselves against injury. Surprisingly, after 200 and 400 μg ml^{-1} of the recovery treatment with the extract, GSTP1 was significantly upregulated indicating the restoration of the antioxidant defense mechanisms.

Peroxide metabolism genes such as AKR1C2, HSP90AA1 and SLC7A11 showed different expression patterns. In particular, the AKR1C2 gene, which catalyzes the conversion of aldehydes and ketones to their corresponding alcohols (Zhang et al., 2014), was downregulated with H_2O_2 treatment and upregulated in a dose-dependent manner by the recovery treatment with the extract (only for 200 and 400 μg ml^{-1}). The activation of this gene indicates a specific cell response to hydrogen peroxide metabolites through the induction of detoxification mechanisms. Heat shock protein 90 kDa alpha (cytosolic) class A member 1 (HSP90AA1) was upregulated by H_2O_2 treatment because it is a pro-apoptotic factor which induces cell death in response to stress. The extract was able to downregulate HSP90 expression leading to the induction of cytoprotective pathways through the inhibition of pro-apoptotic pathways (Alani et al., 2014). Surprisingly, the extract was able to downregulated the SLC7A11 gene which is upregulated by the H_2O_2 treatment. SLC7A11 encodes a subunit of the xCT cystine/glutamate aminoacid transport system, which is involved in the generation of glutathione and the protection of cells from oxidative stress. However, in a recent study the expression of SLC7A11 was shown to promote tumorigenesis and chemotherapy resistance (Martin and Gardner, 2015). The downregulation of SLC7A11 by the extract may therefore be considered as a potential chemo-preventive agent. A schematic representation of the mechanism activated by the ethanol/water crude extract of *Tetraselmis suecica* is reported in figure 9.1.

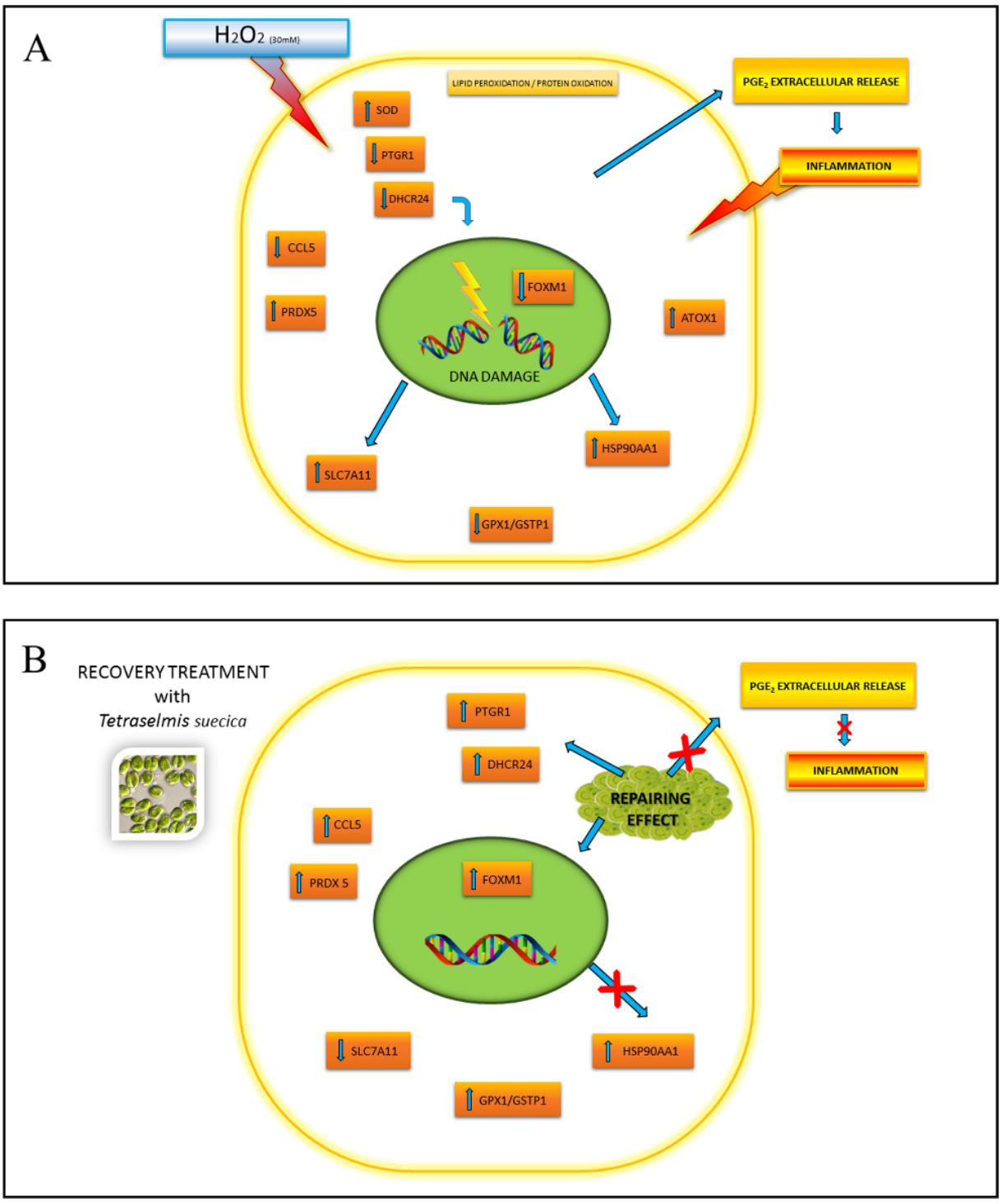

FIGURE 9.1: Schematic representation of the cellular response activated by H_2O_2 (A) and repairing effect induced by Tetraselmis suecica extract (B) after H_2O_2 pretreatment.

In order to demonstrate the activation of an oxidative stress response pathway after *T. suecica* extract recovery treatment, we also analyzed the expression of key proteins involved in antioxidant

mechanisms (GPX4 and DHCR24) and PTGR1. Immunoblot data confirmed gene expression results on the induction of an antioxidant pathway in A549 cells damaged with H_2O_2 and then treated with extract. We found that the physiological increase of the active form of GPX4 protein after 30 mM H_2O_2 treatment was enhanced by recovery treatment with 200 and 400 μg ml^{-1} extract. Another important finding was the increased expression of DHCR24 and PTGR1 proteins induced by extract treatment. The high upregulation of PTGR1 could be linked to a reduction in prostaglandin release by cells. ELISA experiments showed a significant dose-dependent decrease in prostaglandin PGE_2 levels in the culture medium after recovery treatment confirming this hypothesis. To our knowledge, this is the first report that an ethanol/water extract from a marine green microalga acts as an inhibitor of prostaglandin release in an inflammatory response.

Due to difficulties in obtaining sufficient human lung epithelial cells to perform this study, we chose the A549 cell line derived from a lung carcinoma due to its considerable use in the literature as a surrogate cell type (Speit and Bonzheim, 2003; Lopez-Alarcona and Denucolab, 2013; Parashiva et al., 2014; Macnee and Rahman, 1999) due to its high levels of glutathione (Carmichael et al., 1988) and high (non-induced) heme oxygenase 1 (HO-1) gene expression levels (Dubrovskava and Wetterhahn, 1998). We are aware that results obtained from this transformed cell line may not be applicable and immediately transferrable to normal lung epithelial cells in the respiratory tract *in vivo*. Thus, in order to use this extract as a potential cosmetic agent for topical application, we used human epidermidis tissue (EPI-200) as an experimental model and showed that the extract exerted a strong repairing effect after injury caused by hydrogen peroxide.

To date, intervention trials with single antioxidants in pharmacological doses have not supported a repairing effect in humans (Horvath et al., 2015). However, if many antioxidants work in a network, 'total antioxidants' may be a better concept than individual antioxidants. Thus, the potential synergistic effects of bioactive components, such as carotenoids, with different chemical structures and anti-oxidizing activities may be a promising agent for cosmeceutical use. The identification of potent marine microalgal species as peroxide scavengers and repairing agents can lead to new alternative cosmeceutical products or nutritional supplements for prevention of disorders related to oxidative damage, such as cancer, aging and skin inflammation diseases. In order to develop new natural cosmeceutical products for human health applications from marine microalgae, further studies are required to clarify if this bioactivity is ascribable to a single compound, classes of molecules (e. g. carotenoids) or the synergistic effect of several molecules contained in the ethanol/water extract of *Tetraselmis suecica*.

9.2 *Alexandrium andersoni* activates caspase-indipendent programmed cell death in tumor cell lines

This study indicates that an *n*-butanol extract and two of the relative SPE fractions of the dinoflagellate *Alexandrium andersoni* induce high cytotoxicity towards two cancer cell lines (A549 lung cancer and HT-29 colorectal cancer) without affecting normal cell viability (WI-38 and BEAS-

2B cell lines). In the case of A549 cells, the *n*-butanol extract and the active SPE fraction B induced the activation of cell death pathway via necroptosis and extrinsic apoptosis as shown schematically in figure 9.2 A. At concentrations of 400 μg ml^{-1} for the extract and of 1 μg ml^{-1} for the fraction B, TNF-Receptor 1 (TNFR1) was activated which in turn activated CRADD which was responsible for death signaling producing cytotoxicity after 24 h and 48 h. The activation of a caspase-independent apoptotic pathway was also confirmed by the downregulation of cell death inhibitors XIAP and BIRC3 **(**apoptosis inhibitor family-IAP) genes and TRAF2 factor that inhibit caspases and suppress apoptosis (Carter at al. 2013). Activation of TNFR is responsible for cellular stress response signaling in the presence of TRAF2. In contrast, in cells where this factor is inhibited or silenced, an apoptotic response is favored (Gentle et al. 2011). *A. andersoni* extract also caused an overexpression of TNFRSF25 (also known as DR3) resulting in a caspase-independent apoptosis pathway as demonstrated by the upregulation of the AIFM1 gene. DR3 mediates activation of NF-kappa-B and induces rapid apoptosis because it interacts directly with the death domains in signaling transduction (Fang et al. 2008).

Interestingly, we observed a downregulation of anti-apoptotic molecules (BIRC3 and TRAF2) and an upregulation of death receptors (CD27, DR3, TNF and TNFS8) for the crude extract and fraction B. No survival response was induced as confirmed by the downregulation of IGF1R- insulin-like growth factor 1 receptor that is directly involved in malignant cell defense against external insults (Xue et al. 2012). Finally we also found an overexpression of another receptor involved in cell death signaling, CD27, that activates an extrinsic apoptotic pathway. This result was confirmed by the upregulation of BID, Bcl2l-10 and cytochrome-C genes, which are also associated with the mitochondrial pathway. However, notwithstanding the initial activation of this pathway, we did not observe a downstream activation of apoptotic caspases for the extract and fraction B. This may suggest that although cytochrome C was released, the caspase cascade was not activated since the necroptotic pathway was too fast and privileged with respect to intrinsic apoptosis. This was confirmed by the decrease in cell viability in the presence of caspase inhibitor (figure 8.12 E and 8.12 F, see results chapter 8) after treatment with active fraction B. Treatment of A549 cells with *A. andersoni* extract induced an arrest in the G2/M cell cycle phase, which is unusual when cells are defective for the oncogene p53, as in the case of the A549 cell line. To date, only asperolide A (extracted from the marine-derived endophytic fungus *Aspergillus wentii*) has been shown to inhibit cell-cycle progression through a blockage at the G2/M phase (Chandra et al. 2002). Moreover, the lack of nick fragments in the flow cytogram confirms the activation of a caspase-independent pathway as previously discussed.

Also in HT-29 cells, the *A. andersoni* extract and active fraction D directly activated apoptosis through an extrinsic signaling pathway thereby indirectly inducing DNA damage as shown schematically in figure 9.2 B. At concentrations of 400 μg ml^{-1} for the extract and of 1 μg ml^{-1} for the active SPE fraction D two tumor necrosis factors FASLG and TNF genes were upregulated; these in turn activated CRADD that was responsible for death signaling after 24 and 48 h. The significant upregulation of the apoptosis inductors BCL2L11 and Mcl-1 confirmed cell death via apoptosis involving mitochondrial proteins without caspase activation. After 2 h of treatment at 400 μg $ml^{-1}$for the extract and of 1 μg ml^{-1} for the fraction D, there was a downregulation of the V-type proton ATPase subunit G 2 (ATP6V1G2) with a consequent decrease of Kv channel-interacting protein 1, also known as KCNIP1, indicating damage of cell membrane integrity. Therefore, an increase of the DPYSL4 gene, which regulates cytoskeleton modelling, was probably a response to the insult received by the cell membrane.

A. andersoni extract increased gene expression of Gadd45 alpha and Foxl1; at the same time fraction D showed a significant upregulation of Gadd45 alpha and gamma together with Foxl1, indicating and confirming DNA damage. Gadd45 alpha and gamma, p53- and BRCA1-regulated stress-inducible genes, have been characterized as the most important genes targeted by a variety of DNA damaging agents (Sun et al. 2013). Interestingly, the signaling machinery that regulates Gadd45 alpha and Gadd45 gamma induction by genotoxic stress involves both p53-dependent and -independent pathways. Gadd45 alpha together with Gadd45 gamma protein play important roles in suppressing cell proliferation, mediating cell cycle arrest, promoting apoptosis, inducing DNA repair, and stabilizing chromatin assessment (Yang et al. 2013). *A. andersoni* extract and fraction D also induced downregulation of the death receptors CD40 ligand (also known TNFSF5) and EIF5B, which is an initiation factor GTPase that promotes ribosomal engagement for protein synthesis. These results confirm that DNA damage induces activation of the Gadd45 alpha and Gadd45 gamma proteins that arrest cell cycle progression with a consequent block in protein synthesis (Lee et al. 2002). We did not observe the activation of the TRAF2 and NF-kappa-B genes indicating the antiproliferative effect in p53-deficient cancer cells induced by extract and fraction D (Ahmed et al. 2013; Abe et al. 2014). Also in the case of HT-29 cells, none of the caspases (caspases 2, 3 and 9) involved in apoptosis were activated in the presence of the *A. andersoni* treatment.

This is the first report where an extract and relative purified fraction from a marine dinoflagellate induce a caspase independent extrinsic apoptotic pathway activated by Gadd45 alpha and gamma factor in colorectal adenocarcinoma HT-29 cell line which is also p53 defective. This is surprising because Gadd45 alpha and Gadd45 gamma induce G2-M arrest only when p53 is functional (Jin et al. 2002).

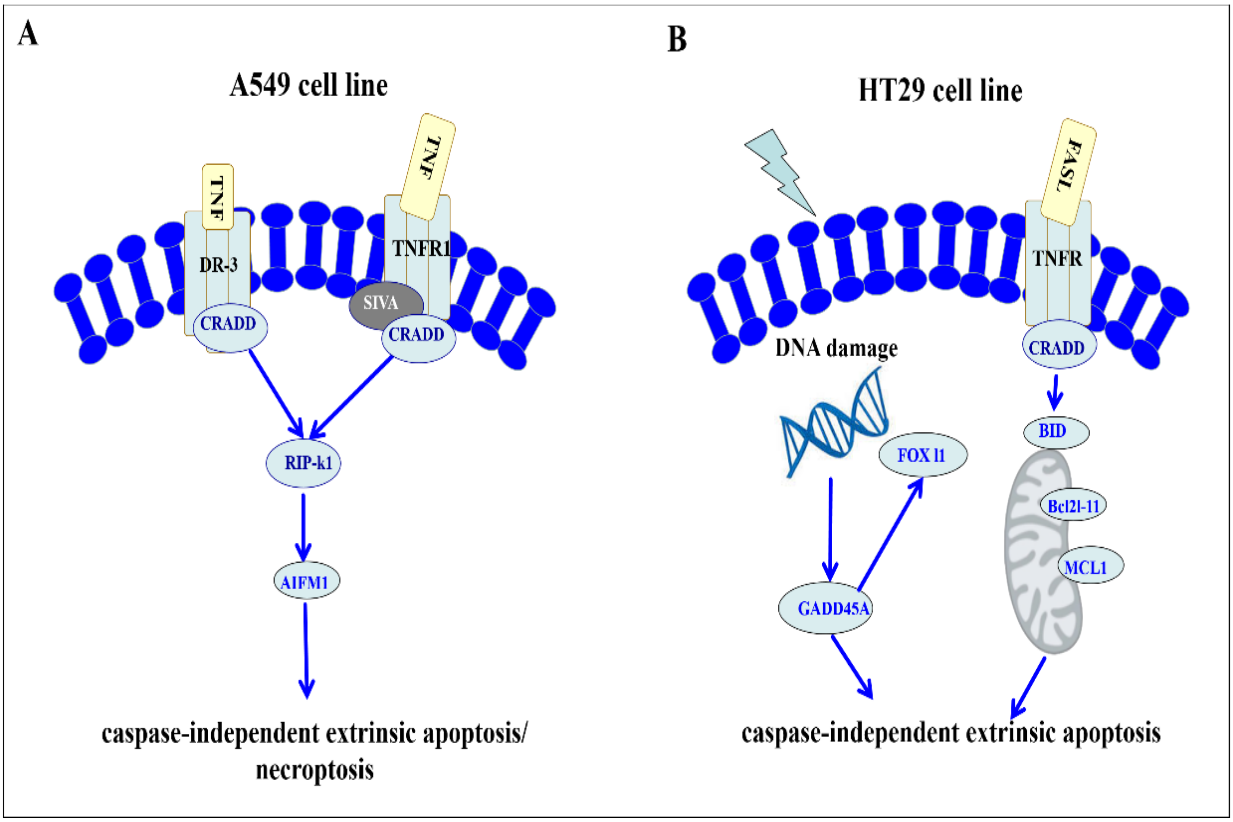

FIGURE 9.2 Schematic representation of pathways induced by *Alexandrium andersoni n*-butanol extract in lung adenocarcinoma A549 (A) and colorectal adenocarcinoma HT-29 (B) cell lines.

In conclusion *A. andersoni* extracts and fractions induced high specific cytotoxicity only towards two highly aggressive cancer cell lines (A549 lung cancer and HT-29 colorectal cancer) without affecting normal lung (WI38) and primary brunch (BEAS2B) cell lines. This cyctotoxicity was induced in both cases through an extrinsic caspase-independent cell signaling pathway involving necroptosis in A549 and GADD45 alpha and gamma factor in HT-29 cells. These findings differ from those reported in another study showing that the carotenoid peridinin from the marine dinoflagellate *Heterocapsa triquetra* induced apoptosis in DLD-1 human colorectal cancer cells by activating both caspase-8 and caspase-9 (Sugawara et al. 2007). Interestingly cell blockage occurred in both cases in the G2-M transition and this has only been reported the compound asperolide A extracted from the marine-derived endophytic fungus *Aspergillus wentii* which has been shown to inhibit cell-cycle progression through a blockage at the G2/M phase (Chandra et al. 2002). Another important finding is that we are probably dealing with two separate molecules, as suggested by the two different active SPE fractions, which induce different responses in the two cancer cell lines. Studies are currently underway to isolate

and characterize these molecules. By way of a coda, our study shows that *Alexandrium andersoni* may represent a new species for chemical and pharmacological research for cancer drug discovery.

CHAPTER 10.

Conclusions and future implications

Future perspectives for marine microalgae as high renewable marine resource

Oceans represent an enormous, untapped and sustainable source of several biotechnological opportunities. Marine resources can effectively offer valid solutions to a variety of issues relevant for humans and for an environmental sustainable life, in order to solve important societal challenges of the twenty-first century. In fact, the study of marine organisms and ecosystems can favourite the discovery of new and more efficacious drugs, the isolation of undiscovered enzymes useful in the industry, to cite a few examples. Furthermore, the creation of new concept of fuel from sustainable marine sources is a new trend in bioengineering, together with the synthesis of biopolymers, new biodegradable plastic materials, the remediation of environmental pollution and the development on large scale of sustainable aquaculture.

Marine microorganisms diversity is almost unlimited and could offers a hug biotechnological potential for their exploitations. Microalgae are microscopic plants that contain potential bioactive materials in the form of proteins, lipids, carbohydrates, carotenes and vitamins. In recent years, considerable interest has been paid to marine microalgae research in the fields of pharmaceuticals, nutraceuticals, cosmeceuticals, and production of biofuels. Biological properties of algae and their components are now studied in many areas of research, as source of antioxidants, antimicrobials, anticancer agents, anti-inflammatory and cardiovascular health, anti-obesity and antidiabetic activity. Knowledge obtained in these years on microalgal world has been soon transferred by industries in products. In fact, microalgae have been widely used for various industrial applications including human and animal nutrition, cosmetics, pharmaceuticals, CO_2 capture, bioenergy production, and nutrient removal from wastewater.

The results showed in this thesis (Marine Biotechnology sections) demonstrate the potential application of microalgae in health care applications. In fact, a dinoflagellate *Alexandrium andersoni* was found to produce specific chemical compounds able to induce selective death signaling pathways in different tumor cell lines. Further studies should examine in depth the chemical characteristics of the natural compounds responsible for the interesting effects. In addition, this is an attempt to improve the methodology for discovering and analysing new lead compounds of marine origin.

Another important outcome of this experimental work is represented by the green microalga *Tetraselmis suecica*, which showed an interesting repairing effect after oxidative cell damage. In particular, the study describes the potential synergistic effect of marine bioactive compounds (e.g. carotenoids). The formulation (the ethanol/water crude extract of *Tetraselmis suecica*) contains a large variety of chemical component with different chemical structures and anti-oxidizing activities that could be promising for cosmeceutical use. This discover of such potent marine microalgal species as peroxide scavengers and repairing mechanisms activator can lead to new alternative cosmeceutical products or nutritional supplements for prevention of disorders related to oxidative damage, such as cancer, aging and skin inflammation diseases. For this reason, an application procedure for patenting these results has been launch, in order to protect the intellectual property.

Further study are request to clarify other important effects and possible applications of marine microalgae. Moreover, there is a big pressure from industrial field to improve cultivation conditions and techniques for the production in large scale of huge amount of marine microalgae. This represent the priority in order to develop new commercial products ready to be launched on the market with competitive prizes.

REFERENCES

Abe, N., Hou, D.X., Munemasa, S., Murata, Y., Nakamura, Y. (2014). Nuclear factor-kappaB sensitizes to benzyl isothiocyanate-induced antiproliferation in p53-deficient colorectal cancer cells. Cell Death and Disease. 5, doi:10.1038/cddis.2014.495.

Ahmed, D., Eide, P. W., Eilertsen, I. A., Danielsen, S. A., Eknæs, M., Hektoen, M., Lind, G. E., Lothe, R. A. (2013). Epigenetic and genetic features of 24-colon cancer cell lines. Oncogenesis. 2, e71.

Alani, B. (2014). Silencing of HSp90 chaperone expression protects against 6-hydroxydopamine toxicity in PC12 cells. J Mol. Neurosci. 52(3), 392-402

Alonso, E., Otero, P., Vale, C., Alfonso, A., Antelo, A., Gimenez-Llort, L., Chabaud, L., Guillou, C., Botana, L. M. (2013). Benefit of 13-desmethyl spirolide C treatment in triple transgenic mouse model of Alzheimer disease: beta-amyloid and neuronal markers improvement. Curr. Alzheimer Res. 10 (3): 279e289.

Altschul, S. F., Madden, T. L., Schäffer, A. A., Zhang, J., Zhang, Z., Miller, W. and Lipman, D. J. (1997). 'Gapped BLAST and PSI-BLAST: a new generation of protein database search programs', Nucleic acids research, vol. 25, no. 17, pp. 3389-3402

Ashkenazi, A., Dixit V.M. (1998). 'Death receptors: signaling and modulation', Science, 81(5381):1305-8

Bartual, A., Arandia-Gorostidi, N., Cózar, A., Morillo-García, S., Ortega, M. J., Vidal, M., Cabello, A. M., González-Gordillo J. I. and Echevarría F. (2014). 'Polyunsaturated Aldehydes from Large Phytoplankton of the Atlantic Ocean Surface (42°N to 33°S)' Marine drugs 2014, 12, 682-699

Ben Kahla-Nakbi, A., Haouas, N., El Ouaer, A., Guerbej, H., Ben Mustapha, K., Babba H. (2016). 'Screening of antileishmanial activity from marine sponge extracts collected off the Tunisian coast', Parasitol Res., 37:258-7

Bergmann W. and Stempien M.F. (1957). 'Contributions to the study of marine products. XLIII. The nucleosides of sponges V The synthesis of spongosine', J Org Chem,2:1557–75

Bringmann, G., Gulder, T.A., Lang, G., Schmitt, S., Stöhr, R., Wiese, J. (2007). 'Large-scale biotechnological production of the antileukemic marine natural product sorbicillactone A', Mar Drugs, 5:23–30

Brunet, C. (2014). Spectral radiation dependent photoprotective mechanism in the diatom Pseudonitzschia multistriata. PLoS ONE. 9, e87015

Burge, C. and Karlin, S. (1997). 'Prediction of complete gene structures in human genomic DNA', J. Mol. Biol. 268, 78-94.

Buttino I., Miralto, A., Ianora, A., Romano, G. and Poulet, S. A. (1999). 'Water-soluble extracts of the diatom *Thalassiosira rotula* induce aberrations in embryonic tubulin organisation of the sea urchin *Paracentrotus lividus*', Marine Biology, vol. 134, no. 1, pp. 147-154

Buttino, I., Miralto, A., Ianora, A., Romano, G. and Poulet, S. A. (1999). 'Water-soluble extracts of the diatom *Thalassiosira rotula* induce aberrations in embryonic tubulin organisation of the sea urchin *Paracentrotus lividus*', Marine Biology, vol. 134, no. 1, pp. 147-154

Camacho, F. G., Rodríguez, J. G., Mirón, A. S., García, M. C., Belarbi, E. H., Chisti, Y., Grima, E. M. (2007). Biotechnological significance of toxic marine dinoflagellates. Biotechnol. Adv. 25: 176-194.

Carballeira, C., Ramos-Gomez, J., Martin-Diaz, L. and DelValls, T. A. (2012). 'Identification of specific malformations of sea urchin larvae for toxicity assessment: application to marine pisciculture effluents', Marine environmental research, vol. 77, pp. 12-22

Carballo-Cárdenas, E.C., Tuan, P.M., Janssen, M., Wijffels, R.H. (2003).Vitamin E (alpha-tocopherol) production by the marine microalgae Dunaliella tertiolecta and Tetraselmis suecica in batch cultivation. Biomol. Eng. 20(4-6), 139-147

Cardozo, K.H.M., Guaratini, T., Barros, M.O., Falcao, V.R., Tomon, A.P., Lopes, N.P., Campos, S., Tores, M.A., Souza, A.O., Colepicolo, P., Pinto, E. (2007). 'Metabolites form algae with economically impact', Comp Biochem Physiol Part C 146: 60-78

Carmichael, J. (1988). Gluthathione and related enzyme activity in human lung cancer cell lines. Br. J. Cancer, 58, 437-440

Carter, B. Z., Mak, D. H., Wang, Z., Ma, W., Mak, P. Y., Andreeff, M., Davis, R. E. (2013). XIAP downregulation promotes caspase-dependent inhibition of proteasome activity in AML cells. Leuk. Res. 37: 974-9.

Chan, E. Y., Longatti, A., McKnight, N.C., Tooze,S.A. (2009). 'Kinase-inactivated ULK proteins inhibit autophagy via their conserved C-terminal domains using an tg13-independent mechanism', Mol Cell Biol., 29(1):157-71

Chandra, D., Liu, J. W., Tang, D. G. (2002). Early mitochondrial activation and cytochrome c up-regulation during apoptosis. J Biol Chem. 277: 50842-54.

Chaudron, Y., Poulet, S. A., Laabir, M., Ianora, A. and Miralto, A. (1996). 'Is hatching success of copepod eggs diatom density-dependent?'. Marine Ecology Progress Series, vol. 144, no. 1-3, pp. 185-193

Chini Zittelli, G., Rodolfi, L., Biondi, N., Tredici, M.R. (2006). Productivity and photosynthetic efficiency of outdoor cultures of Tetraselmis suecica in annular columns. Aquaculture. 261, 932-943

Congcong H. and D. J. Klionsky. (2009). 'Regulation Mechanisms and Signaling Pathways of Autophagy', Annu Rev Genet. 43: 67–93

Costa, C., Karakostis, K., Zito, F. & Matranga, V. (2012). 'Phylogenetic analysis and expression patterns of p16 and p19 in Paracentrotus lividus embryos', Dev. Genes Evol. 222, 245–251

Crook, A. C., Long, M. and Barnes, D. K. a. (2000). 'Quantifying daily migration in the sea urchin *Paracentrotus lividus*', Journal of the Marine Biological Association of the UK, vol. 80, no. 1, pp. 177-178

Culotta, V.C., Yanga, M., O'Halloran, T.V. (2006). Activation of superoxide dismutases: Putting the metal to the pedal. Biochim. Biophys. Acta. 1763(7), 747–758

Curtis, J.E., Hersh, E.M., Butler, W.T., Rossen, R.D. (1971). 'Antigen dose in the human immune response. Dose-relationships in the human immune response to Keyhole limpet hemocyanin', J Lab Clin Med., 78:61–9

Cutignano, A., Nuzzo, G., Ianora, A., Luongo, E., Romano, G., Gallo, C., Sansone, C., Aprea, S., Mancini, F., D'Oro, U. and Fontana, A. (2015). Development and Application of a Novel SPE-Method for Bioassay-Guided Fractionation of Marine Extracts. Mar. Drugs 13: 5736-5749.

D'Andrea, T. (2004). The transcriptosomal response of human A549 lung cells to a hydrogen peroxide-generating system: relationship to DNA damage, cell cycle arrest, and caspase activation. Free Radical Bio. Med., 36(7), 881-896

d'Ippolito, G., Iadicicco, I., Romano, G., Fontana, A. and Iadicicco, O. (2002a). 'Detection of short-chain aldehydes in marine organisms: the diatom *Thalassiosira rotula*', Tetrahedron Letters, vol. 43, no. 35, pp. 6137-6140

d'Ippolito, G., Romano, G., Iadicicco, O., Miralto, A., Ianora, A., Cimino, G. and Fontana, A. (2002b). 'New birth-control aldehydes from the marine diatom *Skeletonema costatum*: characterization and biogenesis', Tetrahedron Lette*rs*, vol. 43, no. 35, pp. 6133-6136

d'Ippolito, G., Romano, G., Caruso, T., Spinella, A., Cimino, G. and Fontana, A. (2003). 'Production of octadienal in the marine diatom *Skeletonema costatum*', Organic Letters, vol. 5, no. 6, pp. 885-887

Dall'Osto, L., Cazzaniga, S., North, H., Marion-Poll, A., Bassi, R. (2007). The Arabidopsis aba4-1 mutant reveals a specific function for neoxanthin in protection against photooxidative stress. Plant Cell. 19(3), 1048-1064

Davidson, E. H., Cameron R. A. and A. Ransick. (1998). Specification of cell fate in the sea urchin embryo: summary and some proposed mechanisms. Development125:3269-3290

Davidson, E. H., J. P. Rast, and P. Oliveri, et al. (25 co-authors). (2002). A genomic regulatory network for development. Science 295:1669-1678

De-Bashan, L.E., Bashan, Y. 2010. Immobilized microalgae for removing pollutants: review of practical aspects. Bioresour Technol; 101: 1611-1627.

Debatin, K. M. (2004). Apoptosis pathways in cancer and cancer therapy. Cancer Immunol Immunother 53: 153–159.

Dellai, A., Laroche-Clary, A., Mhadhebi, L., Robert, J., Bouraoui, A. (2010). 'Anti-inflammatory and antiproliferative activities of crude extract and its fractions of the defensive secretion from the mediterranean sponge *Spongia officinalis*', Drug Dev Res., 71:412–8

Dinnel, P. A., J. M. Link, Q. J. Stober, M. W. Letourneau, and W. E. Roberts. (1989). Comparative sensitivity of sea urchin sperm bioassays to metals and pesticides. Arch. Environ. Contam. Toxicol. 18:748-755

Dragunow, M., Trzoss, M., Brimble, M. A., Cameron, R., Beuzenberg, V., Holland, P., Mountfort, D. (2005). Investigations into the cellular actions of the shellfish toxin gymnodimine and analogues. Environ. Toxicol. Pharmacol. 20: 305-312.

Duboc, V., Röttinger, E., Lapraz, F., Besnardeau, L., Lepage, T. (2005). 'Left-right asymmetry in the sea urchin embryo is regulated by nodal signaling on the right side', Dev. Cell, 9, 147–158.

Dubrovskaya, V. A., Wetterhahn, K.E. (1998). Effects of Cr(VI) on the expression of the oxidative stress genes in human lung cells. Carcinogenesis, 19, 1401-1407

Edge, R., Truscott, T.G. (2010). Properties of Carotenoid Radicals and Excited States and Their Potential Role in Biological Systems. In: Landrum J.T., (editor. Carotenoids) Physical, Chemical, and Biological Functions and Properties. CRC Press. 283–308, Boca Raton, FL, USA

Fang, L., Adkins, B., Deyev,V., Podack, E. R. (2008). Essential role of TNF receptor superfamily 25 (TNFRSF25) in the development of allergic lung inflammation. J. Exp. Med. 205: 1037–1048.

Fiedor, J. and Burda, K. (2014).Potential role of thus as antioxidants in human health and disease. Nutrients. 6(2), 466-488

Fontana, A., d'Ippolito, G., Cutignano, A., Miralto, A., Ianora, A., Romano, G. and Cimino, G. (2007a). 'Chemistry of oxylipin pathways in marine diatoms', Pure and Applied Chemistry, vol. 79, no. 4, pp. 481-490

Fontana, A., d'Ippolito, G., Cutignano, A., Romano, G., Lamari, N., Massa Gallucci, A., Cimino, G., Miralto, A. and Ianora, A. (2007b). 'LOX-induced lipid peroxidation mechanism responsible for the detrimental effect of marine diatoms on zooplankton grazers', Chembiochem: a European journal of chemical biology, vol. 8, no. 15, pp. 18101818

Garcìa, E.J. (2012).Antioxidant Activity by DPPH Assay of Potential Solutions to be Applied on Bleached Teeth. Braz. Dent. J. 23(1), 22-27

Garcia, J., Mujeriego, R., Hernandez-Marine, M. (2000). 'High rate algal pond operating strategies for urban wastewater nitrogen removal', J Appl Phycol., 12: 331-339

Garrido, J.L., Rodríguez, F., Zapata, M. Occurrence of loroxanthin, loroxanthin decenoate, and loroxanthin dodecenoate in Tetraselmis species (Prasinophyceae, Chlorophyta). J. Phycol. 45(2), 366-374 (2009).

Gentle, I. E., Wong, W. W., Evans, J. M., Bankovacki, A., Cook, W. D., Khan, N .R., Nachbur, U., Rickard, J., Anderton, H., Moulin, M., Lluis, J. M., Moujalled, D. M., Silke, J., Vaux, D. L. (2011). In TNF-stimulated cells, RIPK1 promotes cell survival by stabilizing TRAF2 and cIAP1, which limits induction of non-canonical NF-kappaB and activation of caspase-8. J Biol Chem. 286: 13282-91.

Gerlier, D., Thomasset, N. (1986). Use of MTT colorimetric assay to measure cell activation. J. Immunol. Methods. 94 (1-2), 57-6320

Gerwick, W. H. (1994). 'Structure and biosynthesis of marine algal oxylipins', Biochimica et Biophysica Acta, vol. 1211, no. 3, pp. 243-255

Gerwick, W.H., Moore, B.S. (2012). 'Lessons from the past and charting the future of marine natural products drug discovery and chemical biology', Chem Biol., 19:85–98

Glibert, P. M., Seitzinger, S., Heil, C. A., Burkholder, J. M., Parrow, M. W., Codispoti, L. A., Kelly, V. (2005). The role of eutrophication in the global proliferation of harmful algal blooms. Oceanography 18:198–209.

Godhe, A., Rehnstam-Holm, A. S., Karunasagar, I., Karunasagar, I. (2002). PCR detection of dinoflagellate cysts in field sediment samples from tropic and temperate environments. Harmful Algae 1: 361-373.

Gornicka, A. (2011).Transcriptional Profile of Genes Involved in Oxidative Stress and Antioxidant Defense in a Dietary Murine Model of Steatohepatitis. Antioxid. Redox Sign.15(2),

Granville, R. (2008). 'Echinometrid sea urchins, their trophic styles and corresponding bioerosion'. Current Developments in Bioerosion. ed. / Max Wisshak; Leif Tapanila. Berlin Heidelberg New York, Springer, p. 279-304

Guillard, R.R.L. (1975). Culture of phytoplankton for feeding marine invertebrates. In Smith W.L. and Chanley M.H (Eds.) Culture of Marine Invertebrate Animals. Plenum Press, New York, USA. 26-60

Guo, B., Zhai, D., Cabezas, E., Welsh, K., Nouraini, S., Satterthwait, A. C., Reed, J. C. (2003). 'Humanin peptide suppresses apoptosis by interfering with Bax activation', Nature, 423(6938):456-61

Hackett, J. D., Anderson, D. M., Erdner, D. L., Bhattacharya, D. (2004) Dinoflagellates: a remarkable evolutionary experiment. American Journal of Botany 91:1523–1534.

Hansen, E., Eilertsen, H. C., Ernstsen, A. and Genevière, A. M. (2003). 'Anti-mitotic activity towards sea urchin embryos in extracts from the marine haptophycean *Phaeocystis pouchetii* (Hariot) Lagerheim collected along the coast of northern Norway', Toxicon, vol. 41, no. 7, pp. 803-812

Harmelin, J. G., Bouchon, C., Duval, C., Hong J. S. (1980). 'Les échinodermes des substrats durs de l'île de Port-Cros, Parc National (Méditerranée Nord-occidentale)' *Trav Sci Parc Nation de Port-Cros*, vol.6, pp. 25-38

Harris, J.R., Markl, J. (1999). 'Keyhole limpet hemocyanin (KLH): A biomedical review', Micron., 30:597–623

He, J., Yang, Y., Xu, H. Y., Zhang, X., Li, X. M. (2005). Olanzapine attenuates the okadaic acid-induced spatial memory impairment and hippocampus cell death in rats. Neuropsychopharmacology 30: 1511-1520.

Hoppenrath, M., Bachvaroff, T. R., Handy, S. M., Delwiche, C. F., Leander, B. S. (2009). Molecular phylogeny of ocelloid-bearing dinoflagellates (Warnowiaceae) as inferred from SSU and LSU rDNA sequences. BMC Evolutionary Biology 9.

Horváth, G. (2015). Effects of Some Natural Carotenoids on TRPA1 and TRPV1-Induced Neurogenic Inflammatory Processes In: Vivo in the Mouse Skin. J. Mol. Neurosci. 56, 113–121

Hsu, H., Huang, J., Shu, H. B., Baichwal, V., Goeddel, D. V. (1996). 'TNF-dependent recruitment of the protein kinase RIP to the TNF receptor-1 signaling complex' Immunity, 4(4):387-96

Hybertson, B.M., Bifeng, G., Swapan, K. B., McCord, J.M. (2011). Oxidative stress in health and disease: The therapeutic potential of Nrf2 activation. Mol. Aspects Med. 32, 234–246

Ianora, A. and Miralto, A. (2010). 'Toxigenic effects of diatoms on grazers, phytoplankton and other microbes: a review', Ecotoxicology, vol. 19, no. 3, pp. 493-511

Ianora, A. and Poulet, S. A. (1993). 'Egg viability in the copepod *Temora stylifera*', Limnology and Oceanography, vol. 38, no. 8, pp. 1615-1626

Ianora, A., Miralto, A., Buttino, I., Romano, G. and Poulet, S. A. (1999). 'First evidence of some dinoflagellates capacity reducing male copepod fertilization', Limnology and Oceanography, vol. 44, no. 1, pp. 147-153

Ianora, A., Poulet, S. A. and Miralto, A. (1995). 'A comparative study of the inhibitory effect of diatoms on the reproductive biology of the copepod *Temora stylifera*', Marine Biology, vol. 121, pp. 533-539

Iqbal, M., Verpoorte, R., Korthout, H. A. A. J. and Mustafa, N. R. (2013). 'Phytochemicals as a potential source for TNF-α inhibitors', Phytochemistry Reviews, vol. 12, pp. 65-93

Irianto, A. and Austin, B. (2002).Probiotics in aquaculture. J. Fish Dis. 25(11), 633–642

Ivanov, A.V. (2013). HCV and Oxidative Stress in the Liver. Viruses. 5, 439-469

Jeffrey, S.W., Wright, S.W. (1997). Qualitative and quantitative HPLC analysis of SCOR reference algal cultures. In Jeffrey, S.W., Mantoura, R.F.C. and Wright, S.W. (Eds.) Phytoplankton Pigments in Oceanography: Guidelines to Modern Methods, UNESCO Publishing, Paris 343-360

Jiang, Z. D., Ketchum, S. O. and Gerwick, W. H. (2000). '5-Lipoxygenase-derived oxylipins from the red alga *Rhodymenia pertusa*', Phytochemistry, vol. 53, no. 1, pp. 129-133

Jin, S., Tong, T., Fan, W., Fan, F., Antinore, M. J., Zhu, X., Mazzacurati, L., Li, X., Petrik, K.L., Rajasekaran, B., Wu, M., Zhan, Q. (2002). GADD45-induced cell cycle G2-M arrest associates with altered subcellular distribution of cyclin B1 and is independent of p38 kinase activity. Oncogene 21: 8696-8704.

Jo, W.S. (2012). Effect of Microalgal Extracts of Tetraselmis suecica against UVB-Induced Photoaging in Human Skin Fibroblasts. Toxicol. Res. 28(4), 241-248

Jung, J. H., Sim, C. S., Lee, C. O. (1995). Cytotoxic compounds from the two-sponge association. J Nat Prod 58: 1722-1726.

Kita, M., Ohishi, N., Washida, K., Kondo, M., Koyama, T., Yamada, K., Uemura, D. (2005). Symbioimine and neosymbioimine, amphoteric iminium metabolites from the symbiotic marine dinoflagellate Symbiodinium sp. Bioorg. Med. Chem. 13: 5253-5258.

Kobayashi, J., Shimbo, K., Kubota, T., Tsuda, M. (2003). Bioactive macrolides and polyketides from marine dinoflagellates. Pure Appl Chem 75: 337-342.

Kobayashi, J., Tsuda, M. (2004). Amphidinolides, bioactive macrolides from symbiotic marine dinoflagelates. Nat. Prod. Rep. 21: 77-93.

Kupchan, S. M., Britton, R. W., Ziegler, M. F., Sigel, C. W. (1973). Bruceantin, a new potent antileukemic simaroubolide from Brucea antidysenterica. J. Org. Chem. 38: 178-179.

Lawrence, J. M. (2013) 'Sea urchins: Biology and Ecology third edition', Lawrence, J. M. (ed.), Academic Press, Elsevier

Le, K. (2011). Antioxidant potential of microalgae in relation to their phenolic and carotenoid content. J. Appl. Phycol. 24(6), l477-1486

Lee, J. H., Pestova, T. V., Shin, B. S., Cao, C., Choi, S. K., Dever, T. E. (2002). Initiation factor eIF5B catalyzes second GTP-dependent step in eukaryotic translation initiation. PNAS 99: 16689–16694.

Lee, Y.-H., G. M. Huang, R. A. Cameron, G. Graham, E. H. Davidson, L. Hood, and R. J. Britten. (1999). EST analysis of gene expression in early cleavage-stage sea urchin embryos. Development 126:3857-3867

Lem Vet and M. Dicke (1992). 'Ecology of Infochemical Use by Natural Enemies in a Tritrophic Context', Annual Review of Entomology, 37:141-72

Levine, B., Sinha, S., Kroemer, G. (2008). 'Bcl-2 family members: dual regulators of apoptosis and autophagy', Autophagy, 4(5):600-6

Lim, S.L., Chu, W.L., Phang, S.M. (2010). 'Use of Chlorella vulgaris for bioremediation of textile wastewater', Bioresour Technol, 7314-7322.

Linington, R.G., Robertson, M., Gauthier, A., Finlay, B.B., MacMillan, J.B., Molinski, T.F., Van, S.R., Andersen, R.J. (2006). 'Caminosides B–D, antimicrobial glycolipids isolated from the marine sponge *Caminus sphaeroconia'*, J Nat Prod., 69:173–177

Linking Oceans and Human Health: A Strategic Research Priority for Europe, Position Paper 19, (2013). European Marine Board

Locksley, R. M., Killeen, N., Lenardo, M. J. (2001). 'The TNF and TNF receptor superfamilies: integrating mammalian biology', Cell, 104(4):487-501.

López-Alarcóna, C., Denicolab, A. (2013). Evaluating the antioxidant capacity of natural products: A review on chemical and cellular-based assays. Anal Chim. Acta 763, 1-10

Lv, C., Sun, W., Sun, H., Wei, S., Chen, R., Wang, B., Huang, C. (2013). Asperolide A, a Marine-Derived Tetranorditerpenoid, Induces G2/M Arrest in Human NCI-H460 Lung Carcinoma Cells, Is Mediated by p53-p21 Stabilization and Modulated by Ras/Raf/MEK/ERK Signaling Pathway. Mar. Drugs. 11: 316-331.

MacKinnon, S. L., Cembella, A. D., Burton, I. W., Lewis, N., LeBlanc, P., Walter, J. A. (2006). Biosynthesis of 13-desmethyl spirolide C by the dinoflagellate Alexandrium ostenfeldii. J Org Chem. 10 71(23): 8724-31.

Macnee, W., Rahman, I. (1999). Oxidants and Antioxidants as Therapeutic Targets in Chronic Obstructive Pulmonary Disease. Am. J. Respir. Crit Care Med. 160, S58-S65

Maiani, G., et al. (2009).Carotenoids: Actual knowledge on food sources, intakes, stability and bioavailability and their protective role in humans. Mol. Nutr. Food Res. 53, S194–S218

Maier, M.E. (2009). 'Structural revisions of natural products by total synthesis', Nat Prod Rep., 26:1105–24

Margulis, L., Schwartz, K. V. (1998) 3rd ed. New York, USA: W.H. Freeman and Company;. Five Kingdoms – An Illustrated Guide to the Phyla of Life on Earth.

Marrone, V., Piscopo, M., Romano, G., Ianora, A., Palumbo, A. and Costantini, M. (2012). 'Defensome against toxic diatom aldehydes in the sea urchin *Paracentrotus lividus*', PLoS One, vol. 7, no. 2, p. e31750

Martin, L., Gardner, L. B. (2015). Stress-induced inhibition of nonsense mediated RNA decay regulates intracellular cystine transport and intracellular glutathione through regulation of the cystine/glutamate exchanger SLC7A11. Oncogene. 34(32), 4211–4218

Martins, A., Vieira, H., Gaspar, H., Santos, S. (2014). 'Marketed marine natural products in the pharmaceutical and cosmeceutical industries: Tips for success', Mar Drugs, 12:1066–101

McNulty, H., Jacob, R.F., Mason, R.P. (2008).Biologic activity of carotenoids related to distinct membrane physicochemical interactions. Am. J. Cardiol. 101, 20D–29D

Miralto, A., Ianora, A. and Poulet, S. A. (1995). 'Food type induces different reproductive responses in the copepod Centropages typicus', Journal of Plankton Research, vol. 17, no. 7, pp. 1521-1534

Miyaoka, H., Shimomura, M., Kimura, H., Yamada, Y., Kim, H.S., Yusuke, W. (1998). 'Antimalarial activity of kalihinol A and new relative diterpenoids from the Okinawan sponge, Acanthella sp.', Tetrahedron., 54:13467–74

Molinski, T.F., Dalisay, D.S., Lievens, S.L., Saludes, J.P. (2009). 'Drug development from marine natural products', Nat Rev Drug Discov., 8:69–85

Murray, S. A., Garby, T., Hoppenrath, M., Neilan, B. A (2012). Genetic diversity, morphological uniformity and polyketide production in dinoflagellates (Amphidinium, Dinoflagellata). PLoS ONE 7 (6): e38253

Murti, Y., Agarwal, T. (2010). 'Marine derived pharmaceuticals-development of natural health products from marine biodiversity', Int J ChemTech Res.,2:2198–217

Mustafa, E.M., Phang, S.M., Chu, W.L. (2012). 'Use of an algal consortium of five algae in the treatment of landfill leachate using the high-rate algal pond system', J Appl Phycol., 1954-1968

Onodera, K. I., Nakamura, H., Oba, Y., Ohizumi, Y., Ojika, M. (2005). Zooxanthellamide Cs:vasoconstrictive polyhydroxylated macrolides with the largest lactone ring size from a marine dinoflagellate of Symbiodinium sp. J. Am. Chem. Soc. 127: 10406-10411.

Parashiva, P. (2014). In vitro antioxidant studies on diselenodinicotinamide: A potent GPx mimic. Indian J. Chem. 53, 781-786

Passantino A. (2008). 'Application of the 3Rs Principles for Animals Used for Experiments at the Beginning of the 21st Century', Biomed. Sci., 10:27-32

Pattingre, S., Tassa, A., Qu, X., Garuti, R., Liang, X. H., Mizushima, N., Packer, M., Schneider, M. D., Levine, B. (2005). 'Bcl-2 antiapoptotic proteins inhibit Beclin 1-dependent autophagy', Cell 122(6):927-39

Pérez-López, P. (2014). Life cycle assessment of the production of bioactive compounds from Tetraselmis suecica at pilot scale. J. Clean Prod. 64, 323-331

Pertile, P., Zanella, L., Herrmann, M., Joppe, H., Gaebler, S., inventors; Symrise Gmbh & Co., assignee. (2015). Extracts of Tetraselmis sp. for cosmetic and therapeutic purposes. Europe Patent N. EP2,193,785

Peterson, K. J., R. A. Cameron, and E. H. Davidson. (2000). Bilaterian origins: significance of new experimental observations. Dev. Biol. 219:1-17

Pfaffl, M. W. (2001). 'A new mathematical model for relative quantification in real-time RT-PCR', Nucleic acids research, vol. 29, no. 9, p. e45

Pfaffl, M. W., Horgan, G. W. and Dempfle, L. (2002). 'Relative expression software tool (REST) for group-wise comparison and statistical analysis of relative expression results in real-time PCR', Nucleic acids research, vol. 30, no. 9, p. e36

Phang, S.M., Miah, M.S., Yeoh, B.G., Hashim, M.A. (2000). 'Spirulina cultivation in digested sago starch factory wastewater', J Appl Phycol., 12: 395–400

Pohnert, G. (2000). 'Wound-activated chemical defense in unicellular planktonic algae', Angewandte Chemie-International Edition, vol. 39, no. 23, pp. 4352-4354

Pohnert, G. (2002). 'Phospholipase A (2) activity triggers the wound-activated chemical defense in the diatom *Thalassiosira rotula*', Plant Physiology, vol. 129, no. 1, pp. 103-111

Pohnert, G. and Boland, W. (2002). 'The oxylipin chemistry of attraction and defense in brown algae and diatoms', Natural product reports, vol. 19, pp. 108-122

Poulet, S. A., Ianora, A., Miralto, A. and Meijer, L. (1994). 'Do diatoms arrest embryonic-development in copepods?'. Marine Ecology Progress Series, vol. 111 no. 1-2, pp. 79-86

Poulet, S. A., Ianora, A., Miralto, A. and Meijer, L. (1994). 'Do diatoms arrest embryonic-development in copepods?', Marine Ecology Progress Series, vol. 111 no. 1-2, pp. 79-86

Radjasa, O.K., Vaske, Y.M., Navarro, G., Vervoort, H.C., Tenney, K., Linington, R.G., (2011). 'Highlights of marine invertebrate-derived biosynthetic products: Their biomedical potential and possible production by microbial associants', Bioorg Med Chem., 19:6658–74

Raja, R., Hemaiswarya, S., Ashok Kumar, N., Sridhar S. and Rengasamy R. (2008). 'A Perspective on the Biotechnological Potential of Microalgae', Crit Rev Microbiol., 34(2):77-88

Rashid, Z.M., Lahaye, E., Defer, D., Douzenel, P., Perrin, B., Bourgougnon, N. (2009). 'Isolation of a sulphated polysaccharide from a recently discovered sponge species (*Celtodoryx girardae*) and determination of its anti-herpetic activity', Int J Biol Macromol., 44:286–93

Ribalet, F., Berges, J. A., Ianora, A. and Casotti, R. (2007). 'Growth inhibition of cultured marine phytoplankton by toxic algal-derived polyunsaturated aldehydes', Aquatic toxicology, vol. 85, no. 3, pp. 219-227

Ritter, A., Goulitquer, S., Salaün, J.-P., Tonon, T., Correa, J. A. and Potin, P. (2008). 'Copper stress induces biosynthesis of octadecanoid and eicosanoid oxygenated derivatives in the brown algal kelp *Laminaria digitata*', The New phytologist, vol. 180, no. 4, pp. 809-821

Rizzo, P. J. (2003). Those amazing dinoflagellate chromosomes. Cell Research 13: 215–217.

Roger, M. J. R., Reigosa, M. J.; Pedrol, N.; González, L. (2006). 'Allelopathy: a physiological process with ecological implications', Springer, p. 2, ISBN 1-4020-4279-5

Romano, G., Costantini, M., Buttino, I., Ianora, A. and Palumbo, A. (2011). 'Nitric oxide mediates the stress response induced by diatom aldehydes in the sea urchin *Paracentrotus lividus*', PLoS ONE, vol. 6, no. 10, pp. e25980

Romano, G., Miralto, A. and Ianora, A. (2010). 'Teratogenic effects of diatom metabolites on sea urchin *Paracentrotus lividus* embryos', Marine drugs, vol. 8, no. 4, pp. 950-967

Romano, G., Russo, G. L., Buttino, I., Ianora, A. and Miralto, A. (2003). 'A marine diatom-derived aldehyde induces apoptosis in copepod and sea urchin embryos', Journal of Experimental Biology, vol. 206, no. 19, pp. 3487-3494

Sansone, C., Braca, A., Ercolesi, E., Romano, G., Palumbo, A., Casotti, R., Francone, M., Ianora, A., (2014). Diatom-derived polyunsaturated aldehydes activate cell death in human cancer cell lines but not normal cells', PLoS ONE 9 (7), e101220 10.1371

Sea Urchin Genome Sequencing Consortium. (2006). The Genome of the Sea Urchin *Strongylocentrotus purpuratus*. Science (New York, N.Y.), 314(5801), 941–952

Shulin, W. and Wafik S. El-Deiry. (2003). 'TRAIL and apoptosis induction by TNF-family death receptors 1', Oncogene 22, 8628–8633

Sindhu, E.R., Preethi, K.C., Kuttan, R. (2010). Antioxidant activity of carotenoid lutein in vitro and in vivo. Indian J. Exp. Biol. 48, 843-848

Skov, M.J., Beck, J.C., de Kater, A.W., Shopp, G.M. (2007). 'Nonclinical safety of ziconotide: An intrathecal analgesic of a new pharmaceutical class', Int J Toxicol., 26:411–21

Smith A. B. (1999). 'Biomineralization in Echinoderms', Skeletal biomineralization: patterns, processes and evolutionary trends, 5, pp. 413-443

Speit, G., Bonzheim, I. (2003). Genotoxic and protective effects of hyperbaric oxygen in A549 lung cells. Mutagenesis 18(6), 545-548

Spiteller, G. (2003). 'Are lipid peroxidation processes induced by changes in the cell wall structure and how are these processes connected with diseases?', Medical hypotheses, vol. 60, no. 1, pp. 69-83

Su, X., Kamat S. and Heuer A. H. (2000). 'Structure of sea urchin spines, large biogenic single crystals of calcite', *Journal of Materials Science*, vol. 35, no. 22, pp. 5545-5551

Suganthy, N., Karutha Pandian, S., Pandima Devi, K. (2010). 'Neuroprotective effect of seaweeds inhabiting South Indian coastal area (Hare Island, Gulf of Mannar Marine Biosphere Reserve): Cholinesterase inhibitory effect of Hypnea valentiae and Ulva reticulata', Neurosci Lett., 468:216–9

Sugawara, T., Yamashita, K., Sakai, S., Asai, A., Nagao, A., Shiraishi, T., Imai, I., Hirata, T. (2007). Induction of Apoptosis in DLD-1 Human Colon Cancer Cells by Peridinin Isolated from the Dinoflagellate, Heterocapsa triquetra. Biosci. Biotechnol. Biochem. 71: 1069–1072.

Susin, S. A., Lorenzo, H. K., Zamzami, N., Marzo, I., Snow, B. E., Brothers, G. M., Mangion, J., Jacotot, E., Costantini, P., Loeffler, M., Larochette, N., Goodlett, D. R., Aebersold, R., Siderovski, D. P., Penninger, J. M., Kroemer, G. (1999). 'Molecular characterization of mitochondrial apoptosis-inducing factor', Nature 397(6718):441-6

Taylor, F. J. R., Hoppenrath, M., Saldarriaga, J. F. (2008) Dinoflagellate diversity and distribution. Biodivers. Conserv. 17: 407-418.

Taylor, R. L., Abrahamsson, K., Godhe, A. and Wangberg, S.-A. (2009). 'Seasonal variability in polyunsaturated aldehyde production potential among strains of *Skeletonema marinoi* (bacillariophyceae)', Journal of Phycology, vol. 45, no. 1, pp. 46-53

Tosti, E., Romano, G., Buttino, I., Cuomo, A., Ianora, A. and Miralto, A. (2003). 'Bioactive aldehydes from diatoms block the fertilization current in ascidian oocytes', Molecular reproduction and development, vol. 66, no. 1, pp. 72-80

Vacquier, V. D., Swanson, W. J. and M. E. Hellberg. (1995). What have we learned about sea urchin sperm bindin? Dev. Growth Differ. 37:1-10

Varrella, S., Romano, G., Ianora, A., Bentley, M. G., Ruocco, N. and Costantini, M. (2014). 'Molecular response to toxic diatom-derived aldehydes in the sea urchin *Paracentrotus lividus*', Marine Drugs, vol. 12, pp. 2089-2113

Varrella, S., Romano, G., Ruocco, N., Ianora, A., Bentley M.G. and Costantini M. (2014). 'First morphological and molecular evidence of the negative impact of diatom-derived hydroxyacids on the sea urchin Paracentrotus lividus', Toxicol. Sci.151(2):419-33

Vidoudez, C., Casotti R., Bastianini, M. and Pohnert G. (2011). 'Quantification of Dissolved and Particulate Polyunsaturated Aldehydes in the Adriatic Sea', Mar. Drugs, 9, 500-513

Vignesh, S., Raja, A., James, R. A. (2011). 'Marine drugs: Implication and future studies', Int J Pharmacol., 7:22–30

Voigt, A., Berlemann, L.A., Winklhofer. (2016). 'The mitochondrial kinase PINK1: functions beyond mitophagy', J Neurochem139 Suppl 1:232-239

Walsh, C. J., Leggett, S. R., Strohbehn, K., Richard H. Pierce and John W. (2008). Sleasman Effects of in vitro Brevetoxin Exposure on Apoptosis and Cellular Metabolism in a Leukemic T Cell Line (Jurkat). Mar. Drugs 6: 291-307.

Wan-Loy Chu. (2012). 'Biotechnological applications of microalgae', IeJSME: 6 (Suppl 1): S24-S37

Wheeler, B., White, M.P., Stahl-Timmins, W., Depledge, M.H. (2012). Does living by the coast improve health and wellbeing? Health & Place 18:1198-1201

Wichard, T., Poulet, S.A., Halsband-Lenk, C., Albaina, A., Harris, R. (2005). 'Survey of the chemical defense potential of diatoms: Screening of fifty one species for a, b, c, d-unsaturated aldehydes', J Chem Ecol 31: 949–958.

Wright, J. L. C., Cembella, A. D. (1999). Ecophysiology and biosynthesis of polyether marine biotoxins. In: Anderson DM, Cembella AD, Hallegraeff GM (Eds.) Physiological Ecology of Harmful algal Blooms. NATO ASI series, Springer-Verlag, Berlin Heidelberg, New York.

Xin Luo and W. Lee Kraus. (2012). 'On PAR with PARP: cellular stress signaling through poly(ADP-ribose) and PARP-1', Genes Dev., 26(5):417-32

Xue, M., Cao, X., Zhong, Y., Kuang, D., Liu, X., Zhao Z., Li, H. (2012). Insulin-like growth factor-1 receptor (IGF-1R) kinase inhibitors in cancer therapy: advances and perspectives. Curr. Pharm. Des. 18: 2901-13.

Yang, Z. F., Zhang, W., Li, D. (2013). Inhibition of the mTOR/STAT3 Gadd45a Suppresses Tumor Angiogenesis. J. Biol. Chem. 288: 6552-6560.
Yip, K. W. and Reed, J. C. (2008). 'Bcl-2 family proteins and cancer', Oncogene, 27, 6398–6406

Zhang, B. (2014). Human 3-alpha hydroxysteroid dehydrogenase type 3 (3α-HSD3): the V54L mutation restricting the steroid alternative binding and enhancing the 20α-HSD activity. J. Steroid Biochem Mol. Biol. 141, 135-43

Zhang, Z. D., Green, B. R., Cavalier-Smith, T. (1999). Single gene circles in dinoflagellate chloroplast genomes. Nature 400: 155–159.